Functional MRI in Asleep and Awake Infants – New Frontiers

Dr. Graham King

MB BCh BAO, BE, MRCPI, MRCPCH, MSc, PGDip

Student Number: 19328533

Trinity College Institute of Neuroscience,

School of Psychology,

Trinity College Dublin

Thesis submitted in fulfilment of the requirements for the degree of

Doctor of Philosophy (PhD)

to Trinity College Dublin, the University of Dublin.

2025

DECLARATION AND PERMISSION

This thesis has not been submitted as an exercise for a degree at this or any other University. It is entirely my own work, except where duly acknowledged in the text. Full and informed consent was obtained from human subjects.

I agree to deposit this thesis in the University's open access institutional repository or allow the library to do so on my behalf, subject to Irish Copyright Legislation and Trinity College Library conditions of use and acknowledgement. I consent to the examiner retaining a copy of the thesis beyond the examining period, should they so wish (EU GDPR May 2018).

GRAHAM KING

Graham King

ACKNOWLEDGEMENTS

I would like to thank my supervisor, Prof. Rhodri Cusack, the Thomas Mitchell Professor of Cognitive Neuroscience and Director of Trinity College Institute of Neurosciences. I would like to thank him for giving me the opportunity to pursue this thesis, for his support and guidance, and for his patience as I balanced my clinical and academic work commitments during this thesis period.

I would like to thank my clinical supervisor for this thesis, Prof. Eleanor Molloy, Professor of Paediatrics Trinity College Dublin, without whose input and support I would not have been able to achieve the clinical-academic components of this thesis. Further I would like to thank her for her advice and mentorship during my thesis period.

I would like to thank Prof. Adrienne Foran (consultant neonatologist) and Dr. Ailbhe Tarrant (consultant radiologist) for all their help setting up this project and conducting this research work in the Rotunda Hospital Dublin. In addition, I am very grateful to Prof. Eleanor Molloy (consultant neonatologist) and Dr. Angela Byrne (consultant radiologist) who facilitated this project's commencement and ongoing work in the Coombe Hospital Dublin.

I would like to thank Mr. Sojo Joseph, MRI Radiographer Trinity College Institute of Neurosciences, who helped set up the scanning paradigm and environment, helped problem solve equipment issues, and who so carefully and professionally rose to the challenge of scanning the infant participants both awake and asleep.

I am especially grateful to my colleagues in the Cusack Lab during my thesis period. This group includes Áine Dineen, Clíona O'Doherty, Chiara Caldinelli, Anna Kravchenko, Enna-Louise Darcy, and Jessica White. You all were very hard working and very supportive colleagues, and special thanks for all the help with participant recruitment and for all your tips helping me to learn python coding. In addition, I would like to thank Dr. Anna Truzzi, Postdoctoral Research Fellow, who in addition to helping recruitment and scanning of the infant participants, ensured my smooth on-boarding when I joined the Cusack Lab team, and supervised the timelines and project management of the project.

I would like to thank the infant participants and their parents from the Rotunda Hospital Dublin and the Coombe Hospital Dublin who generously gave their time towards this project (FOUNDCOG project: www.foundcog.org) and thesis.

I would like to thank the developing Human Connectome Project team (dHCP) (KCL-Imperial-Oxford Consortium, London, UK) for the use of their open data repository. Covid-19 related delays had a significant impact on the commencement/timings of the FOUNDCOG project, and so I was delighted to have the dHCP open data available to work with during the Covid-19 lockdowns/restrictions.

I want to especially thank my parents (Raphael and Alan) for their support of my education, my career, and for the many meals cooked for me in to allow me time to write this thesis. Similarly, I would like to thank my parents-in-law (Tess and Tiernan) who through their many generous offers of childcare have greatly helped me achieve the time commitment needed for this thesis.

Finally, I would like to thank my wife, Sadhbh, and my son, Oisín. Sadhbh has had to juggle both her medical career and extra parenting responsibility (both Oisín and baby bump) to allow me the time to write up this thesis and has constantly shown me the love and encouragement needed to balance my busy clinical and academic commitments. Thank you, Sadhbh. During my thesis period Oisín has been both a wonderful newborn and now an aged 3-year-old young man. Oisín has both been an infant participant in this study/project and has kindly understood (I hope!) when I have disappeared during evenings/weekends while writing up this thesis. Thank you, Oisín.

CONTRIBUTOR STATEMENT

The FOUNDCOG (www.foundcog.org) project includes a team of post-graduate PhD candidates, postdoctoral fellows and research assistants, all led by the principal investigator Prof. Rhodri Cusack. Numerous members of the team with various backgrounds (physics, psychology, neuroscience, and clinical neonatology) worked towards the common goal of using magnetic resonance imaging as a tool to understand infant brain development during their first year of life. Various steps in this thesis involved the contribution of input from colleagues, and I am very grateful for this.

Specific tasks/contributions that I was directly involved in include (but is not limited to) the following: drafting and submitting ethics applications for the hospitals and university (including numerous updates to ethics), managing the recruitment of infants in the participating hospitals, authoring the Trinity College Institute of Neuroscience (TCIN) 'Standard Operating Procedures for Infant MRI Scanning' (and amending same for COVID precautions), designing data forms and collecting hospital data for neonatal ICU (NICU) participants, designing data forms and collecting data (perinatal, demographic, parental) for controls (term) infants, organising and collecting of Ages & Stages data, designing and collecting Parental Feedback Questionnaire data, co-designing and testing the infant scanning environment (equipment purchasing, testing, problem solving), supervising the wellbeing and comfort of the infants during the scanning visit (I was present as the paediatric doctor for each scan), and designing and managing the pathway for anatomical MRI reporting of incidental findings.

The conversion of DICOM images to NIFTI format and logging of MRI runs/images achieved was managed by Clíona O'Doherty. The main pre-processing pipeline was co-authored (python code) by various members of the project team. I contributed towards this coding (editing the infant template mask, quality control checking, and coding for region-of-interest extraction).

I personally designed, analysed (python coded), carried out statistics, and first authored all works relating to functional connectivity analyses (fingerprinting analysis, brain state analysis, and classification analysis). I also first/principal

authored the chapter (article 'in-submission') on awake infant scanning methodology. I would like to acknowledge the initial written contributions of my colleagues (Áine Dineen, Clíona O'Doherty, Anna Truzzi, Chiara Caldinelli, and Jessica White) towards the initial draft of this chapter. I would like to thank Clíona O'Doherty for creating the illustration (Figure 3-3) in the 'Infant Scanning' section of the methodology chapter. I would also like to thank Áine Dineen for creating the illustration (Figure 3-7) in the 'Infant Attention' section of the methodology chapter. I would also like to thank Amy Burke and Maebh Healy for helping me with the many hours tagging of infant facial video footage (work included in the methodology chapter).

This research was funded by an ERC Advanced Grant 2017 – FOUNDCOG 787981.

Open data were provided by the developing Human Connectome Project, KCL-Imperial-Oxford Consortium funded by the European Research Council under the European Union Seventh Framework Programme (FP/2007-2013) / ERC Grant Agreement no. [319456].

PUBLICATIONS AND PRESENTATIONS

Peer-reviewed and related directly to this thesis:

- King, G., Truzzi, A., Cusack, R., 2023. The confound of head position in within-session connectome fingerprinting in infants. NeuroImage 265, 119808. https://doi.org/10.1016/j.neuroimage.2022.119808

Manuscripts in preparation:

- King, G., Dineen, A., O'Doherty, C., Truzzi, A., Caldinelli, C., D'Arcy, E.L., White, J., Kravchenko, A., Zaadnoordijk, L., Burke, A., Healy, M., Joseph, S., Molloy, E., Foran, A., Tarrant, A., Byrne, A.T., Cusack, R., Practicalities of scanning an Awake Infant functional MRI cohort. [*in submission*].

Conference presentations - Oral:

- International Neonatology Association Conference (2023). *Functional Connectivity MRI analysis in infancy – Is awake richer?* King, G., Dineen, A., O'Doherty, C., Truzzi, A., Caldinelli, C., D'Arcy, E., White, J., Kravchenko, A., Molloy, E., Foran, A., Tarrant, A., Byrne, A.T., Cusack, R.
- Irish Neonatal Research Symposium (2023). Infant Brain Functional MRI – A New Awakening. King, G., Dineen, A., O'Doherty, C., Truzzi, A., Caldinelli, C., D'Arcy, E., White, J., Kravchenko, A., Molloy, E., Foran, A., Tarrant, A., Byrne, A.T., Cusack, R.
- Organization for Human Brain Mapping, Montréal, Canada (2023). 100 Babies: Lessons from Awake Infant fMRI at 2 Months. Dineen, Á., King. G, O'Doherty, C., Truzzi, A., Caldinelli, C., D'Arcy, E., White, J., Kravchenko, A., Zaadnoordijk, L., Burke, A., Healy, M., Joseph, S., Molloy, E., Foran, A., Tarrant, A., Byrne, A., Cusack, R.
- Trinity College Dublin School of Psychology (Neuroscience) Research Symposium (2023). 100 Babies: Lessons from Awake Infant fMRI at 2 months. King, G., Dineen, A., O'Doherty, C., Truzzi, A., Caldinelli, C., D'Arcy, E., White, J., Kravchenko, A., Molloy, E., Foran, A., Tarrant, A., Byrne, A.T., Cusack, R.

Conference presentations - Poster:

- Organization for Human Brain Mapping (2021). *Characteristics of the Preterm Infant Connectome in the early postnatal period*. King, G., Truzzi, A., Cusack, R.
- Fetal Neonatal Neurology Conference (2021). Exploring the connectome in preterm infants in the early postnatal period. King, G., Truzzi, A., Cusack, R

SUMMARY

In recent years, the improved survival of very/extremely preterm infants has led to a higher prevalence of neurodevelopmental impairment. As such, increased attention has turned towards biomarkers for early diagnosis/prognosis. Historically, neurological insults during the early preterm period (while in the neonatal intensive care unit) took the form of macroscopic lesions leading to cerebral palsy, blindness/deafness, or other severe motor/cognitive impairment. However, today, very/extremely preterm infants mostly avoid macroscopic brain injury and are instead later diagnosed with more subtle deficits, such as disorders of attention, executive function, or learning. Here we investigate how functional neuroimaging can be used to probe individual differences in infant brain function. Specifically, we examine functional connectivity.

In the first study, we critically examine existing methods for measuring the individual functional connectome (a.k.a. 'fingerprint'), which is portion of functional connectivity that can identify the individual and be linked to their behaviours. Recent research has assessed whether a functional fingerprint exists in young infants. We hypothesised that various confounding variables, including brain state (asleep versus awake), might impact this functional connectome in infants (and its potential as a neuroimaging biomarker). Analysing data from a large open infant cohort, we identified confounding variables that seriously impact infant functional fingerprinting, including motion, head size, inter-session interval and head position in the head coil.

Next, we acquired functional MRI (fMRI) from a cohort of infants as part of the FOUNDCOG study (www.foundcog.org). The first 100 infants (75 term and 25 preterm born infants) were included in this analysis. The majority of previous studies have scanned infants asleep, and the practical challenges and important methodological steps needed to achieve awake infant fMRI data is discussed in detail. Methods used resulted in successful completion of awake fMRI runs and good infant comfort/attendance (as reported by researcher and parents).

Individual versus shared components of the infant functional connectome were identified in preterm and term infant groups, and the impact of brain state (awake versus asleep) on these was assessed. Results from this 2-month old infant cohort, showed that there is a different pattern of fMRI connectivity between sleep and awake (movies) states, and that there appear subtle differences between preterm and term functional connectivity in both states.

Lastly, we examined the relationship between connectivity, brain state and prematurity. We used simple machine learning models to examine whether brain state impacted the classification of preterm and term born infant groups. Results indicated that functional connectivity data from 2-month aged infants can classify brain state (asleep/movies) during a scan (both ex-preterm and term born infants) and can weakly predict scan age (when training on asleep state only). It is felt that methodological challenges in our analysis limited our ability to classify and predict birth gestation.

Finally, study protocols are being shared with the foetal/infant/toddler neuroimaging community (FIT'NG community) which is an increasingly active and growing community of researchers. This is in the hope that both this and future work will lend towards identifying potential functional MRI biomarkers in this pre-verbal infant population.

ABBREVIATIONS

aEEG, amplitude integrated EEG

ASQ, Ages and Stages Questionnaire

BOLD, blood oxygen level dependent signal

BSID, Bayley scales of infant toddler development

CGA, corrected gestational age

CLD, chronic lung disease (aka bronchopulmonary dysplasia)

cUS, cranial ultrasound

dHCP, Developing Human Connectome Project

DMN, Default Mode Network

dMRI, diffusion MRI

DWMA, diffuse white matter abnormality

EEG, electroencephalography

ELBW, extremely low birth weight

EPT, extremely preterm

FA, fractional anisotropy

FC, functional connectivity

fMRI, functional MRI

fNIRS, functional near infra-red spectroscopy

FWD, frame-wise displacement

GA, gestational age

ISC, inter-subject correlations

ISFC, inter-subject functional connectivity

ISS, inter-subject similarity (shared)

LH, left hemisphere

MRI, magnetic resonance imaging

MRS, magnetic resonance spectroscopy

NDI, neurodevelopmental impairment

NEC, necrotising enterocolitis

NICU, neonatal intensive care unit

OFC, occipital-frontal circumference

PMA, post-menstrual age

RH, right hemisphere

ROI, region-of-interest

rsfMRI, resting state fMRI

RSM, representational similarity matrix

RSNs, resting state networks

SD, standard deviation

SIS, state-independent similarity

sMRI, structural MRI

SNR, signal-to-noise ratio (a.k.a. temporal signal-to-noise ratio, tSNR)

SNR-coil, SNR estimated for each point in the head coil space

SNR-group, SNR-coil values resliced back into an individual participant's functional space (and re-sampled using Schaefer ROIs).

SNR-individual, SNR calculated from the participant's functional timeseries

SVC, support vector classification

SVM, support vector machine

SVR, support vector regression

TEA, term equivalent age

VLBW, very low birth weight

VPT, very preterm

WMI, white matter injury

WSS, within-subject similarity

LIST OF FIGURES

LIST OF TABLES

Table of Contents

CHAPTER 1 INTRODUCTION

1.1 BRAIN DEVELOPMENT IN PRETERM INFANTS

Preterm birth is defined by World Health Organization (WHO) as all births before 37 completed weeks of gestation (World Health Organization, n.d.). Preterm birth can be divided based on gestational age: extremely preterm (<28 weeks); very preterm (28 to <32 weeks); moderate to late preterm (32 to <37 weeks). Across 184 countries, the rate of preterm birth ranges from 5% - 18% of babies born (World Health Organization, n.d.).

The rate at which extremely premature (EPT) infants being born is increasing. In Ireland the 2018 report on mortality risk among very low birth weight (VLBW) infants (born between 2014-2016) recommended that resuscitation should be administered to all infants born at 23 weeks who present in a favourable condition. In 2018 in Ireland, 89% of infants born at 23 weeks gestation were offered resuscitation compared to 42% in 2014 (Leitao et al., 2020).

The brain is developing in many important ways during this period. From the 24th week of gestational age (GA) to term-equivalent age of 40 weeks GA, the main events in brain network development consist of: (1) growth of thalamocortical connections, (2) growth of long-range cortico-cortical connections, (3) growth of short range cortico-cortical connections, and (4) pruning of connections based on initial endogenous, and then subsequent exogenous activity (Kostović and Jovanov-Milosević, 2006). The growth of cortico-cortical connections is paralleled by the emergence of functional inter- and intra- hemispheric synchronisation, which increase rapidly between approximately the 30th to 35th week GA (Koolen et al., 2016). This increase in neural activity/synchronisation is largely accounted for by the growth of neural connections in grey matter (i.e., synapse and dendrites), long-range axons, and myelination, all of which are elements essential for the organization of distributed functional networks (Tau and Peterson, 2010).

In cerebral white matter, pre-oligodendrocytes (pre-OLs) begin ensheathment of axons at approximately 30 weeks of gestation. In the premature period, this process is critical for axonal growth and differentiation and, as a downstream

consequence, the development of the cerebral cortex, cerebral white matter, thalamus, basal ganglia, and more distant grey matter (Back et al., 2002). Any pre-OLs disruption can acutely causes cell death followed by chronic replenishment of the pre-OLs pool. However, these pre-OLs fail to differentiate and en-sheath white matter axons, with resulting impact on myelination and impaired development of the grey matter structures (Kinney and Volpe, 2018).

After birth, infancy continues to be a period of rapid brain growth, largely by dendritic and axonal expansion and progressive myelination (Huttenlocher et al., 1982). During the early postnatal period a number of complex neurobiological processes take place (e.g. myelination, axonal pruning, synaptic pruning, synaptogenesis) in an ordered manner across the brain (Barkovich and Barkovich, 2019; Dubois et al., 2020; Levitt, 2003). Different rates of coordinated brain developmental processes occurring during infancy include: synaptogenesis (Huttenlocher and de Courten, 1987); myelination of cortical connections (Miller et al., 2012); and refinement of cortical microstructure (T. A. Smyser et al., 2016).

1.1.1 The multiple hit hypothesis of preterm birth

The multiple hit hypothesis posits that the risk of white matter injury (WMI) increases with cumulative exposure to multiple perinatal risk factors (Barnett et al., 2018; Van Steenwinckel et al., 2014). Further WMI and impaired WM development may be accompanied by a more global insult also involving the grey matter, which is nowadays qualified by the term *encephalopathy of prematurity*, first proposed by Volpe (Volpe, 2009).

Infection/Chorioamnionitis:
In a Swiss multi-centre cohort study (2000-2007) of EPT infants with proven sepsis, affected infants had worse neurodevelopmental outcomes independent of other risk factors (Schlapbach et al., 2011). Perinatal infection is recognised as an important risk factor for WMI in the premature population (Chau et al., 2012; Glass et al., 2008; Schlapbach et al., 2011).

Chronic Lung Disease:

In a study (Ball et al., 2010) the relationship between chronic lung disease (CLD) and WMI was investigated using diffusion MRI and measures of fractional anisotropy (FA) and diffusivity. Preterm infants with CLD had significantly increased radial diffusivity (RD) and significantly reduced FA within the centrum semiovale, corpus callosum and inferior longitudinal fasciculus ($p<0.05$) compared to their peers (controlling for degree of prematurity and age at scan) (Ball et al., 2010).

Necrotising enterocolitis:
In a recent systematic review of studies of cohorts (2010 – 2018) of infants with necrotising enterocolitis (NEC) from high-income countries the overall rates of severe neurodevelopmental impairment (NDI) ranged from 25% - 59% (Jones and Hall, 2020). NEC is often accompanied (during the NICU course) by other common complications of prematurity such as longer intubation, CLD, and retinopathy of prematurity. Whether these are a result of NEC or an indication of an infant's level of vulnerability, these complications compound the risk for NDI (Hickey et al., 2018) and can be considered a cumulative insults as per the multiple hit hypothesis.

In this context of the multiple hit hypothesis, Irish rates of inflammatory morbidities in the preterm population have been sourced. According to the 'Very Low Birth Weight Infants in the Republic of Ireland Annual Report 2018' commonly considered inflammatory morbidities had the following rates (% of the total population in the year): small for gestational age (22%), chronic lung disease (18%), any late infection (late onset sepsis, meningitis) (10%), and necrotising enterocolitis (6%) (Leitao et al., 2020). Preterm infants with these inflammatory morbidities could serve as a cohort with a specific type of brain injury.

1.2 NEURODEVELOPMENTAL OUTCOMES OF PRETERM INFANTS

While preterm mortality (Lui et al., 2019), severe intra-ventricular haemorrhage (Yeo et al., 2020) and rates of cerebral palsy (Pascal et al., 2018) have decreased in recent decades, this improved survival without major motor deficits has not yet been matched by a reduction in rates of neurodevelopmental

impairment with high rates of intellectual, behavioural, social and emotional impairments persisting into adult life (Johnson and Marlow, 2017).

From a recent meta-analysis of low mortality countries (neonatal mortality rates <5) it was seen that 24.5% (95% CI: 20.2–28.8%) of survivors born at <28 weeks developed moderate/severe neurodevelopmental impairment (all inclusive of motor, visual, hearing, speech, and higher cognitive or social/executive dysfunction) and 33.9% (95% CI: 28.6–39.3%) of survivors had mild neurodevelopmental impairment. For infants born at 28–31 weeks, 12.2% (95% CI: 6.1–18.2%) had moderate/severe and 16.5% (95% CI: 13.6–19.3%) mild neurodevelopmental impairment (Blencowe et al., 2013). Similarly in a systematic review (infants born 2006-2016) investigators showed that at 2 years corrected age 1 in 6 infants had some cognitive delay, with overall pooled prevalence showing mild cognitive delay in 14.3% and moderate-severe cognitive delay in 8.2% (Pascal et al., 2018).

It has been known for some time that extremely low birth weight (ELBW) infants who avoid the classical motor/visual/cognitive impairments of prematurity have increased risk of symptoms of autism, inattention, anxiety, and obsessive compulsive disorder (Fevang et al., 2016). Two meta-analyses of data from studies of very preterm cohorts have reported small to medium effect sizes (0.25 SD to 0.57 SD) for deficits in inhibition, working memory, planning, cognitive flexibility and verbal fluency (Aarnoudse-Moens et al., 2009; Mulder et al., 2009). Further, preterm birth is associated with decreased academic performance in school age children (> 5 years old) (Twilhaar et al., 2018), and has been associated with decreased intelligence (Allotey et al., 2018), executive function, and processing speed through to adolescence (Brydges et al., 2018) and an increase risk for attention problems in adulthood (Breeman et al., 2016).

Executive function disorders, common in preterm children, are often associated with widespread, subtle abnormalities of white and grey matter rather than focal lesions (Anderson et al., 2017; Boardman et al., 2010). As such, neurodevelopmental outcomes in these domains may be better predicted with 'connectome-type' analyses that include measures of segregation and integration (Fischi-Gomez et al., 2016)

1.3 BIOMARKERS AND NEUROIMAGING

During their time in the neonatal intensive care unit (NICU), preterm infants have a rapid rate of brain development that occurs at the same time as they are often critically ill, exposed to numerous medical interventions, and unusual sensory stimuli (Huppi et al., 1998). Currently, being born very/extremely premature is in itself one of the strongest indicators of impacted long-term developmental outcomes, with the degree of prematurity associated with severity (Eves et al., 2021; Johns et al., 2018; Johnson and Marlow, 2017; O'Reilly et al., 2020).

With higher very/extremely preterm infant survival, and as a result a significant prevalence of neurodevelopmental impairment, attention has turned towards biomarkers for early diagnosis and intervention. Early intervention programmes for preterm infants have a positive influence on cognitive and motor outcomes during infancy, with the cognitive benefits persisting into pre-school age (Spittle et al., 2012).

The NIH Biomarkers Definitions Working Group defined a biomarker as:

> *"a characteristic that is objectively measured and evaluated as an indicator of normal biological processes, pathogenic processes, or pharmacologic responses to a therapeutic intervention" (Downing, 2001)*

The potential clinical application of a biomarkers includes: determination of the presence or absence of disease; staging of a disease; determination of risk prognosis; or prediction and monitoring of clinical response to an intervention (Downing, 2001).

While screening tools aim to rule in all affected persons (high sensitivity) this is often at the cost of being overly inclusive (low specificity). In contrast, for diagnostic tests, higher importance is put on achieving the correct diagnosis (high specificity) at the cost of being less inclusive (lower sensitivity) (Castellanos et al., 2013). Various infant neuroimaging techniques have lent

themselves to infant screening/diagnostics/prediction of neurodevelopmental impairment and these are summarised below.

1.3.1 Cranial ultrasound

Serial cranial ultrasound (cUS) is used to detect early intra-ventricular haemorrhage (IVH), and subsequent peri-ventricular leukomalacia (PVL) and/or cystic change. The American Academy of Pediatrics state that serial cUS is important in delineating fully overt brain injury, including cystic white matter injury (Hand et al., 2020). Serial cUS is safe, relatively inexpensive, and readily available at the bedside for serial imaging of brain injury and its evolution.

However, in recent years there has been a trend towards decreasing overall rates of IVH, for example, in one large study in New Zealand and Australia from 24% in 1995 to 21% in 2012 (Yeo et al., 2020). The Vermont Oxford Network (VON) Database is used worldwide to measure rates of common preterm morbidities. In 2017, VON demonstrated an overall 24.6% incidence of IVH and an 8.1% rate of severe IVH (defined as grade III or IV) among more than 50,000 VLBW infants (Hand et al., 2020).

Despite skilled personnel performing serial cranial ultrasound measures in these populations, the sensitivity of cUS is restricted due to its resolution and acoustic window. It has been seen that cUS is less sensitive in assessing the more common mild but diffuse white matter injury, periventricular white matter lesions and punctate cerebellar haemorrhages, and it cannot detect myelination, abnormalities in the integrity of cerebral white matter and grey matter structures, connectivity, gyral maturation, or cortical malformations (Inder et al., 2021; Ou et al., 2014). Further, a recent meta-analysis has shown how the sensitivity and specificity of IVH as a biomarker for extended neurodevelopmental outcomes (cognitive/social/executive) is lacking (Hollebrandse et al., 2020). As a result, attention has turned from cUS towards other imaging modalities to identify more subtle biomarkers of NDI in the preterm population.

1.3.2 Anatomical MRI

Acquired brain lesions are common in preterm infants routinely imaged at term-equivalent age, but not all predict an adverse neurodevelopmental outcome. In a recent 3T MRI study of preterm infants born < 33 weeks gestation it was seen that 76% of infants had acquired lesions on term equivalent age (TEA) MRI (Arulkumaran et al., 2020). However, for an infant with no focal lesion at TEA MRI is only 45% sensitive and 61% specific for normal neurodevelopmental outcome at 20 months age (Arulkumaran et al., 2020).

In recent years it has been seen how MRI studies of preterm infants with moderate/severe (i.e., not mild) brain injury on conventional MRI have been shown to be strong predictors of neurodevelopmental outcomes (Anderson et al., 2017; Collins et al., 2021; Dimitrova et al., 2021a, 2021b; Hintz et al., 2015; Parikh et al., 2020; Woodward et al., 2012, 2006). Similarly, a recent meta-analysis of MRI at TEA showed that MRI predicts cerebral palsy or low motor score on the Bayley Scale of Infant Development (BSID) with a range of positive predictive value of 60%-67% (Guillot et al., 2021).

In contrast, for cognition, TEA magnetic resonance imaging (MRI) demonstrates low positive predictive value and high negative predictive value (Guillot et al., 2021). Importantly, it was seen that the prognostic value of MRI did vary between studies, and the variance related principally to the tools used and the breadth of evaluation of brain abnormalities (Guillot et al., 2021). Other literature has found similar results regarding the prediction of cognitive/intellectual outcomes. In a systematic review of very preterm (VPT) infants undergoing TEA MRI showed that TEA MRI had limited ability to predict outcomes such as neurocognitive or behavioural impairments at 18 months corrected age (van't Hooft et al., 2015). Further, Hintz et al. (2018, 2015) have recently indicated that adding MRI to early and late cUS did not improve prediction of severe intellectual disability or neurodevelopmental impairment at 6 to 7 years of age (Hintz et al., 2018, 2015).

In Ireland it is not current clinical practice to provide routine TEA MRI for VPT infants. However, as suggested in the review by Hand et al., term MRI is offered to high-risk infants (infants with grade 3 or 4 IVH, seizure, severe sepsis, other

severe infection/inflammation) however only after a conversation with the family regarding the limitations of this test for estimation of long-term prognosis (Hand et al., 2020).

1.3.2.1 Advanced anatomical MRI

In recent years more advanced anatomical MRI techniques have shown promise as potential biomarkers. Many of these use objective scoring systems and/or measure new surface-based parameters.

In a study of very preterm born infants, researchers combined TEA quantitative mapping of periventricular white matter lesions with a simple clinical classification tool. In so doing it was seen that impairments in visual, motor, and cognitive functions, and pre-school age outcomes could be predicted (Cayam-Rand et al., 2019). In a study of VPT infants without severe brain injury on MRI, multivariable linear regression was used to assess the value of diffuse white matter abnormality (DWMA) volume to predict cognitive and language scores on BSID at 2 years corrected age. While controlling for known predictors of Bayley-III scores (i.e., socioeconomic status, gestational age, sex, and global brain abnormality score), it was seen that DWMA volume remained a significant predictor of cognitive and language scores at 2 years (Parikh et al., 2020). In another study from the dHCP group (London, UK) including VPT infants, multivariable regression models were used (adjusting for GA, sex, socioeconomic status, and injury score on MRI) and showed that regional measures of surface area and curvature independently explained more than one-third of the variance in cognitive and language scores at 2 years corrected age (Kline et al., 2019).

Engelhardt et al. have studied folding of the cortex in VPT infants (without major brain injury on conventional MRI) by using cortical cartography methods (cortical surface area/gyrification index). They have shown that both the antenatal growth and the preterm postnatal course disrupts cortical development (insula, superior temporal sulcus, and ventral portions of the pre- and postcentral sulci in both hemispheres) with abnormalities evident at TEA (Engelhardt et al., 2015).

In summary, while these advanced anatomical MRI methods have shown links/correlation with later neurodevelopment, these methods have not yet been tested as prognostic indicators in the clinical domain.

1.3.3 Diffusion MRI

Diffusion MRI (dMRI) characterizes the direction-dependent diffusion of water molecules in the brain and is contingent on the organisation and density of axonal fibres. Diffusion MRI has been used to examine structural connectivity (cf. functional MRI connectivity) and microstructural injury in preterm infants.

In preterm infants, diffusion MRI has revealed significant differences in the microstructure throughout the white matter and altered structural brain networks as early as term equivalent age (Ball et al., 2013, 2010; Barnett et al., 2018; Batalle et al., 2017; Counsell et al., 2006; Dimitrova et al., 2020; Parikh et al., 2020). Data also suggests that, while individual risk factors are associated with altered dMRI characteristics in the white matter, exposure to 'cumulative' risk factors during the preterm period is associated with an increased vulnerability for white matter injury (Barnett et al., 2018).

In a study of preterm infants (without focal abnormality on anatomical MRI), dMRI at TEA was correlated with structural connectivity between the thalamus and the cortex at term, and this mean thalamocortical connectivity across the cortex explained 11% of the variance in cognitive scores (BSID) at 2 years age (Ball et al., 2015).

Using dMRI in older, ex-preterm, infants has also shown impaired structural connectivity and correlations with NDV outcomes. In as study of very preterm infants using dMRI scanning at 7 years of age, it was seen that infants with lower gestational age at birth, infection, or higher neonatal brain abnormality score, had reduced structural connectivity at 7 years and this was predictive of impaired intelligence quotient (Thompson et al., 2016).

1.3.4 Electroencephalography

In addition to MRI, investigators have looked at electroencephalography (EEG) as a potential biomarker of neurodevelopmental outcomes of VPT infants. This stems from the realisation that while WMI is associated with a reduction in cortical complexity and volume (and with neurodevelopmental impairment), that grey matter damage, due to loss of connections rather than cell loss, is also a major factor in long-term disability (Dean et al., 2014).

Compared to other imaging modalities EEG has good temporal resolution and whole-cortex coverage, but poor spatial resolution. To date most systematic reviews and meta-analyses have included mostly studies of amplitude-integrated EEG (aEEG) rather than raw (12-lead) EEG. In a study of VPT using an aEEG scoring system (Burdjalove score) it was seen that the predictive value of the aEEG score for neurodevelopmental outcome at 2 years age (BSID) was low (Burger et al., 2020). Similarly in a prospective cohort study in VPT infants who underwent continuous aEEG during the first 4 days of life, it was seen on univariate analyses that there were some associations between aEEG and cognitive outcomes, but these were no longer significant after adjustment for confounders (Feldmann et al., 2020).

In a meta-analysis by Fogtmann et al. (2017) the prognostic test accuracy of aEEG or conventional EEG early in life in preterm infants was examined with respect to prediction of later neurodevelopmental outcome. All studies included were at high risk of bias and heterogeneity was evident among the studies (heterogeneity in aEEG and EEG variables, neurodevelopmental outcomes, and threshold values). Ultimately investigators recommended that the prognostic value of aEEG and EEG should be used only as a scientific tool at present (Fogtmann et al., 2017).

1.4 FUNCTIONAL MRI

1.4.1 Introduction to functional MRI

In 1990 Ogawa identified the Blood Oxygen Level Dependent (BOLD) signal as a potential signal for functional imaging of the brain, and Kwong and Ogawa produced the first images using BOLD as an endogenous contrast agent in 1992 (Kwong et al., 1992). This BOLD signal is the most used MRI measure of brain function. The BOLD signal relies on the fact that haemoglobin has different magnetic properties when bound to oxygen, and as such it acts as an 'endogenous contrast agent' with good contrast to noise and spatial specificity when measured using T2*-weighted MRI sequences (Logothetis et al., 2001). Specifically, oxy-haemoglobin is diamagnetic, i.e., weakly repulsed from magnetic fields, and deoxy-haemoglobin is paramagnetic, i.e., attracted to externally applied magnetic fields, and so a change in their ratio leads to a susceptibility difference between the blood and its surrounding tissue (Pauling and Coryell, 1936).

As neuronal activity is accompanied by an increase in blood flow to the local blood vessels and by an increased demand for oxygen, an increase in blood flow results in a change in the ratio of oxygenated to deoxygenated haemoglobin which is measured by the blood oxygenation level dependent (BOLD) signal used in functional MRI (fMRI). MR pulse sequences sensitive to T2* show a stronger signal where there is more oxygenated blood. This small signal increase is the BOLD signal that is recorded during an fMRI timecourse (Huettel et al., 2014).

The haemodynamic response function (HRF) to a specific stimulus reflects the changes in blood flow that accompany the timecourse of the BOLD signal change, which is delayed from the onset of neural activity by a few seconds. The signal increases about 2 seconds after neural activity increases then reaches a plateau at 5 to 8 seconds. After the neuronal activity/stimulation stops the signal falls to baseline in 8 to 11 seconds, after briefly dipping below the baseline (a phenomenon known as the undershoot) (Huettel et al., 2014). Interestingly there is both a longer time to peak of the HRF and a decrease in peak amplitude of the HRF in infants relative to adults (Figure 1-1).

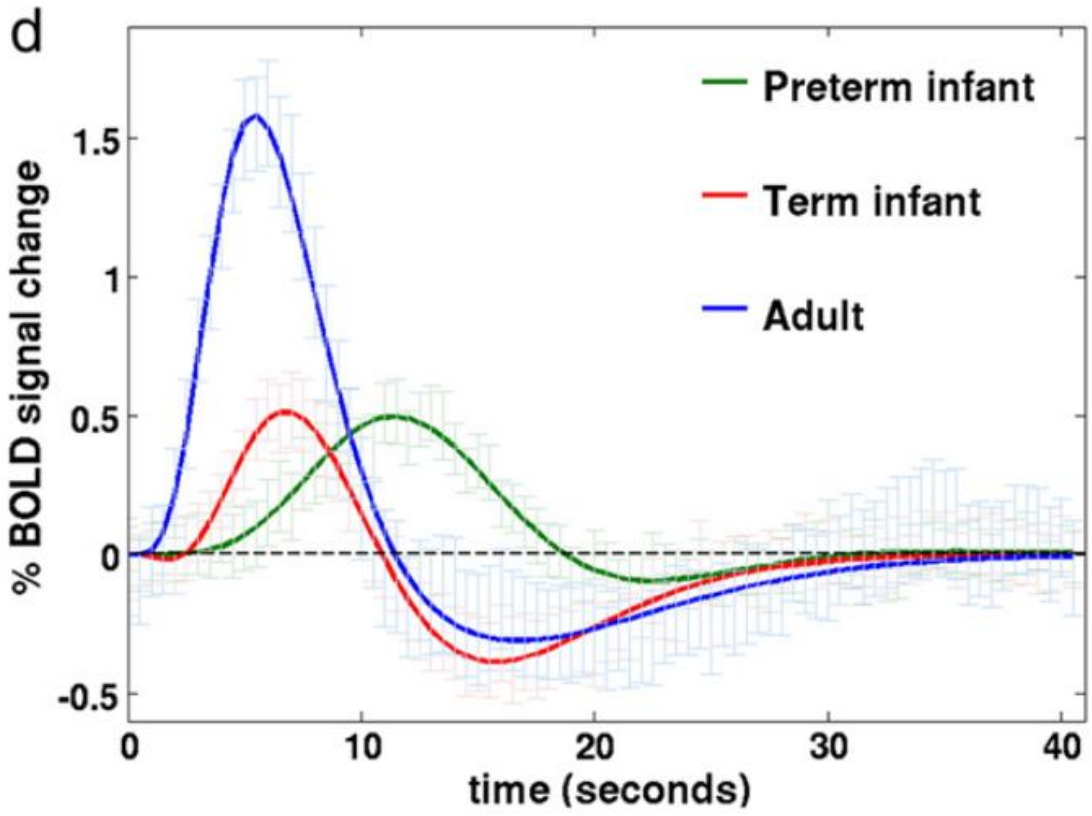

Figure 1-1 Peristimulus timeseries plots.

Arichi, T., Fagiolo, G., Varela, M., Melendez-Calderon, A., Allievi, A., Merchant, N., Tusor, N., Counsell, S.J., Burdet, E., Beckmann, C.F., Edwards, A.D., 2012. Development of BOLD signal hemodynamic responses in the human brain. NeuroImage 63, 663–673. https://doi.org/10.1016/j.neuroimage.2012.06.054. Peristimulus timeseries plots for the (a) adult; (b) term equivalent infant; (c) preterm infant groups. A decrease in the time to peak of the HRF, and an increase in peak amplitude is seen with increasing age.

The HRF is thought to be tightly spatially coupled to electrodynamics which gives the BOLD signal an excellent spatial resolution. Also, as changes in haemodynamics in the brain occur in reaction to neuronal activity, the MRI signal changes in real-time. As such, changes in the voxel intensity over time can suggest where and when the neuronal activity is occurring. By repeatedly measuring BOLD signal over a period of time (i.e. multiple images/volumes), relative increases and decreases of the signal can be interpreted as changes in activity (Logothetis et al., 2001).

In typical task-based fMRI, the BOLD signal is recorded throughout an entire task, and then subdivided at the analysis stage into different conditions, usually "on" (experimental) and "off" (baseline) trials. By revealing the differential

haemodynamic responses associated with each condition, this comparative approach produces results detailing brain regions believed to be implicated in the various mental operations required to complete the task.

In resting state fMRI (rsfMRI), however, the awake participant (adult in this example) is either staring at a crosshair in the scanner or is with eyes shut (i.e. no specific task). Among the benefits of rsfMRI over task-based fMRI is that it can be used even in those individuals who are unable to perform an in-scanner task, due to age (e.g., infants) or clinical status (e.g., who may be unable to produce a motor response).

1.4.2 Functional connectivity MRI

Functional connectivity (FC) is defined as the temporal dependence of neuronal activity patterns of anatomically separated brain regions (Aertsen et al., 1989; Friston et al., 1993).

In a groundbreaking experiment showing how a task activation map and a resting state correlation map showed many spatial similarities , Biswal et al. (1995) were the first to show that intrinsic fluctuations at rest hold information about the inherent functional organization of the brain (Biswal et al., 1995). These intrinsic fluctuations have low frequency (<0.1 Hz) (Biswal et al., 1995) and as they represent brain region activity during rest, they were termed resting-state fMRI (Biswal et al., 1995; Cordes et al., 2001; Lowe et al., 1998).

Functional connectivity is formally defined as any statistical relation between time series (Friston, 2011) and it is typically estimated using a Pearson correlation between the BOLD time series of two brain regions of interest. Pearson's correlation values range from -1 (fully negative) to +1 (fully positive), and 0 indicates no relationship between the two signals.

The two most used approaches in FC MRI analysis included independent component analysis and seed-based analysis. Independent component analysis is a data-driven method that defines resting state networks (RSNs) by subdividing the rs-fMRI sequences into spatial components that have similar

temporal patterns. Seed-based methods define a region-of-interest, or "seed region," and then study how the time series of the BOLD signal in such "seed region" is correlated with the time series of all other voxels in the brain, producing correlation coefficients that define levels of connectivity between the "seed region" and the rest of the brain (Bijsterbosch et al., 2017) (Figure 1-2).

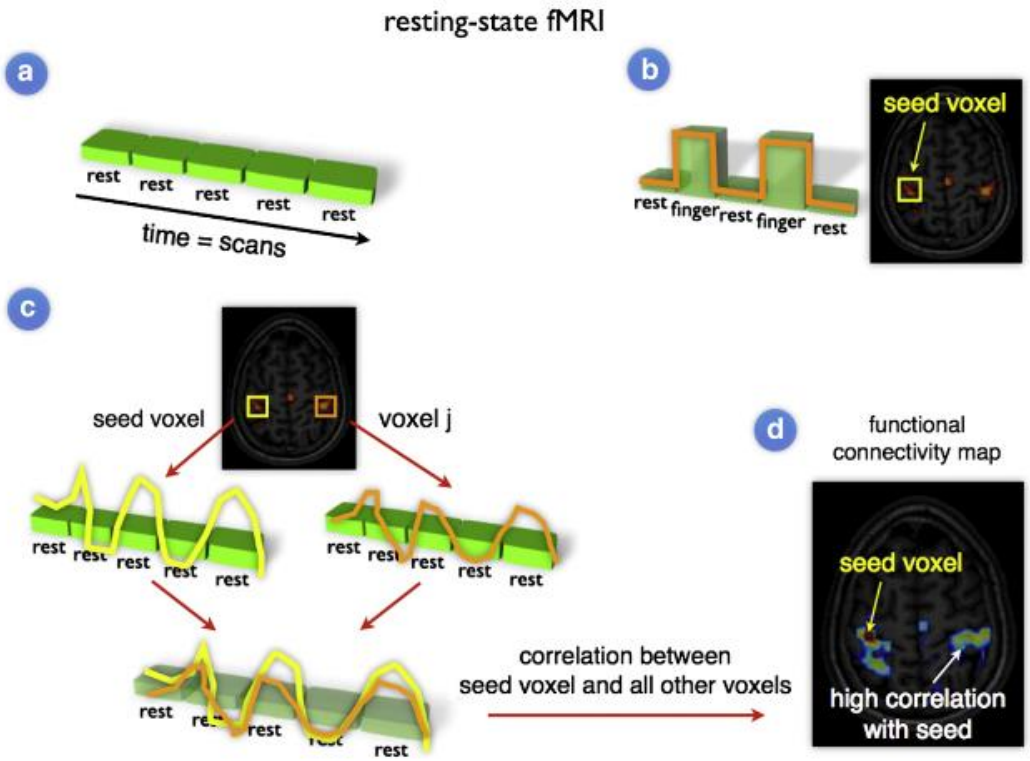

Figure 1-2 Schematic of resting-state fMRI.

(van den Heuvel, M.P., Hulshoff Pol, H.E., 2010. Exploring the brain network: A review on resting-state fMRI functional connectivity. European Neuropsychopharmacology 20, 519–534): Conventional task-dependent fMRI can be used to select a seed region of interest (panel b). To examine the level of functional connectivity between the selected seed voxel i and a second brain region j (for example a region in the contralateral motor cortex), the resting-state time-series of the seed voxel is correlated with the resting-state time-series of region j (panel c). A high correlation between the time-series of voxel i and voxel j is reflecting a high level of functional connectivity between these regions. Furthermore, to map out all functional connections of the selected seed region, the time-series of the seed voxel i can be correlated with the time-series of all other voxels in the brain, resulting in a functional connectivity map that reflects the regions that show a high level of functional connectivity with the selected seed region (panel d).

1.5 FUNCTIONAL CONNECTIVITY MRI IN ADULTS/ADOLESCENTS

Several adult studies FC MRI studies have shown a high level of functional connectivity between the homologous regions in the two hemispheres, and also between regions of other known functional networks, like the primary visual network, auditory network and higher order cognitive networks (Biswal et al., 1997; Buckner et al., 2008; Cordes et al., 2000; De Luca et al., 2006; Greicius et al., 2003; Morgan et al., 2018a; Vertes et al., 2012).

FC MRI has proven valuable for its ability to discriminate individual differences and patient groups. Multivariate machine learning approaches have shown that there is information in FC MRI to classify healthy adults from clinical populations including ADHD (Lake et al., 2019), schizophrenia (Bassett et al., 2012; Liu et al., 2011), Alzheimer's disease (Koch et al., 2012), major depressive disorder (Craddock et al., 2009), and autism (Nielsen et al., 2013). Further, adult FC MRI research has shown how these functional networks change during physiological/pathological development with age (Gao et al., 2015a; Morgan et al., 2018b; Vertes and Bullmore, 2015) and that these changes can be linked with individual behaviour (Finn et al., 2015; Gordon et al., 2017; Gratton et al., 2018; Rosenberg et al., 2016).

Interestingly, FC MRI studies of preterm born adults have also shown differences in FC networks versus controls (White et al., 2014), with differences in FC associated with preterm adult intelligence (Bäuml et al., 2017), preterm adult language (Constable et al., 2013), preterm adult emotional processing (Ho et al., 2015; Johns et al., 2019).

1.6 FUNCTIONAL CONNECTIVITY MRI IN INFANTS

In recent years, a growing literature regarding the infant functional connectome has developed. Precursors of mature functional networks have been observed as early as during the foetal period (Turk et al., 2019). Studies of infant FC MRI at birth have shown infant functional networks appearing more mature in the sensorimotor networks (e.g. somatosensory, motor, visual, and auditory)

compared to the association networks (e.g. default mode, executive control, and attention networks) (Doria et al., 2010; Eyre et al., 2021; Fransson et al., 2007; Gao et al., 2015a; Linke and Cusack, 2015; Smyser et al., 2011, 2010).

Initially, higher-order networks were thought topologically incomplete in neonates but then to show increasing connectivity during infancy (Fransson et al., 2011; Gao et al., 2015b, 2015a). However, recent work has suggested that indeed adult-like functional networks are evident in asleep neonates under specific experimental parameters: network-detection algorithms tuned to long-range connections; using surface-based registration (versus volume-based registration), and when per-subject data quantity increases (Sylvester et al., 2022). Also, in a recent large cohort of term born infants scanned at 37 – 43 weeks post-menstrual age (PMA), an adult-like topology was found in RSNs in the primary sensory, motor, visual, and auditory cortices, while in association RSNs maturation in FC was also found across the age span (Eyre et al., 2021).

Preterm birth can affect the functional connectome. In preterm infants, RSNs have been identified as young as 29 weeks PMA (Doria et al., 2010) and even at 26 weeks PMA (Smyser et al., 2010). It is known that the immature brain is susceptible to injury inherent to both being born early and living in the NICU environment until term corrected age (Brummelte et al., 2012; Ferguson et al., 2012; Smith et al., 2011). Despite no macroscopic injury (conventional MRI or cUS), studies have shown various network-specific differences in resting-state functional MRI (rsfMRI) connectivity between very preterm and term infants when scanned at term equivalent age (Ball et al., 2016; C. D. Smyser et al., 2016b). Further, Eyre et al. found that preterm birth is associated with decreased functional connectivity at term across all defined RSNs in a dose-dependent manner (Eyre et al., 2021).

Neuro-pathologies associated with the preterm neonate (such as post-haemorrhagic or moderate/severe DWMA) have been shown to result in differences in functional connectivity at term equivalent age (Arichi et al., 2014; Duerden et al., 2019; He and Parikh, 2015; Smyser et al., 2013). These disruptions to functional networks in graduates from the NICU have been shown to correlate significantly with motor impairment at 4 and 8 months of age (Linke

et al., 2018), cognitive and motor impairment (Peyton et al., 2020) and behavioural inhibition at age 2 years (Sylvester et al., 2018).

1.7 FUNCTIONAL CONNECTIVITY MRI AS A POTENTIAL BIOMARKER IN INFANTS

Resting state fMRI during the pre-verbal (infant), task-competent (infant/toddler) periods has the potential to act as a marker of later neurodevelopment (Cusack et al., 2018; Linke et al., 2018). An earlier ability to identify an individual with an atypical developmental trajectory might facilitate more accurate diagnoses and prognoses of developmental disorders and lead to earlier and individualized treatment (Ciarrusta et al., 2020; Emerson et al., 2017; Horien et al., 2022).

Functional connectivity analyses increase the features under study by a power of two—from univariate activity in N brain regions to interactions between 'NxN pairs' of brain regions. This vastly expands the space for both within- and between-subject variation (Finn et al., 2017). It is this principal that drives the idea of a distinct/unique FC RSN pattern that is unique to the individual (termed the 'connectome').

Functional connectome fingerprinting using fMRI was first reported by Miranda-Dominguez et al. where they showed how a model-based approach toward characterizing rsfMRI was capable of identifying a so-called ''connectotype'', or functional fingerprint in individual adult participants. Using a simple linear model (that proposed that the activity of a given brain region can be described by the weighted sum of its functional neighbouring regions), they showed that the resulting coefficients corresponded to a personalized model-based connectivity matrix that was capable of predicting the timeseries of each subject (Miranda-Dominguez et al., 2014). They further showed that the model's ability to discriminate an individual was driven by unique connections in higher order control regions in frontal and parietal cortices (Miranda-Dominguez et al., 2014). In 2015 Finn et al. devised their method of functional fingerprint identification and showed that fingerprint connectivity profiles predicted levels of fluid intelligence in adults (Finn et al., 2015). Importantly, these individual

differences in brain connectivity have been shown to be predictive of individual differences in behaviour in adults (Finn et al., 2015; Ousdal et al., 2020).

Kaufman et al. averaged fingerprint identification accuracy across various tasks and defined this as '*connectome distinctiveness'*, as it resembled how well an individual's connectome discriminates that person from the rest of the cohort. They showed how connectome distinctiveness increased with age with the most significant increase coinciding with puberty (slopes peaking at 14.5 ± 1.8 years) (Kaufmann et al., 2017). These researchers also demonstrated how a delay in this differentiation period is associated with mental health problems, with weaker connectome distinctiveness reflecting higher level of symptom burden (Kaufmann et al., 2017).

Since this early work individual functional connectomes have been shown to be predictive of age in older children and adults (Nielsen et al., 2019), cognitive ability in adults (Finn et al., 2015; Rosenberg et al., 2016; Sripada et al., 2020; Yamashita et al., 2018) and risk of autism in infants/children (Emerson et al., 2017) and autism/ADHD scores in adults (Lake et al., 2019). It is this ability to map individual brains to individual behaviours that is crucial to developing neuroimaging based biomarkers (Finn et al., 2017).

Recently, a number of groups have used fingerprinting to test whether stable individual differences in the functional connectome are present in infants (infants less than 1 year of age) (Ciarrusta et al., 2021; Dufford et al., 2021a; Hu et al., 2021a; Q. Wang et al., 2021; Y. Wang et al., 2021). To date, these results are quite disparate and reasons for this are analysed and discussed in this thesis.

Another research method taking advantage of this unique functional connectome is the investigation of 'brain age'. Using the functional connectome and mathematical models, brain age studies examine the difference between the predicted versus observed chronological age of an individual, assessing which RSNs are driving any difference, and whether a difference may be related to an individual's behaviours/development. Through this idea of predicting brain age using rsfMRI, is hoped to allow identification of functional connectivity

architecture during brain development, and as such the potential to find biomarkers of typical and atypical neurodevelopment.

Brain age analyses have been studied in adult groups (Meier et al., 2012) and in adolescent/younger adult groups (Dosenbach et al., 2010). Only a few studies have used functional connectivity brain age analyses in children including toddlers (Kardan et al., 2022) and infants (aged 6 – 12 months) (Pruett et al., 2015). These early studies have had some success and results from these early studies are discussed in this thesis.

1.8 BRAIN STATE IN INFANT FUNCTIONAL CONNECTIVITY

Until recently, most infant fMRI studies have included infants asleep (Figure 1-3). It has been felt that the ability to study infants who are awake is typically precluded by patient motion during acquisition, with reports of neonates studied while awake particularly limited (Hendrix and Thomason, 2022). However, it is hypothesised that brain state (asleep versus awake) might impact the functional connectome and its potential characteristic as a neuroimaging biomarker.

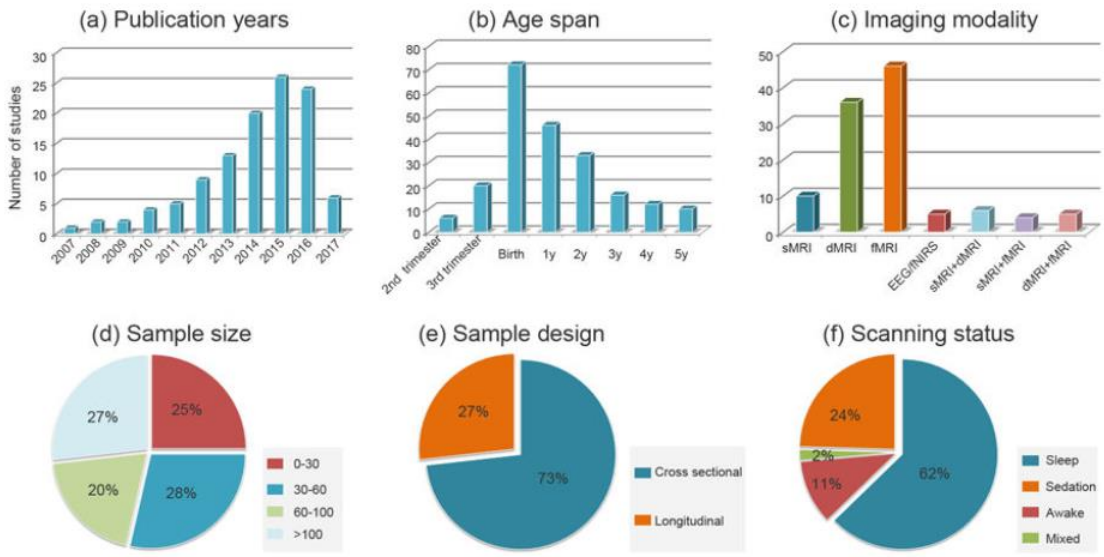

Figure 1-3 Research summary of developmental connectomics from infancy to early childhood.

(*Cao, M., Huang, H., He, Y., 2017. Developmental Connectomics from Infancy through Early Childhood. Trends Neurosci 40, 494–506. https://doi.org/10.1016/j.tins.2017.06.003*): The publications are

summarized and plotted as distribution histograms according to their publication years (a), age span (b), imaging modality (c) as well as pie charts regarding sample size (d), sample design (e), and scanning status (f). sMRI, structural MRI; dMRI, diffusion MRI; fMRI, functional MRI; EEG, electroencephalography; fNIRS, functional near-infrared spectroscopy

Indeed, in the very first awake infant fMRI study (Dehaene-Lambertz, 2002) brain activity evoked by speech was assessed in a small group of awake and asleep 3 month old infants. This study showed that listening to speech activates a large subset of the temporal lobe, with a significant left-hemispheric dominance in both awake and asleep infants. However, additional activation in right prefrontal cortex was seen only in 'awake' infants (Dehaene-Lambertz, 2002).

In 2004 a research group devised a technique known as 'inter-subject functional connectivity (ISFC)' analysis in order to detect similar spatiotemporal activity patterns in adults experiencing the same stimulus (movie) (i.e. stimulus driven synchronisation of brain responses across people) (Hasson et al., 2004). Adopting this ISFC method, recent fingerprinting studies (using rest and movie conditions) have shown that, despite the fact that a shared stimulus would be presumed to decrease between-subject variability (less unique), in fact individual differences in connectome (both activity and functional connectivity) persisted above the shared response (Finn et al., 2020; Vanderwal et al., 2017; Wang et al., 2017). In addition, one study has shown that data collected during movie watching in a cohort of adults (Human Connectome Project dataset) improved functional connectivity-based behaviour prediction (cognition and emotion scores) compared to data from the same adults collected at rest (Finn and Bandettini, 2021). These findings suggest that movie watching may fall into the "spotlight" category of conditions/states making them desirable for individual differences research (Finn et al., 2017).

Applying movie watching to infant FC MRI paradigms may not only increase individual differences (movies versus asleep brain state) in the connectome, but may also lend itself to improved compliance in the scanner (Vanderwal et al., 2015). However, to date no literature exists comparing awake (movies) and asleep state functional connectivity in infants in the same session. It is unknown whether awake infant state (movie watching) also enhances individual

variability in connections, and perhaps more precise relationships with behaviours (i.e. potential to act as a neuroimaging biomarker).

1.9 AIMS AND OBJECTIVES OF THIS THESIS

As an infant's first year of life is rich in brain growth and development, this period has the potential for functional fingerprinting to act as a biomarker of brain development. While infant fMRI fingerprinting is a relatively new area of research already various research groups have published mixed/conflicting results. This thesis aimed to investigate some confounding variables that impact infant functional fingerprinting success. It was hoped that lessons learned would inform future infant fingerprinting studies.

In this thesis it was decided to prioritise the awake (movie watching) state, with infants viewing of naturalistic movie clips and picture stimuli. Awake infant fMRI is challenging, and this study aimed to investigate what factors lead to successful data collection and a positive experience for the infant participant, parents and researchers.

One obvious fact in MRI functional connectivity neuroimaging research is that comparing asleep infant data to awake child/adult data is not a pure comparison due the difference in brain state. This thesis aimed to assess whether the functional connectivity (connectome) is impacted by state (asleep/awake), and whether the strength and pattern of functional networks/edges would differ between infant states. It was hypothesised that due to the visual stimulus, that the awake state would contain additional/evoked connectivity. How this additional/evoked connectivity compares to previous (traditional) asleep connectivity was to be assessed.

It was felt that differences in functional connectomes between states may be subtle and as such it was decided to explore the use of simple machine learning models as a method of further analysis of infant connectomes. Using these machine learning models it was hoped that there may be a difference in classification/prediction of dependent variables (birth gestation and brain/scan age) between data from asleep versus awake states, highlighting any predictive connectivity features/edges that lend towards greater success.

CHAPTER 2 FUNCTIONAL CONNECTOME FINGERPRINTING IN INFANTS – IMPORTANT CONFOUNDS

2.1 ABSTRACT

Individuals differ in their functional connectome, which can be demonstrated using a "fingerprinting" analysis in which the connectome from an individual in one dataset is used to identify the same person from an independent dataset. Recently, the origin of these fingerprints has been studied by examining if they are present in infants. The results have varied considerably, with identification rates from 10-90%. When fingerprinting has been performed by splitting a single imaging session into two split-sessions (within session), identification rates were higher than when two full-sessions (between sessions) were compared. This study examined whether a methodological difference could account for this variation. It was hypothesized that the infant's exact head position in the head coil may affect the measured connectome, due to the gradual inhomogeneity of signal-to-noise in phased-array coils and the breadth of possible positions for a small infant head in a head coil. This study examined the impact of this using resting state functional MRI data from the Developing Human Connectome Project second release. Using functional timeseries, fingerprinting identification was high (84-91%) within a session while between sessions it was low (7%).Using N=416 infants' head positions, a map of the average signal-to-noise across the physical volume of the head coil was calculated and was used (independent group of 44 infants with two scan sessions) to demonstrate a significant relationship between head position in the head coil and functional connectivity. Using only the head positions (signal-to-noise values extrapolated from the group average map) of the independent group of 44 infants, high identification success was achieved across split-sessions (within session) but not full-sessions (between sessions). Using a model examining factors influencing the stability of the functional connectome, head position was seen as the strongest of the explanatory variables. We conclude within-session fingerprinting is affected by head position and future infant functional fingerprint analyses must use a different strategy or account for this impact.

2.2 PUBLICATION DETAILS

This chapter was published previously as follows:

King, Graham[1,2], Truzzi, Anna[1], Cusack, Rhodri[1], 2023. *The confound of head position in within-session connectome fingerprinting in infants*. NeuroImage 265, 119808. https://doi.org/10.1016/j.neuroimage.2022.119808

[1] Trinity College Institute of Neuroscience and School of Psychology, Rm 3.22 Lloyd Building, Trinity College Dublin, Dublin 2, Ireland
[2] Neonatology Department, The Rotunda Hospital, Parnell Square, Dublin 1, Ireland

Contributions:

Graham King: Conceptualization, Methodology, Formal analysis, Investigation, Visualization, Writing – original draft, Writing – review & editing.
Anna Truzzi: Formal analysis, Writing – review & editing.
Rhodri Cusack: Conceptualization, Methodology, Supervision, Funding acquisition, Writing – review & editing.

2.3 INTRODUCTION

In the Human Connectome Project a large cohort of adults was scanned twice, and the functional connectivity MRI pattern (functional connectome) from a person in the first scan could be used to find that person among the connectomes from the second scans with high accuracy – a procedure that has been dubbed "fingerprinting" (Finn et al., 2015). Fingerprinting shows that a significant proportion of individual variance in functional connectivity is trait-like, or intrinsic to the participant and constant across time, and only weakly impacted by the modulations in brain state that occur across sessions (Finn et al., 2015; Miranda-Dominguez et al., 2014). Importantly, these individual differences in brain connectivity have been shown to be predictive of individual differences in behavior in adults (Finn et al., 2015; Ousdal et al., 2020). This suggests that fingerprinting captures a functionally important component of the connectome.

Recently, a number of groups have used fingerprinting to test whether stable individual differences in the functional connectome are present in infants (infants less than 1 year of age) (Ciarrusta et al., 2021; Dufford et al., 2021a; Hu et al., 2021a; Q. Wang et al., 2021; Y. Wang et al., 2021). The results are quite disparate. A cohort of 31 asleep preterm infants scanned in two rsfMRI sessions separated by a few weeks had an identification rate of just 3/31 (10%) (Ciarrusta et al., 2021). In another cohort of 30-40 term infants scanned at 1 month and 9 months the identification rate was 50-65% (Dufford et al., 2021a). A rsfMRI study of 239 asleep infants (aged 39 – 59 weeks PMA) reported moderate-to-good reliability (intraclass correlation 0.40 – 0.78) (Y. Wang et al., 2021). A recent study of 40 healthy term infants scanned asleep at 1 week of age, found a connectome identification rate of 100%, leading the authors to report that the connectome fingerprint is already present in neonates (Q. Wang et al., 2021).

It is believed that a methodological difference may be largely responsible for the disparity of these results, namely whether fingerprinting is calculated by comparing two different scanning sessions or is derived from within a scanning

session. A straightforward way to conduct fingerprinting within a session, for example, is to compare the connectome derived from the first half of a rsfMRI session with the connectome from the second half of the same session (Q. Wang et al., 2021). Supporting the importance of this methodological difference, in a study using both methods, the reported across-session identification was much lower (13-20%) than within-session identification (50-65%) (Dufford et al., 2021a).

Two explanations were considered for why across-session identification was lower than within-session identification:

One explanation is that the connectome may be unstable in the infant brain. The extent to which the functional connectome is reproducible across time at the participant level (i.e., "stable") is an area of much interest in recent years. It has been shown to be stable across 'days to weeks' in adults (Finn et al., 2017, 2015; Horien et al., 2019; Kaufmann et al., 2018; Miranda-Dominguez et al., 2014; Vanderwal et al., 2017) with identification accuracies up to approximately 90%. Further, the functional connectome has been seen to be stable across 'years' in children/youths and adults (Jalbrzikowski et al., 2020; Miranda-Dominguez et al., 2018). However, it might be that in the highly plastic and rapidly changing infant brain, connectomes are unstable within an individual infant. Across the 8-month gap between the two scans in the Yale group study (Dufford et al., 2021a), there are large changes in functional brain organization. Synaptic connections change rapidly through the first year (Huttenlocher and de Courten, 1987). Myelination commences at approximately 20 weeks PMA and rapidly progresses over the first 2 years of infant life (Barkovich, 2005); and neurovascular changes in infants occur over a matter of days, which will affect the functional MRI (fMRI) signal (Kozberg and Hillman, 2016). The instability of the infant connectome may lead to lower across-session than within-session fingerprint identification rates.

In contrast to the idea that the infant connectome is unstable is a recent publication from the Baby Connectome Project (Hu et al., 2021a) which has reported higher identification rates suggesting that infant connectomes are unique and stable over months. In this study 104 term born infants were scanned at least twice at different sessions (between ages 16 – 874 days)

resulting in 806 longitudinal rsfMRI scans. The study used a fine-grained infant-specific mid-cortical functional parcellation map with 602 cortical regions-of-interest (ROIs) (higher parcellation is known to improve connectome distinctiveness). Importantly this study used feature selection-based identification by estimating the differential capability of an edge by its standard deviation (SD) across subjects. The peak threshold value for SD was found to be 0.95 – 0.98 for optimum identification rate and using this optimum threshold the correct identification rate was approximately 66% across the group (in contrast to 47% without feature selection) (Hu et al., 2021a).

A second explanation for why across-session identification is lower than within-session identification is that within-session fingerprinting may be affected by an artifact of the acquisition process, the head position in the MRI head coil. Head coils with many receiving coils are used for fMRI to provide high signal-to-noise, but these are gradually inhomogeneous across the volume of the head coil, with the signal closest to the receiver elements a factor of 2 – 3 times higher than in the center of the coil (Ghotra et al., 2021; Hughes et al., 2017). Despite using the same head coil, different infants will have different head positions due variable initial placement of the head, followed by idiosyncratic application of the head cushions on each side of the infant's head. As a result, head position will be more similar within a session compared to between different sessions. If the signal-to-noise field was completely homogenous, or completely heterogenous, head position would not lead to signal-to-noise ratio (SNR) differences. However, as the signal-to-noise field has a gradual inhomogeneity with smooth changes then head position may lead to substantial modulations in SNR. In this case a small amount of head position change (common within session, i.e. across split-session analyses) will lead to only small changes in SNR, but larger differences in head position (common between sessions, i.e. across full-session analyses) will lead to larger differences in SNR (and resulting functional connectivity pattern). As a result, the similarity of the functional connectome may be more similar during split-session analyses due to this similarity of head position (SNR artifact). Put in another way, within session fingerprinting may be decoding head position in the MRI scanner, rather than, or in addition to, capturing individual differences in the brain connectivity.

2.3.1 Aims and objectives

The aim of this study was to investigate factors leading to increased infant functional fingerprinting ability when comparing within-session analysis to across-session analysis.

To achieve this aim the following objectives were tasked:

- To calculate functional connectivity using fMRI data from a large cohort of infant participants
- To compare functional connectome identification (fingerprinting) ability from within-session versus across-session analyses
- To determine whether infant head position in the head coil has an impact on the fingerprinting ability
- To investigate other confounders/variables that likely also impact fingerprinting ability
- To discuss important learning/decisions for future infant fingerprinting studies.

2.4 METHODS

2.4.1 Cohort and pre-processing details

Open data from the Developing Human Connectome Project (dHCP) second release (http://www.developingconnectome.org/data-release/second-data-release/) was used. Infants were recruited and imaged at the Evelina Newborn Imaging Centre, St Thomas' Hospital, London, United Kingdom. Minimal accompanying metadata was issued with the dHCP Data Release 2.0.

Rs-fMRI data had been obtained using multiband x9 acceleration echo-planar imaging (TE/TR: 38/392 ms) providing 2300 volumes with an isotropic resolution of 2.15 mm. fMRI data was pre-processed as per the dHCP Data Organization (http://www.developingconnectome.org/data-release/second-data-release/release-notes/) and as stipulated in the dHCP publication (Fitzgibbon et al., 2020).

The main steps of the pre-processing pipeline included (Fitzgibbon et al., 2020):

- Estimation of the susceptibility distortion field
- Registration of blood oxygen level dependent (BOLD) images with native T2 space and the neonatal atlas space
- Susceptibility and intra- and inter-volume motion correction (slice-to-volume motion correction, dynamic susceptibility distortion correction, and estimation of motion nuisance regressors) (Andersson et al., 2017)
- FSL TOPUP (Andersson et al., 2003) was used to estimate the susceptibility-induced off-resonance field (creating a voxel displacement field). Further, FSL EDDY was used to correct for the susceptibility-by-movement distortion by estimating rate-of change of off-resonance fields with respect to subject orientation (Andersson et al., 2001, 2018)
- Denoising: regression of signal artifacts related to head motion, cardiorespiratory fluctuations and multiband acquisition, together with single-subject ICA noise bespoke components identified with the FMRIB's ICA-based Xnoiseifier (FIX) (Salimi-Khorshidi et al., 2014).

Following pre-processing and quality control 512 fMRI sessions were included in the dHCP data release (416 participants with 1 scan, 48 participants with 2 scans). The 416 participants with one scanning session included 34 who were born preterm and 382 who were born term.

The infants with two rsfMRI scanning sessions (n = 48) were born between 25 – 37 weeks post-menstrual age (PMA) (median 31.7 weeks PMA, IQR 5.8 weeks) and scanned first (preterm session) between 29 – 37 weeks PMA (median 34.9 weeks PMA, IQR 2.5 weeks) and again (term session) at term age (median 41 weeks PMA, IQR 2.1 weeks). These infants (n = 48) had a birth weight range between 0.54 kg and 3.06 kg (median 1.7 kg, IQR 0.9 kg), and consisted of 33 males (15 females) and 31 singletons (17 multiples). MRI scans were reviewed for incidental findings by a specialist perinatal neuroradiologist who scored each subject using a radiological score (score range 1 to 5; a score of 3 or greater indicated incidental findings with either possible clinical and/or analysis significance). Of the 48 infants with two rsfMRI sessions, 28 had a radiological score of 3 or greater (17 had a score below 3, and 3 infants did not receive a score).

2.4.2 Registration and Region-of-Interest analysis

A region-of-interest (ROI) analysis was carried out using the Schaefer 400 functional parcellation (Schaefer et al., 2018) in the individual infants' functional spaces [See Appendix]. This functional parcellation has been shown to perform similarly to the Glasser multi-modal parcellation when evaluated using the 'distance-controlled-boundary-coefficient' (a measure that allows for comparison of parcellation with different spatial resolutions)(Zhi et al., 2021). The adult T1 MNI-152 template was used facilitate registration of the Schaefer-400 to the dHCP 40-week infant template (Schuh et al., 2018), following the procedure described in (Cabral et al., 2020). As the infant skull is very close to the cortex it was noted that the adult cortex registered to this and as a result the skull was removed from infant images by taking background tissue, label 4 in the dHCP 40-week atlas (https://gin.g-node.org/BioMedIA/dhcp-volumetric-

atlas-groupwise), thresholding at 1000, inverting the mask, and applying it to the dHCP T1 infant template. It was also noted that registration led to the inferior visual cortex being dragged down, likely due to the small infant cerebellum, and so the cerebellum was masked out in the infant and adult templates. To do this in the adult template a mask of the cerebellar region 95-120 (AAL3 template 62 from https://www.oxcns.org/aal3.html) was created, inverted, and applied to the T1 adult template. The infant cerebellum was masked using tissue type 6 (dHCP 40-week atlas), thresholding by 300, inverting, and applying the mask to the T1 40-week template.

The transformation from the adult T1 MNI-152 template (cerebellum stripped) to the dHCP 40-week infant template (skull and cerebellum stripped) was carried out with ANTS (http://stnava.github.io/ANTs/). This transformation was then applied to the MNI-space Schaefer atlas. The FSL transform (provided by the dHCP release) was used to transform Schaefer-400 from the dHCP 40-week atlas space to the individual infants' functional spaces.

2.4.2.1 Quality Control

Quality control showed that there were artifacts in rsfMRI images from some participants leading to signal loss in some ROIs. For each session, ROIs with a signal intensity less than 3 standard deviations below the mean across ROIs were defined as outliers. ROIs which met this outlier definition across >10% of the sessions were taken as ROI deviants and were removed, leaving 387 ROI (from original 400) for subsequent analysis (ROIs removed included bilateral prefrontal cortex lateroventral areas, limbic-temporal pole areas, and visual centers-extra striatal areas).

A quality control of the FSL transform (used in this analysis to transform Schaefer-400 from the dHCP 40-week atlas space to the individual's functional space) was also conducted. This quality control involved visualizing the overlay of the Schaefer-400 over both the functional brainmask and the mean BOLD image of the timeseries while in the individual functional space. This was done for all 96 sessions (48 participants with both preterm and term sessions from the dHCP Data Release 2.0, 2019). This FSL transform was adjudged to have been ineffective (in at least 1 of the 2 sessions) for 4 out of the 48 participants.

These 4 participants were removed leaving the cohort with 44 participants remaining (88 sessions).

Motion can have a strong effect on rsfMRI, and even sleeping infants occasionally move in the scanner (Cusack et al., 2018). To quantify this, the mean framewise displacement in a session was used (Power et al., 2012).

2.4.3 Connectivity and Connectome Stability calculations

2.4.3.1 First order (across time) analysis

Segments of the functional timeseries were derived from both full sessions (full timeseries, 2300 volumes, 15 mins) or split-sessions (partial timeseries). To create a split-session segment a session was split into two smaller segments by removing 60 seconds (154 volumes) from the middle of a session's timeseries and labelling the two remaining sections as 'split-sessions' (Q. Wang et al., 2021).

Each segment was filtered to the functional connectivity (FC) frequency range (0.1 – 0.01 Hz) using nilearn (https://nilearn.github.io/modules/generated/nilearn.signal.clean.html). For each segment, the functional connectivity of every pair of ROIs was calculated using Pearson correlation (r) between their timeseries to yield the connectome. When a sample's r value is near +1 or -1 its distribution is highly skewed, making it difficult to apply tests of significance for the population's correlation coefficients. To tackle this, often Fisher's r-to-Z transformation is used to yield a z-distribution that is approximately normally distributed (Bijsterbosch et al., 2017). In this study's case, a histogram of Pearson correlation values for all edges (387 x 387) for all 88 segments (44 participants with two runs/segments) was calculated and showed that nearly all r values were between -0.3 and +0.50 (i.e. weak correlations with little skew), and such it was felt that there was no need for Fisher's r-to-Z transformation of the first order correlations in this study.

2.4.3.2 *Second order (across segment) analysis*

For correlation across segments (full or split-sessions) the similarity of the resulting ROI by ROI connectome for each participant's first segment was then compared to each participant's second segment using Spearman correlation (across-segment correlation). Following calculation of functional connectivity (Pearson correlation across the timeseries) it is well recognized that the resulting values may not be normally distributed (Kriegeskorte et al., 2008) and so a second order Pearson correlation would be inappropriate. As a result, Spearman correlation was used to assess the higher order (across full-sessions or across split-sessions) comparison of functional connectivity (ROI based edges). Spearman correlation has been used in other connectivity studies (Ahmadi et al., 2023; Gruskin and Patel, 2022; Mahadevan et al., 2021; Sun et al., 2022) and has been shown to be more powerful in non-linear, skewed data sets (Ahmadi et al., 2023). The within-participant Spearman correlation gives an indication of the stability of the connectome for that participant (a.k.a 'connectome stability').

2.4.3.3 *Connectome stability based identification (fingerprinting)*

The connectome-based identification (ID) method followed that suggested by Finn et al. (Finn et al., 2015). Identification was performed across pairs of segments with the first order connectivity matrix from one segment the 'target' and the other the 'database'. The target and database had to be selected from different timepoints (either across full-session segments, or, across split-session segments). Similarity was defined as the Spearman rank correlation coefficient between the various pairs of target and database matrices. If the target and database pair with the highest similarity originated from the same participant, this was considered a 'match'. The percentage of participants where identification was correctly predicted was calculated for the total number of participants (44 participants). This ability to 'match' (highest similarity with self) is thought to be due to a connectome 'fingerprint' whose stability allows correct identification (fingerprinting).

2.4.4 Using Signal-to-Noise to examine the Impact of Head Position

Traditionally the signal-to-noise ratio (SNR) is calculated from the functional timeseries of a session. Of note, it is recognized that ICA denoising (dHCP pre-processing pipeline) artificially inflates the SNR of the functional timeseries shipped with this Data Release 2.0 (Fitzgibbon et al., 2020). Despite this fact, this study used the minimally pre-processed data to determine both the real SNR and the SNR resulting from head position alone (see explanations of both of these below).

2.4.4.1 Estimation of Signal-to-Noise using functional timeseries

SNR was calculated as the mean BOLD signal divided by the detrended standard deviation (SD) (Friedman and Glover, 2006) for the timeseries at each voxel in native space. Detrending was carried out using nilearn (https://nilearn.github.io/dev/modules/generated/nilearn.image.clean_img.html). For segments consisting of full-sessions, the SNR was calculated from the full timeseries. For segments consisting of split-sessions, the SNR was calculated from each of two split timeseries (leaving out 60 secs from the middle of the session as described previously for functional connectivity). The resulting segment-specific SNR map allowed extraction of edge values using the Schaefer 40-week atlas in the individual's space. These SNR values were labelled as 'SNR-individual' (to discern them from 'SNR-group' values, as described below).

2.4.4.2 Estimation of Signal-to-Noise using Head Location

The signal-to-noise ratio (SNR) across the head coil was calculated as follows:

- A group of 416 participants with a single session (34 preterm, 382 term) was used. This group was independent of the 44 participants with two sessions (preterm and term sessions).
- The SNR for each individual was calculated from the fMRI timeseries at each voxel in native space as the mean signal across time divided by the detrended standard deviation (SD) across time (Friedman and Glover, 2006)
- Our goal was to quantify SNR variation across the coil. The internal structure of the brain (e.g., the contrast between grey and white matter) was not present in the SNR maps and instead the well-

established multi-channel receive coil sensitivity profile (Wiggins et al., 2006) was dominant (i.e., lower signal further from the coil). An exception to this was round the edge of the brain, where there was a thin band of lower SNR values, consistent with CSF signal. As a result, the SNR images were masked with a brain mask that had been eroded by a 1 voxel (2.1mm).

- Each individual's fMRI data had an accompanying affine transformation matrix, comprising the translation, rotations, and scaling, to map the voxel coordinates into the frame of reference of the MRI scanner (i.e., mm for x, y and z relative to the isocenter). Using this, the SNR maps from each individual were resliced to a common 1 mm isotropic grid into the scanner's space using the MNI152_T1_1mm atlas shipped with FSL (Fonov et al., 2009).
- These individual maps were averaged across the 416 participants (using a soft mean), giving an estimated SNR for each point in the head coil (termed 'SNR-coil'). Figure 2-1 shows the proportion of the 416 participants used to calculate the soft-mean for each voxel of the SNR-coil map.
- The group average map (SNR-coil) was then used to predict the SNR for each ROI of each individual, from the position and orientation of their head. These predicted SNR values, labelled here as 'SNR-group' values, represent the SNR values resulting from the position, orientation, and shape of the head relative to the head coil.

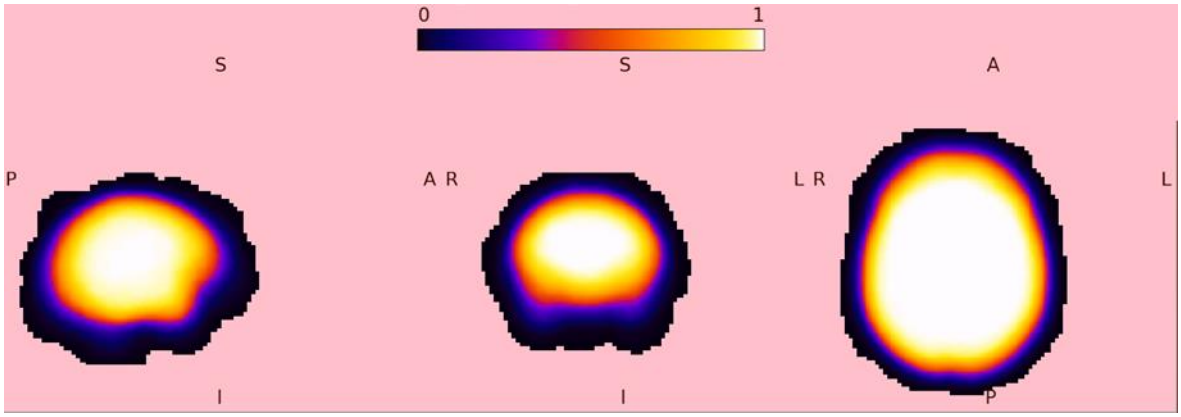

Figure 2-1 Proportion (colorbar: 0 – 1) out of total 416 participants used to calculate the soft-mean for each voxel of the SNR-coil map.

More centrally all participants contribute towards the SNR-coil, while most peripherally only some of the 416 participants contribute.

For full-session segments (across session analysis) SNR-coil was resampled to the individual's native space and the values extracted in the ROIs from the Schaefer 40-week atlas in that individual's space.

For split-session segments (within session analysis) two head positions were chosen (positions at volume 537 and volume 1763 of the functional MRI timeseries for a session). Volume 537 represents the head position in the middle of the first segment, the volume that FSL MCFLIRT would realign to if working on only the first split of the session. Volume 1763 similarly represents the head position in the middle of the second split-session segment. The 6 rigid-body motion parameters (dHCP Data Release, Quality Control data), 3 translations and 3 rotations, represent the head position relative to the initial volume (volume 0). These 6 motion parameters for each head position were translated to FSL – FLIRT format and the resulting matrices were used to re-orient the individual's Schaefer 40-week atlas, using FSL FLIRT, to the two head positions in their individual participant functional space. For the 44 participants with two sessions, SNR-group values were extracted from the SNR-coil map (using FSL fslmeants) for both of the two reoriented Schaefer 40-week atlas head positions for each of 88 sessions (creating 176 SNR-group value matrices for all 176 split-sessions).

2.4.4.3 Fingerprinting – a comparison of SNR-group and SNR-individual

In order to compare their ability to mediate fingerprinting we assessed whether SNR-group or SNR-individual in one segment (full-session/split-session) better predicted functional connectivity in another segment. We implemented this using an ordinary least squares multiple linear regression function (https://www.statsmodels.org/stable/generated/statsmodels.regression.linear_model.OLS.html).

The standardized regression coefficients this yielded were used to assess predictor strength. The regression model took the form:

Equation 1

$$c_{ij}^{(p,2)} = \beta_{ij}^{SNR} s_i^{(p,1)} s_j^{(p,1)} + \beta_{ij}^{FC} c_{ij}^{(p,1)} + a$$

where

$c_{ij}^{(p,e)}$ is the functional connectivity of the edge between regions i and j for participant p and segment number e (session/split)

β_{ij}^{SNR} is the standardized regression coefficient of SNR (SNR-individual/ SNR-group) for the edge

$s_i^{(p,e)}$ is the SNR value (SNR-individual/ SNR-group) of region i for participant p and segment e

β_{ij}^{FC} is the standardized regression coefficient of functional connectivity for this edge

a is a constant

SNR (SNR-group/SNR-individual) and functional connectivity were both standardized to obtain z-scores, so that the beta parameters became comparable and indicative of the variance explained. The focus of fingerprinting is on individual differences, and so a separate regression model was conducted for each edge to model the variance across the 44 participants. Regression was repeated for segments comprising two full sessions and for segments comprising two split-sessions. It was repeated in both directions (the dependent variable (c_{ij}) being from segment 1 or segment 2). SNR-group and SNR-individual were entered consecutively into Equation 1.

It can be seen (Figure 2-2) that for whole-session segments all coefficients are low with both SNR-group and SNR-individual values comparable to the coefficient for FC. For split-session segments both SNR-group and SNR-individual coefficients are higher and approximately 40% of the magnitude of the coefficient for FC. Figure 2-2 shows that for both whole-session and split-session segments, SNR-individual had less predictive power for individual differences than SNR-group (SNR-coil map sampled by individual head position). This suggests that coil sensitivity dominates the predictive power of SNR, and that this is best estimated using group-average data. In this regard, it was decided to use the SNR-group measure for further analyses in this current study.

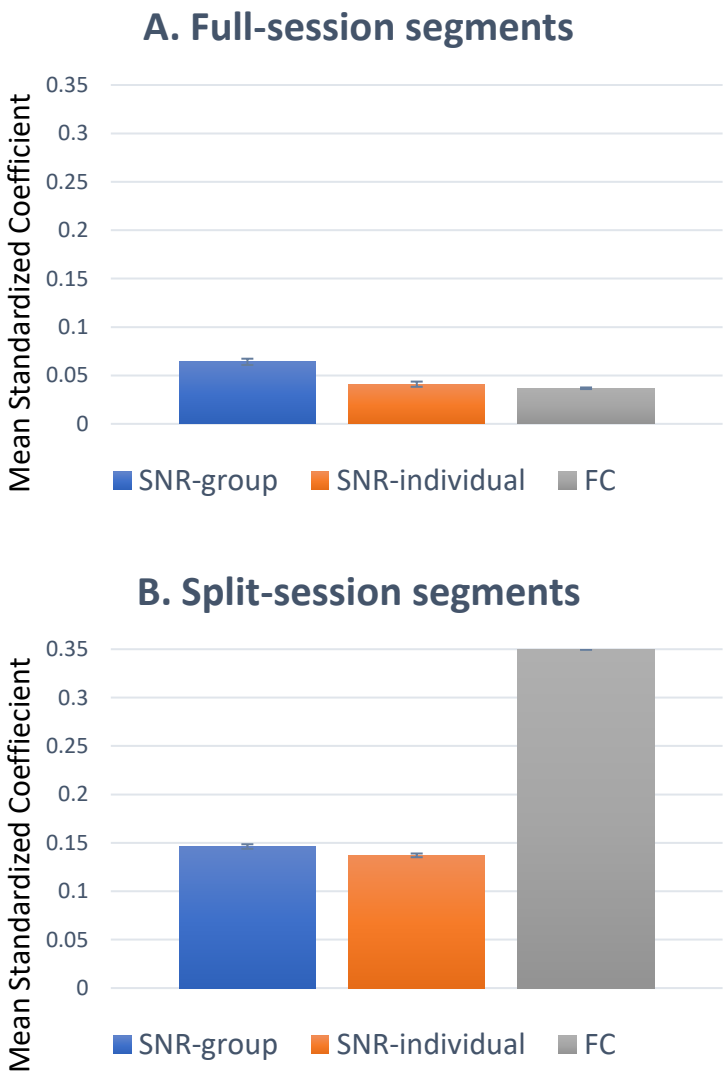

Figure 2-2 Mean standardized coefficients (95% confidence intervals)

a) full-session segments (149,381 edges); b) split-session segments (298,762 edges). SNR-group coefficients are higher than SNR-individual suggesting that coil sensitivity dominates the predictive power of SNR.

2.4.5 Head Position and Functional Connectivity

The relationship between the predicted SNR (SNR-group) values and functional connectivity (FC) was explored using linear regression. For each of the 74,691 edges, a linear model across the 416 participants with one session was fitted (Equation 2). The rational for using a linear regression model 'for each edge' (linear regression across participants) was to examine the relationship between functional connectivity and SNR (SNR-group) due purely to head position. An

edge represents the connection between two ROIs, and while that connection is consistent in terms of anatomical regions, the position of the edge in the head coil space changes with head position. This study examined whether a change in head position in the head coil space (SNR-group value) may or may not result in a change in functional connectivity at that same edge.

Equation 2

$$c_{ij}^{(p)} = \beta_{ij} s_i^{(p)} s_j^{(p)} + a$$

where

p is the participant number

c_{ij} is the functional connectivity of edge connecting regions *i* and *j*

s_i and s_j are the SNR-group of regions *i* and *j*

β_{ij} is the slope of the relationship for this edge

a is a constant

The statsmodels ordinary least squares linear regression function was used (https://www.statsmodels.org/stable/generated/statsmodels.regression.linear_model.OLS.html). Values for functional connectivity and SNR-group were standardized (z-score). Non-zero β values would indicate a consistent relationship between 'SNR due to head position' and functional connectivity. A permutation test was used to test this. As the regression model is not entirely independent of the input values (the same 416 sessions were used to define the SNR-coil) it was decided to cross-validate in an independent group of 44 preterm participants each with two scans (88 sessions).

2.4.6 Head Position and Fingerprinting

Firstly, to examine the similarity of SNR-group values across participants and across segments (full-session or split-session), the Spearman rank correlation coefficient between the various pairs of target and database SNR-group matrices was used (similar to 2.4.3.3 above). Again, if the target and database pair with the highest similarity originated from the same participant, this was considered a 'match' and the percentage of participants where identification was

correctly predicted was calculated (using only these head position derived SNR-group values).

Secondly, to quantitatively compare the impact of head position (SNR artifact) with the functional connectivity signal that drives fingerprinting, both the functional connectivity and SNR (SNR-group) from the first segment were entered as standardized regressors to predict the functional connectivity in the second. This was implemented using an ordinary least squares multiple linear regression function (https://www.statsmodels.org/stable/generated/statsmodels.regression.linear_model.OLS.html).
The standardized regression coefficients this yielded were used to assess predictor strength. The regression model took the form:

Equation 3

$$c_{ij}^{(p,2)} = \beta_{ij}^{SNR} s_i^{(p,1)} s_j^{(p,1)} + \beta_{ij}^{FC} c_{ij}^{(p,1)} + a$$

where

$c_{ij}^{(p,e)}$ is the functional connectivity of the edge between regions i and j for participant p and segment number e (session/split)

β_{ij}^{SNR} is the standardized regression coefficient of SNR-group for the edge

$s_i^{(p,e)}$ is the SNR-group value of region i for participant p and segment e

β_{ij}^{FC} is the standardized regression coefficient of functional connectivity for this edge

a is a constant

SNR-group and functional connectivity were both standardized to obtain z-scores, so that the beta parameters became comparable and indicative of the variance explained. The focus of fingerprinting is on individual differences, and so a separate regression model was conducted for each edge to model the variance across the 44 participants. Regression was repeated for segments comprising two full-sessions and for segments comprising two split-sessions. It was repeated in both directions (the dependent variable (c_{ij}) being from segment 1 or segment 2).

2.4.7 Factors impacting Connectome Stability

2.4.7.1 Individual explanatory variables

For the 44 participants with two sessions, the relationship between connectome stability and one other individual explanatory factor (head size, inter-session interval, and motion respectively) was examined using a scatter plot and Pearson correlation (with confidence interval and p-value).

2.4.7.2 Factors impacting Connectome Stability - Multiple explanatory variables

To assess the degree to which head position (SNR-group) impacts connectome stability (dependent variable) and compare it to other explanatory variables, an ordinary least squares multiple linear regression model was used for full-sessions (Equation 4) and split-sessions (Equation 5) respectively. (https://www.statsmodels.org/stable/generated/statsmodels.regression.linear_model.OLS.html). The 44 participants with two sessions were included in this model. In all instances the explanatory variables were standardized (z-score) prior to inputting into the regression model.

Across full-session segments (Equation 4) the dependent variable was connectome stability across full-sessions (44 values). The five ($i = 5$) explanatory variables considered included: mean SNR-group (mean across the two full-sessions); mean framewise displacement (FWD) (mean across the two sessions); inter-session interval (weeks); age at first session (post-menstrual age); and mean occipital-frontal circumference (OFC) (mean across the two sessions).

Equation 4

$$s^p = \sum_{i=1}^{5} \beta_i x_i^p + a$$

where,

i is the number of explanatory variables

s^p is connectome stability for participant p

x_i^p is explanatory variable number i for participant p

β_i is standardized regression coefficient number i

a is a constant

Across split-session segments (Equation 5) the dependent variable was connectome stability across split-sessions (88 values). The two ($i = 2$) explanatory variables considered were mean SNR-group (mean across the two split-sessions) and mean FWD (mean across the two split-sessions).

Equation 5

$$s^{(p,e)} = \sum_{i=1}^{2} \beta_i x_i^{(p,e)} + a$$

where,

e is session number, where $e \in \{1, 2\}$

i is the number of explanatory variables$s^{(p,e)}$ is connectome stability for participant p session e

$x_i^{(p,e)}$ is explanatory variable number i for participant p session e

β_i is standardized regression coefficient number i

a is a constant

2.4.8 Ethics Statement

Data was obtained from the dHCP Data Release 2 (2019) with permission. In order to protect data participants, these open data have been pseudonymized and subjected to post-collection processing (data processing) at source to remove any data elements that could otherwise be reconstructed and/or processed to reveal facial features of the data participants. Analysis of this data was approved by the Trinity College Dublin School of Psychology Research Ethics Committee (ID: SPREC082021-02).

2.4.9 Data and Code

Data from the Developing Human Connectome Project (dHCP) second release was used (http://www.developingconnectome.org/data-release/second-data-release/). Data were provided by the developing Human Connectome Project, KCL-Imperial-Oxford Consortium funded by the European Research Council under the European Union Seventh Framework Programme (FP/2007-2013) / ERC Grant Agreement no. [319456]. We are grateful to the families who generously supported this trial.

Scatter plots were used to demonstrate correlations along with Pearson correlation and Pearson partial correlation statistics (r-value, 95%CI, and p-value). A p-value <0.05 was considered significant for the correlations shown in scatter plots (labelled with *).

Brain images were displayed using FSLeyes for planar visualization (https://git.fmrib.ox.ac.uk/fsl/fsleyes/fsleyes/). Connectome Workbench was used for cortical surface visualization (https://www.humanconnectome.org/software/connectome-workbench).

Bash scripts and python code used in this chapter/analysis are available at: https://github.com/Grahamgithubking/head_position

2.5 RESULTS

2.5.1 Functional Connectivity and Fingerprinting

Similar to Dufford et al. (2021), it was seen that fingerprint identification was much higher across split-session segments than across full-session segments (Dufford et al., 2021a). Across full-session segments only 3 of 44 (7%) of infants' connectomes ranked highest (connectome correctly identified across sessions), while within a session (across split-session segments) 40/44 (91%) of preterm and 37/44 (84%) of term infants ranked highest (Table 2-1).

Table 2-1 Functional Connectome: Stability Across versus Within sessions

	Across-sessions (88 full-sessions)	**Within-sessions (176 split-sessions)**	
		Preterm (88 splits)	**Term (88 splits)**
Within-participant correlation (mean)	0.17	0.37	0.46
Between-participants (shared) correlation (mean)	0.13	0.07	0.18
Identification Success	3/44 (7%)	40/44 (91%)	37/44 (84%)

Fingerprinting might fail across sessions either because an individual's connectome is unstable, or because relatively, different people have a more similar connectome across sessions. To differentiate these possibilities, within-participant and between-participant connectome similarity was examined, using Spearman (second-order) correlations (Table 2-1). Across full-session segments the within-participant correlation (connectome stability) was low, with the mean of 44 participants ($r = 0.17$) only slightly higher than the mean of the across-participant (shared) correlation ($r = 0.13$). The 44x44 representational similarity matrix (RSM) had no obvious leading diagonal (no significant

correlation within a participant across the two full-sessions) (Figure 2-3). In contrast, Spearman correlations within a participant were much higher when comparing split-session segments (within a session) at both preterm age and term age (Table 2-1 and Figure 2-3). This shows that within-session fingerprinting is more effective because the similarity of the connectomes within a participant are much higher.

Overall, this picture of strong self-identification within a session (across split-session segments) but weak self-identification across sessions (across full-session segments) is consistent with either of the two explanations – it might be because infant connectomes are unstable over weeks, and/or because of various artifacts contributing towards high within-participant correlation during within session analysis.

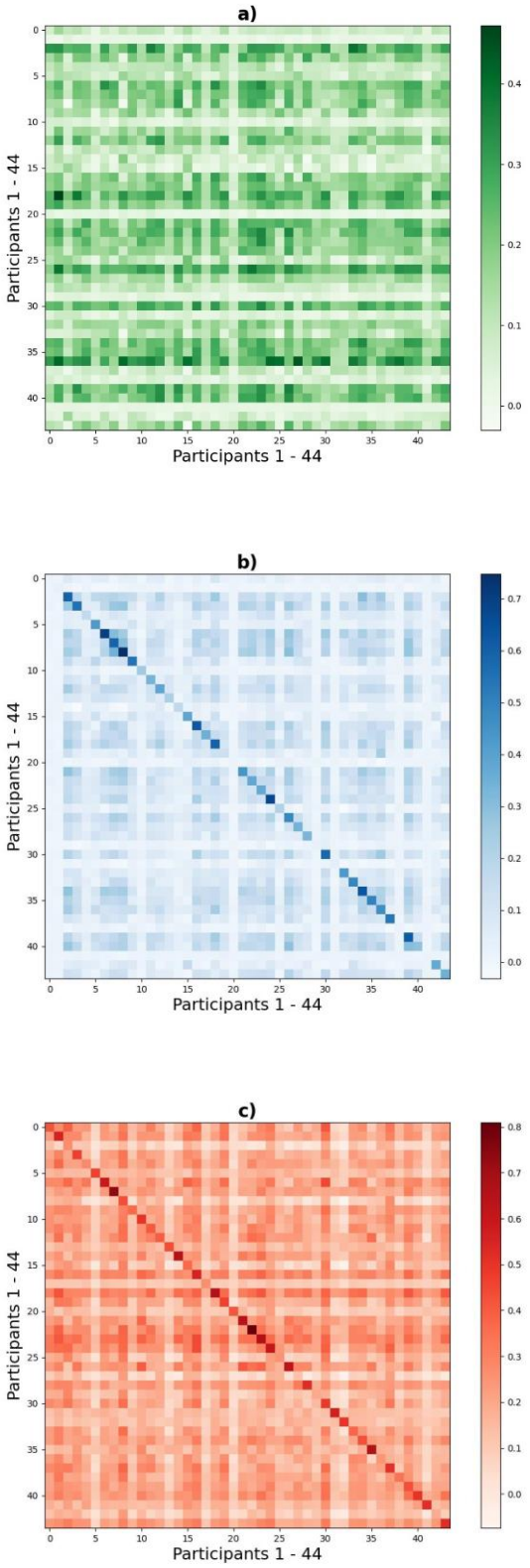

Figure 2-3 Representational Similarity Matrices (44 participants with two sessions).

Second order Spearman correlations of functional connectivity: a) across sessions, b) across split-segments at preterm session, c) across split-segments at term session

2.5.2 Head Position and Functional Connectivity

To demonstrate the variability of head position for the 44 participants, FSL fslstats was used to calculate the centroid ('center of gravity') of the functional brainmask for a session. This gave the centroid in mm coordinates (x, y, z scanner directions). To illustrate the variability in centroid position the centroids (x, y coordinates) for both preterm and term sessions (44 participants) were plotted on a 2-dimensional scatter plot (Figure 2-4). This plot shows a clear distribution of centroids with variability in the posterior - anterior direction (range: -5mm to +29mm) and the left - right direction (range: -14 to +7mm). There was more variability in centroid position in the preterm session compared to the term session.

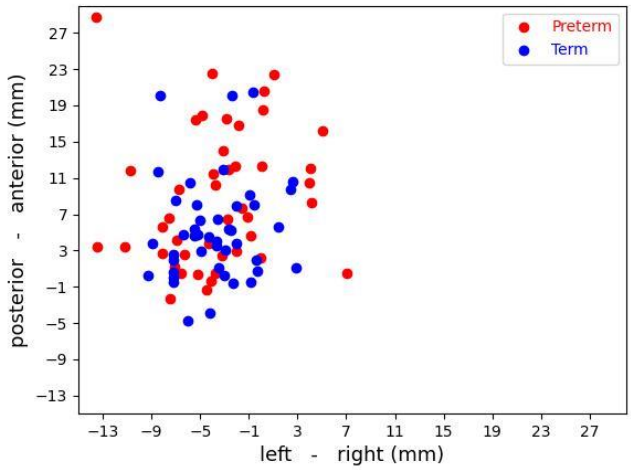

Figure 2-4 Centroids of brainmasks in scanner space for 44 participants (preterm & term sessions).

For a 20mm displacement in either direction, this could result in an approximate 50% decrease in SNR values in the dHCP dedicated neonatal head coil (values derived from data on phantom analysis by Hughes et al. (Hughes et al., 2017)

To test the hypothesis that differences in SNR due to head position affect connectome fingerprinting, an estimate of the SNR across the volume of the coil (SNR-coil) was derived and then used to estimate each individual's SNR based on location of their head (termed 'SNR-group'). This was illustrated for two

participants in the scanner frame of reference (Figure 2-5) and in the brain frame of reference (Figure 2-6).

The scanner frame of reference (Figure 2-5) depicts the individual's Schaefer 40-week atlas resliced into MNI152 reference space and overlayed onto the SNR-coil. Head position and distance from the head coil directly are seen to influence the pattern of SNR across the brain. Using the brain frame of reference (Figure 2-6), the SNR-coil was resliced to individual space and mapped to the mid-cortical thickness surface (T2w) using Connectome Workbench. Based on position in the head coil, it can be seen that the mid-cortical thickness surface has a variable pattern of SNR across the various sessions (preterm and term examples).

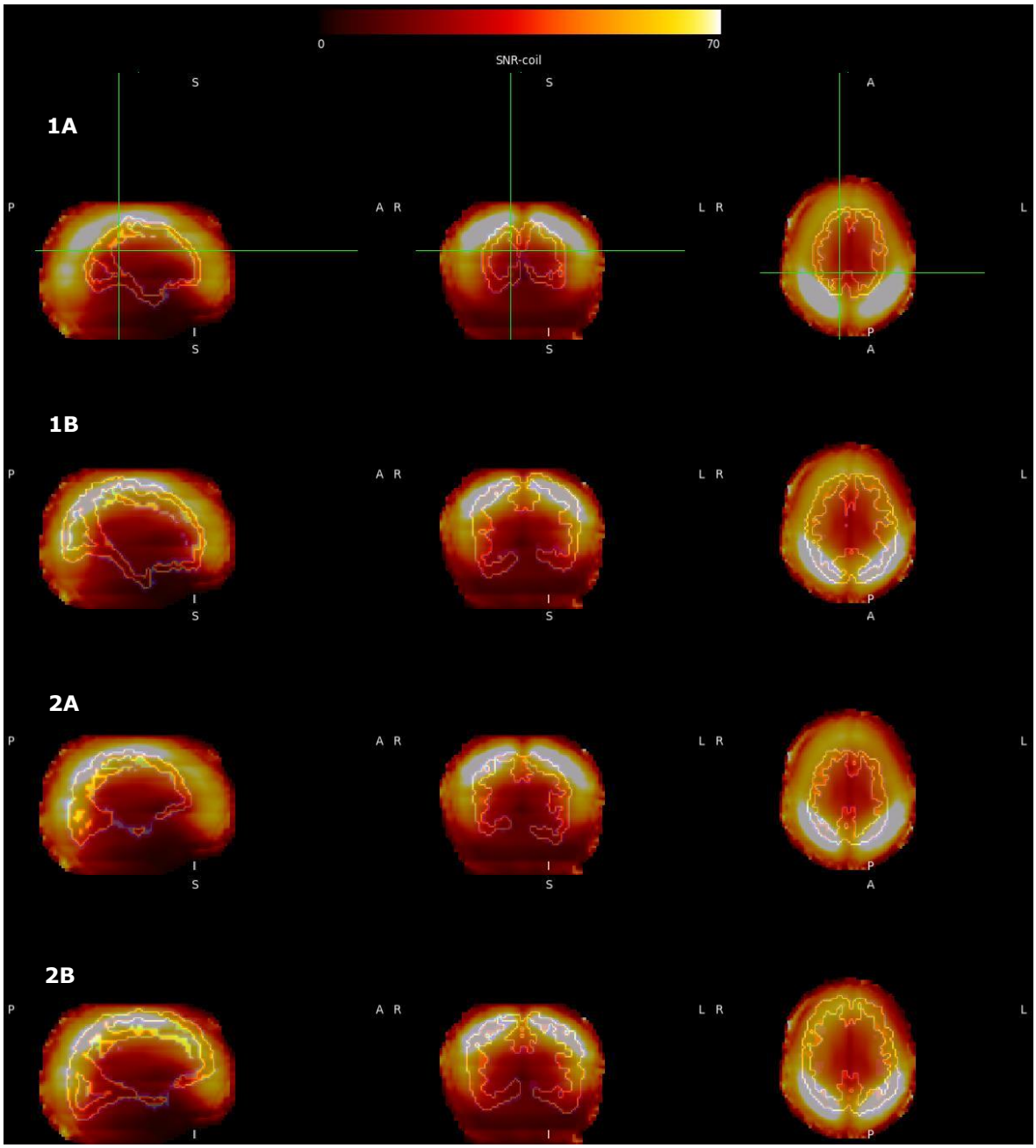

Figure 2-5 Impact of Head Position - *Scanner Frame of Reference*:

Schaefer 40-week atlas resliced from individual space to MNI152 reference and overlayed on SNR-coil. Two example preterm participants with two sessions were chosen: (1A) Participant 1 at 29.9 weeks PMA (1B) Participant 1 at 38.4 weeks PMA. (2A) Participant 2 at 35.8 weeks PMA (2B) Participant 2 at 42.1 weeks PMA.

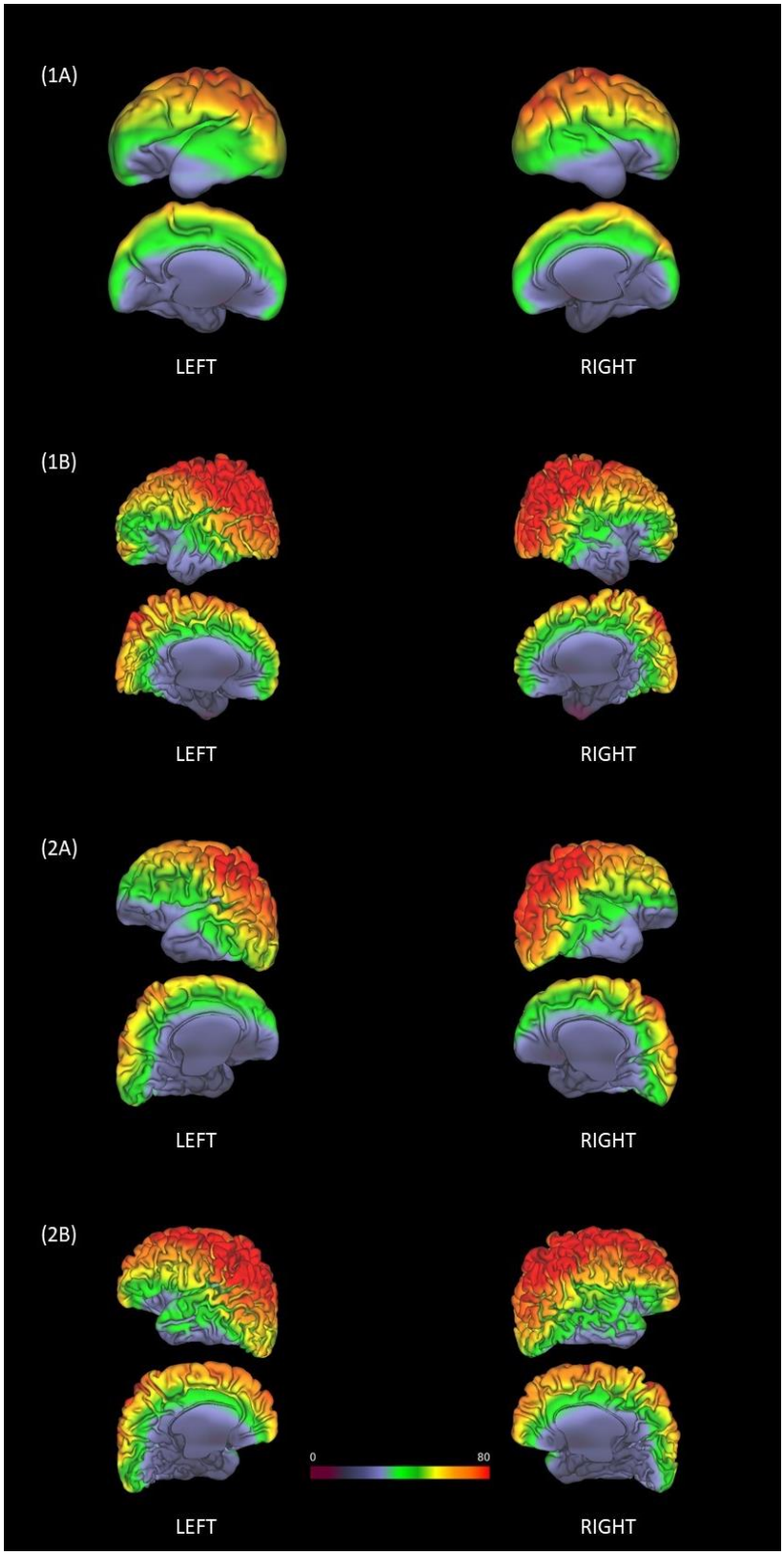

Figure 2-6 Impact of Head Position - *Brain Frame of Reference*:

SNR-coil resliced to individual space and mapped to mid-cortical thickness surfaces (T2w) (Left + Right). Two example preterm participants with two sessions were chosen: (1A) Participant 1 at 29.9 weeks PMA (1B) Participant 1 at 38.4 weeks PMA. (2A) Participant 2 at 35.8 weeks PMA (2B) Participant 2 at 42.1 weeks PMA.

To demonstrate how SNR covaries with FC, a pair of parcels (ROIs) from the Default Mode Network (DMN) were chosen. Within the DMN regions one pair was selected based on having the highest mean functional connectivity across the 88 sessions (Mean r = 0.595). This was the edge between the inferior parietal lobe (IPL) and the dorsal pre-frontal cortex (PFCd) (Schaefer regions 174 and 175) on the left hemisphere (LH). Across the 88 sessions (44 participants with 2 sessions) functional connectivity was plotted against SNR-group values for this edge (Figure 2-7). The relationship showed that there was a positive correlation between FC and SNR (r = 0.3, 95%CI 0.09-0.48, p<0.005).

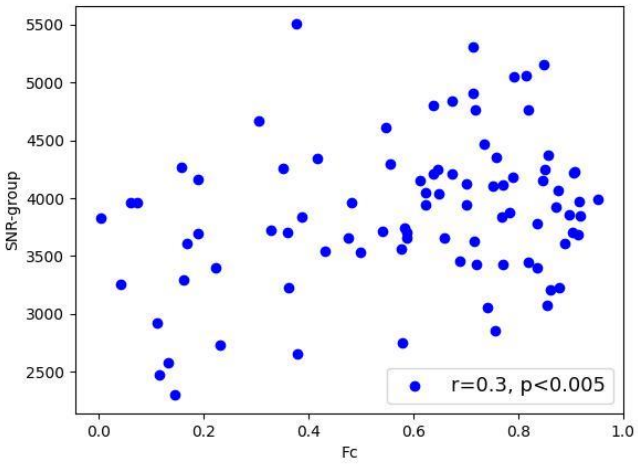

Figure 2-7 SNR-group values covary with FC (Schaefer ROI edge 174-175)

Next, using ordinary least square regression across 416 participants for each edge, the relationship between SNR-group and functional connectivity was examined. For each of the 74,691 edges the β (slope) for the fit was calculated across all 416 participants and a histogram of Beta values was plotted (Figure 2-8). The one-sample t-test showed the β values were significantly different from zero (p<0.0001) indicating a significant relationship between predicted (based on head position) SNR values and functional connectivity.

In this analysis, although a significant relationship was seen between SNR-group values and functional connectivity across the 416 participants, there was a slight possibility of circularity due to the fact that the same data was used to both a)

generate the group average 'SNR-coil', and, b) compare the relationship between SNR-group and functional connectivity values in the same cohort. In light of this, this significant relationship was cross-validated in the independent sample of 44 participants (each with both preterm and term sessions) whose sessions' data were not used in the calculation of SNR-coil. Using Equation 2 for the 88 independent sessions, the relationship between SNR-group and functional connectivity was re-examined. The histogram of 74,691 slopes (β) (Figure 2-9) was seen and the one-sample t-test for the fits of the β for the edges was again significantly different from zero ($p<0.0001$).

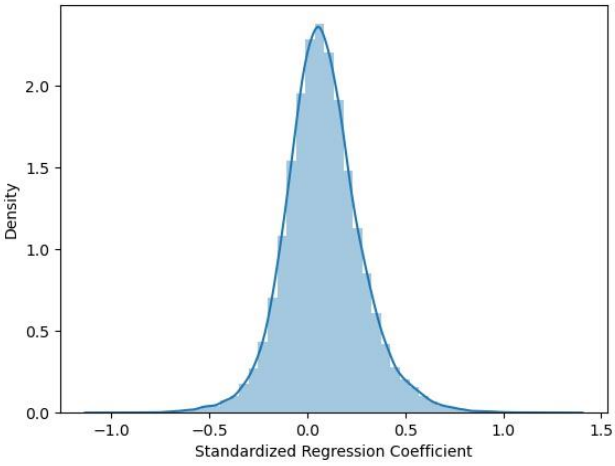

Figure 2-8 Histogram of standardized coefficient values (slopes) of 74,691 edges (linear regression across 416 participants with one session) for the relationship between functional connectivity and SNR due to head position (SNR-group). Mean coefficient = 0.08

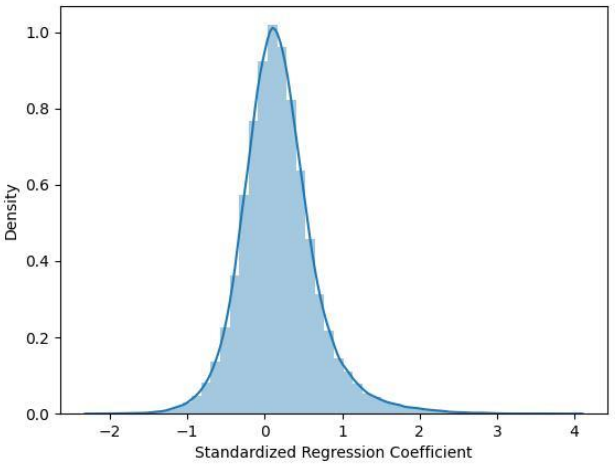

Figure 2-9 Histogram of standardized coefficient values (slopes) of 74,691 edges (linear regression across independent group of 44 participants with both a preterm and term session) for the relationship between functional connectivity and SNR due to head position (SNR-group). Mean coefficient = 0.18

2.5.3 Head Position and Fingerprinting

The similarity of SNR-group values (derived from head position) across participants for each segment (full-session or split-session) were calculated using Spearman rank correlation (Table 2-2). Across sessions, correlation values were comparable within-participant and between-participants (0.90 vs 0.89). As a result, identification was low (9%). Within sessions, correlation values within-participant were higher (0.99) compared to between-participants (0.90-0.92) allowing identification rates of 98-100%.

Table 2-2 Head position (SNR-group values): Stability Across versus Within sessions

	Across-sessions (88 full-sessions)	**Within-sessions (176 split-sessions)**	
		Preterm (88 splits)	**Term (88 splits)**
Within-participant correlation (mean)	0.90	0.99	0.99
Between-participants (shared) correlation (mean)	0.89	0.92	0.90
Identification Success	4/44 (9%)	44/44 (100%)	43/44 (98%)

To quantitatively compare the impact of head position (SNR artifact due to head position) with the functional connectivity signal that drives fingerprinting an ordinary least squares multiple linear regression function was used (Equation 3). Both the functional connectivity and SNR-group from the first segment were

entered as standardized regressors to predict the functional connectivity in the second segment.

Figure 2-10 shows the mean standardized coefficients (95% confidence intervals marked) for SNR-group and functional connectivity. Across full-session segments (149,381 edges), SNR-group is twice as predictive as functional connectivity. This shows that SNR-group is of critical concern. In split-session segments (298,762 edges) the mean standardized coefficients are higher. Functional connectivity is the strongest predictor (mean 0.35, 95%CI 0.349 – 0.351) but SNR-group still accounts for considerable variance (mean 0.15), at approximately 40% that of functional connectivity.

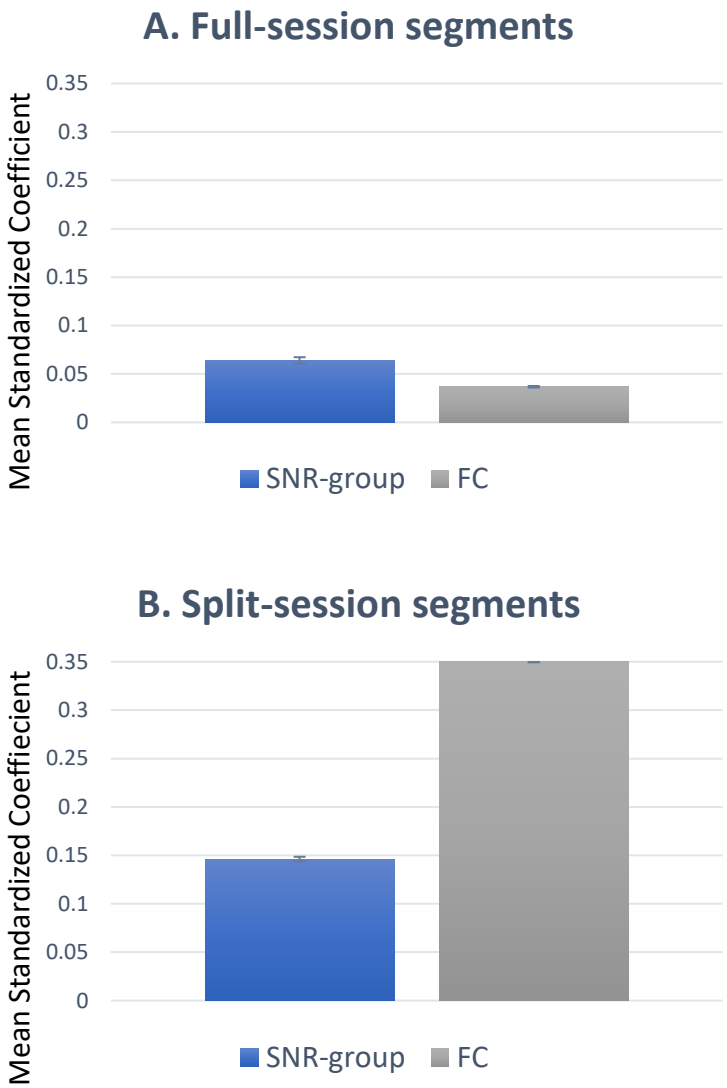

Figure 2-10 Mean standardized coefficients (95% confidence intervals)

a) full-session segments (149,381 edges); b) split-session segments (298,762 edges). Across split-session segments SNR-group accounts for considerable variance.

2.5.4 Factors impacting Connectome Stability

2.5.4.1 Connectome Stability and Head Size

Some participants may have a higher overall SNR, because the critical ROIs in the cortex are closer to the coil – for example because their head is larger. An overall higher SNR might be expected to lead a more accurate assessment of

the connectome, and greater stability (higher Spearman correlation) across scans. Of the 44 participants with two sessions, 39 infants had head size (occipital frontal circumference, OFC) measured at both sessions. OFC was seen to positively correlate with connectome stability (Pearson r = 0.38, 95%CI 0.08 – 0.62, p<0.016) (Figure 2-11).

This correlation was not independent of mean SNR-group across the two sessions (Pearson partial correlation correcting for mean SNR-group was r=0.10, 95%CI -0.23, 0.41, p<0.55). This suggests that a larger head size is associated with increased stability of the connectome and this relationship is likely influenced by a closer approximation of a larger head to the receiver coils (higher SNR).

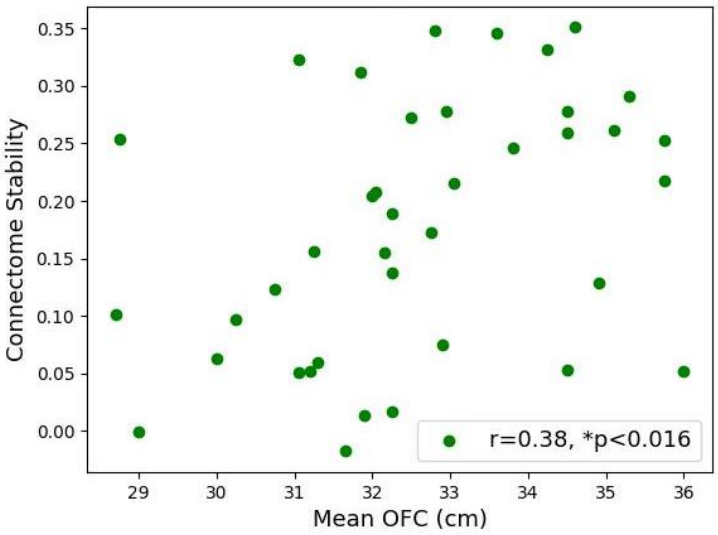

Figure 2-11 Functional connectome stability (second order Spearman correlation) versus mean occipital-frontal circumference across two sessions

2.5.4.2 Connectome Stability and Session Interval

The effect of inter-session interval on connectome stability was examined using a scatter plot (Figure 2-12, a) with Pearson-r = -0.47 (95% CI -0.67, -0.2), p <0.001. This significant negative correlation indicates that there is also a true component of connectome stability that drifts with development. This negative correlation between inter-session interval and connectome stability was maintained even when correcting for the difference in functional connectivity (difference between preterm and term sessions' mean connectivity) (Pearson

partial correlation r -0.45 (95%CI -0.66, -0.17), p<0.003) indicating that although functional connectivity increases with older post-menstrual age (Figure 2-12, b) that the difference in functional connectivity between the preterm and term session is not the explanatory factor for this relationship between inter-session time interval and connectome stability.

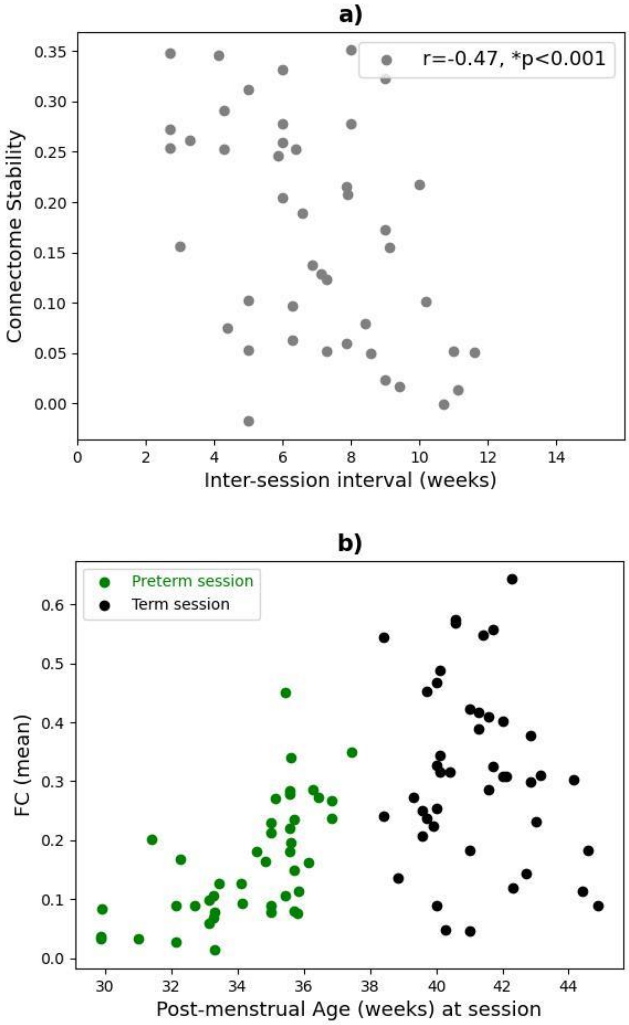

Figure 2-12 Connectome stability and session interval.

a) Functional connectome stability (second order Spearman correlation) versus inter-session interval. Preterm connectome stability is negatively correlated with inter-session interval, b) Mean functional connectivity (mean of first order Pearson correlations for 387 ROIs) at session versus post-menstrual age (PMA) at session.

2.5.4.3 Connectome Stability and Motion

The dHCP cohort was scanned without sedation and so had considerable motion artifact (Fitzgibbon et al., 2020). As a result, the dHCP pre-processing pipeline

does not perform motion censoring in order to minimize the potential loss of participants or timepoints. Instead, the dHCP use a 'less aggressive' ICA-based denoising procedure and authors conclude that this ICA-based denoising procedure is qualitatively similar to using spike regression in periods of time when motion is worst (Fitzgibbon et al., 2020).

Connectome stability (across sessions) in this preterm population was negatively correlated with mean framewise displacement (Pearson r -0.5 (95%CI -0.7, -0.24), p = 0.0005) (Figure 2-13). This negative correlation was independent of mean SNR-group values (mean across two sessions) (Pearson partial correlation: r -0.4 (95%CI -0.62, -0.11) p<0.008) indicating that head motion has a negative effect on connectome stability that is independent of SNR-group (SNR due to head position in the head coil space).

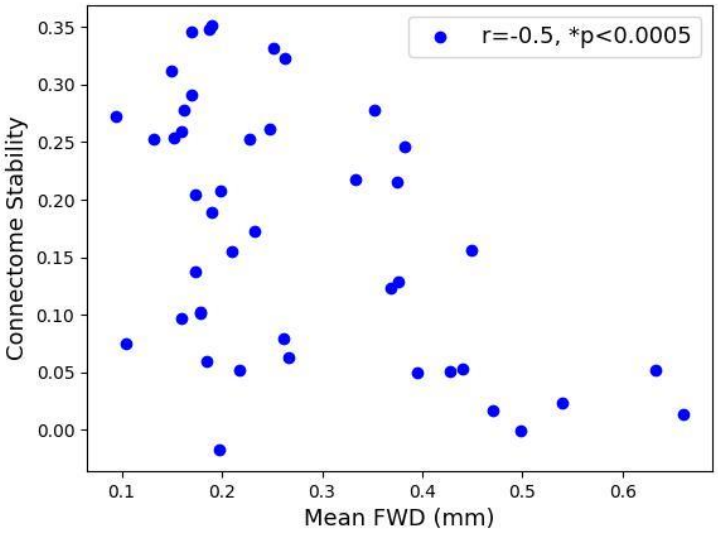

Figure 2-13 Connectome stability versus mean framewise displacement (mean of the FWD across two sessions).

Preterm connectome stability is negatively correlated with head motion.

2.5.4.4 *Multiple explanatory variables*

Using Equation 4 and Equation 5 the relative impact of specific explanatory variables on connectome stability were compared. Figure 2-14 shows that, across full-session segments, motion (FWD) is strongly negatively related (β = -0.38, p<0.013) with connectome stability, while SNR-group (SNR based on an individual's head location within the head coil) is positively related (β = 0.36, p<0.05). Across split-session segments (Figure 2-14), motion (FWD) was much less related (β = -0.11, p<0.27) to connectome stability compared to head location within the head coil (β = 0.38, p<0.000). In summary, it appears that head position has a considerable relationship to connectome stability, and overall was the strongest factor found, particularly in the across split-session analysis.

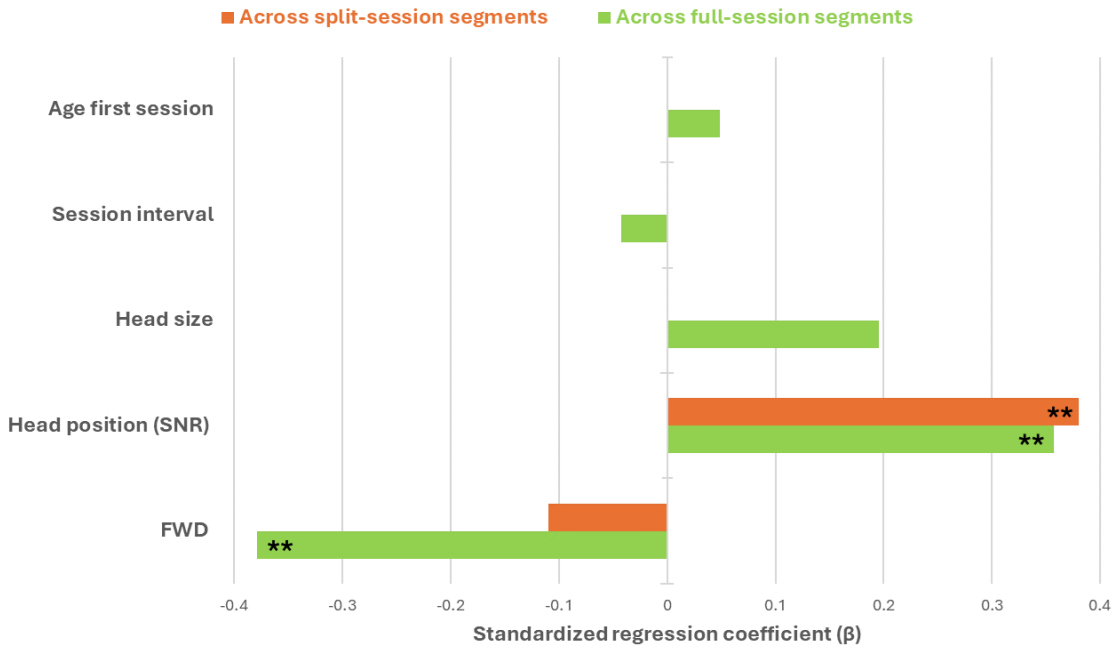

Figure 2-14 Relative impact of explanatory variables on connectome stability across full-session (5 variables) and split-session (2 variables) segments.

****two-tailed p-value<0.05. [Age first session, preterm session post-menstrual age; Session interval, interval (weeks) between preterm and term session; Head-size, mean occipital-frontal circumference (cm) across two full-sessions; Head-position, mean SNR-group (SNR due to head position) across two full/split-session segments; FWD, mean framewise displacement (mm) across two full/split-session segments]**

2.6 DISCUSSION

This study showed that the stability of measured connectomes in infants was found to be affected by several factors. The infant's head position relative to the head coil affected the regional SNR, which was empirically found to covary with functional connectivity. Head position alone, in combination with the inhomogeneity of the phased-array head coil, was found to lead to 98-100% success in split-session (within-session) fingerprinting, without any information from an individual's functional connectivity. The significant impact of head position may explain the high fingerprinting identification derived from the within-session method. As a result, the authors of this study propose that within-session fingerprinting must account for this impact, and that care be taken in across-session fingerprinting to control for head position/SNR induced artifacts. Consistent positioning within the head coil across infants is also important.

It was also found that the time interval between sessions negatively correlated with connectome stability, which suggests that the infant connectome may change gradually across time. Furthermore, head motion was found to negatively correlate with connectome stability. Our model of multiple explanatory variables impacting connectome stability showed that head position was the strongest variable found particularly during within-session (across split-session) analysis.

Today fMRI research uses phased array head coils due to their gain of higher SNR in the cortex. However, as the number of head-coil channels increase the inhomogeneity of the distribution of the SNR across the brain also increases, and as a result consistency of head position is imperative for reliable whole-brain functional connectivity analysis and regional functional connectivity estimates. This study has shown how position in native space directly impacts on SNR and that nodes with higher SNR have higher functional connectivity.

Infant head circumference changes rapidly during the first year of life, approximately from 27 cm at 29 weeks gestation (youngest session in this cohort), through 34 cm at term, and 45 cm at 1 year old (50 percentiles) (Department of Health UK et al., 2009). Both a changing head size and head

re-positioning (across sessions) therefore impacts on functional connectivity. Across-session identification methods need to be aware of this added variance. Within-session identification methods have less variance due to the constant position of the head and, as a result, identification methods (functional fingerprinting methods) are falsely improved by this confound.

Research groups examining the infant functional connectome continue to use an array of head coils including those with 8-channels (Y. Wang et al., 2021), both 12-channels and 32-channels (Dufford et al., 2021a), 32-channels only (Hu et al., 2021a) and the dHCP bespoke 32-channels (Ciarrusta et al., 2021; Q. Wang et al., 2021). In the last 10 years or so various groups have looked at designing infant sized head coils. A group in Massachusetts designed custom-sized 32 channel head-coils including for term neonates and 6 month old infants (Keil et al., 2011). These were made to specific set sizes to fit the 95% diameters of these age groups. Similarly another research group designed an 8 channel infant head coil customized to fit the average head of a 6 month old infant (Scheef et al., 2017). Data from the dHCP has been analyzed in this study and recent studies (Ciarrusta et al., 2021; Q. Wang et al., 2021). The dHCP group use a customized infant 32 channel head coil designed using term age infants head sizes (Hughes et al., 2017). To achieve centrality of head position, they use thin inflatable cushion devices to achieve consistent head position within the head coil (Hughes et al., 2017). However, the dHCP infant head coil was not designed to accommodate preterm infant head sizes such as those 44 infants with two sessions (dHCP Data Release 2.0, 2019) whose connectome stability across sessions was analyzed in this study.

Designing head coils that can adapt to the large range of head sizes from preterm through to late infant ages is important for connectome analysis across this time period. In Montreal a research group have tested a pneumatic-based 13 channel infant head-coil that adapts to infant head dimensions (27 weeks PMA to 6 weeks post-term) and which results in a 2.22 fold increase in SNR at the cortex compared to a standard 32 channel adult head-coil (Rios et al., 2018). Most recently a research group in MIT (USA) have designed their own close-fitting 32 channel infant head-coil for ages 1 – 18 months and have tested it both in vitro (phantoms) and in vivo (infant cohorts) (Ghotra et al., 2021; Kosakowski et al., 2021). Their infant head-coil can be adjusted in the anterior-

posterior and lateral dimensions to obtain a snug fit to the infant's head. The tight fit of their infant head coil results in a gain of SNR (2.7 SNR gain in brain regions, compared to adult head coil). These developments in infant head coil design are timely and, for reasons outlined in this paper, this ability to repeatedly approximate the head coil as close as possible to the infant cortex will likely help mitigate much of the variance associated with head position across sessions.

In the interim, however, infant fMRI research groups using a fixed head coil size (and therefore inducing a variable distance between the cortex and the receiver coils across infants and sessions) could consider correcting for head position in the head coil. This correction would take the form of: calculating the SNR for the space within the head coil (SNR-coil) (ideally using independent participants); calculating the first-order functional correlations for each edge (ROI to ROI); dividing the functional edge value by the product of the two SNR values derived from head position (having resampled SNR-coil to the individual's native space and extracted the two SNR values for the edge); and creating an edge matrix of corrected functional edge values. There-after second-order correlations (across infants and sessions) may show more consistent values within a subject (across sessions) then across subjects (across sessions), perhaps allowing a better measure of fingerprinting (connectome stability) ability in infancy.

2.6.1 Conclusion

Research into infant functional connectivity depends heavily on avoiding confounds that are unique or exaggerated in infancy compared to older children/adults. This study has highlighted an important confound namely that infant functional connectome analysis must consider world head position in their design and analysis methods. This study draws attention to the importance of recent developments in head coil design and the emergence of head coils that are adjustable (allowing more closer approximation to the infant cortex). Ideally these head coils should also produce homologous coil coverage.

This study has focused on the effect of head position on functional connectivity measurements in the context of 'fingerprinting'. However, the head-position induced variation in SNR may have consequences on other measures. For example, it might mask true individual differences in functional connectivity and add noise or bias to longitudinal measures of functional connectivity during development or at other points of the lifespan.

It is hoped that these findings contribute towards both the newly emerging literature on the topic of infant functional connectivity and towards improved methodological practice for longitudinal functional connectivity studies at all age groups.

CHAPTER 3 PRACTICALITIES OF SCANNING AN AWAKE INFANT FUNCTIONAL MRI COHORT

3.1 ABSTRACT

In recent years, task fMRI with awake infants in the scanner watching engaging visual stimuli has been performed by a small number of research groups. To date, usable fMRI data has primarily been achieved in a select few infants who tolerated multiple repetitions of the same paradigm, highlighting the difficulty in acquiring useful fMRI data at a reasonable scale in an awake infant population. The Foundations of Cognition Project (FOUNDCOG) builds on previous recent advances in the field of awake infant fMRI and aims to conduct the largest and first longitudinal study of infants scanned with awake task-based fMRI to date. This chapter examines the methodology used to achieve awake fMRI scans at the 2-month age scanning visit and investigates: recruitment methods and success; task type (movies versus pictures) achieving most fMRI data quantity and quality (less motion); infant behaviours during awake tasks/runs; and caregiver perceptions of their infant's experience.

Two cohorts of infants (term controls and NICU graduates) were recruited from two maternity hospitals in Dublin, Ireland. Research MRI scans were conducted at the Trinity College Institute of Neuroscience campus, and infants attended one visit for a total duration of 2.5 hours. Video stimulus fMRI runs consisted of cartoon and natural movies showing scenes/contexts that infants would experience during the first year of life. Picture stimulus fMRI runs consisted of objects (looming) relating to the movie scenes. A flexible paradigm allowed switching between the home-screen (baby sensory/calming clips) and video and pictures runs. The caregiver was encouraged to be as hands-on as possible both in the MRI magnet room and the MRI control room. Additional data was achieved through the tagging of infant facial camera footage and through caregiver feedback (questionnaire).

Of the first 100 infants attending for 2-month age scanning, most infants achieved 2 completed video runs and 1 completed picture run. Of the full group, 80 infants fell asleep allowing achievement of 80 asleep resting-state fMRI runs, and 70 T2-weighted anatomical MRI runs. A median of 19 minutes (IQR 8.4 min) of awake data (from 98 infants) was obtained, with slightly more awake date from videos compared to pictures runs. Motion (FWD) was less than 1.3mm for the 75% percentile (videos < 1.26mm, pictures <1.36mm), and less than 2.7mm for the 90% percentile (videos < 2.6mm, pictures <2.8mm) of all awake

frames acquired. Tagging of infant facial camera footage showed infants were interested/attending the visual images 85% of the time, fussing/vocalising 4% of the time, and falling asleep in 15% prior to the end of the awake run. Caregivers' feedback showed that 90% agreed that their infant was comfortable during scanning, and 91% felt that their infant contributed useful awake/asleep fMRI data from the scanning visit.

In summary, it appears that 2-month age is an opportune age to achieve infant fMRI data (at a reasonable scale) and that prioritising awake fMRI does not preclude the acquisition of resting state and anatomical sequences later in the protocol (most 2-month-olds fall asleep). It is felt that caregiver presence contributed towards optimal decision making using the dynamic/flexible scanning protocol. Positive parental feedback is important as it confirms acceptability of conducting infant MRI studies at this early age (both awake/asleep) and as such it is hoped that this will ensure good ongoing attendance in this longitudinal study.

3.2 PUBLICATION DETAILS

This chapter is currently under review with the title "Practicalities of scanning an Awake Infant functional MRI cohort"

Graham King[1,2,3], Áine Dineen[1], Cliona O'Doherty[1], Anna Truzzi[1], Chiara Caldinelli[1], Enna-Louise D'Arcy[1], Jessica White[1], Anna Kravchenko[1], Lorijn Zaadnoordijk[1], Amy Burke[1], Maebh Healy[1], Sojo Joseph[1], Eleanor Molloy[2, 4, 5], Adrienne Foran[3, 6], Ailbhe Tarrant[3, 6], Angela T Byrne[2, 4], Rhodri Cusack[1]

[1]Trinity College Institute of Neuroscience, Trinity College Dublin, Dublin, Ireland
[2]The Coombe Hospital, Dublin, Ireland
[3]The Rotunda Hospital, Dublin, Ireland
[4]Children's Health Ireland at Crumlin, Dublin, Ireland
[5]Paediatrics and Child Health, Trinity College Dublin, Dublin, Ireland
[6]Children's Health Ireland at Temple Street, Dublin, Ireland

Contributions:

Conceptualisation: GK, ÁD, COD, A Truzzi, LZ, EM, RC.
Methodology: GK, ÁD, COD, A Truzzi, ELD, RC.
Recruitment and Resources: GK, ÁD, A Truzzi, CC, ELD, JW, AK, SJ, EM, AF, A Tarrant, ATB, RC.
Investigation: GK, ÁD, COD, A Truzzi, CC, ELD, JW, AK, EM, AF, A Tarrant, ATB, RC.
Ethics and Project administration: GK, A Truzzi, LZ, ELD, JW, EM, AF, A Tarrant, ATB, RC.
Data Curation and Pre-processing: GK, ÁD, COD, A Truzzi, RC.
Writing – original draft: GK, RC.
Writing – review & editing: GK, ÁD, COD, A Truzzi, RC.
Funding acquisition: RC

3.3 INTRODUCTION

Anatomical MRI in infants is only partially predictive of atypical development, as at this early age the brain has enormous plasticity and may develop normally despite considerable structural injury (Anderson et al., 2017; Inder et al., 2021). Measures of infant brain function have the potential to offer rich information during the pre-verbal and pre-locomotor period (Cusack et al., 2016). Functional MRI (fMRI) provides a measure of activity across the brain with better spatial localization than alternatives such as electroencephalography. There has been good progress in addressing the challenges of fMRI in infants (Cusack et al., 2018; Korom et al., 2022; Pollatou et al., 2022) and it has been used to explore both typical and atypical development.

The majority of infant fMRI studies have been of the asleep state (Cusack et al., 2018). In clinical settings, sedation is still used widely in children (El-Dib, 2020) but for ethical reasons, it is not often used for research and so most studies have adopted the 'feed & wrap' technique (Almli et al., 2007; Gilmore et al., 2004), including large projects with asleep infant fMRI such as the Developing Human Connectome Project (http://www.developingconnectome.org), the Baby Connectome Project (http://babyconnectomeproject.org) and the ongoing HEALthy Brain and Child Development study (https://hbcdstudy.org/).

3.3.1 Traditional task fMRI studies in infants

In contrast to functional connectivity analysis, task fMRI measures the signal change in response to an external stimulus (Kwong et al., 1992). Task fMRI has been performed in sleeping infants, for example to explore the detection of and discrimination of speech or non-speech auditory stimuli (Baldoli et al., 2015; Blasi et al., 2015, 2011; Dehaene-Lambertz, 2002; Dehaene-Lambertz et al., 2010; Graham et al., 2013; Perani et al., 2011; Wild et al., 2017). Other asleep studies have focused on infant discrimination of joint angles (Dall'Orso et al., 2018) or the discrimination of somatosensory (Williams et al., 2015) and

nociceptive stimuli (Baxter et al., 2021; Duff et al., 2020; Goksan et al., 2015). Further, some researchers have measured learning in the asleep infant using deviant auditory stimuli (Sylvester et al., 2021) and associative motor/auditory stimuli (Dall'Orso et al., 2021). One challenge of using fMRI in sleeping infants to assess task responses is that sleep affects cognition. In adults, sleep has been shown to affect both task- and connectivity- fMRI (Tagliazucchi et al., 2012). Similarly, infant awake/asleep state has been shown to have different results to the same stimuli (Dehaene-Lambertz, 2002). As a result, care is needed when comparing fMRI studies between asleep versus awake states.

3.3.2 Awake infant fMRI literature

In recent years, task fMRI with visual stimuli has been used in infants awake in the scanner, to examine the processing of coherent motion (Biagi et al., 2015), retinotopy (Ellis et al., 2021c), the discrimination of categories (faces/bodies/objects/scenes) using movie clips and still images (Deen et al., 2017; Kosakowski et al., 2022), and the segmentation of movies into events (Yates et al., 2022). With regards infant learning, awake task fMRI has been used to assess the discrimination of repeated versus novel visual stimuli (Tristan S. Yates et al., 2023), and memory for sequences of visual stimuli (Ellis et al., 2021a). In these studies, fMRI data (useful for analyses) has primarily been achieved in a select few infants (sub-group) who tolerated multiple repetitions of the same paradigm/run. These studies have highlighted the difficulty in acquiring useful fMRI data across representative samples of an awake infant population.

In the paediatric clinical environment movie clips have been used in older children to avoid sedation (Raschle et al., 2012). In the research setting previous teams have used a changing visual stimulus (sometimes classified as a 'movie') to display changing faces (Schultz and Pilz, 2009), point-light-displays (Sifre et al., 2018), or series of changing objects (Deen et al., 2017).

However compared to these previous stimuli, naturalistic paradigms (movie clips) aim to evoke a more natural pattern of neural responses (Vanderwal et al., 2019) and, due to their dynamic nature and complexity, induce multiple

patterns of neural responses during the same task avoiding the need for multiple separate experiments (Bartels and Zeki, 2005, 2004; Hasson et al., 2010, 2004; Vanderwal et al., 2019). Naturalistic movies allow various analytical approaches based on task induced and task independent activity including: conventional task-based (time-locked/model) analysis, inter-subject (model-free) analysis, and traditional connectivity (resting-state) analysis (Vanderwal et al., 2019).

The FOUNDCOG project builds on previous recent awake infant fMRI studies (Ellis et al., 2021b, 2021a, 2020; Yates et al., 2021) by using, in one paradigm, naturalistic stimuli (Hasson et al., 2010) in the form of short movie clips and also sequences of picture (objects) stimuli. The project includes fMRI in 2- and 9-month-old infants who are awake during scanning.

This chapter discusses the important methodological steps applied to the first 100 babies recruited to the project when they attended for their first (2 months age) awake scanning visit. This study prioritizes the awake state during infant viewing of naturalistic movie clips and picture stimuli. Practical methodology and lessons learned to date are shared in this manuscript. Data from this cohort (100 babies) who attended for their 2-month age scan is used in further analyses in this thesis.

3.4 METHODS

3.4.1 Experimental Groups and Recruitment

Two cohorts were recruited from the Coombe Hospital and Rotunda Hospitals (Dublin, Ireland): i) Control - babies born at term (37-42 weeks gestation) without any known brain injury; and ii) Neonatal Intensive Care Unit (NICU) graduates with at least one prior neuro-imaging investigation (cranial ultrasound or hospital MRI brain) while in the NICU (i.e., infants investigated for potential brain injury). Most common indications for neuroimaging in the NICU include prematurity (screening for intra-ventricular haemorrhage/peri-ventricular leukomalacia) and hypoxic ischemic encephalopathy (late preterm/term infants).

Exclusion criteria for both cohorts comprised: known congenital abnormalities; contraindications to undergo MRI; known visual impairments; vulnerable parent(s); and parental refusal to consent to incidental findings being reported to the collaborating paediatric consultant. Specific to the NICU cohort was an additional exclusion criterium, namely retinopathy of prematurity (ROP) reaching Stage 3 or that needed treated (laser/injections).

For the control group, mothers were initially approached on the post-natal wards by both research assistants and neonatal doctor, while for the NICU group, the neonatal doctor only approached the parents. If they expressed interest, the parents were given an information leaflet, and their contact details were recorded. Parents were then called around 4-6 weeks later, to explain the study and ask if they would like to participate.

Ethical approval was granted by the ethics committees of the Coombe Hospital, Rotunda Hospital, and Trinity College Dublin [See Appendix].

Prior to the first attendance of any infant for research MRI scanning, the Paediatric/Neonatal Doctor (G.K.) drafted the new 'Infant MRI Standard Operating Procedures' (SOPS) document for the Trinity College Institute of Neuroscience (TCIN) [See Appendix]. This document addressed the following (not limited to): the procedure for infant MRI scanning; roles and responsibilities

of relevant personnel; infant MRI safety; infant emergency procedures; and infant screening procedures. This document was approved by the TCIN MRI Committee members.

3.4.2 Equipment and Task Stimuli

3.4.2.1 MRI Hardware

Neuroimaging was acquired on a Siemens 3T MAGNETOM Prisma MRI scanner at the Trinity College Institute of Neuroscience. The protocol included task fMRI, resting state fMRI (rsfMRI), and T2-weighted anatomical images. Task fMRI was acquired as long as the infant was awake, but if the infant fell asleep then rsfMRI and T2 images were acquired. Only the bottom half of the 64 Siemens head/neck coil was used, to allow the infant an un-interrupted view of the visual stimuli projected on the bore of the scanner (Figure 3-1). This use of the bottom half head coil was validated previously where it was shown that head motion is still the predominant disruptor of intact fMRI data and not the signal-to-noise gradient at the anterior brain where there is an absence of receiver coils (Ellis et al., 2020). In the current study an additional 4-channel surface coil was placed on the inner edge of the head coil (invisible to the infant's field of view) to attempt to receive further signal from frontal areas of the brain.

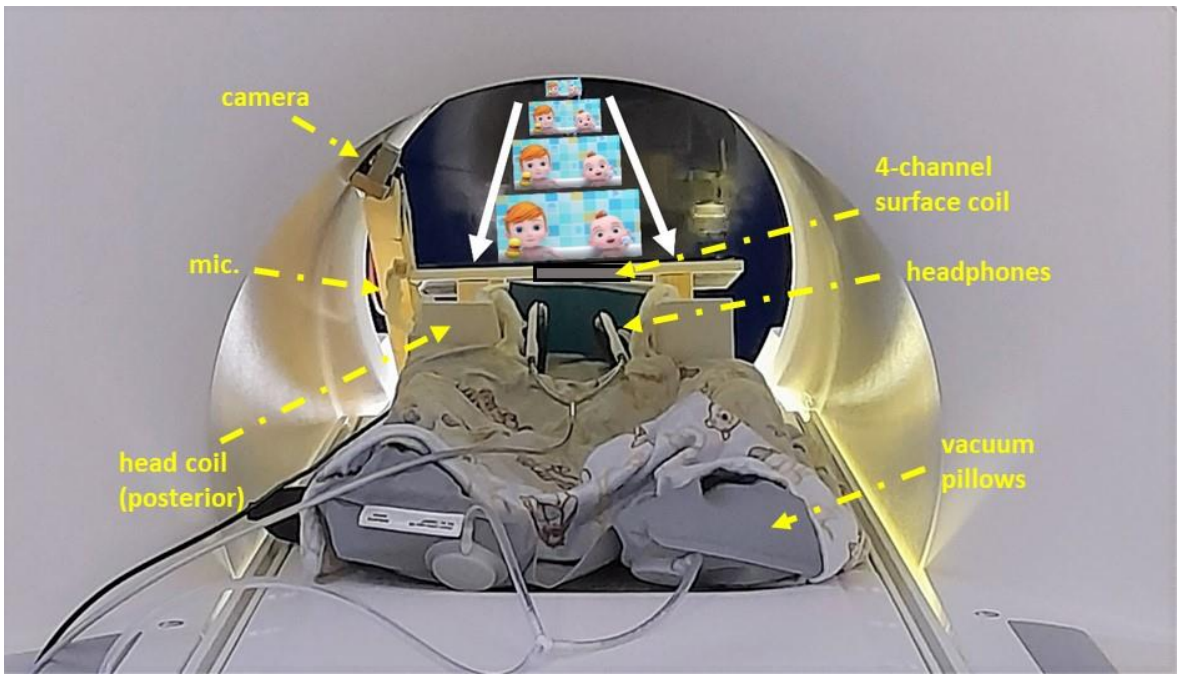

Figure 3-1 Equipment setup for awake infant fMRI scanning at 2 months corrected age.

3.4.2.2 MRI Sequences

For fMRI the CMRR (https://www.cmrr.umn.edu/multiband/) gradient-echo multiband EPI sequence was used (acceleration factor 4), 3 x 3 mm in-plane, 36 slices of 3 mm plus 10% gap, phase encoding anterior-to-posterior, repetition time (TR) 610 ms, echo time (TE) 32 ms, flip angle 40 degrees, echo spacing 0.54 ms. Before the first fMRI scan, two spin-echo reference protocols were acquired for distortion correction, one with phase encoding anterior-to-posterior and the other posterior-to-anterior, with the same geometry but without multiband for better tissue contrast (TR=2,260 ms, TE=32 ms, FA=40 degrees, 10 volumes).

If the infant was awake, two paradigms were alternated, starting with videos (485 volumes, 5 min 3 s) and then pictures (510 volumes, 5 min 18 s). If the infant fell asleep, resting-state fMRI (1000 volumes, 10 min 17 s) was acquired and then a T2-weighted anatomical sequence, an acoustic noise-reduced scan: 100 contiguous near-axial slices, GRAPPA acceleration factor of 3, voxel size 1 mm × 1 mm x 1 mm, coverage of the whole head and a field of view 192 mm, TR 6090 ms, TE 84 ms, flip angle 150 degrees, echo spacing 12 ms, and duration 4 min and 5 s.

3.4.2.3 MRI Motion and Field Distortion Correction

MRI data were converted from DICOM to NIfTI format using dcm2niix (https://github.com/rordenlab/dcm2niix) (Li et al., 2016). Motion was determined using FSL MCFLIRT (Jenkinson et al., 2002) and the 6 motion parameters (3 translation, 3 rotation) were used to calculate framewise displacement (FWD, in mm) (Power et al., 2012) using Nippype software algorithm (Gorgolewski et al., 2011). Following motion correction with FSL MCLIRT, the field distortion estimation from FSL TOPUP (Andersson et al., 2003) was then applied to the EPI data to correct for susceptibility distortion (iterated each time the infant was positioned in the head coil, i.e. once per session).

3.4.2.4 Visual Projection

The visual stimuli were projected using an ultra-high-definition (UHD) video projector located in a room behind and adjacent to the actual MRI magnet room itself. The UHD projector light beam travelled through the wave guide (through the wall of the MRI magnet room) towards a 'front surface' mirror secured at the correct angle on a wooden frame. The angle of the projector beam and the mirror were such to allow the projected image to be reflected upwards onto the ceiling of the bore of the MRI scanner (Figure 3-1).

Video projectors with a narrow beam width ("long throw") are designed for large rooms and tend to be very bright. A balance between these factors was chosen, with an Optoma UHD30 projector, which has a 4K (or 2160p) to ensure that the projected image had adequate resolution. Visual acuity at 2 months of age is thought to be approximately 20/150 to 20/215 (Banks and Salapatek, 1978; Daw, 2013; Sokol, 1978). At 2-months-old infant visual accommodation is pre-programmed for near targets and they can accommodate to 25cm (Currie and Manny, 1997). It is known that infants have decreased peripheral visual acuity compared to central (foveal) acuity. A 2-months-old an infant has approximately 20/300, 20/600, and 20/1200 visual acuity at the central, 10-degree and 30-degree visual field angles from the fovea (Courage and Adams, 1996). As a result, a 2-month-old infant may miss a salient object if it appears more than 30-degrees away from the fovea. As infants' eyes were approximately 30 cm away from the projected image, the image proportions were chosen to ensure that the images appeared within the 30-degree visual field angle and salient elements of the visual scene were large and central in the image.

3.4.2.5 Visual Stimuli

There were two main awake tasks: videos and pictures. An ideal session would consist of 2 video runs, 2 pictures, 1 resting state, and 1 T2 anatomical scan. The video task was prioritized at the start of the MRI session. It was not typical for the entire set to be achieved in one session.

Based on learning from previous online infant studies, video clips were chosen for their ability to attract infants' attention (Tran et al., 2017) and consisted of both cartoon and natural movies. Clips were chosen such that the content of each clip featured a coherent scene depicting a context that an infant may

experience in the first year of life, e.g., a supermarket, bathroom, or restaurant (Figure 3-2). These clips included various content classified by various semantic and perceptual properties. Semantic categories included animate/inanimate (Konkle and Caramazza, 2013), indoor/outdoor (Kravitz et al., 2011), faces/objects/body parts/scenes (Deen et al., 2017). The chosen final six 22.5s clips (contexts) are shown in six colour codes in an example video run events file (Table 3-1). During a full 5 min video run each infant saw two repetitions of the 6 videos, each a different randomly selected order. Each repetition began with an attention getter stimulus (https://osf.io/wakqf). Subsequent video runs for the same infant would always use the same two orders.

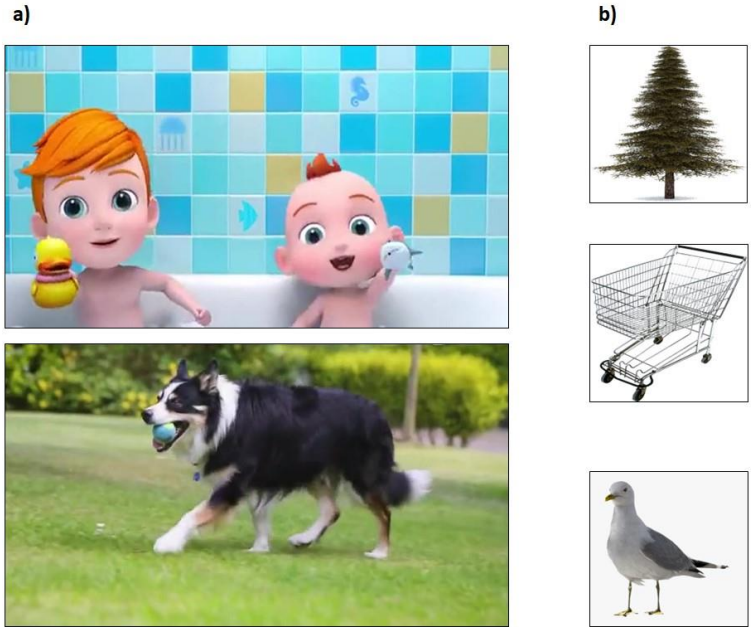

Figure 3-2 Examples of frames from a) Videos, b) Pictures runs

Videos – 'bath time' and 'dog' videos; Pictures – 'tree', 'shopping cart', and 'seabird' pictures

Picture stimuli chosen consisted of six pairs of object types chosen to relate to each of the six contexts in the videos task and to be something an infant may encounter in the first year of life (e.g., 'supermarket' video = [shopping cart + shelves]). Object types were decided by comparing the similar brain responses between adult pilot study video and picture runs. Picture runs featured still images looming towards the infant for 3 s. For each type of object, 3 instances (examples/instances of the object) were shown. The pictures task was repeated

twice per fMRI run giving a final design of [6 contexts x 2 object types x 3 instances x 2 repetitions], totaling 5 min of scanning.

Table 3-1 Example of a video run events file

onset (s)	duration (s)	trial_type
1	8	attention_getter
9	23	bathsong.mp4
32	23	dog.mp4
55	23	moana.mp4
78	23	forest.mp4
101	23	minions_supermarket.mp4
124	23	new_orleans.mp4
147	4	attention_getter
151	23	forest.mp4
174	23	moana.mp4
197	23	new_orleans.mp4
220	23	minions_supermarket.mp4
243	23	dog.mp4
266	23	bathsong.mp4

3.4.3 Infant Scanning

In contrast to previous infant fMRI studies with multiple visits, (Deen et al., 2017; Ellis et al., 2020) infants and parent(s) visited the centre just once per timepoint (in this case 2-months-old). A scanning visit consisted of 2.5 hours duration. Following the initial arrival, check-in, and completion of documentation by the parent, this left approximately 2 hours of time in the MRI department. The basic structure of the 2 hours was 2 sessions with at least one significant breaktime between them. Starting in the awake state an infant would have a maximum of 20mins of actual scanning and if still awake would then have a breaktime. If the first awake session was cut-short due to the baby falling asleep during an awake run, then the infant would proceed to the 15-20min of asleep

sequences (10 min rsfMRI, a T2, and in some cases a T1 sequence). An infant would then have a breaktime (whether still asleep or if they woke). After the breaktime a second session would start with the infant awake (if the infant fell asleep once more the asleep sequences were not repeated/duplicated). In summary, the small number of infants who facilitated both sessions contributed a total of 2 awake (20mins each) periods and 1 asleep (15-20min) period, totalling 60 mins of scanning time (spread out over the 2 hours in the MRI department). Most infants achieved a proportion of this maximum (i.e., 1 awake period and 1 asleep period). During a session an infant sometimes fussed. Quick remedies included gentle reassuring tactile stimulation, and/or giving the infant a soother (dummy/pacifier) and/or using sucrose drops (sweet water) dropped onto their tongue/lips to sooth them. If these measures failed, the infant took a breaktime with their parent.

3.4.3.1 Hearing Protection

Various methods of hearing protection have been discussed by the infant neuroimaging community (Korom et al., 2022). Some employ in-ear earplugs (McJury, 2022) or small foam pads that stick to the infant's ear (Abujarir et al., 2012) but these are unreliable when used under ear defenders, as they often fall out/off, which is not ascertained until the end of the scan. They are also a source of stress to the relaxed awake infant prior to starting the scan and so were not adopted in this protocol. Instead, thin MRI-compatible headphones with good passive noise attenuation of 25 dB (Optoacoustics OptoActive II) (https://www.optoacoustics.com/medical) were adopted. A camera (see later) allowed monitoring of the headphone placement throughout the scan. Furthermore, the OptoActive II headphones contain a microphone to monitor the sound level inside at the infant's ear in real-time, allowing displacement to be detected and remedied. Passive attenuation was sufficient given the length of the scans but if the infant fell asleep, for additional protection active noise cancellation (ANC) was employed. Successful ANC required a 16-20 s learning phase to be completed while the scanner gradients are running, without headphone audio, and when the participant is not moving or vocalizing. Through piloting with adults, it was concluded that ANC calibration would not be reliable while the infant was awake and so it was only used if they fell asleep.

3.4.3.2 Infant Monitoring

During MRI scanning infants were placed supine on a vacuum cushion positioning system (Figure 3-1). This was both to maintain their body position but also to provide them with reassurance due to the 'nest-like' tactile support on all sides. In concordance with the awake infant fMRI protocol from the Yale group (Ellis et al., 2020) no straps or physical constraints were used to ensure that infants felt non-threatened and calm. While research groups scanning asleep infants often use infant immobilizer devices (Golan et al., 2011) this current study found that awake infants remained calm and attentive in a peripheral nest support. At all times a team member was beside the infant next to the entrance to the MR magnet bore. Infants were watched (in real time) via the MR compatible camera (https://www.mrc-systems.de/en/products/mr-compatible-cameras) focused on the face. An Optoacoustics noise-cancelling MR compatible microphone was also positioned beside the infant so that vocalization (and/or fussing) could be monitored in real time during a scan (Figure 3-1).

3.4.3.3 Paradigm Menu Flowchart

Due to the flexibility demanded by an infant scanning session, a bespoke experimental paradigm was coded using PsychoPy (Peirce et al., 2019). The custom python program recorded and saved all event onsets, TR timings, and various other logs needed for analysis.

The awake portions of this paradigm prioritized infants having a constant visual stimulus to keep them calm and engaged. This was achieved using a home screen video playing inside the scanner. If an infant was fussing (for example, triggered by headphones placement or being laid down on the MRI table), once they entered the scanner bore, they often settled and were engaged by the home screen video already playing above them. Home screen video clip options included either baby sensory movies (fireworks or dancing clouds with fun music), or a calmer option that has been shown to promote stillness in child MRI (Vanderwal et al., 2015).

From this home screen, any task (videos, pictures, resting blank visual with or without pink noise) could be launched. A decision aid was used by the paradigm controller/researcher to navigate these decisions easily (Figure 3-3). The only visual downtime (no home screen video) was a blank screen while the paradigm

waited to receive the sync pulse from the MRI scanner. This brief lack of display often led to a short moment of fussing from the infant, highlighting the essential nature of constant visual engagement for infant fMRI scanning.

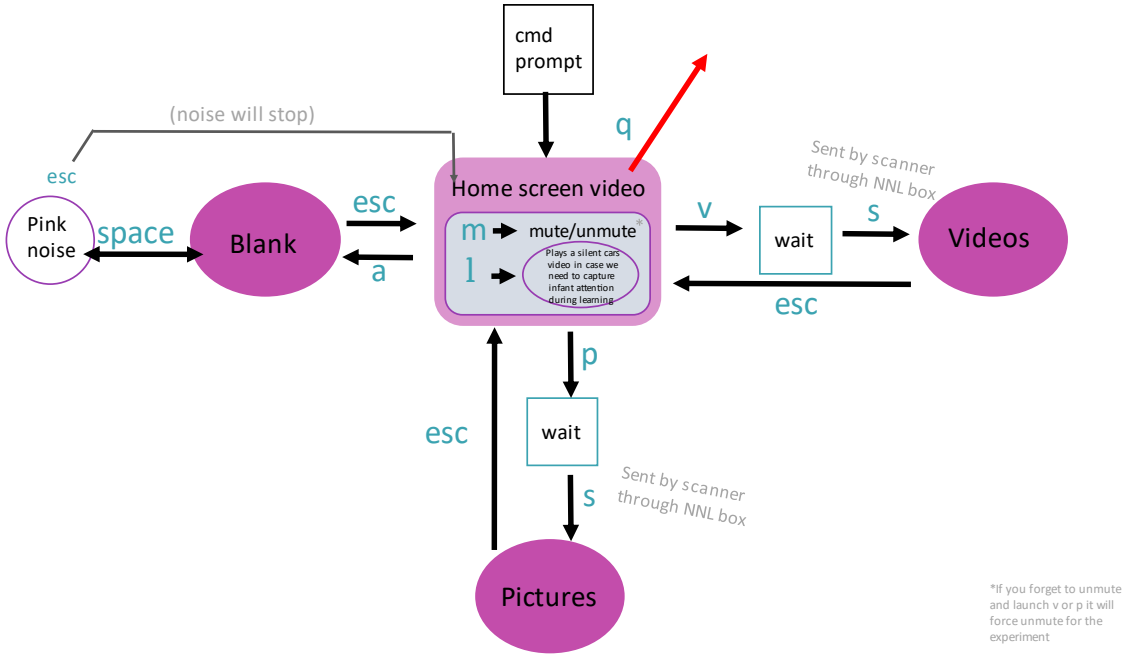

Figure 3-3 Decision aid for paradigm controller using custom python program. (image courtesy of Clíona O'Doherty, Cusack Lab, Trinity College Dublin).

3.4.4 Team Researcher and Caregiver Roles

3.4.4.1 Team Researcher Roles

While scanning an infant, four researchers were present as well as the infant's caregiver(s). Each team member played an equally crucial role in ensuring scan success (Table 3-2). The radiographer focused on MRI safety, positioning the infant on the table correctly, and running the MRI sequences. The clinician (paediatric doctor or nurse) was tasked with screening the infant's health on the day and ensuring the infant remained comfortable and well throughout. A 3rd member of the team ('paradigm controller') was responsible for running the experimental paradigm on the paradigm computer and closely communicating with the radiographer to manage what sequences would be run as the session progressed. The 'paradigm controller' also recorded notes during the session and promptly handled any spurious technical issues. Finally, a 4th team member

was responsible for meeting and greeting the infant and parent, chaperoning them safely in the MRI department, and helping them with documentation (consent, MRI safety and questionnaire forms).

Table 3-2 Researchers' Roles Descriptors

	Title:	Focus of work:
1.	Radiographer	MRI safety and sequences
2.	Clinician	Infant wellbeing and safety
3.	Paradigm controller	Running the dynamic/flexible computer paradigm
4.	4th member	'front of house' and parent support

3.4.4.2 Caregiver Role

Caregiver participation and engagement with scanning was crucial for the success of data collection. Caregivers (in this case, almost exclusively parents) played an important role in crucial turning points of the scanning session, most commonly the transition periods when the infant was going in or out of the MRI scanner. Where able the caregiver was asked to lay their infant down on the MRI table and later pick them up when needed. The presence of their caregiver, and face-to-face interaction with them, provided reassurance and allowed the infant stay as comfortable as possible. Caregivers were keen to be involved and nearly all caregivers played this role (only one or two caregivers were precluded from entering the MRI room due to a positive finding on the MRI safety questionnaire). While the infant was in the MRI scanner the caregiver returned to the MRI control room. There they could see their infant on the facial video camera, hear them on the microphone speakers and see the visual stimuli being shown to the infant (separate screen).

3.4.5 Data Collected

Data collection comprised MRI brain images, in-bore (MRI) facial camera footage, and timing log files. A healthy control infant's birth and current baseline health data was collected using the relevant Clinical Research Form [See Appendix]. Specific to NICU cohort was the collection of healthcare data pertaining to their clinical course in the NICU. This was done using the NICU

Clinical Research Form [See Appendix]. Due to the longitudinal nature of the project, data was pseudonymized to allow collation of participants' data sets.

3.4.5.1 Developmental and Learning Environment Data

During the scanning visit the Ages & Stages (Squires and Bricker, 2009) and Ages & Stages Social-Emotional (Squires et al., 2012) questionnaires were complete by the caregiver. Questionnaires were selected based on the infant's corrected age (age since their due date) so that all infants (Control and NICU) were as closely comparable from a physiological maturation metric.

3.4.5.2 Infant attention during awake scanning

Facial camera footage allowed the level of attention that the infant was paying to the visual stimulus to be retrospectively tagged based on behavioural observation. Tagging was conducted using ELAN tagging software (Nijmegen: Max Planck Institute for Psycholinguistics, 2022). Tags were assigned if the infant demonstrated the action for a duration of at least 1 second. Tags were defined as per the 'Definitions of Tags' document [See Appendix].

3.4.5.3 Caregiver Feedback

At the end of the scanning visit, a caregiver was given a feedback questionnaire. This questionnaire contained 14 questions with Likert-type responses. Questions were related to the knowledge of fMRI before/after the visit, the experience during the scanning, their perception of their infant's state during scanning, whether they felt their infant's state may/may-not have allowed the gathering of data, and whether the caregiver felt that fMRI may be used in the clinical domain in the future. The full set of questions can be seen in the 'Parental Feedback Questionnaire' [See Appendix].

3.5 RESULTS

3.5.1 Recruitment and Cohort characteristics

A key factor in recruitment of the control group was research staff availability and clinical restrictions (Covid-19 restrictions, restrictions on visiting hours to avoid busy clinical doctor/nursing rounds etc.). An important factor in the recruitment of the NICU participants was the need to find the optimal timing – approaching the parents closer to the NICU discharge date, but not too late that the opportunity to meet the parents 'in-person' was missed. Parents of 685 infants agreed to be contacted after discharge from their maternity hospital. Of these 685 infants, all were contacted 4-6 weeks later by email or phone, and eventual overall participation rate was 15% (defined as having attended for the 2-month age research MRI scan). Of these 100 infants, 75 were full-term controls, while 25 were infants recruited from the NICU. This represents a participation rate of 13% (75 of 591) for parents of controls and 27% (25 of 94) for parents of NICU infants. These first 100 infants attended their research scan between August 2021 and October 2022.

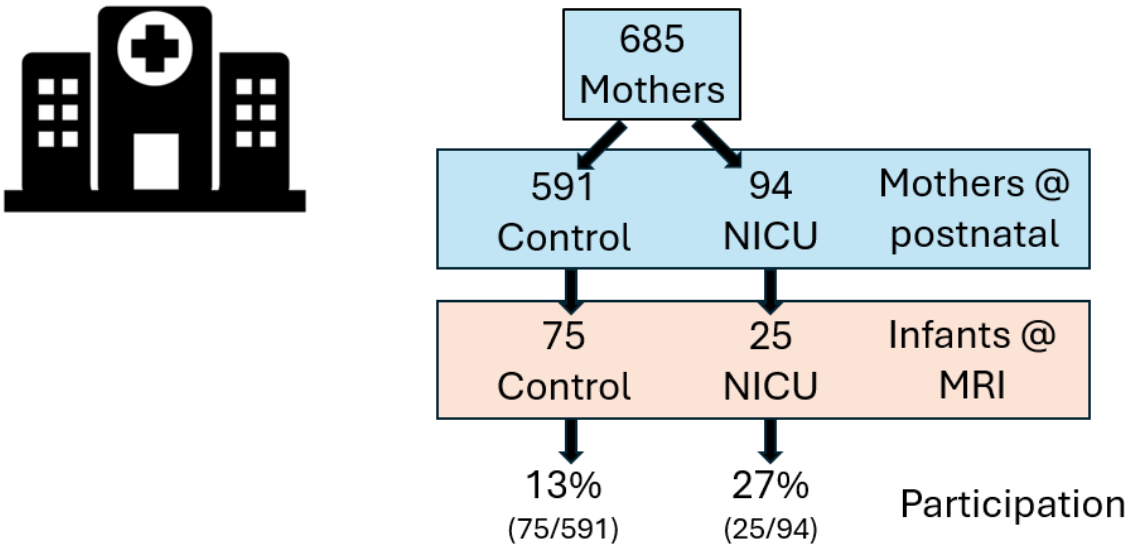

Figure 3-4 Participation rates (Aug 2021 – Oct 2022): control versus NICU participants

3.5.2 MRI

Several important realizations were made during the progression of the project. Firstly, it was noted that the running order of a 'scout' sequence followed by 'field maps' (both with home screen clips) took approximately 2.5 mins. This delayed the start of the first video run, which led to loss of infant engagement. Realizing this, the order was therefore changed so that the initial scout was followed directly by the first video task run, engaging the infant's attention earlier.

Two control infants had no MRI data recorded (neither anatomical nor functional). At 2-months age 92 (71 controls, 21 NICU) of the first 100 infants contributed at least one 'completed' (all frames) awake fMRI run while 98 (73 controls, 25 NICU) of them contributed a 'partial' (minimum 50 frames) awake run or better.

Considering partial runs (minimum 50 frames): 270 video runs (from 98 infants), 182 picture runs (from 87 infants), and 80 asleep rsfMRI runs (from 80 infants) were obtained (Table 3-3). Similarly, run counts for the NICU sub-group were calculated (Table 3-3). However, when counting completed (all frames) runs only: 194 video runs (from 92 infants), 109 picture runs (from 70 infants), and 79 asleep rsfMRI runs (from 79 infants) were obtained.

Table 3-3 Number of runs of fMRI data collected (runs, no. infants contributing)

	Awake	**Videos**	**Pictures**	**rsfMRI**	**Anatomy**
ALL (100)	452 (98)	270 (98)	182 (87)	80 (80)	70 (70)
NICU (25)	107 (25)	69 (25)	38 (20)	20 (20)	18 (18)

The overall trend of these counts shows that, when counting partial runs (min 50 frames), 2-month infants contributed approximately 3 video and 2 picture runs each, while, when counting 'completed' runs (all frames), 2-month infants

contributed approximately 2 video and 1 picture runs each. Once asleep, infants tolerated the rsfMRI run without waking and so the number of rsfMRI runs remained constant (80% of infants).

Analysing by state (awake vs resting) and stimulus type (video vs picture), the number of frames per subject were summed together and converted to unit of minutes (multiplying by TR=0.61 sec). A median of 19.1 minutes (IQR 8.4 min) of awake fMRI data was acquired for the group, with higher minutes of video versus picture runs. The histograms of the number of infants achieving minutes of fMRI data by state and by task are shown (Figure 3-5). In Figure 3-5 it shows that video runs remain more robust (minutes fMRI are similar when comparing any length run versus completed runs) compared to picture runs which suffer more from partial run acquisitions. It is thought that there are two main explanations for this: firstly, it is known that infants find animation more engaging than static objects/pictures (Tran et al., 2017); secondly, after the initial scout MRI sequence, the first visual task run was designated a video run, so infants encountered the video run earlier in the paradigm introducing a potential ordering effect (in the absence of counter-balancing).

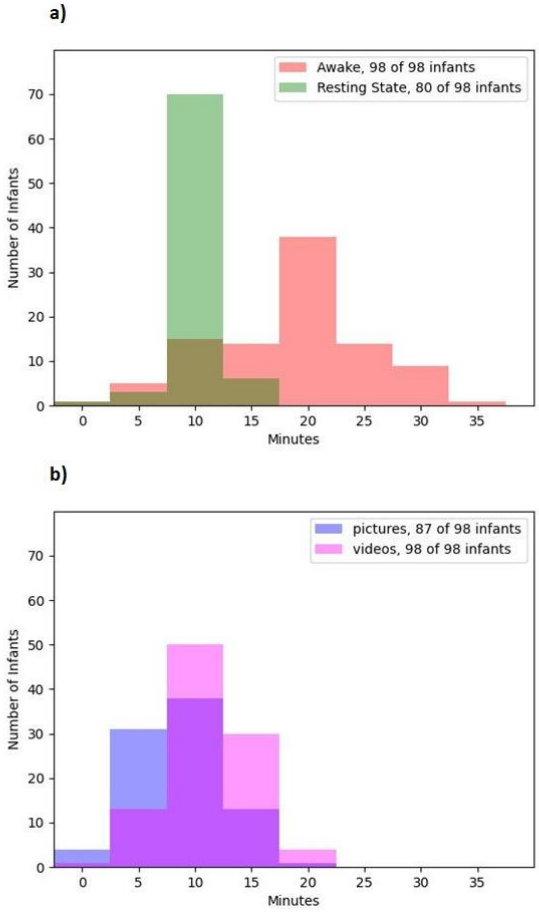

Figure 3-5 Number of infants achieving fMRI (minutes): a) awake versus asleep; b) video versus picture runs

Many infants fell asleep, allowing resting state (80%) and anatomical (70%) data to be collected. A quiet (noise-reduction) T2-weighted anatomical sequence was prioritized in these 2-month-old infants. During a typical session resting state functional scans were acquired before the quiet T2 sequence. It was observed that the sudden drop in sound level between resting state and quieter T2 anatomical sequences caused infants to wake. It was speculated that the infants missed the constant rhythm of the EPI gradient fields and to remedy this, pink noise was played through the infant earphones during the transition from resting state to anatomical sequences. This simple remedy greatly increased the success rate of collecting high quality anatomical data. In total 70 of the 100 infants (70%) acquired a T2 anatomical sequence while asleep. A similar proportion, 18 of 25 NICU infants (72%) had T2 anatomical images obtained.

3.5.3 Coverage and Head Motion

As expected, using the posterior half of the head coil alone resulted in a clear decrease in functional signal received from the frontal regions of the brain (Figure 3-6). Framewise displacement values were available for 97 of the first 100 infants; two infants had no fMRI data obtained, and one NICU cohort infant did not have correct reference scans obtained (this infant's data has yet to be pre-processed for motion parameters).

To allow visualization of the amount of awake motion (FWD) for the both the group and the individual participant, a stepped histogram (cumulative to 100% of each participant's frames for all their runs) was plotted (Figure 3-6) for both awake videos (97 of 100 participants) and awake pictures (86 of 100 participants). Concatenating the FWD for every frame of all runs for all participants, allowed calculation of the FWD distribution for the whole group. Table 3-4 shows the percentile values for chosen percentiles (25 – 95%) for both the full group and the NICU group only. While infants are awake chosen FWD percentiles range from 0.2 to 4mm, however more than 75% of all frames have a FWD below 1.3mm (with video runs, 1.26mm, even better than picture runs, 1.36mm) and more than 90% of all frames have a FWD below 2.7mm (video runs, 2.6mm, better than picture runs, 2.8mm).

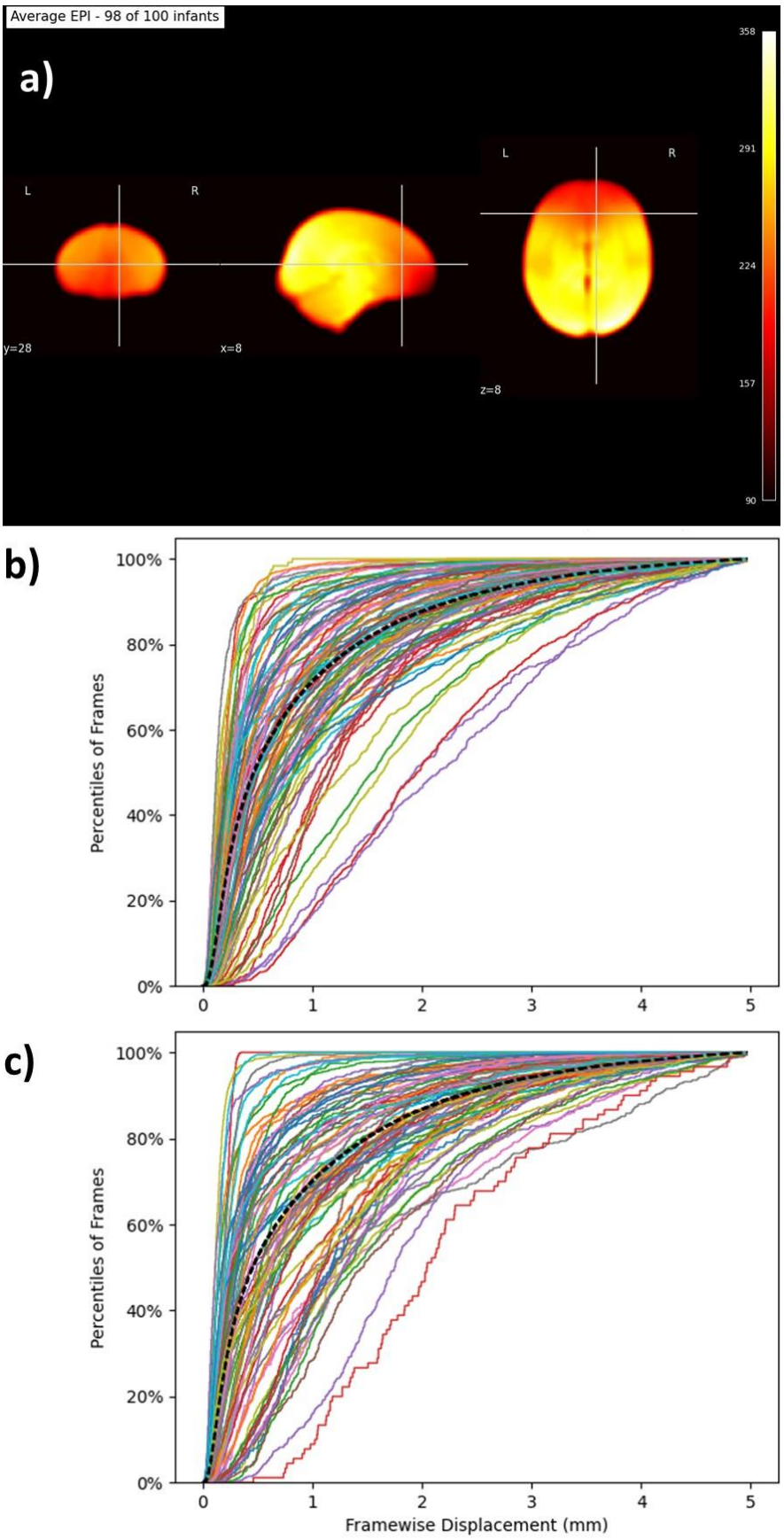

Figure 3-6 Functional signal and motion estimates

a) Group mean functional signal acquired (functional images normalized to infant template). b) Percentiles of frames acquired versus FWD (mm) for each infant achieving awake video runs c) Percentiles of frames acquired versus

FWD (mm) for each infant achieving awake picture runs. [dashed line (--) = FWD distribution of whole group]

Table 3-4 Framewise displacement (mm) at various percentiles of all frames (TRs).

	25%		50%		75%		90%		95%	
	ALL	NICU	ALL	NICU	ALL	NICU	ALL	NICU	ALL	NICU
Awake	0.21	0.24	0.49	0.59	1.3	1.5	2.7	3.2	4	4.7
Video	0.22	0.24	0.5	0.57	1.26	1.48	2.6	3.1	3.9	4.46
Pictures	0.2	0.24	0.49	0.62	1.36	1.66	2.8	3.4	4.2	5
rsfMRI	0.09	0.08	0.13	0.13	0.19	0.19	0.28	0.27	0.38	0.34

(TRs) for 'ALL' runs for all participants (n=97) and 'NICU' participants (n=24)

3.5.4 Infant attention during awake imaging

3.5.4.1 Camera footage

Of the first 100 babies, two infants did not have any awake fMRI runs obtained. For another 5 infants the facial camera had technical difficulties and did not record any footage. Facial camera footage and awake fMRI data was collected for the remaining 93 infants. The videos for the runs for 63 (48 control and 15 NICU) of these infants have been cropped and tagged to date.

This sample of 63 infants contributed a total of 285 awake fMRI runs, of which 268 (94%) had useable camera footage, more than 18 hours of facial camera footage during awake fMRI. Of the 268 runs of awake fMRI (213 control, 55 NICU) 166 were video runs (130 control, 36 NICU) and 102 were pictures runs (83 control, 19 NICU). Of the 268 runs with useable video, 252 were complete recordings (94%) and 16 were partial recordings (12 of which had a delayed onset (4.5%) and 4 of which terminated early (1.5%)). Of the 268 runs, 223 were recorded manually (and retrospectively cropped to align with the runs with second precision) while 45 runs were recorded automatically (and the recordings therefore aligned with the runs with millisecond precision).

3.5.4.2 Inter-rater reliability

To date, two researchers have tagged this camera footage data. As there is a huge volume of facial camera footage to be tagged, it was decided that the camera footage for one run would be tagged by one research tagger. The camera data for the 63 infants was distributed evenly (similar number of runs, control runs, and NICU runs) to both taggers. To measure the reliability of tagging between two taggers Cohen's kappa method was used and an inter-rater reliability (IRR) score was measured during 3 initial pilot periods. This was done using *scikit learn* in python (https://scikit-learn.org/stable/modules/generated/sklearn.metrics.cohen_kappa_score.html).

Cohen's kappa was calculated using the following equation:

Equation 6

$$\boldsymbol{\kappa = (p_0 - p_e) \div (1 - p_e)}$$

where,

$\boldsymbol{\kappa}$ is the kappa statistic (a number between -1 and 1. The maximum value means complete agreement; zero or lower means chance agreement).

p_0 is the empirical probability of agreement on the label assigned to any sample (the observed agreement ratio), and

p_e is the expected agreement when both annotators assign labels randomly.

The two pilot tagging periods were conducted in a '*plan – do – check – act*' structure. Pilot 1 consisted of 23 camera runs (videos and pictures). Both taggers tagged all runs (Table 3-5). Reasons for certain scores were analysed by re-exploring the tagging files on a per run basis. Agreement was reached on how to improve tags 'interest_scanning' and 'eyes_closed_awake' and tag definitions were revised appropriately prior to Pilot 2. Pilot 2 consisted of 14 camera runs (videos and pictures). Pilot 2 scores improved for 'interest_scanning' and 'eyes_closed_awake', however it was noted that the tag 'sleepy' was inconsistently tagged between taggers. Again, the definition of 'sleepy' was revised and agreed. Pilot 3 consisted of a further 25 runs. Overall, after Pilot 3, the six main tags were seen to have good IRR (Table 3-5), including an improvement for the IRR of the tag 'sleepy'. Of note, the IRR score for 'interest_scanning' in the final IRR assessment is lower as these 25 runs contained a high proportion of camera footage of infants interested (and eye

scanning the stimuli) for practically the full run duration. This affected the Cohen's kappa denominator (probability of chance) for this tag. Following this 'check' of Pilot 3 it was determined that there was no further requirement to 'act' and the Pilot 3 definitions were formally adopted. On the basis of these definitions a further 206 runs have been tagged to date. The runs included in Pilot 1 and Pilot 2 were amended in line with the revised definitions for inclusion in analysis.

Table 3-5 Tagging facial camera footage: inter-rater reliability (3 Pilots)

		Interest scanning	***Sleepy***	***Asleep***	***Eyes closed awake***	***Fussing***	***Vocalising***
Pilot 1 - IRR	*Cohens*	0.39	0.75	0	0.62	0.66	0.75
	% time in use	0.68	0.02	0	0.05	0.15	0.17
Pilot 2 - IRR	*Cohens*	0.63	0.28	0.86	0.73	0.79	0.72
	% time in use	0.59	0.11	0.05	0.13	0.09	0.1
Pilot 3 - IRR	*Cohens*	0.47	0.74	0.92	0.39	0.84	0.77
	% time in use	0.68 (#)	0.01	0.02	0.04	0.25	0.24

= this tag was present in most runs and across large sweeps of the run, as a result the Cohen's kappa denominator (probability of random/chance) is high, however these tags are accurate and prevalent.

3.5.4.3 Infant attention

The proportion of time that each of the five main tags were present is shown (Figure 3-7). In summary, 'interest_scanning' (infant is interested in and conducting eye scanning of the visual stimulus) was tagged approximately 85% of the time, with 'fussing' and 'vocalizing' tagged approximately 4% of the time. In just less than 20% of runs tagged to date, there are periods of the infant being 'sleepy', with infants falling 'asleep' in 15% of runs prior to the fMRI run being stopped. 'Eyes_closed_awake' usually co-occurred with 'fussing'. Overall, there are similar results for controls versus NICU babies and for the visual stimulus presented (Figure 3-8). A two-way mixed ANOVA (task, cohort) was run for each of the 11 tags. No effect of 'cohort' was found for any tag, although the median proportion of time spent 'interest scanning' was lower in the NICU

(75%) than control cohort (88%). More time 'interest_scanning' was found for videos compared to pictures (p=0.001) and less time was spent asleep during videos compared to pictures (p=0.026). This suggests that the infants found the videos to be more interesting and engaging than the pictures (but it should also be noted the video task was always presented first).

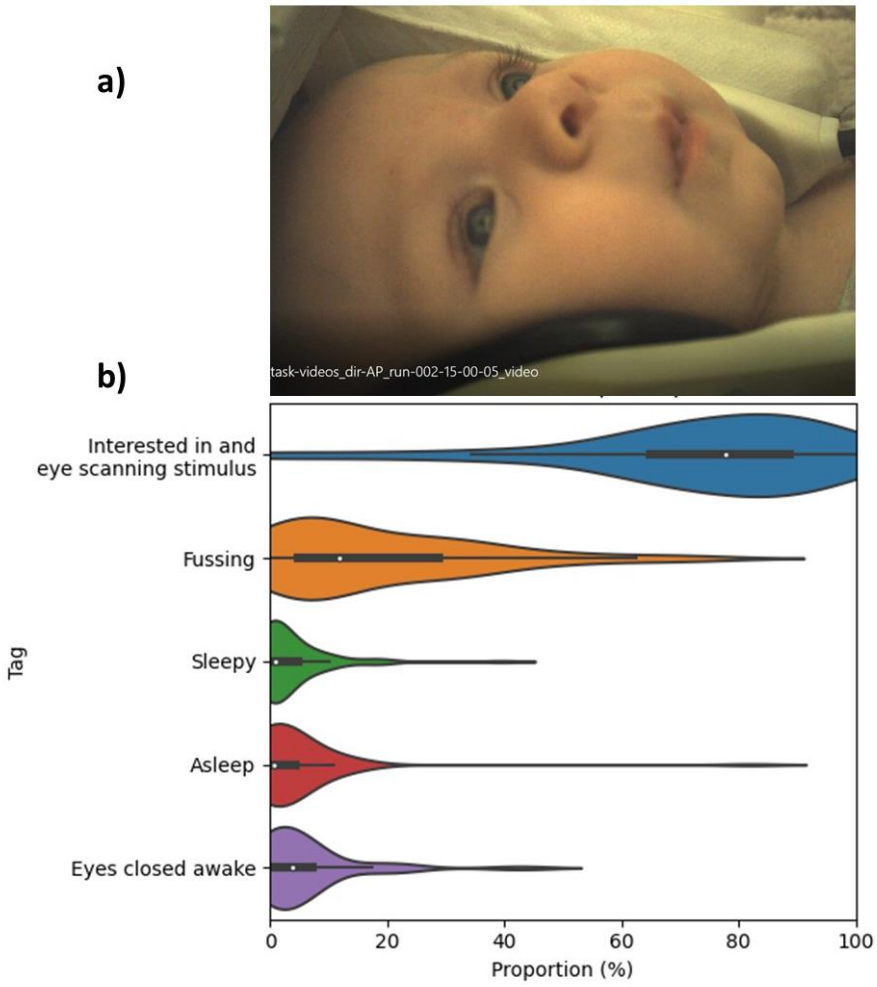

Figure 3-7 a) Example of facial camera view (used for infant monitoring and tagging), b) Violin plots - proportion of time that the 5 main tags were present (268 runs for 63 participants tagged)

Note: Infant facial photograph given with parental consent/permission for publication/thesis.

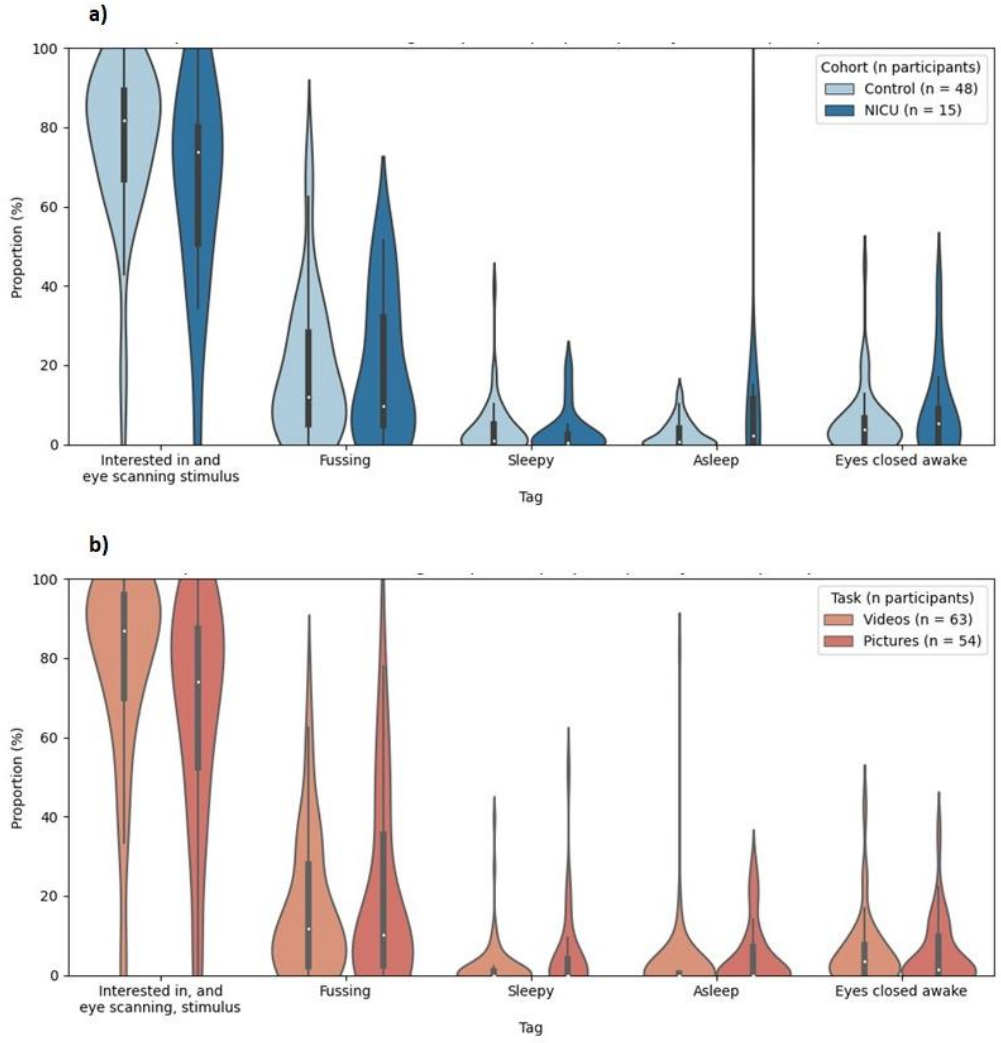

Figure 3-8 Violin Plots of proportion of time (%, awake runs) per participant that a tag was present. a) cohorts (Control vs NICU) and b) tasks (Videos vs Pictures)

(Image courtesy of Ms Áine Dineen, Cusack Lab, Trinity College Dublin).

3.5.5 Incidental Findings

Anatomical T2 images were acquired in 70 infants (52 of the 75 control infants and 18 of the 25 NICU infants). Two control and one NICU participants' images had severe movement artefacts, but the remaining 67 were shared with collaborating paediatric radiologists, who found incidental findings in two (3%), which were then followed up by the collaborating paediatricians. Despite some of the 17 NICU infants having known radiological findings on previous clinical imaging, there were no new (un-related) incidental findings made in any research anatomical scans.

3.5.6 Caregiver Feedback

Of these first 100 infants, 63 infants' caregivers attended following the introduction of an additional 'parental feedback questionnaire' (the other 37 parents attended prior to the commencement of the questionnaire). Of these possible 63 caregivers, 58 completed a questionnaire (5 did not). Questionnaires (58 total) were analysed, and any specific questions not answered were deemed 'NA'. Questions in this parental feedback questionnaire are shown in the Appendix [See Appendix].

Results of the questionnaire show a positive attitude towards infant fMRI scanning (

Figure 3-9). Parents of 52 infants (90%) agreed or strongly agreed that their infant was comfortable during scanning (only 1 parent disagreed). Parents of 53 infants (91%) agreed or strongly agreed that their child's participation contributed towards 'usable awake' MRI data, while parents of 43 infants (91%) who fell asleep (47 infants fell asleep) agreed or strongly agreed that their child's participation contributed towards 'usable asleep' MRI data. Parents appeared to learn/understand more clearly the different types of research MRI used. Prior to attending parents of 14 infants (24%) did not understand the difference between structural MRI (sMRI) compared to functional MRI (fMRI), but after attending the 2-month scanning, this reduced to parents of 5 infants (9%), representing an improvement in understanding following time spent scanning/participating as caregivers.

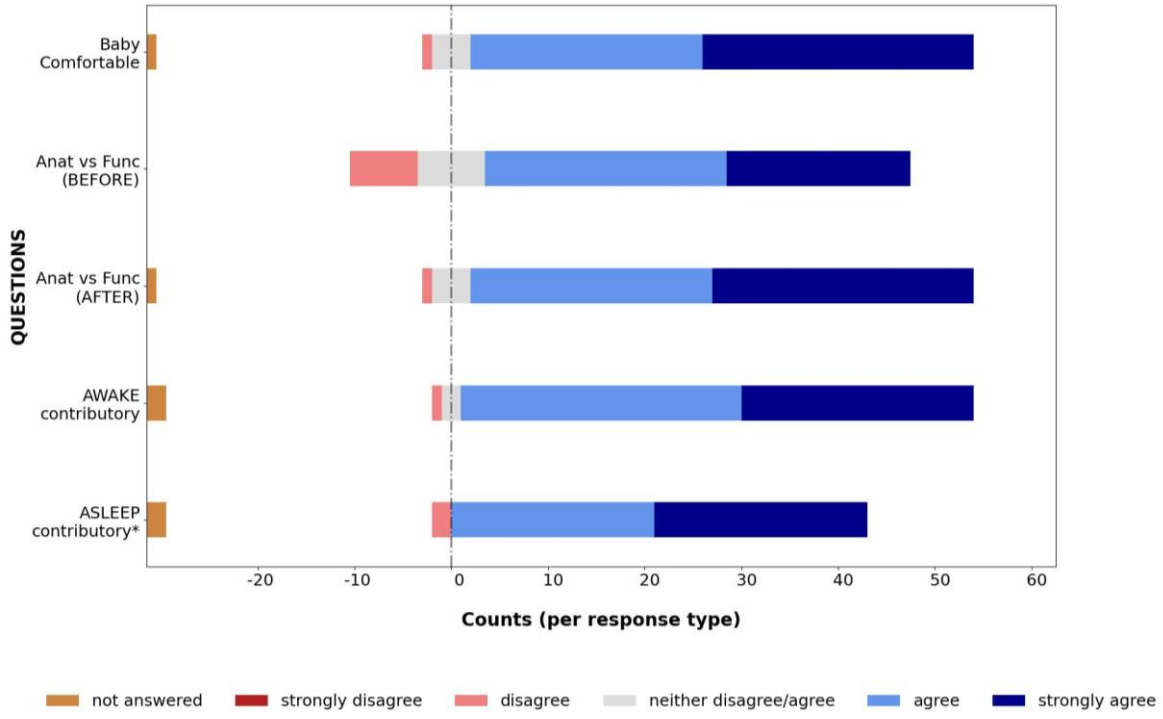

Figure 3-9 Parent feedback (58 of 63 possible respondents): Counts of answers to Likert-type questions

[* = out of the 47 respondents whose infant fell asleep]

3.6 DISCUSSION

It is hoped that brain functional MRI data captured during these awake infant fMRI (naturalistic movie clips and pictures) runs will allow the investigation of the emergence of semantic representation in infancy, allow longitudinal analyses (similar stimuli repeated at 9-month timepoint), allow a multitude of analytic approaches (time-coded models, model-free, and traditional connectivity analyses), and potentially shed light on typical and disrupted (NICU group) development.

To date, this current study's methods have resulted in 92 out of 100 infants achieving at least one full awake run with many infants providing multiple runs. It was seen that most 2-month-old infants stay awake and settled for approximately 15 minutes (average 2 complete video runs and 1 picture run) of awake task-based fMRI scanning. In this current study a median of 19.1 (IQR 8.4) minutes of awake fMRI data was acquired for the group. Importantly it was discovered that infants tolerated the movie runs better than the picture runs. This was likely due to the fact that movie clips are animate and dynamic while also possibly due to the fact that the movie clips were always presented first (element of ordering effect and participant fatigue perhaps). In a recent survey of 54 international expert researchers (81% from north America) in infant/toddler neuroimaging only 5 of the 54 experts responding had experience in awake task-based fMRI studies in infants (Hendrix and Thomason, 2022). These experts surveyed felt that 80-90% of scans resulted in usable data for young infants (< 3 months age) who underwent task-based fMRI scans (Hendrix and Thomason, 2022). This current study's results to date confirm the reported success rates of awake fMRI in this specific age group.

This study has discovered important practical consideration which it is felt have contributed greatly to this study's success:

Firstly, such was the importance of gaining an infant's attention at the earliest stage of the scan that it was decided to record field map sequences only after the first video run (5 mins) was achieved (and using the home screen distractor at the same time).

Secondly, it was seen that the ability to play audio into the infant headphones was a critical success measure as during periods of transition (awake and waiting for visual stimuli, or asleep and switching from fMRI gradients to anatomical quieter gradients) infants often benefited from lullabies or white noise to keep them in a relaxed/asleep state. Interestingly, it was realised that infants often woke up during the transition from resting fMRI (louder) to anatomical MRI (quieter) sequences due to the considerable drop off in volume of the gradient fields. Using audio input (white noise) during this transition achieved decreased rates of spontaneous waking at this important junction. In addition to audio input, the infant headphones used in this study had the capability of active noise cancellation, however it was discovered that the 'learning phase' needed at the start of the fMRI sequence was not amenable to maintaining a settled attentive awake infant.

Thirdly, despite prioritizing task-based awake runs, it was found that most awake infants ended up falling asleep (80% achieving resting-state fMRI) during the same session. This discovery is thought unique to this age group and should be considered for future infant fMRI study designs. Unlike other similar study paradigms (Ellis et al., 2020) this current study never attempted anatomical sequences when an infant was awake, opting instead to repeat task-based runs for as long as the infant remained comfortable and cooperative. In addition to achieving rsfMRI runs, 70% (52/75 controls and 18/25 NICU) achieved anatomical images, which was higher than expected, and so future similar paradigms should note this to allow design of analysis steps (registration of anatomical to template).

Fourth, this current study did not use real-time motion monitoring software but instead depended on the facial camera footage and the opinion of the researcher present in the scanner to decide whether excessive infant motion would warrant intervention (e.g. taking a break, changing stimulus, parent attending the infant). The motion (FWD) data of these first 100 participants compares well to thresholds used in previous studies. Compared to motion thresholds (0.5mm translation/rotation) used by the MIT group (Deen et al., 2017; Kosakowski et al., 2022) most of this current study's participants' awake frames (TRs) would not be scrubbed, with video runs being better than picture runs (Figure 3-6). Similarly, comparing to the Yale group (Ellis et al., 2021a, 2021b; Tristan S.

Yates et al., 2023; Yates et al., 2022), this current study's awake data would have few excluded frames (based on a 3mm translation threshold) and very few runs (participants) would be excluded. However, future awake infant scanning could consider the use of Framewise-Integrated Real-time MRI Monitoring (FIRMM) which has been shown to improve rates of usable fMRI data in sleeping infants (Badke D'Andrea et al., 2022).

Fifth, this study recognized the importance of the caregiver being visible by the infant during placement on the scanner table and encouraged the caregiver to stay nearby at-hand during the session (in the MRI control room). Caregivers watching (infant facial camera) and hearing (noise-cancelling microphone) their infant during a scan allowed parental feedback facilitating the adapting of the scanning protocol to meet the state of the infant (for example, switching back to movie stimuli if preferred over picture stimuli). It is felt that caregiver presence contributed towards correct decision making using the dynamic/flexible scanning protocol. Parents' attitudes surveyed were very positive towards the 2-month age scan visit with a dominant feeling that their infant was comfortable and provided usable data (self-reported). This positive parental feedback is important as it confirms acceptability of conducting infant MRI studies at this early age and as such it is hoped that this will ensure good ongoing attendance in this longitudinal study.

In the current study paediatric radiologists reported 2 (3%) of 67 infants with anatomical sequences having an incidental finding. This rate is similar to the median 3% (IQR 1.75 – 5.25%) reported by experts in a recent survey (Hendrix and Thomason, 2022). Recently the dHCP group reported a 47% incidental finding rate in their 500 healthy term infants scanned asleep (most findings consisting of subdural haemorrhage, punctate white matter lesions and caudothalamic sub-ependymal cysts) all of which had no clinical correlation/significance at Bayley Scales of Infant Development (BSID) at 18 months (Carney et al., 2021). The infants in the dHCP study were scanned within 1 week of birth, and as such the higher rates of incidental findings are likely in part explained due to this earlier proximity to birth date (i.e., resolution of birth related radiological findings had not yet occurred).

Finally, the infant fMRI community has recently published articles aiming to address the challenge of fetal, infant and toddler MRI research (Spann et al., 2023) and how the community of neuroscientists, neonatologists, radiologists and engineers are combining their expertise to advance learning in this cohort (Pollatou et al., 2022). It is hoped this report of this current study's methodology, and initial measures of success, adds valuable information to this collective effort.

CHAPTER 4 EXAMINING FUNCTIONAL CONNECTIVITY IN AWAKE AND ASLEEP INFANTS

4.1 ABSTRACT

Most infant fMRI studies to date have compared infant asleep connectivity to adult awake resting-state connectivity. In adults, it has been seen that functional connectivity has state-like components in that tasks modulate FC patterns in both the group and individual level. Recent literature has shown how asleep infants (6 to 12 months age) had functional connectivity resembling adult sleep more closely than adult awake state.

This study aimed to determine whether different functional connectivity patterns exist in young infants who are both asleep and watching movies (free viewing of naturalistic movies) in the same session, and whether a stimulus-evoked (shared) connectivity exists in movies state in young infants. Further, this study investigated if state difference in connectivity (i.e., movies minus asleep) accounted for any stimulus-evoked connectivity in the movies state. Whether findings differed between term born and preterm born infants was also assessed.

Infants (75 term born, 29 preterm born) attending as part of the FOUNDCOG project undertook MRI scanning at 2-months age (corrected age for preterm). Infants watched naturalistic movies (485 frames, 5 mins) during awake movies runs, and underwent asleep fMRI (1000 frames, 10 mins) if they fell asleep (76 infants). Within-subject similarity (WSS) was calculated as the Pearson correlation of each ROI x ROI (edge) across the timeseries (frames) for that infant. Inter-subject similarity (ISS) (stimulus-evoked connectivity) was calculated as the Pearson correlation of an infant's timeseries calculated pairwise between each infant's own run with all other infants' runs within a group. Final group connectivity matrices (400 by 400 Schaefer et al. ROI-level, and 14 by 14 Yeo et al. network-level) were calculated by averaging across all connectivity (WSS/ISS) from infants in a particular group (asleep/movies/term/preterm sub-groups).

Results showed that young infants had strong and consistent patterns of connectivity in both states (movies and asleep) measured in the same scanning session. In both asleep and movies states, the within network connectivity was higher compared to between networks (with visual, somatomotor, dorsal attention and salience ventral attention networks having the highest FC).

Compared to visual and somatomotor networks, lower within-network functional connectivity was seen in the limbic, control and default mode networks. Infants born preterm had similar connectivity in limbic network edges in both states (while term born infants had relatively lower limbic connectivity in the awake state compared to asleep state). Analysis showed how cortical edges containing the somatomotor and default networks (left/right/inter-hemispheres) dominated the pattern of stimulus-evoked (ISS) connectivity in term infants watching movies, while in preterm born infants this finding was limited to edges containing the somatomotor network only. State differences (movies minus asleep) in connectivity patterns did not appear related to the stimulus-evoked (ISS) connectivity seen (both term and preterm groups).

Overall, this study shows subtle differences in connectivity between asleep and awake (movies) states in young infants (term and preterm groups), and that these differences do not appear driven by a shared visual stimulus (the movie).

4.2 INTRODUCTION

4.2.1 Adult functional connectivity, task and arousal state

In adolescent/adult studies, resting state fMRI (rsfMRI) is usually acquired when participants are awake while letting their minds freely wander. The resulting resting state networks (RSNs) are dominated by low frequency BOLD signal fluctuations, have distinct spatial patterns and time courses. To some extent they appear to be invariant across mental state, as they are present even during sleep and anaesthesia (Vincent et al., 2007), and functional connectivity (FC) during resting and task evoke networks with many similarities in adults (Smith et al., 2009). However, there is also evidence that FC reflects a mixture of spontaneous and task-evoked activities. In a paradigm using MEG and fMRI during rest versus movie watching (task) in adults, it was seen that rest and task networks were different (Betti et al., 2013). In adults, it has been seen that functional connectivity has state-like components in that tasks modulate FC patterns in both the group and individual level (Finn et al., 2017; Gratton et al., 2018). In a further adult study of functional connectivity, it was seen that task-evoked activity is not independent from spontaneous activity, and that engaging in a task may suppress spontaneous activity and its inter-regional correlation (Lynch et al., 2018). This difference in connectivity between states is also seen at younger ages and in a study of children/adolescents different functional connectivity patterns were derived across states (resting/movies) which allowed a predictive model accurately determine state (resting versus movie watching) (Sanchez-Alonso et al., 2021)

Furthermore, when fMRI was acquired while adults were asleep, connectivity was found to be different to their awake resting-state patterns (Tagliazucchi et al., 2012), primarily in associative networks (frontoparietal control networks and default networks primarily) (Houldin et al., 2021; Spoormaker et al., 2012) reflecting the effects alterations in cognition/consciousness in sleep. Even when awake, adult resting state fMRI is susceptible to confounds due to differences in arousal, and indeed in children/adolescents studies bespoke movies commanding attention have been seen to improve compliance/data (Vanderwal et al., 2015).

4.2.2 Infant functional connectivity

Functional connectivity (resting/asleep) MRI does not require the performance of specific tasks in the scanner, thereby removing one of the most difficult obstacles in functional neuroimaging of the infant brain. Instead, fcMRI examines the temporal correlation of spontaneous blood-oxygen level dependent (BOLD) signals in the absence of any external tasks.

In a large longitudinal rsfMRI (asleep) study of infants during the first 2 years of life researchers showed that local FC and bilateral symmetric FC emerge in newborns (forming adult-like primary visual and motor-sensory networks), however higher-order FC networks experience dramatic long-range synchronization/connectivity during the infant postnatal period (Gao et al., 2015b). Indeed this infant developmental period was marked by a maturation sequence from primary sensorimotor/auditory to visual to attention/default-mode, and finally executive control networks (Gao et al., 2015a).

Despite the fact that functional networks in preterm born infants develop during rapid neural growth during the NICU period (third trimester period) (Doria et al., 2010), group-level differences within these functional networks have still been seen in infants born premature and scanned asleep at TEA (C. D. Smyser et al., 2016b). Multiple studies to date have shown alterations in functional connectivity network development associated with prematurity (Cao et al., 2017; Doria et al., 2010; Fransson et al., 2007, p. 20; Smyser et al., 2010). These infant fMRI studies carried out during sleep have reported weaker functional connectivity in preterm born infants, compared to term-born controls, in areas involved in motor function (Smyser et al., 2010) to regions associated with motor, cognitive, language, and executive functions (Gozdas et al., 2018) or frontal cortex and basal ganglia (Ball et al., 2016). These findings may be linked to the motor or other impairments observed in preterm infants with structural or microstructural brain lesions in the preterm brain (Linke et al., 2018; Rogers et al., 2018; Smyser et al., 2019).

Infant functional connectivity has been exclusively assessed in the sleep state. This is the most practical method of scanning in young infants (mitigating upset/movement) and experts agree that this method is largely successful up to approximately 3-4 months of age (feed & wrap technique) (Hendrix and Thomason, 2022). In recent years there have been a number of large projects which have included asleep infant fMRI analysis such as the Developing Human Connectome Project (http://www.developingconnectome.org), the Baby Connectome Project (http://babyconnectomeproject.org) and the ongoing HEALthy Brain and Child Development study (https://hbcdstudy.org/).

Despite the immaturity of long-range connectivity as newborns, the neonatal brain already shows early formation of resting-state networks and a significant overlap with the mature adult brain networks (81%) (De Asis-Cruz et al., 2015). Multiple infant studies have now consistently shown that infants demonstrate asleep functional networks similar to those of the large-scale functional network architecture seen in older paediatric and adult populations (Doria et al., 2010; Fransson et al., 2011, 2009, 2007; Lin et al., 2008; Smyser et al., 2010). However, most studies to date have been comparing infant asleep FC to awake adult resting-state connectivity. This difference in state presents a considerable confound.

In the very first awake infant fMRI study (Dehaene-Lambertz, 2002) brain activity evoked by speech was assessed in a small group of 3 month old infants, some of whom were awake and some asleep. This study showed that listening to speech activates a large subset of the temporal lobe, with a significant left-hemispheric dominance in both awake and asleep infants. However, additional activation in right prefrontal cortex was seen only in awake infants. This lack of prefrontal activation in asleep infants indicates the influence of infant state – perhaps attention - on the task. Attention has also been assessed in an event-related study of awake infants, aged 3 – 12 months, performing a visual cuing task. When attention was triggered/manipulated, fMRI activity showed that attention networks (frontal regions) activated more strongly for attention events. This effect was seen at 3 months, suggesting that these regions function early in development (Ellis et al., 2021b). However, these results also suggest that these networks are less engaged when an infant is in a state of less attention (with the extreme end of this spectrum being asleep) and has

associated implications for sleep/awake states in infant functional connectivity analyses.

These results hint at the fact that infant asleep state analysis should not be directly compared to adult resting state (awake) analysis. Indeed, one study has shown how asleep infants (6 to 12 months age) had functional connectivity resembling adult sleep more closely than adult awake state (Mitra et al., 2017).

The stage of sleep also impacts FC in adults, with results from one study providing support for contrasting functions for non-rapid eye movement (NREM) quiet sleep and rapid eye movement (REM) active sleep, wherein the adult brain is purposefully driven into a different FC configuration in NREM and is then returned to a wakefulness-like configuration in REM (Houldin et al., 2021). Sleep stage level can have an impact on FC in neonates also, and indeed a fNIRS combined with EEG study assessed FC in neonates and showed that inter-hemispheric FC was stronger during active sleep (REM) than quiet sleep, whereas intra-hemispheric short-range FC was enhanced during quiet sleep relative to active sleep (Lee et al., 2020). Indeed, the typical practice of measuring FC using MRI in infants during natural sleep may not be appropriate, since newborn sleep is physiologically heterogeneous and each sleep state is associated with a different functional connectivity network pattern (Tokariev et al., 2019, 2016). Further, different groups of infants cannot be presumed to sleep similarly, for example preterm born infants also demonstrate impaired sleep architecture, decreased sleep efficiency, and abnormal sleep patterns relative to their term-born counterparts at birth, at comparable post-conceptual ages (Eiselt et al., 1997; Horne et al., 2000).

It is likely that the variability in brain state during infant asleep studies has played a part in the heterogeneity of results, and indeed stability of the functional connectome in infants, across sessions, has been seen to be low-moderate when infants were asleep (Ciarrusta et al., 2021; Dufford et al., 2021b; Hu et al., 2021b; G. King et al., 2023; Q. Wang et al., 2021).

4.2.3 Inter-subject functional connectivity

Brain activity during a task reflects an unknown mixture of spontaneous and task-evoked neural activities. As such, the task-dependent FC should reflect the changes in both task-evoked networks and spontaneously emerging networks. If the task-dependent FC is due to the task-evoked activity, its pattern reflects the network interactions directly involved in information processing for task execution. If the task-dependent FC is attributed to ongoing activity, its pattern is driven by the brain's functional re-organization or adaption to facilitate the task (Lynch et al., 2018). Indeed in a simultaneous EEG and fMRI study in adults researchers observed that spontaneous alpha-rhythm power fluctuations largely explain task evoked fMRI response variance in extrastriate, thalamic, and cerebellar areas (Becker et al., 2011). Further task-evoked changes in FC patterns have been seen to allow the tracking of mental state in adults (windows as short at 22 seconds) with high accuracy (Gonzalez-Castillo et al., 2015).

In recent years, movies have been used in fMRI analysis in children. The idea of using movies to improve compliance is not new; labs and hospitals have been showing cartoons during structural MRI sequences to improve image quality and avoid sedation during paediatric scanning (Raschle et al., 2012). Using movies has been shown to improve compliance in a fMRI study involving 3 – 7 year old children (Vanderwal et al., 2015). As such, many fMRI studies in the last decade or so have used movies to investigate functional brain development in children aged approximately 4 years age or older (Table 1: (Vanderwal et al., 2019)).

Naturalistic stimuli carry rich information to engage subjects in a more behaviourally relevant context (unlike the task free resting state in adults) while inducing highly reliable responses within and across adult subjects (Finn and Bandettini, 2021; Gal et al., 2022; Hasson et al., 2010, 2004; Sanchez-Alonso et al., 2021; Vanderwal et al., 2019). The most commonly used naturalistic stimuli in paediatric research has been movies which provide a compelling mixture of visual and auditory events to maintain the child's cooperation (e.g., language, face processing, social interactions, different camera angles, music) and are amenable to FC analyses (i.e., identification of spatially separate brain regions or voxels that have correlated BOLD signal time-courses) (Sanchez-Alonso et al., 2021).

Hasson et al. described the idea of a time-locked stimulus shared across participants and the associated intersubject correlations (ISCs), in which the BOLD-signal time course in voxel A of subject 1 is correlated with the time course in voxel A of subject 2, and so on (Hasson et al., 2004) (Figure 4-1). Building on the work by Hasson et al., Simony et al. proposed the use of intersubject functional connectivity (ISFC) during sustained and naturalistic stimulation to extract task-evoked functional connectivity without contributions from ongoing activity or non-neuronal noise (Simony et al., 2016) (Figure 4-1).

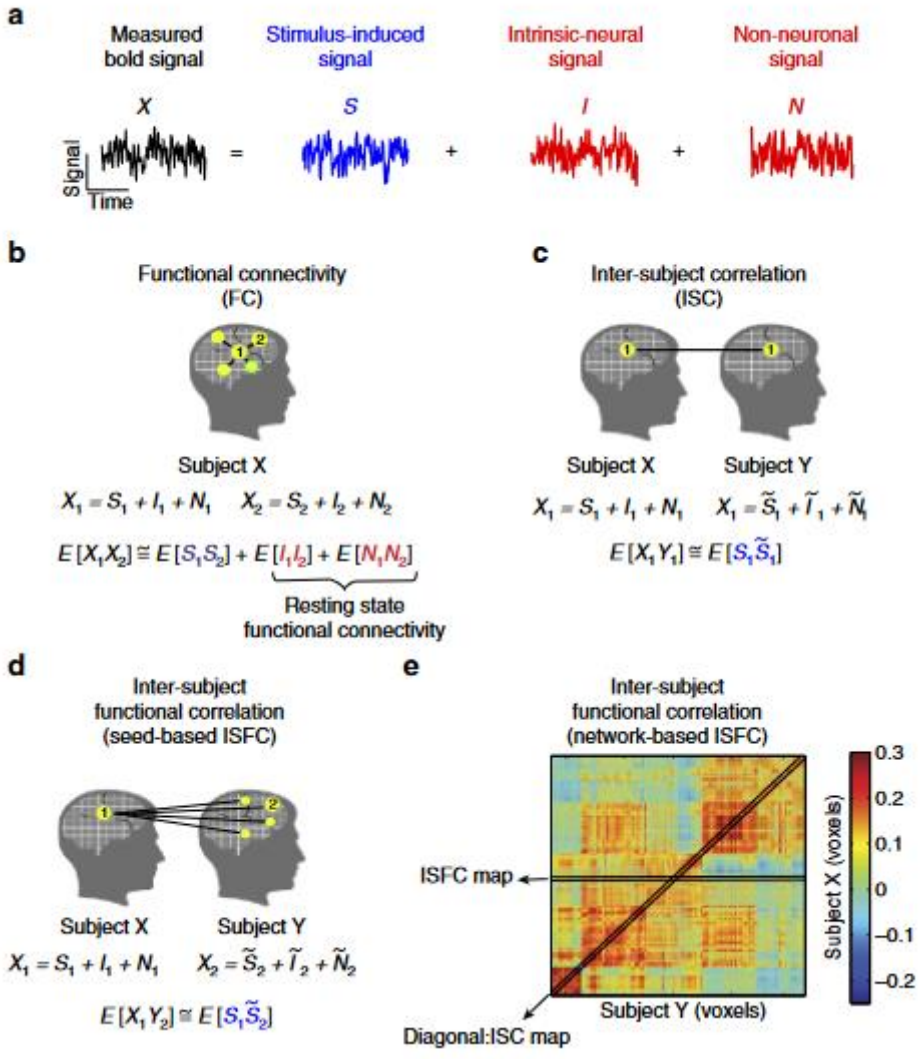

Figure 4-1 Inter-subject functional correlation (ISFC) method.

***Simony, E., Honey, C.J., Chen, J., Lositsky, O., Yeshurun, Y., Wiesel, A., Hasson, U., 2016. Dynamic reconfiguration of the default mode network during narrative comprehension. Nat Commun 7, 12141. https://doi.org/10.1038/ncomms12141*. (a) During task processing the measured BOLD signal can be decomposed into stimulus induced signal (blue),**

intrinsic neural signal (spontaneous fluctuations) and non-neuronal signal (for example, physiological noise) (red). (b)Seed-based functional connectivity (FC) is the Pearson correlation between a time course extracted from a seed region (1) in subject X, and all other regions in the same subject, for example, region (2). This can be estimated as the sum of stimulus-induced correlations (blue) and intrinsic neural correlations (red), which are difficult to separate. (c) Point-to-point inter-subject correlations (ISC): stimulus-induced correlation (blue) between time courses from the same region (for example, region 1) across subjects X and Y. ISC reveals stimulus-induced within-region correlations that are shared across subjects. (d)Seed-based ISFC is the Pearson correlation between a time course extracted from one region in subject X and all other regions in subject Y (for example, Region 1 in subject X versus region 2 in subject Y). (e) Network-based ISFC are the Pearson correlations between a network of brain regions in subject X and a network of brain regions in subject Y. This correlation matrix computed across brains (the diagonal represents ISC) filters out intrinsic and non-neuronal correlations and highlights stimulus-induced inter-regional correlations that are shared across subjects.

The ISFC method has unique strengths in that it requires few assumptions about the structure of the stimulus (which features are important) or the neural response (the haemodynamic response) and so can achieve strong stimulus-driven signal (Finn, 2021). This may lend itself to infant fMRI analysis.

Combining the ISFC method and naturalistic paradigms (movies) can produce rich neural responses in both shared (inter-subject) (Nastase et al., 2019) and idiosyncratic components (Finn et al., 2020). Already, in older children, ISFC has been shown to correlate strongly with behavioural/developmental outcomes such as cognition scores in children 3 – 12 years old (Richardson et al., 2018), age, and measures of attention in children 4 – 6 years old (Moraczewski et al., 2018).

4.2.4 Aim and Objectives

The aim of this study was to assess at the group level, the possibility that functional connectivity MRI analysis in awake infants attending movies in the scanner may contain different and rich information compared to asleep data alone. This study therefore aimed to compare functional connectivity patterns between sleeping and awake movie watching in young infants. To achieve this aim the following objectives were tasked:

- To determine whether functional connectivity showed different patterns in asleep state versus movies state (free viewing of naturalistic movies)
- To use the inter-subject functional connectivity method (Hasson et al., 2004; Simony et al., 2016) to attempt to isolate stimulus-evoked changes in connectivity, by determining if there is a shared connectivity and if so, whether the connectivity is significant at the group level, and what cortical pattern does this shared connectivity take.
- To see if a state-independent (across-state) connectivity exists, and if so to compare this state-independent connectivity to any connectivity shared within states.
- To investigate if state difference in connectivity (i.e., movies minus asleep) accounts for any task-evoked (shared) connectivity in the movies state in these young infants.
- To assess whether preterm born infants (scanned at 2 months corrected age) have different findings (these objectives) to term born infants (scanned at 2 months age), and if so, what is the difference in magnitude or pattern of any differences.

4.3 METHODS

4.3.1 Participants

The first 100 infants recruited as part of the FOUNDCOG study were included. This consisted of 75 term controls and 25 graduates of the NICU (see previous, Figure 3-4). To allow more data representing the preterm group, four additional NICU participants (scanned Oct – Dec 2022) were included in the preterm group (in addition to the first 25 NICU participants). Details of the detailed practical setup for awake (movies) and asleep infant fMRI scanning are given previously in this thesis (Chapter 3).

Infants attended for scanning at 2 months post-menstrual age (all infants born either term or preterm were each corrected to their PMA). All infants were scanned in the same Siemens Prisma 3T MRI scanner in the one visit/session. For as long as the infant remained awake and attending the stimuli, two awake run paradigms were alternated, starting with movies run and then pictures run. As movies runs were achieved more successfully (more runs achieved and less motion) and as the 6 movie clips were at least 23 seconds duration, it was felt that this awake task run was best placed for analysis of functional connectivity (rsfMRI) in this infant population (picture runs were not included in this analysis). If the infant fell asleep, we acquired resting-state fMRI (1000 volumes) and then a T2-weighted anatomical sequence, as detailed previously in this thesis (Chapter 3). These infants fell asleep naturally (no sedation) having commenced the session awake.

4.3.2 State/Stimulus

All infant movie and asleep data came from distinct functional runs (i.e. no concatenation of volumes/frames). Movie runs were collected while infants watched 6 short movie clips. Movie runs meeting the motion criteria were 5 min (485 volumes) long. Infants' eyes were approximately 30 cm away from the projected image, and the image proportions were chosen to ensure that the images appeared within the 30-degree visual field angle and salient elements

of the visual scene were large and central in the image. Audio input was included and consisted of the audio of the movie-clip (ANC was not included).

The order of the 6 movie clips (23 seconds each) an infant saw were randomly chosen (counterbalanced as the study progressed) to make up the 5 minute movies run. Despite infants seeing different orders of movie clips (during the 480 frames/5 mins), we collapsed across all 6 movie clips to assess the "general effect" of awake movie watching on functional connectivity, and to allow increased power in our analysis. While some would have concern that this collapsing would confound the interpretation of results, a previous study in 10 healthy adults viewing four distinctly different movies showed the frontoparietal network becoming more integrated with other networks during movies and did not differ significantly across the four conditions/movies (Vanderwal et al., 2019). While the exact timings of the visual images during the movies run were not relevant for analysis, it was important to ascertain whether the infant participants attended the images during the movies run. This assessment has been conducted at the group level (see Section 3.5.4) and has shown that for approximately 85% of the time during a movie run infants were interested in and using their eyes to scan the visual image in front of them (with fussing/crying approximately 4% of the time). Future work will involve including/excluding specific movie runs for analysis based on the predominant infant state/behaviour in the corresponding facial camera footage.

As has been shown previously in this thesis (3.5.4.3 Infant attention), the tag 'interest_scanning' (i.e. the infant was interested in and conducting eye scanning of the visual stimulus) was tagged approximately 85% of the time (while 'fussing' and 'vocalizing' was tagged approximately 4% of the time) in the movies runs.

Infant asleep runs were collected during natural sleep with the display turned off, without visual stimulation. Sleep state was not assessed by EEG/other, but all infants were assumed to be asleep based on extended eye closure and stillness, as viewed both by the researcher in the scan room, and online via an MR-safe camera (radiographer controlling the MRI run). The asleep fMRI run was stopped as soon as it was felt that the infant was no longer asleep. Asleep

runs were 10 min long (1000 volumes). Asleep runs (surviving motion thresholds) were successfully obtained in 76 infants (56 term controls and 20 preterms). To match the movies run duration, only one portion of the asleep run was chosen (i.e. a portion of 480 consecutive frames).

4.3.3 Code

The code used for pre-processing, data handling, analysis, statistics, and output graphics is available at (please contact to request access permissions): https://github.com/Grahamgithubking/foundcog_pipeline/tree/master/graham_code

4.3.4 Pre-processing

For fMRI runs the CMRR (https://www.cmrr.umn.edu/multiband/) gradient-echo multiband EPI sequence was used (acceleration factor 4), 3 x 3 mm in-plane, 36 slices of 3 mm plus 10% gap, phase encoding anterior-to-posterior, repetition time (TR) 610 ms, echo time (TE) 32 ms, flip angle 40 degrees, echo spacing 0.54 ms.

MRI data were converted from DICOM to NIfTI format using dcm2niix (https://github.com/rordenlab/dcm2niix) (Li et al., 2016). The FMRIB Software Library FSL was used in the pre-processing steps (Smith et al., 2004).

Motion was determined using FSL MCFLIRT (Jenkinson et al., 2002), using the middle volume as the standard reference, and the 6 motion parameters (3 translation, 3 rotation) were used to calculate framewise displacement (FWD, in mm) (Power et al., 2012) using Nippype software algorithm (Gorgolewski et al., 2011).

Two spin-echo reference protocols were acquired for distortion correction each time the infant was positioned in the head coil (i.e. once per session), one with phase encoding anterior-to-posterior and the other posterior-to-anterior, with

the same geometry as the fMRI run but without multiband for better tissue contrast (TR=2,260 ms, TE=32 ms, FA=40 degrees, 10 volumes).
Following motion correction with FSL MCFLIRT, the field distortion estimation from FSL TOPUP (Andersson et al., 2003) was then applied to the EPI data to correct for susceptibility distortion. One subject (of these 100 participants) was excluded due to failing to obtain field maps.

As a T2-weighted anatomical scan was not presumed/expected during the session (not needed as an inclusion criterion) a bespoke method of co-registration/normalisation of the functional images was devised. To allow co-registration of a subject's multiple fMRI runs, a co-registration reference run was chosen (with asleep/resting state being the preferred co-registration run in any subject who had both resting state and movie runs). The mean of this chosen run was used as the co-registration reference. The mean images of a subject's other runs were then co-registered (FSL FLIRT) using 12 DOF. Using the transformation matrices (from these co-registrations) the mean image of each run was re-oriented (applyXFM) to the space of the reference run. Averaging (ants.AverageImages) these mean images produced a single average volume in the reference space.

For spatial normalisation to a common group space, a 2 – 5 month age infant T2-weighted template was used (Fonov et al., 2009). Using FSL FLIRT (cost function=mutual info, DOF=12) the single average volume was linearly registered (normalised) to the infant template. Combining both transformations (using fsl.utils.ConvertXFM) a subject's distortion corrected (FSL TOPUP) functional runs were then both co-registered to the reference run and normalised to the template (applyXFM). The runs were then smoothed using a gaussian kernel (FWHM=5.0) using fsl.SMOOTH to allow for inaccuracies of spatial normalisation. Of note, functional runs were not slice time corrected as the TR was short at 0.61sec, and a multiband EPI sequence was used. Global signal reduction (GSR) was not applied as this analysis aimed at determining differences between groups of infants with different noise characteristics and so the effect of GSR was not certain (Murphy and Fox, 2017).

4.3.5 Quality Control

Infants were excluded in analysis if they had known structural abnormalities on previous anatomical MRI (while in the NICU) or current anatomical MRI (if T2-weighted scan achieved) scans. As a result, this excluded four NICU infants from the dataset.

To check adequacy of the co-registration/normalisation step the single average volume (EPI image) for a subject (in the template space) was overlayed on the segmented (csf/grey/white matter) infant template. Quality control consisted of checking this fit for all subjects. One subject was excluded due to poor normalisation to template.

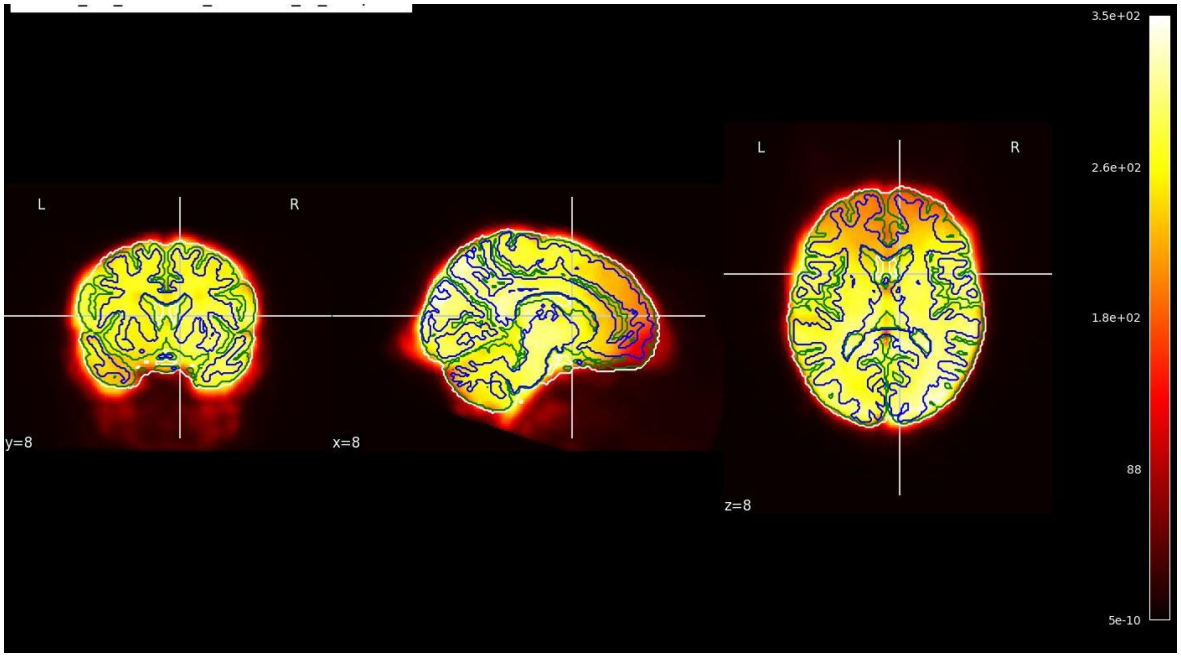

Figure 4-2 Quality Control (repeated for each subject): overlay of the single average volume (EPI) for an example subject on the segmented infant template.

For the 77 infants (of 100 participants) who did provide a T2-weighted anatomical scan (not presumed/expected) during the session, the T2-weighted anatomical image (co-registered to the reference run and transformed to the template using the same transformation as the EPI data) was also used as quality control check. This allowed determination of adequacy of grey/white matter fit.

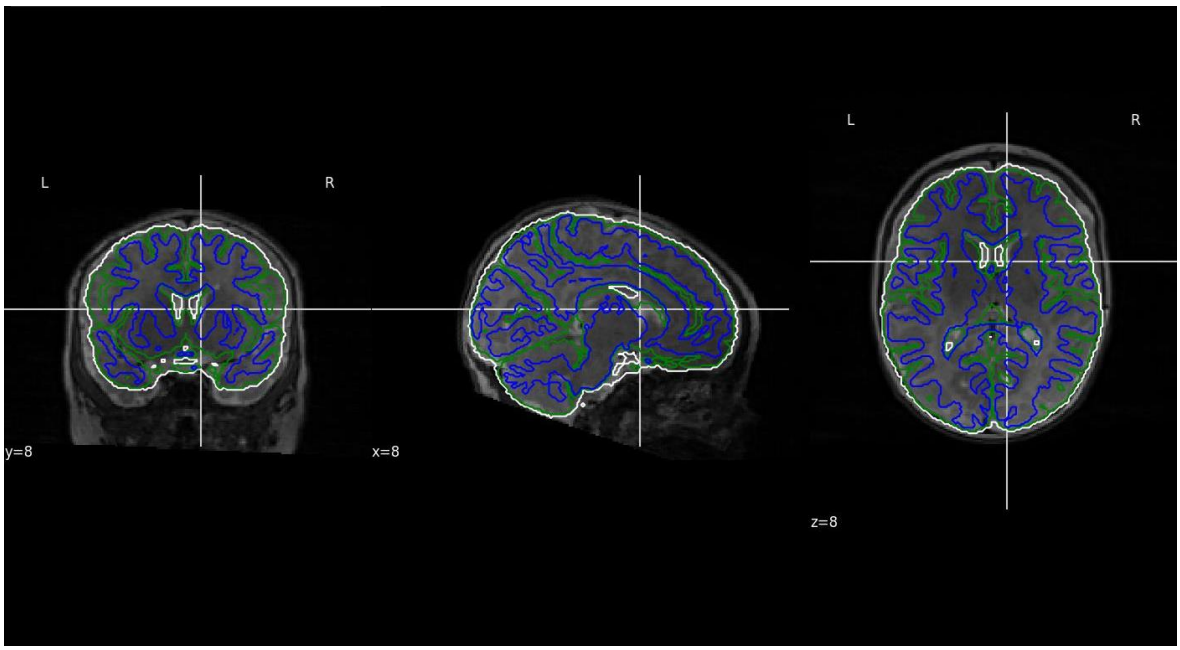

Figure 4-3 Quality Control (77 of 100 subjects): overlay of the T2-weighted anatomical for an example subject on the segmented infant template.

Further, it was noted that the shipped NIHPD 02-05 template mask was not including a considerable amount of the infants' temporal lobes. As such the mask was manually edited to allow inclusion of the missing parts of the temporal lobes. This manually edited mask was used to adjust the T2-weighted template used for normalisation to template. The co-registration/normalisation step was repeated for all runs/images using this updated/edited T2-weighted template.

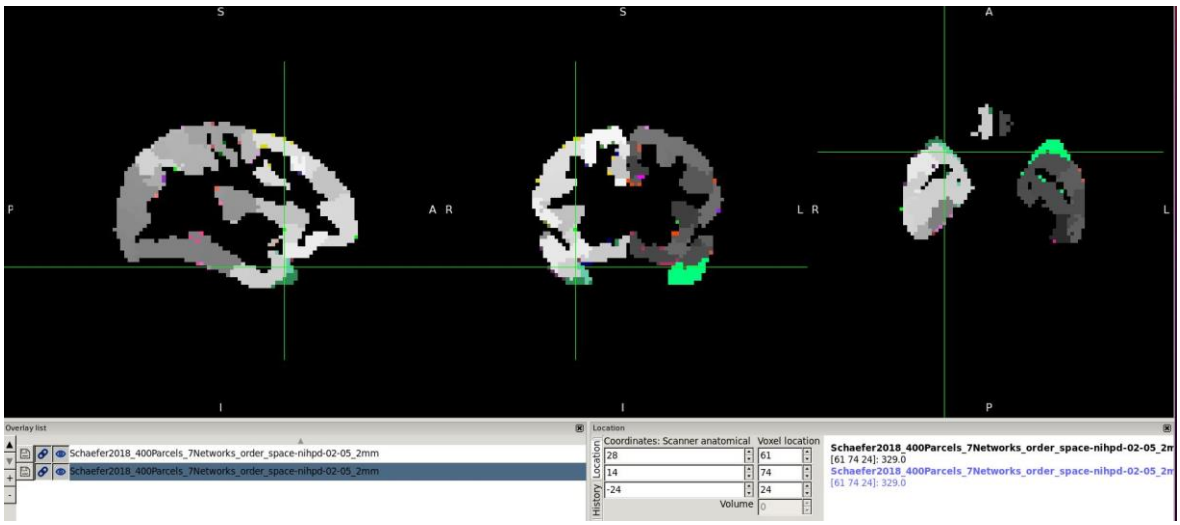

Figure 4-4 View of the manually added/edited mask (green) of the NIHPD 02-05 month infant template.

4.3.6 Motion threshold

In keeping with other recent studies (Ellis et al., 2021b; Yates et al., 2022) in awake infant fMRI a FWD threshold of 3mm was chosen. However, where other awake studies have usually kept runs with 50% of volumes meeting this threshold, we instead required that less than 10% of volumes could meet this threshold (in keeping with the approximated number of similar volumes in the asleep runs). This motion threshold criterion was termed 'standard motion threshold'. In further/stricter analyses (termed 'stricter motion threshold') we limited this FWD threshold to 0.5mm (i.e. less than 10% of volumes of the whole run were allowed to have 0.5mm FWD or greater, for the run to be included).

4.3.7 Brain parcellation

The Schaefer 400 parcellation (7 networks) atlas (Schaefer et al., 2018) was used for parcellation. Details of these parcels/networks can be found in the appendix [See Appendix]. This is an adult parcellation based on the 7 functional connectivity networks as determined by Yeo et al. (Thomas Yeo et al., 2011a). The 7 functional networks consist of: visual, somatomotor (smtr), dorsal attention (dsattn), ventral attention (sva), limbic, frontoparietal control, and default networks.

Table 4-1 Number of parcels per functional network

Functional Network	No. parcels in network
LH_visual	31
LH_smtr	37
LH_dsattn	23
LH_sva	22
LH_limbic	13
LH_control	22
LH_default	52
RH_visual	30
RH_smtr	40

RH_dsattn	23
RH_sva	25
RH_limbic	13
RH_control	30
RH_default	39

Left hemisphere (LH), right hemisphere (RH)

To construct individual functional connectivity matrices, we averaged BOLD activity over all voxels in each parcel. This signal extraction was conducted using nipreps (https://www.nipreps.org/niworkflows/1.0/api/niworkflows.interfaces.images.html).

4.3.8 Functional connectivity

Functional connectivity was examined at the group level (FC matrices of the average FC across a group) for initially term born infants (healthy controls), and then separately for preterm born infants (NICU graduates).

As the movie runs were 480 TRs (volumes) in duration (5 initial volumes were discarded due to T1 equilibrium effects), the asleep runs were therefore similarly shortened to 480 consecutive TRs in length. This was so that both movies and asleep runs would contain the exact same number of volumes. Any infants with repeat sessions of movie watching (meeting the motion threshold criterion) had the session with the lowest mean FWD chosen as the selected session representing that infant.

4.3.8.1 Within-subject similarity (within state)

Within-subject similarity (WSS) was calculated as the Pearson correlation of the timeseries for a parcel with every other parcel across the number of TRs (volumes) within the subject's own run. The group-level connectivity was calculated as the mean of all subjects' WSS in the group. Group-level connectivity matrices were created by averaging across each infant in the group.

4.3.8.2 *Inter-subject similarity (within state)*

To calculate inter-subject similarity (ISS) within each state (asleep-asleep, movie-movie) the inter-subject functional connectivity method was used (Hasson et al., 2004). Pearson correlation of the timeseries was calculated pairwise (between each subject's own run with all other subjects' runs) within the group (avoiding autocorrelation with self/same subject). The pairwise correlation was taken as the average of the two (400 by 400) off-diagonal matrices from the correlation (800 by 800) array. The group-level shared similarity was calculated as the mean of all subjects' ISS in the group. To prevent leak (autocorrelation with another subject of similar characteristic) any sub-groups (e.g. preterm/term) were strictly pairwise correlated (ISS) with only subjects from their respective sub-group. Final connectivity matrices (400 by 400) were created by averaging across all infants in the group.

4.3.8.3 *State-independent similarity (across states)*

To calculate similarity across states (asleep-movie), we used inter-subject functional connectivity (Hasson et al., 2004) by Pearson correlating the timeseries between each subject's own run (in one state) with all other subjects' runs in the other state (avoiding autocorrelation with self/same subject). This was to assess whether there was any shared/evoked functional connectivity that was independent of the infant's awake/asleep states. This across-states similarity was termed 'state-independent similarity' (SIS).

4.3.8.4 *Connectivity resolution*

For both awake and asleep analyses connectivity was examined at the Schaefer et al. parcel level (400 by 400) and the Yeo et al. 7-network level (14 by 14, as each network was separated into hemispheres). Network level connectivity was determined by calculating the arithmetic mean of the corresponding parcels of the 2-dimensional parcel level connectivity array. Parcels located on the leading diagonal (within parcel timeseries correlation) of the parcel level array (400 by 400) (i.e. value of '1') were not included in the arithmetic means for their respective networks.

To examine the within (intra-) network connectivity compared to the inter-network connectivity (Yeo et al. 7 networks), the intra-network connectivity was

taken as the value of the main diagonal of the 14x14 network level FC matrix. The inter-network connectivity was calculated as the average connectivity between the selected network and the other 13 networks (including left and right hemispheres) in that row of the FC matrix.

4.3.9 Timeseries signal cleaning

As less than 10% of volumes were allowed to meet the FWD threshold (i.e. 90% of volumes had to be below the chosen FWD threshold) in any run (movie or asleep), it was decided to keep the 480 consecutive volumes/frames intact, and no volume scrubbing/censoring was applied. As the segment length was relatively short (480 volumes) and the high pass filter was 0.01Hz, it was considered that there was no real need to detrend the segment.

4.3.9.1 Signal cleaning for Within-subject (Individual) Similarity

Steps of signal cleaning for WSS included the following (in order): band pass filtering; confound regression; and z-scoring.
For band pass filtering the signal was filtered between 0.01 and 0.1 Hz (as is common in infant/child connectivity literature). For confound regression the corresponding motion parameter file (FSL MCFLIRT motion correction) containing estimated 3 rotations and 3 translations for each TR was uploaded. Confound regression includes fitting a linear model using motion estimates as regressors then subtracting it out from the signal. The output was z-scored meaning the timeseries were shifted to zero mean and scaled to unit variance.

4.3.9.2 Signal cleaning for Inter-subject (Group) Similarity

For ISS, steps of signal cleaning were limited (as by the nature of correlation across subjects, it is only the task-evoked signal that is shared, and not noise). As such signal cleaning steps included: band pass filtering (0.01 – 0.1 Hz); z-scoring the output. Confound regression of motion parameters was not included (unlike in the case of WSS).

4.3.10 Network Edge Dissimilarity – Calculation

To determine how dissimilar network-level edge connectivity was comparing one edge to all other edges, Welsh's t-test (unequal variance t-test) was used (Equation 7). This was calculated using the sample of connectivity values (all infants) for that edge and comparing it to the sample (all infants) of the average connectivity of all other edges (except that edge). Welsh's t-test results in a ratio where the numerator is the difference in the means between two samples, and the denominator is the dispersion/variability of the two samples. The higher the t-test value the more dissimilar that edge compared to all other edges.

$$t = \frac{\overline{X}_1 - \overline{X}_2}{\sqrt{\frac{s_1^2}{N_1} + \frac{s_2^2}{N_2}}}$$

Equation 7

$\overline{X}$ = mean of sample
s^2 = variance of sample
N = number of data points in the sample

To visualise the dissimilarity (t-test values) for each edge (network-level), and to compare inter-hemispheric and inter-network patterns, Circos plots were created using pycirclize for python (https://moshi4.github.io/pyCirclize/).

4.3.11 Significance testing

To determine significant parcel-parcel (Schaefer et al. 400 parcels) or network-network (Yeo et. al 7 networks) edges/connections, the group mean was bootstrapped (1,000 resamples). The bootstrap python function from SciPy (SciPy v1.14.0 Manual, n.d.) was used. This returned the bootstrap distribution (i.e. the values of the mean for each of the 1,000 resamples).

Table 4-2 SciPy function parameters for bootstrapping

Statistic	Mean
Vectorized	True
Axis	0 (first dimension of 3D array)
N_resamples	1,000
Batch	10
Method	'basic'
Random state	Numpy random number generator

Significance (p values) were determined using a 1-tail test for each of the positive or negative correlation values respectively. The proportion of the 1,000 resamples (bootstrapped distribution) of the statistic (mean) that had the opposite direction (positive/negative) to the original value (i.e. that were less than zero for originally positive correlations) gave the p-value for the positive correlations. Likewise, the proportion of the 1,000 resamples of the statistic that had the opposite direction to the original value (i.e. that were greater than zero for originally negative correlations) gave the p-value for the negative correlations.

To allow for multiple comparisons correction (105 comparisons for network-level analysis and 80,200 comparisons for parcel-level analysis), the 'FDRcorrection' python function from Statsmodels (Statsmodels, n.d.) used the Benjamini/Hochberg method for independent or positively correlated tests (Benjamini and Hochberg, 1995).

Table 4-3 Parameters for Statsmodels multiple comparisons correction function

Alpha (family-wise error rate)	0.025 (1-sided)
Method	Poscorr#
Is_sorted	False

These corrected p-values were used to determine the significant values of the group mean connectivity matrix (two-tailed p-values=0.05). Functional connectivity matrix edge values were displayed where $p<0.05$ (otherwise matrix edge values were set to 'nan').

For a difference is group means, on each bootstrap resample, the mean from one group was subtracted from the mean of another group to create a sampling distribution of the mean difference. The p-values were defined as the proportion of resamples with the opposite sign of the original effect (x2 for 2-tailed t-test). Similarly, these p-values were corrected for multiple comparisons (as previously).

4.4 RESULTS

4.4.1 Impact of T1 equilibrium effects on movies runs

For any full movie run, the EPI timecourse (averaged across all 400 ROIs) and the corresponding full FWD file were plotted as % change relative to the mean for the run (black lines). Further, the group average EPI and FWD timecourses were plotted as % change relative to the mean for the group averages.

In total 95 infants contributed timecourses to this analysis (dark shaded areas). An increase in the EPI values was noted for the first 5 TRs (Figure 4-5). This is thought to be due to T1 equilibrium effects of the EPI sequence. As a result of this realisation, all data used from movies runs was taken from the 5th TR (volume) onwards, in order to mitigate this T1 equilibrium effect.

Thereafter, the EPI signal increased slowly until the mid-point of the run, followed by a slow decrease in the signal in the second half of the run. The inverse is seen in the FWD values (slightly less FWD until the mid-point, followed by slowly increasing FWD through the second half of the run) (Figure 4-5). It is felt that the novelty of the first movie clip (first half of the run) and including the mid-point attention-getter, both commanded attention (less FWD). Following the mid-point of the run (second half) an infant got slightly less attentive (more FWD).

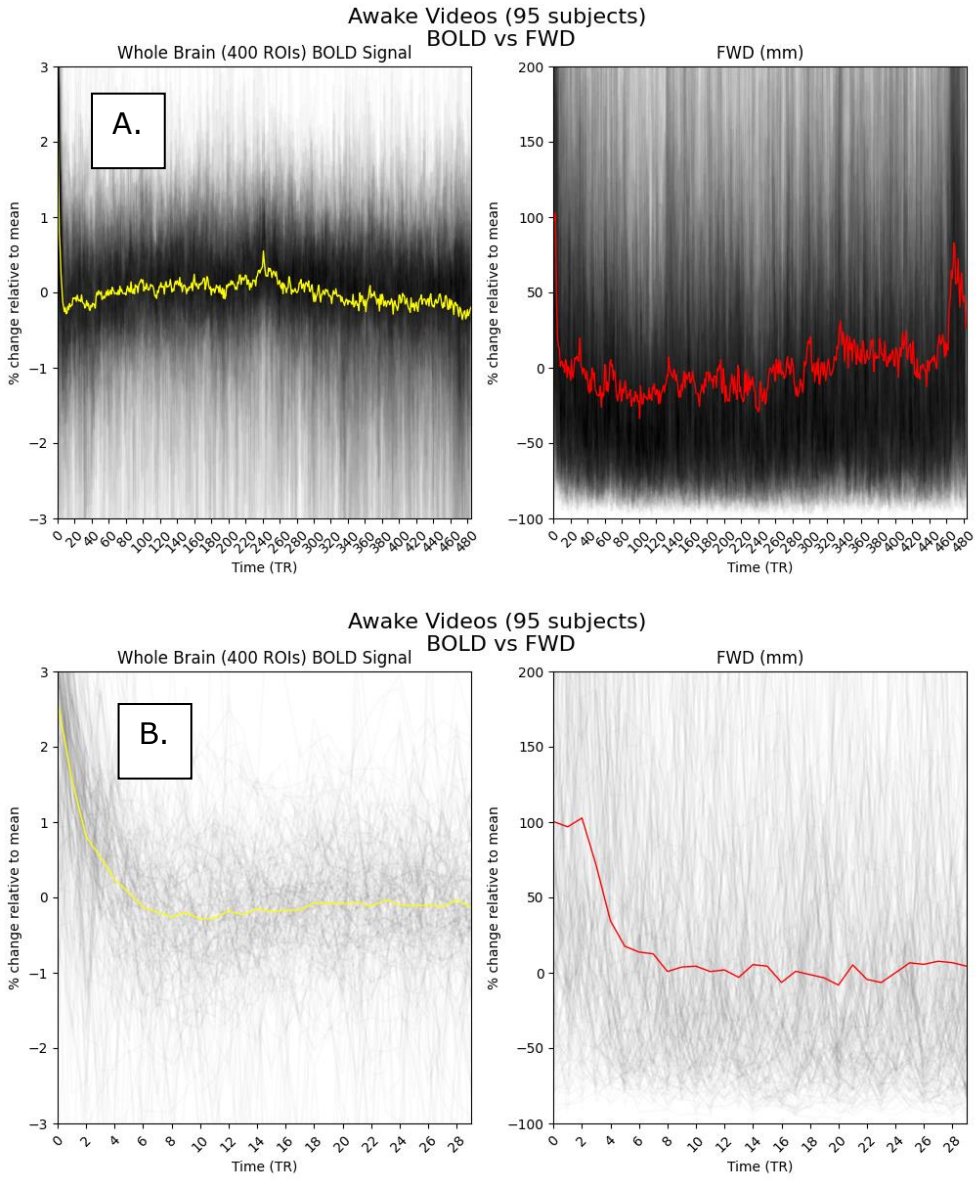

Figure 4-5 Movies runs: change in EPI signal and FWD over time.

Change in EPI signal (% change relative to mean) and change in FWD (% change relative to mean) over time (TR). Individual subject's BOLD/FWD is in transparent grey. Group mean (95 subjects) signal is in yellow (BOLD) and red (FWD). A) Full movie timecourses (0-485TRs); B) x-axis zoom of the first 30 TRs (0-30TRs) of a movies timecourse.

4.4.2 Impact of early movement on asleep runs

For any full asleep (resting state) run the EPI timecourse (averaged across all 400 ROIs) and the corresponding full FWD file were plotted as % change relative

to the mean for the run (black lines) (Figure 4-6). Further, the group average EPI and FWD timecourses were plotted as % change relative to the mean for the group averages.

In total 76 infants contributed timecourses to this analysis. As seen previously in both movies and asleep runs, there is an increase in BOLD signal for the first 5 TRs (T1 equilibrium). In addition, in the asleep runs, the predominant pattern is a lower BOLD signal for the first approximately 60 TRs (Figure 4-6). This is thought to be due to an asleep infant's early sleep state at the start of the run. Infants had been awake watching movies and had just fallen/transitioned to asleep. As a result it is likely that they transitioned to a state of active sleep (rapid eye movement sleep) with associated motion (Uchitel et al., 2022). This motion can be seen with the corresponding drop in BOLD signal (slowly recovering) over the period. Realising this, the first 64 frames (i.e. 5 TRs due to T1 equilibirium effects plus 59 TRs due early motion in sleep) of the asleep EPI run were avoided in further analyses.

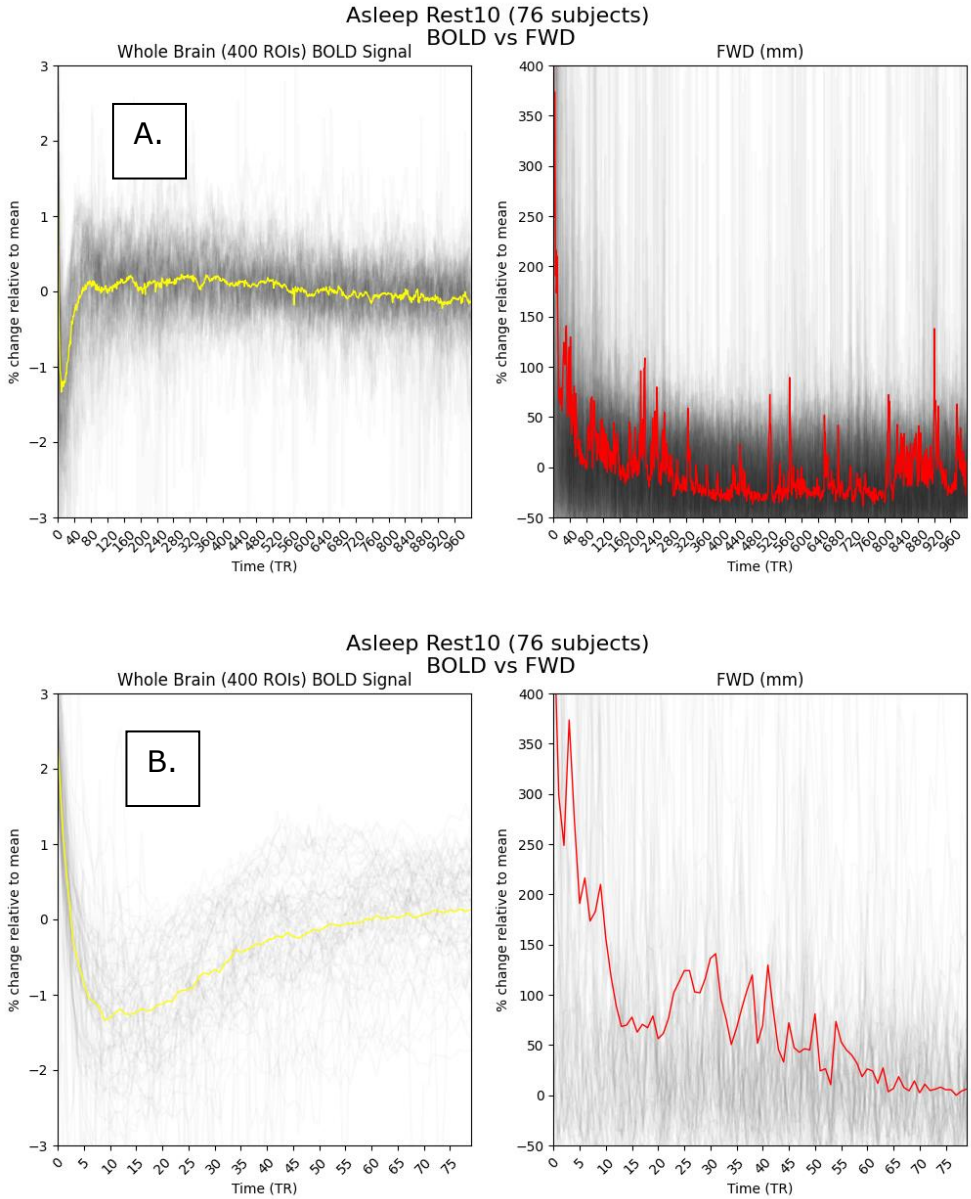

Figure 4-6 Asleep runs: change in EPI signal and FWD over time.

Change in EPI signal (% change relative to mean) and change in FWD (% change relative to mean) over time (TR). Individual subject's BOLD/FWD is in transparent grey. Group mean (76 subjects) signal is in yellow (BOLD) and red (FWD). A) Full asleep timecourses (0-1000 TRs); B) x-axis zoom of the first 80 TRs (0-80 TRs) of an asleep timecourse.

4.4.3 Participants contributing functional runs

The first 75 term control participants were included (as seen previously Figure 3-4). To allow more data representing the preterm group, four additional NICU participants (scanned Oct – Dec 2022) were included in the preterm group (in

addition to the first 25 NICU participants, seen previously Figure 3-4). Of the 75 control participants, two did not have any functional MRI data. Of the 29 NICU (preterm) participants: one was excluded due to not having field maps; four were excluded due to having known structural brain pathology; and one was excluded due to poor registration to template. The remaining 96 infants (73 controls, 23 NICU) had functional runs (movies and asleep) assessed to see if they met the defined motion thresholds for inclusion. The number of participants contributing runs meeting the standard motion threshold are shown in Figure 4-7. The number of participants contributing runs meeting the stricter motion threshold are shown in Figure 4-8.

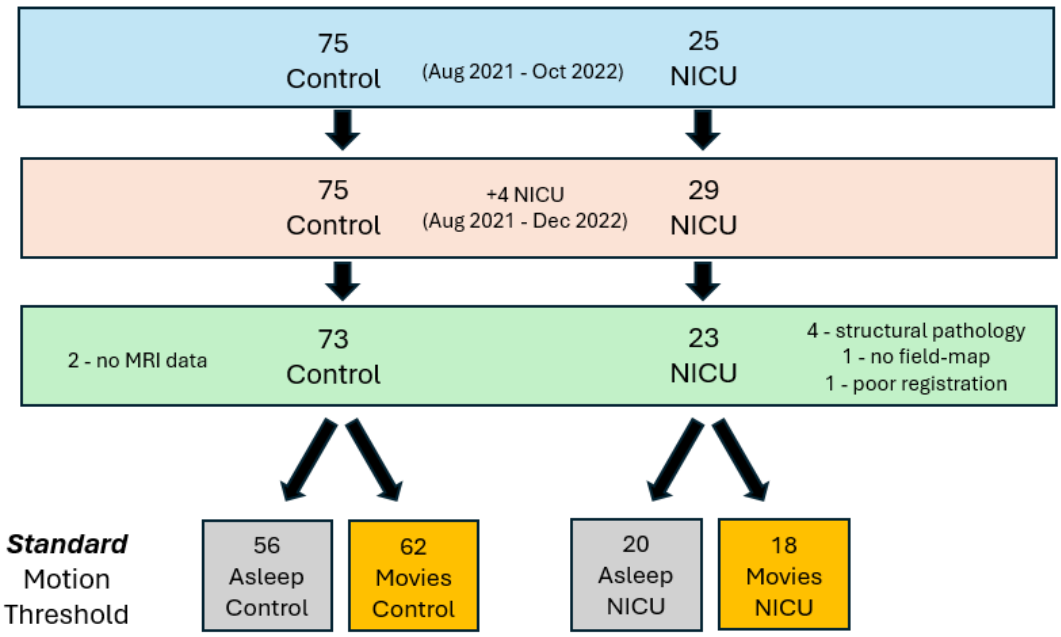

Figure 4-7 Number of participants (Control/NICU) contributing runs meeting the standard motion threshold

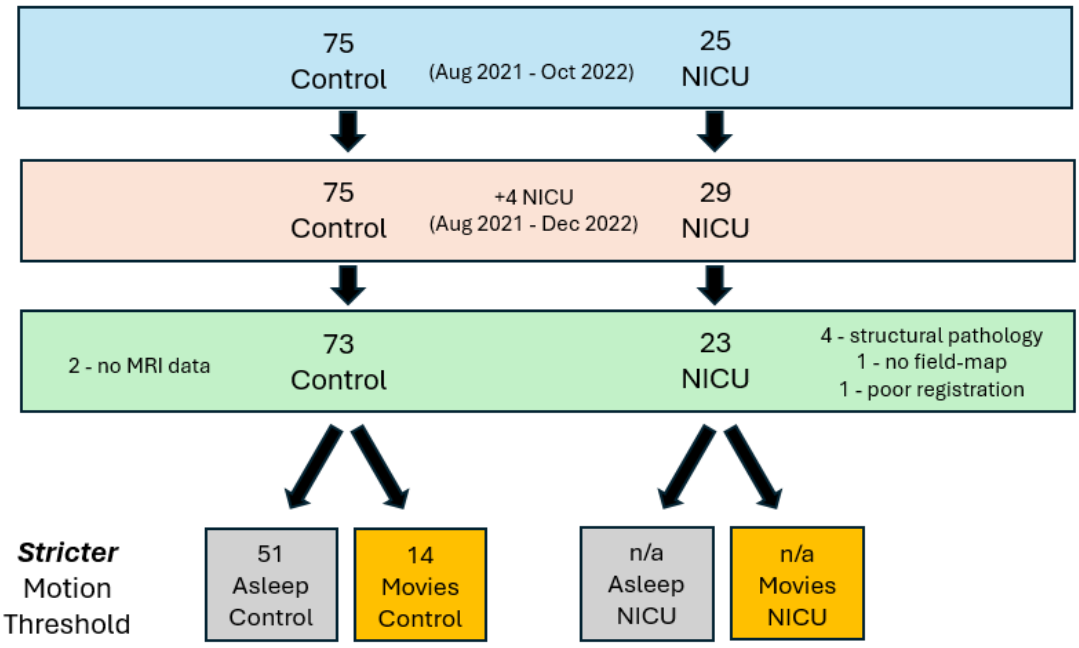

Figure 4-8 Number of participants (Control/NICU) contributing runs meeting the stricter motion threshold

4.4.4 Asleep state functional connectivity

Asleep functional connectivity was calculated for term born infants (controls). For each of the 56 term born infants who fell asleep one asleep run (480 frames) was selected. For the stricter motion threshold, 51 infants (51 runs) were included (5 infants' runs failed to survive the stricter motion threshold).

Table 4-4 Asleep – group average characteristics

	Motion threshold 3mm 56 infants (mean/std; min-max)	**Motion threshold 0.5mm 51 infants (mean/std; min-max)**
Gestational age (weeks)	39.2/1.1; 37.0-41.7	39.2/1.1; 37.0-41.7
Scan age (mo.)	2.34/0.39; 1.6-3.5	2.33/0.39; 1.6-3.5
FWD (mm)	0.18/0.09; 0.07-0.64	0.16/0.05; 0.07-0.29

4.4.4.1 Asleep state: within-subject similarity (WSS)

The group average FC was very similar when comparing the standard motion versus stricter motion thresholds (Figure 4-9) with all FC values being positive correlations. The within network connectivity was higher compared to between networks (with visual and somatomotor networks having the highest FC). Highest inter-hemispheric connectivity was seen in the visual and somatomotor networks. Lowest connectivity, both bilateral and inter-hemispheric, was between pairs containing the somatomotor and any of limbic/control/default networks (Figure 4-9).

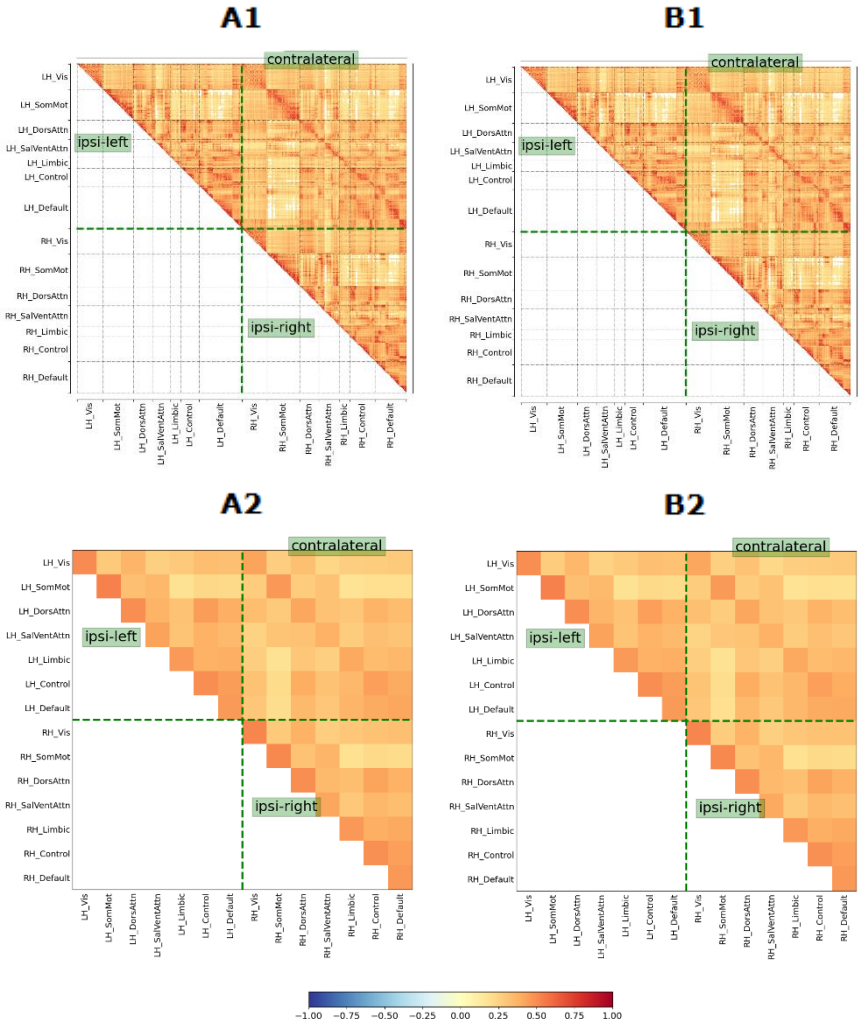

Figure 4-9 Asleep: within-subject similarity of functional connectivity.

A1) Schaefer et al. 400 parcel level; A2) Yeo et al. 7 network level; B1) Schaefer et al. 400 parcel level (FWD < 0.5mm); B2) Yeo et al. 7 network level (FWD < 0.5mm). Values shown surviving bootstrapping significance p<0.05 (with multiple comparisons correction).

Examining network edge dissimilarity (Figure 4-10), the top 20 t-values (t-values range: 5 to 9) included within network edges (visual, somatomotor, control, dorsal-attention), only one inter-hemispheric homologous edge (somatomotor), and inter-hemispheric network edges containing the somatomotor - limbic networks. Examining the subset of infants (n = 51 infants) who met the stricter motion threshold requirements, top 20 t-values (t-values range: 4.75 to 8.5) included the same within network edges (visual, somatomotor, control, dorsal-attention), and inter-hemispheric network edges containing the somatomotor - limbic and somatomotor – default networks (Figure 4-10).

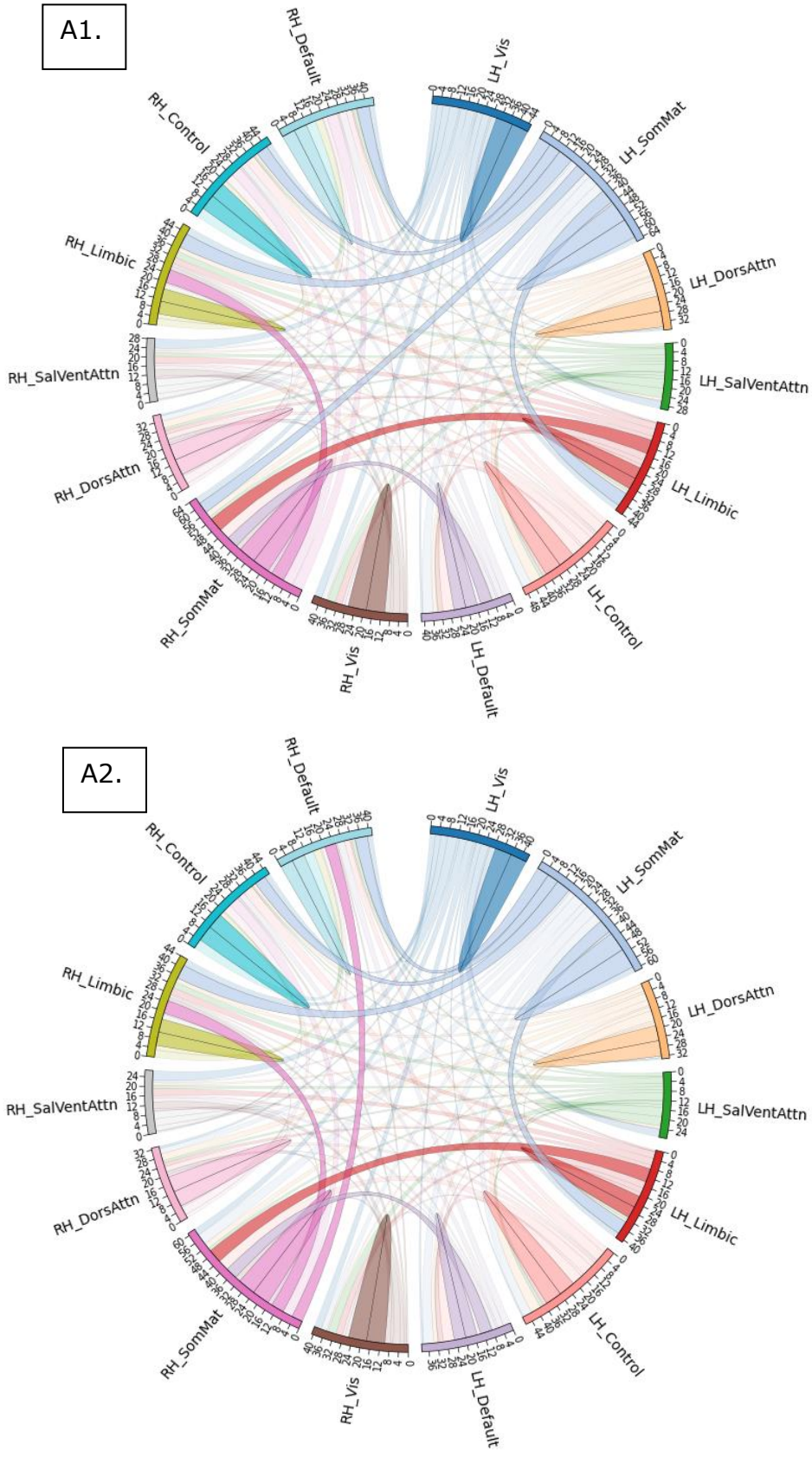

Figure 4-10 Asleep within-subject similarity: Network Edge Dissimilarity (t-values).

A1) normal motion threshold; A2) stricter motion threshold.

4.4.4.2 *Asleep state: inter-subject similarity (ISS)*

As a sanity check, we calculated inter-subject similarity during sleep. As there is no driving stimulus, there is no reason for synchronisation of fluctuations across different subjects. The shared similarity (inter-subject) of infant functional parcels/networks during natural sleep was assessed by correlating the functional connectivity matrix of one infant pairwise with all other infants asleep. Group FC matrices at the Schaefer 400 parcel level showed practically no significant shared connectivity (Figure 4-11). This is reassuring.

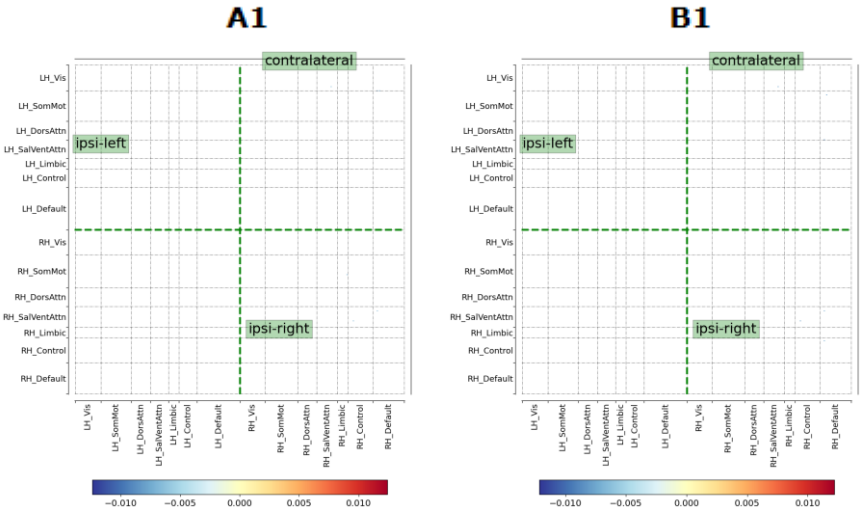

Figure 4-11 Asleep: inter-subject similarity of functional connectivity.

A1) Schaefer et al. 400 parcel level; B1) Schaefer et al. 400 parcel level (FWD < 0.5mm); Values shown surviving bootstrapping significance p<0.05 (with multiple comparisons correction).

4.4.5 Movies state functional connectivity

For each term born infant (healthy control) who watched movies an average of 1.8 (min-max: 1-4) runs survived the motion threshold criterion (an average of 1.1 runs per infant were excluded). For the stricter motion threshold, an average of 1.2 (min-max: 1-2) runs per subject survived the motion threshold criterion (an average of 1.3 runs per infant were excluded). Of infants with multiple

eligible runs, the one run with the least motion was chosen to represent that infant.

Table 4-5 Movies – group average characteristics

	Motion threshold 3mm 62 infants (mean/std; min-max)	**Motion threshold 0.5mm 14 infants (mean/std; min-max)**
Gestational age (weeks)	39.2/1.1; 37.0-41.7	38.7/1.2; 37.0-41.0
Scan age (mo.)	2.43/0.45; 1.6-3.6	2.3/0.36; 1.8-2.9
FWD (mm)	0.58/0.36; 0.14-1.53	0.2/0.04; 0.14-0.27

Characteristics of the infants included in the movies analysis are shown (Table 4-5). Most apparent is the difference in motion (FWD) between the standard and stricter motion groups, and the number of infants included in the respective groups (only 14 infants met the stricter motion threshold criterion). Of note, the motion (FWD) range (0.14 – 0.27) in the movies/awake stricter threshold group is not dissimilar to the motion range seen in the asleep runs (0.07 – 0.29) (Table 4-4).

4.4.5.1 Movies state: within-subject similarity (WSS)

The group average FC was comparable between the standard motion versus stricter motion thresholds (Figure 4-12) with the main difference being that between network FC values were weaker in the stricter motion threshold analysis. All FC values were positive correlations. The within network connectivity was higher compared to between networks (with visual, somatomotor, dorsal attention and salience ventral attention networks having the highest FC). Highest inter-hemispheric connectivity was seen in the visual and somatomotor networks. Lowest connectivity, both bilateral and inter-hemispheric, was between pairs containing the limbic plus other networks (Figure 4-12).

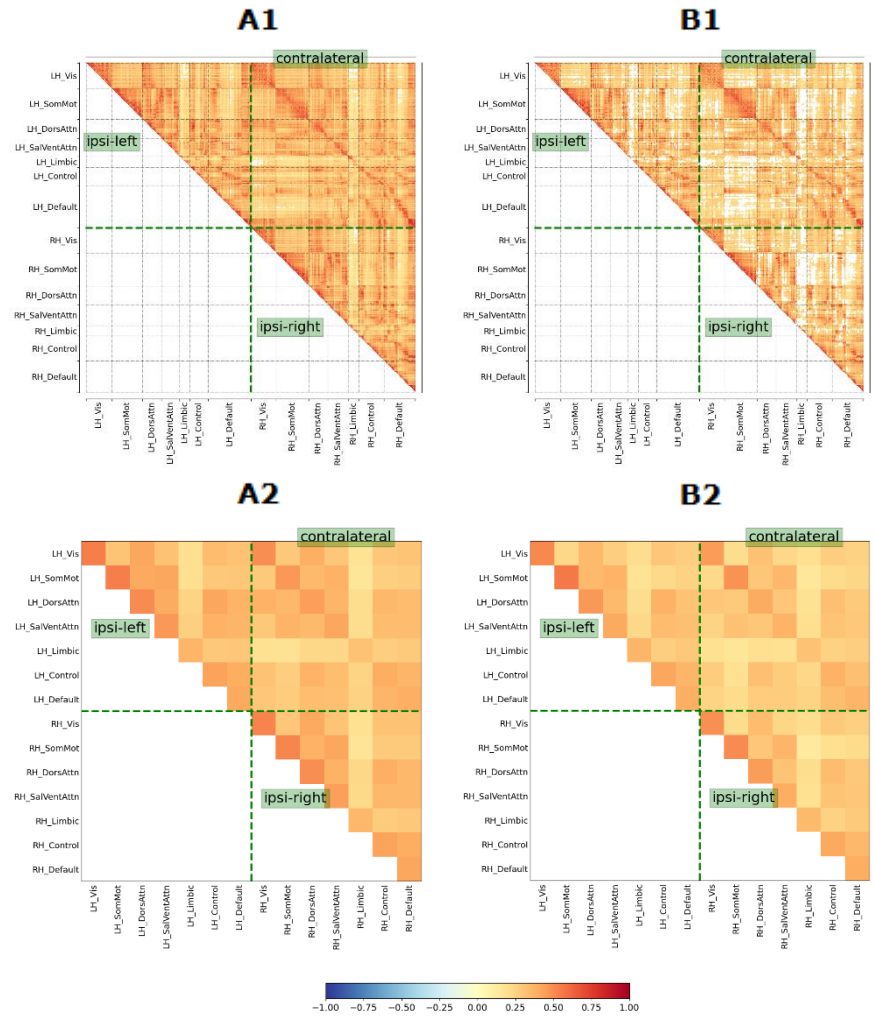

Figure 4-12 Movies: within-subject similarity of functional connectivity.

A1) Schaefer et al. 400 parcel level; A2) Yeo et al. 7 network level; B1) Schaefer et al. 400 parcel level (FWD < 0.5mm); B2) Yeo et al. 7 network level (FWD < 0.5mm). Values shown surviving bootstrapping significance p<0.05 (with multiple comparisons correction).

Examining network edge dissimilarity (Figure 4-13), the top 20 t-values (values range: 5.8 to 11.6) included within network edges (visual, somatomotor, dorsal-attention), inter-hemispheric homologous edges (visual and somatomotor), and both bilateral intra-hemispheric and inter-hemispheric network edges containing the limbic network (i.e. limbic paired with any of; visual, somatomotor and salience ventral attention networks). Examining the subset of term born infants who met the stricter motion threshold requirements (n = 14 infants), the top 20 t-values (values range: 3.0 to 9.5) included the same within network edges (with the addition of the control network), similar bilateral homologous edges (with the addition of dorsal-attention network), and similar inter-hemispheric network edges (containing the limbic network) when compared to the standard motion threshold analysis (Figure 4-13).

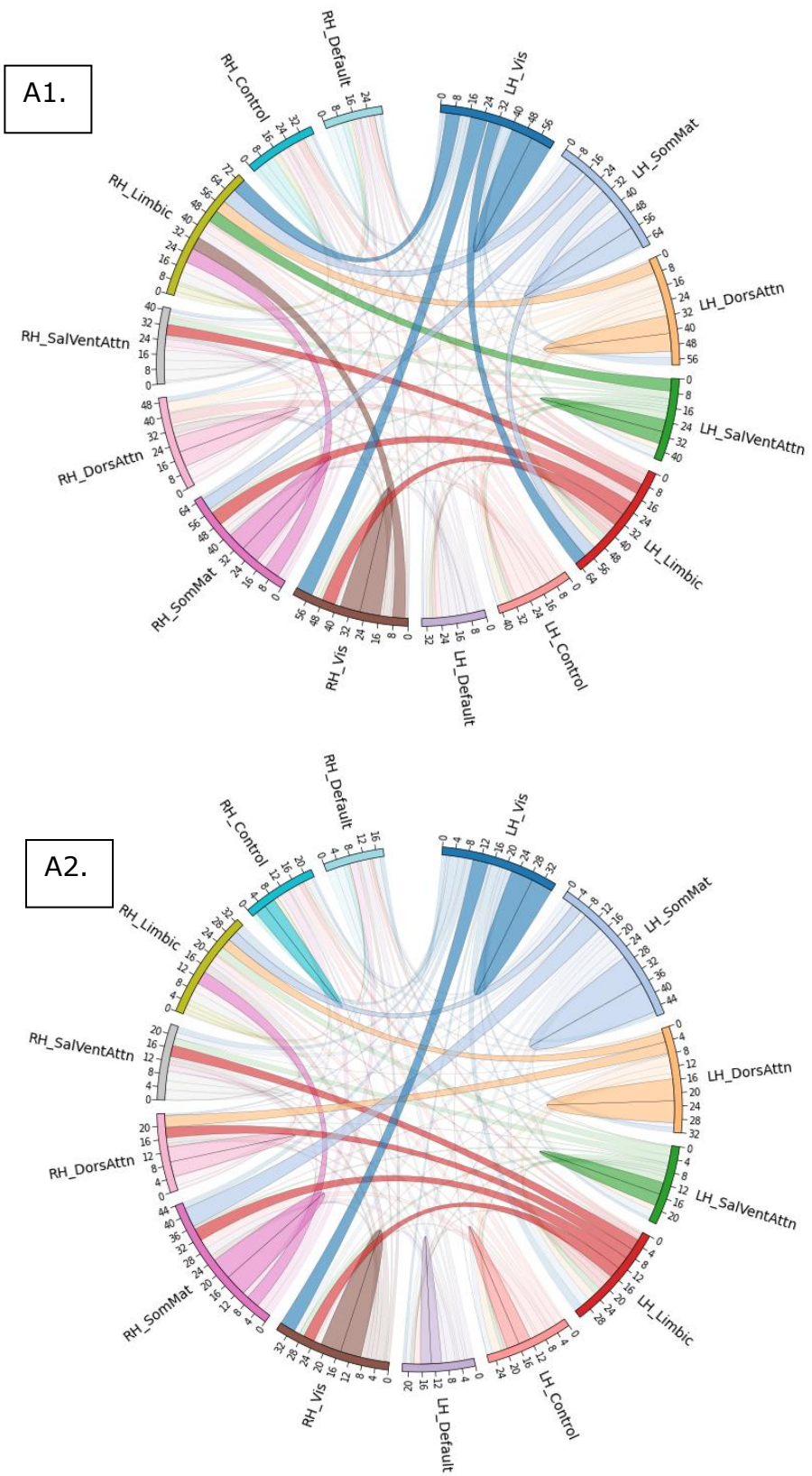

Figure 4-13 Movies within-subject similarity: Network Edge Dissimilarity (t-values).

A1) normal motion threshold; A2) stricter motion threshold.

4.4.5.2 Movies state: inter-subject similarity (ISS)

The shared similarity of term born infant functional connectivity during movie watching was assessed by correlating the functional connectivity matrix of one infant pairwise with all other infants watching movies, using the inter-subject functional connectivity method (Hasson et al., 2004; Simony et al., 2016).

We found that correlation (r values) was lower (Figure 4-14; colorbar range -0.1 to +0.1) compared to awake/movies within-subject similarity. Interestingly the stricter motion threshold connectivity matrix showed stronger positive connectivity and less negative connectivity (compared to standard motion threshold matrix) (Figure 4-14). Focussing on the stricter motion threshold, and comparing to within-subject similarity, the shared inter-subject similarity matrix shows a higher proportion of between network edges that are positively correlated (compared to the number of within network edges). Only the somatomotor network stands out as a notable within network connectivity edge (bilaterally and inter-hemispheres). The main between network edges are edges containing the somatomotor network (plus another) and the default network (plus another), with unilateral and inter-hemispheric edges being equally strong. Interestingly, the small negative connectivity seen in edges containing the visual networks (standard motion threshold) largely disappear (i.e. non-significant for the stricter motion threshold) and edges containing visual networks seem to not have shared (evoked) connectivity during the movies state (Figure 4-14).

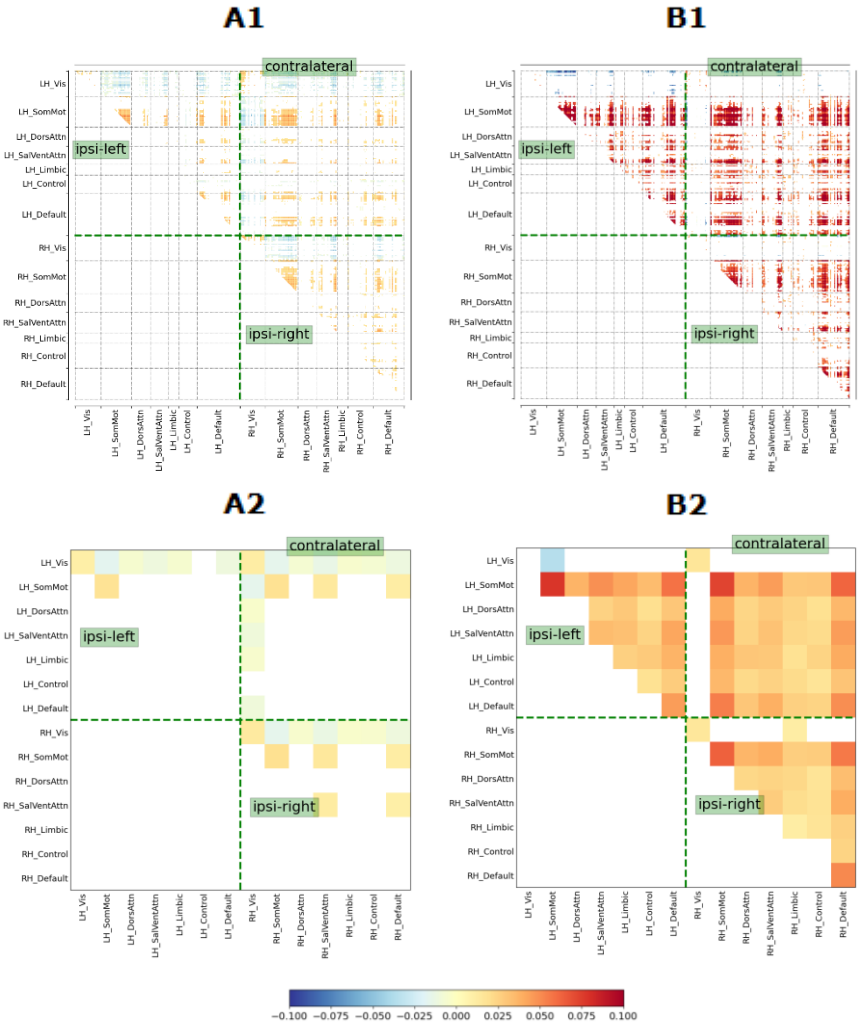

Figure 4-14 Movies: inter-subject similarity of functional connectivity.

A1) Schaefer et al. 400 parcel level; A2) Yeo et al. 7 network level; B1) Schaefer et al. 400 parcel level (FWD < 0.5mm); B2) Yeo et al. 7 network level (FWD < 0.5mm). Values shown surviving bootstrapping significance p<0.05 (with multiple comparisons correction).

Looking at network edge dissimilarity (Figure 4-15), the top 20 t-values were similar for both motion thresholds (values range: 3.3 to 7.9 for standard motion; 2.8 to 5.0 for stricter motion). For both motion thresholds, top 20 dissimilar edges included only one within network edge (somatomotor), and only one inter-hemispheric homologous edge (somatomotor). Both the left and right visual networks contributed dissimilar edges (in the top 20) on the ipsi- and contra-lateral hemispheres.

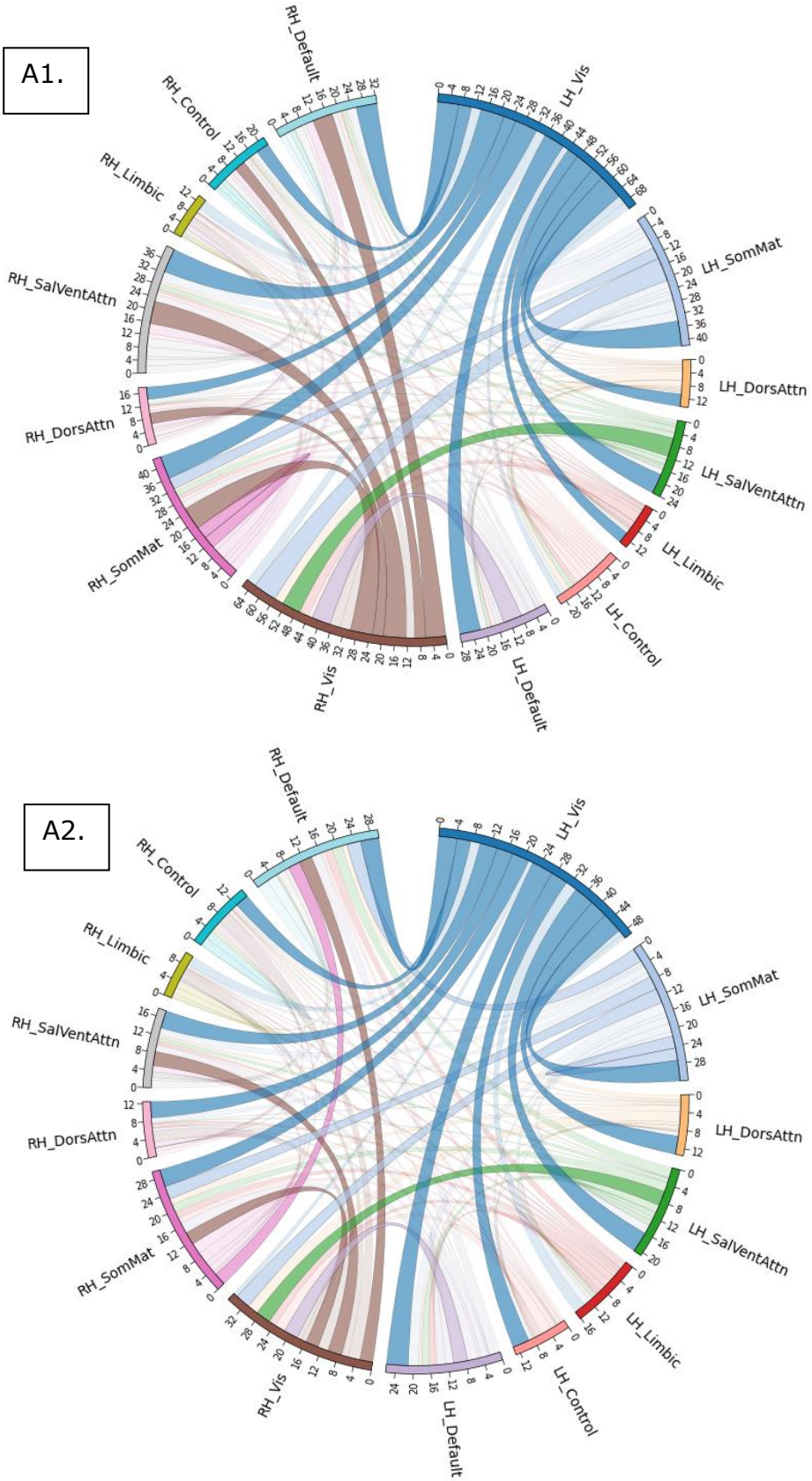

Figure 4-15 Movies inter-subject similarity: Network Edge Dissimilarity (t-values).

A1) normal motion threshold; A2) stricter motion threshold.

4.4.6 State-independent similarity (SIS)

The similarity of infant functional parcels/networks across states (asleep-movie) was assessed by Pearson correlating the functional timeseries of one asleep infant pairwise with all other infants watching movies (and vice versa, averaging across the two directions), i.e. using the inter-subject functional correlation method across subjects and states (Hasson et al., 2004).

Table 4-6 State-independent similarity

	Motion threshold 3mm	**Motion threshold 0.5mm**
No. infants	62 (movies) + 56 (asleep) = 118	14 (movies) + 51 (asleep) = 65

Functional connectivity matrices showed minimal significant connectivity independent of whether infants were watching movies or asleep (i.e. shared between infants across movies and asleep states) (Figure 4-16). This fact, coupled with the fact that the asleep state showed minimal significant shared connectivity (Figure 4-11), indicate that the positive shared connectivity values seen in the movies state (Figure 4-14) appear unique.

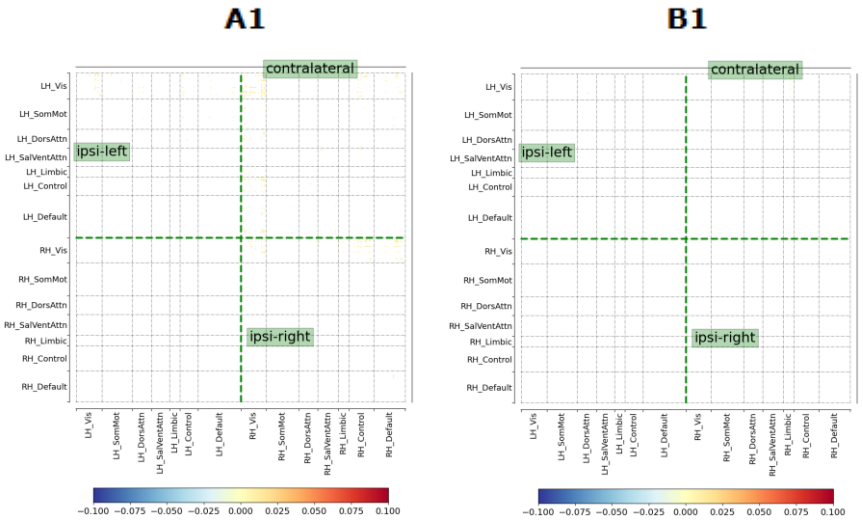

Figure 4-16 State-independent Similarity: inter-subject connectivity across states.

A1) Schaefer et al. 400 parcel level; B1) Schaefer et al. 400 parcel level (FWD < 0.5mm). Values shown surviving bootstrapping significance p<0.05 (with multiple comparisons correction).

4.4.7 State Differences

To compare FC across states, we first examined the overall whole brain average connectivity strength. As apparent from Figure 4-9 and Figure 4-12 , there was a positive correlation across most regions, suggesting a common global signal driving global FC. It is believed that global signal variations reflect both widespread brain activity in response to stimulation and also noise, such as modulations in global signal through motion (Murphy et al., 2009). Therefore, it is important to first assess whether there are differences in this overall global component when comparing states.

Mean within-subject FC for movies was 0.34 (std 0.10) versus 0.33 (std 0.12) for asleep state, with no significant difference ($p<0.67$). Mean shared (inter-subject) FC for movies was 0.002 (std 0.010) versus 0.000 (std 0.010) for asleep state, with no significant difference ($p<0.46$). State-independent connectivity had mean 0.000 (std 0.010). These differences are shown in Figure 4-17 and zoom in Figure 4-18.

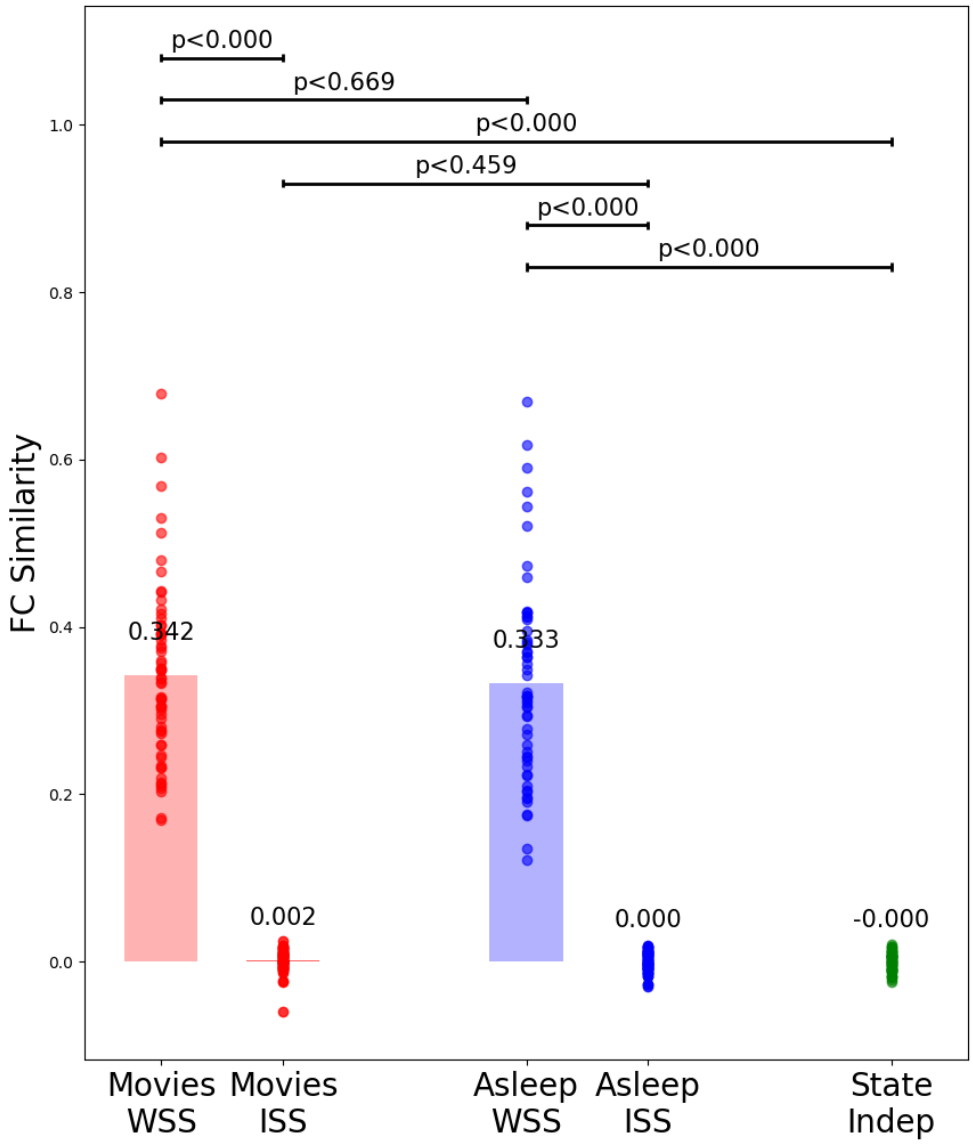

Figure 4-17 Functional connectivity (standard motion threshold).

Average connectivity (across 400 parcels/ROIs) for each infant (dots shown) and group average (bar) for within subject similarity (WSS) and inter-subject similarity (ISS) in both movies and asleep states respectively. State independent similarity (SIS) (green) is the inter-subject similarity across states.

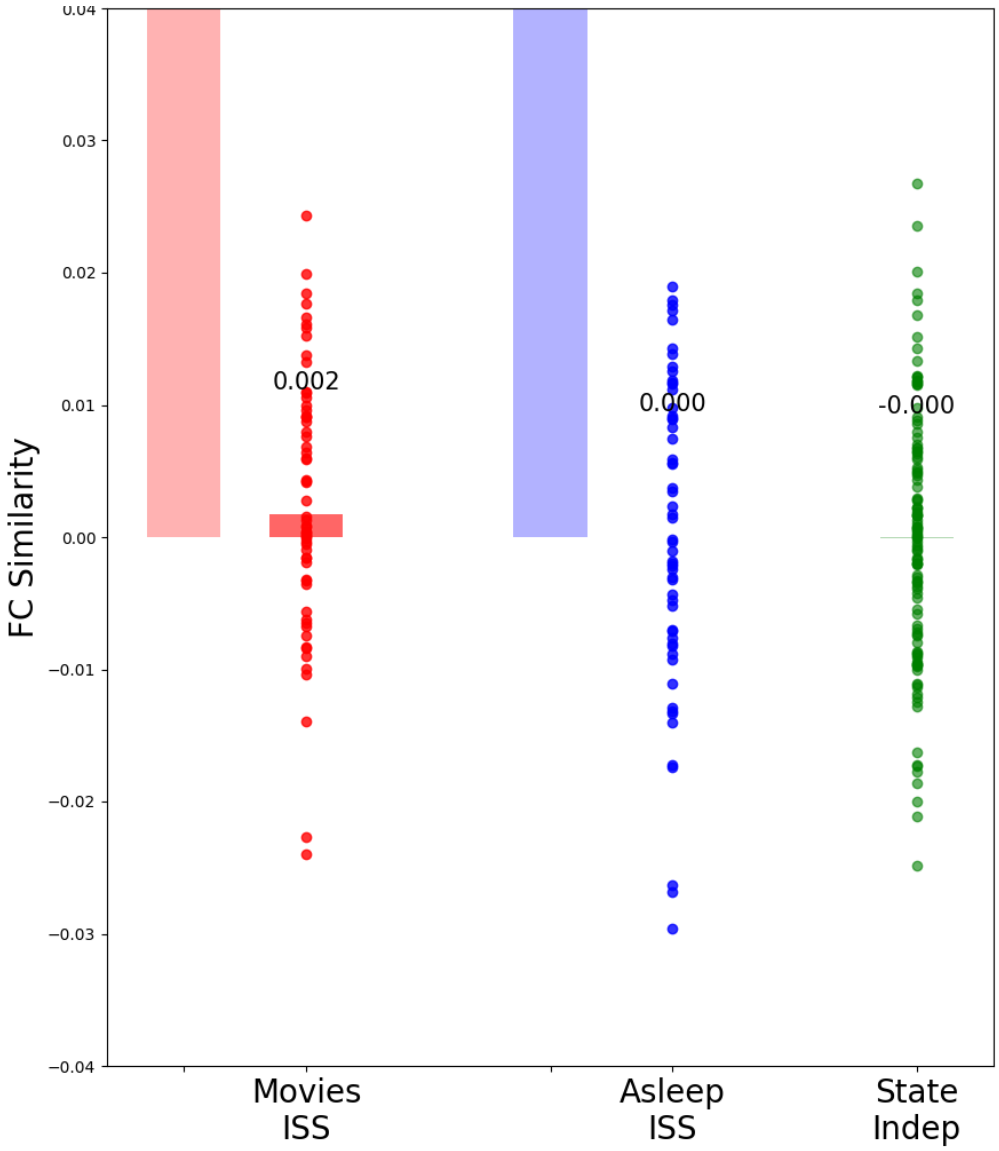

Figure 4-18 Functional connectivity (standard motion threshold): y-axis zoom.

Zoom of Figure 4-17 y-axis. Average connectivity (across 400 parcels/ROIs) for each infant (dots shown) and group average (bar) for inter-subject similarity (ISS) in both movies and asleep states respectively. State independent similarity (SIS) (green) is the inter-subject similarity across states.

Analysing infants with runs that met the stricter motion threshold, mean within-subject FC for movies was lower at 0.30 (std 0.08) versus 0.33 (std 0.12) (i.e. like previous) for asleep state, with no significant difference ($p<0.28$). At the stricter motion threshold, mean shared (inter-subject) FC for movies was higher at 0.025 (std 0.024) versus -0.001 (std 0.010) (i.e. like previous) for asleep state, with a significant difference ($p<0.002$). Again, state-independent

connectivity had mean 0.000 (std 0.02). These differences are shown in Figure 4-19 and zoom in Figure 4-20.

The reduction in global FC when stricter motion thresholds are applied suggests that global signal variation due to motion made an important contribution to activity in many regions, generally elevating FC. However, the lower global FC seen in the movie vs. asleep state, might be due either to greater motion-induced noise in the movie condition (reducing signal correlations for evoked signal) or due to more modularity in the brain with lower correlations between different brain systems, as has been seen before in states of greater arousal (conscious vs. anaesthetised, (Naci et al., 2018)). Modularity will be discussed further later, when changing patterns of FC are considered.

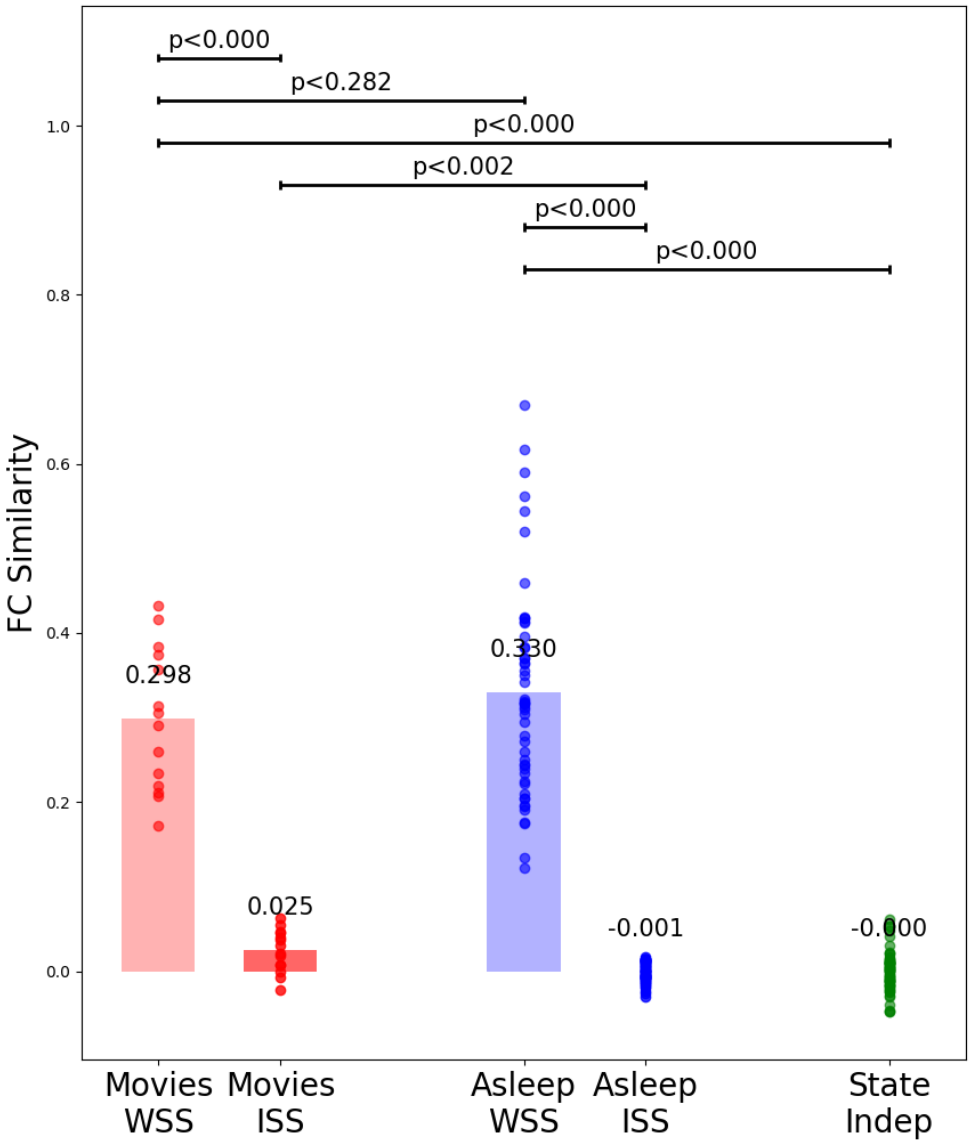

Figure 4-19 Functional connectivity (stricter motion threshold).

Average connectivity (across 400 parcels/ROIs) for each infant (dots shown) and group average (bar) for within subject similarity (WSS) and inter-subject similarity (ISS) in both movies and asleep states respectively. State independent similarity (SIS) (green) is the inter-subject similarity across states.

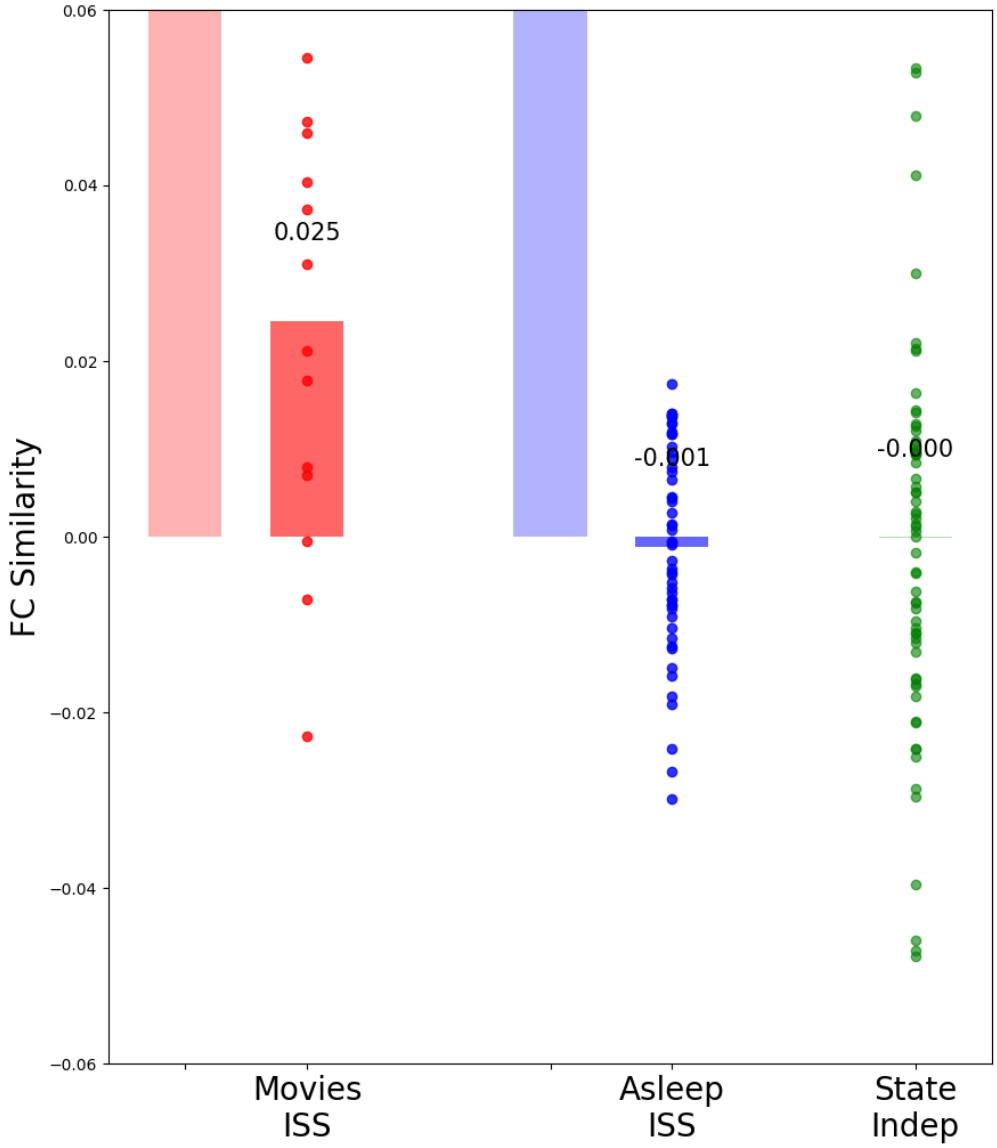

Figure 4-20 Functional connectivity (stricter motion threshold): y-axis zoom.

Zoom of Figure 4-19 y-axis. Average connectivity (across 400 parcels/ROIs) for each infant (dots shown) and group average (bar) for inter-subject similarity (ISS) in both movies and asleep states respectively. State independent similarity (SIS) (green) is the inter-subject similarity across states.

Next, to investigate differences in the pattern of connectivity between states, we examined at an edge level the difference in FC between states (Figure 4-21). Comparing the state difference FC (movies – asleep) for the standard motion threshold group, the state difference was small and connectivity differences were negative (due to asleep FC having slightly higher than movies FC). These negative connectivity differences were seen in edges (right/left and inter-hemispheres) containing the limbic network (as edges containing the limbic

network had lower FC in the movies state). Similarly, as the control and default network (within network) edges had lower FC in the movies state, the state difference was slightly negative in these networks (Figure 4-21). The task-evoked connectivity contained weakly negative connectivity in edges containing the visual network while the task-evoked connectivity contained weakly positive connectivity in the somatomotor edges (right/left/inter-hemispheres) (Figure 4-21). In short, this qualitative comparison of functional edge matrices (state difference versus task-evoked) suggested that the state difference in connectivity pattern did not seem to be related to the task-evoked connectivity pattern (using data from infants meeting the standard motion criteria) (Figure 4-21).

Functional connectivity differences were assessed using data from infants meeting the stricter motion threshold (Figure 4-22). The same colorbar scales (i.e. Pearson-r correlation ranges) were used in Figure 4-22 as were used in the standard motion threshold analysis (Figure 4-21). Edges containing the limbic network showed negative connectivity differences (Figure 4-22). This resembled the pattern for the standard motion threshold group (Figure 4-21). The control network still showed a negative connectivity difference (as movies state control network connectivity was lower than asleep state). Most notable in the task-evoked connectivity was the higher connectivity (positive correlation values) in the stricter motion threshold group (Figure 4-22). While bilaterally visual network edges were largely non-significant, edges containing the somatomotor network or containing the default network comprised the main task-evoked connectivity (right/left/inter-hemispheres) (Figure 4-22). For edges containing the somatomotor or default networks, within network connectivity was higher than between network connectivity (Figure 4-23). This qualitative comparison of functional edge matrices, at the stricter motion threshold analysis, appears to suggest that state differences in connectivity pattern do not account for the task-evoked connectivity seen.

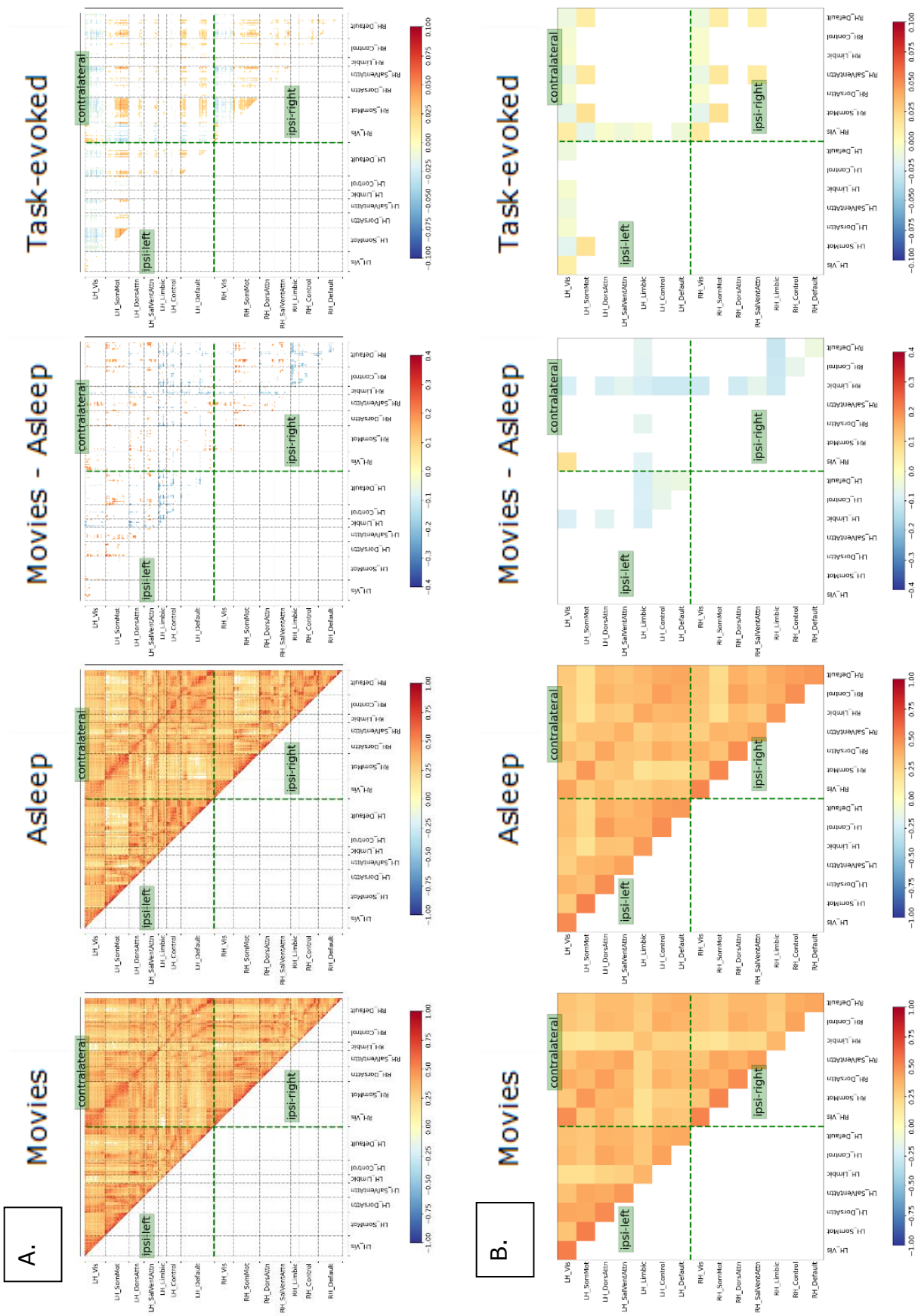

Figure 4-21 State Difference versus Task-evoked Connectivity; <u>Standard</u> motion threshold (>90% of frames with <3mm FWD).

Functional connectivity with two levels of resolution; A. (top) Schaefer et al. 400-region functional parcellation, B. (bottom) Yeo et al. 7 -network parcellation. Functional connectivity matrices corresponding to FC during movie watching (far left), asleep state (middle left), FC difference during movie relative to asleep (middle right), and the task-evoked FC using the inter-subject approach (far right). The colorbar indicates the average Pearson correlation values (only significant correlations are displayed, $p<0.05$, corrected for multiple comparisons). Abbreviations for Yeo parcellation: LH, left hemisphere; RH, right hemisphere; Vis, visual; SomMot, somatomotor; DorsAttn, dorsal attention; SalVentAttn, salience ventral attention; Limbic; Control; Default.

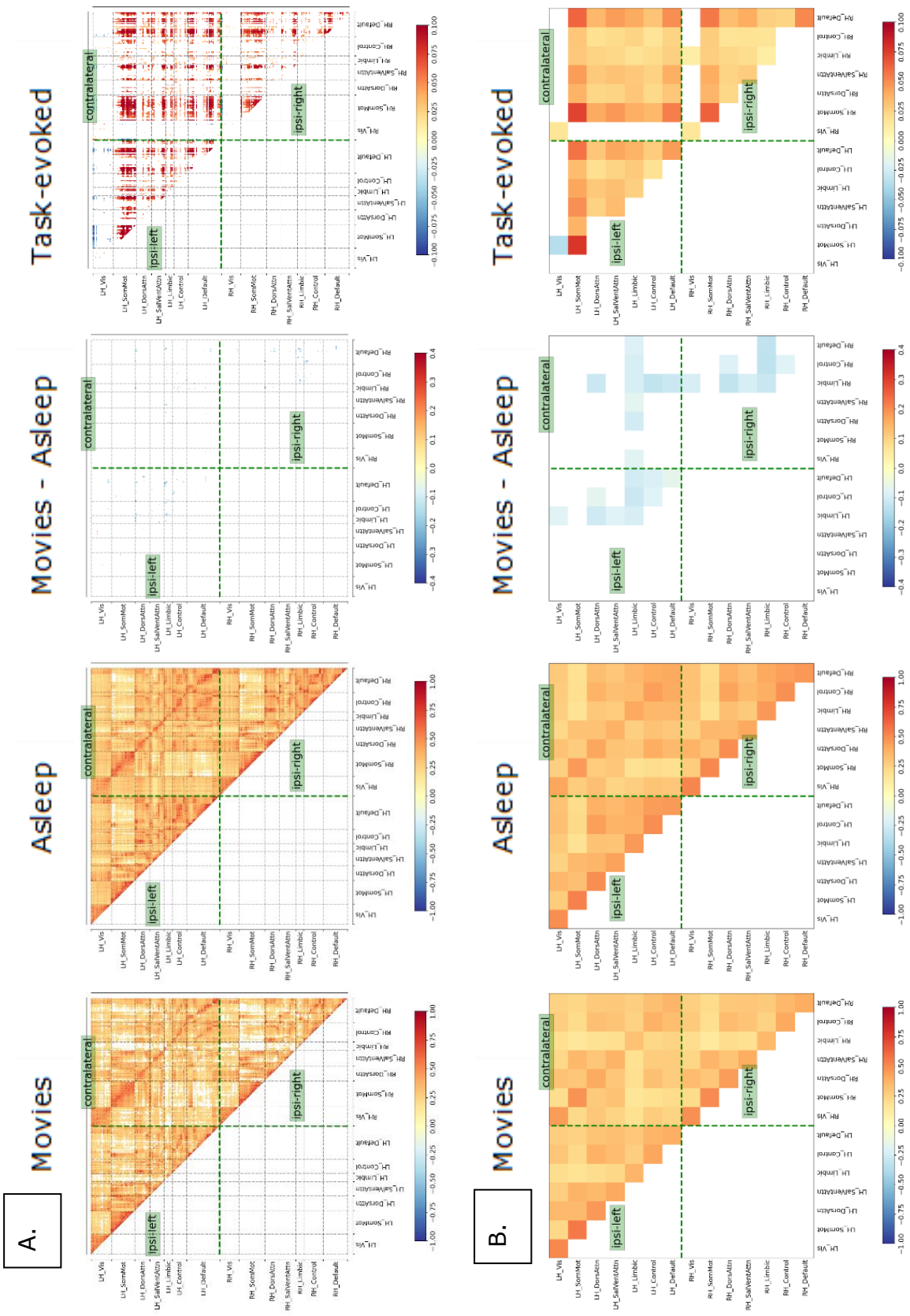

Figure 4-22 State Difference versus Task-evoked Connectivity; <u>Stricter</u> motion threshold (>90% frames with <0.5mm FWD).

Functional connectivity with two levels of resolution: A. (top) Schaefer et al. 400-region functional parcellation, B. (bottom) Yeo et al. 7 -network parcellation. Functional connectivity matrices corresponding to FC during movie watching (far left), asleep state (middle left), FC difference during movie relative to asleep (middle right), and the task-evoked FC using the inter-subject approach (far right). The colorbar indicates the average Pearson correlation values (only significant correlations are displayed, p<0.05, corrected for multiple comparisons). Abbreviations for Yeo parcellation: LH, left hemisphere; RH, right hemisphere; Vis, visual; SomMot, somatomotor; DorsAttn, dorsal attention; SalVentAttn, salience ventral attention; Limbic; Control; Default.

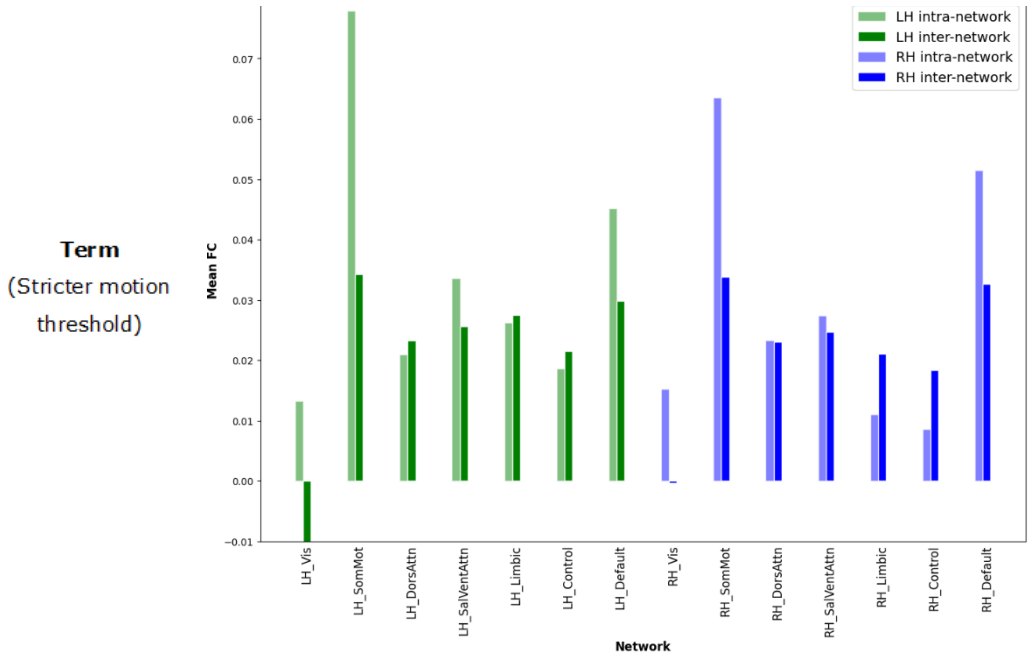

Figure 4-23 Shared movie (inter-subject) connectivity: intra- versus inter-network connectivity values (Yeo et. al 7 networks).

4.4.8 Prematurity

For infants born preterm group average functional connectivity matrices were calculated for asleep and movies states. Findings were compared to the data from term born infants (previous).

4.4.8.1 Preterm Infants: Asleep state

Data from 20 preterm born infants (20 runs) falling asleep were included (data meeting the standard motion threshold criteria). Characteristics of the preterm infants are shown in Table 4-7.

Table 4-7 Asleep – Preterm group average characteristics

	Motion threshold 3mm 20 infants (mean/std; min-max)	**Motion threshold 0.5mm (mean/std; min-max)**
Gestational age (weeks)	32.5/2.9; 28.6-36.9	n/a
Scan age (mo.)	2.5/0.53; 2.0-4.1	n/a
FWD (mm)	0.21/0.16; 0.10-0.65	n/a

The group average within-subject functional connectivity matrix showed a very similar pattern of asleep connectivity between the preterm group (Figure 4-24) and term groups (Figure 4-9) with within network connectivity highest in visual and somatomotor networks and lowest connectivity seen in edges consisting of somatomotor and either limbic/control/default networks.

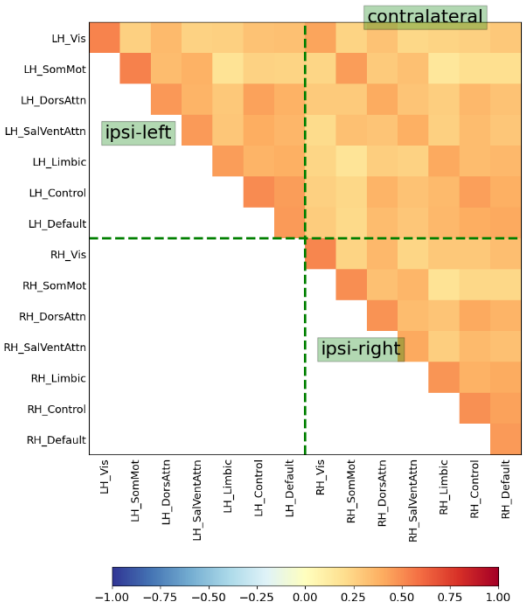

Figure 4-24 Preterm infants: Asleep within-subject similarity of functional connectivity.

Yeo et al. 7 network level. Values shown surviving bootstrapping significance p<0.05 (with multiple comparisons correction).

Examining network edge dissimilarity between the 20 preterm infants (Figure 4-25), t-values (range 3.1 to 5.7) had a similar pattern to term infants (Figure 4-10). Comparable to term infants, within network edge dissimilarity was higher (most networks) and similarly preterm infants had intra- and inter-hemispheric network edges that were notably dissimilar (somatomotor – limbic) (Figure 4-25).

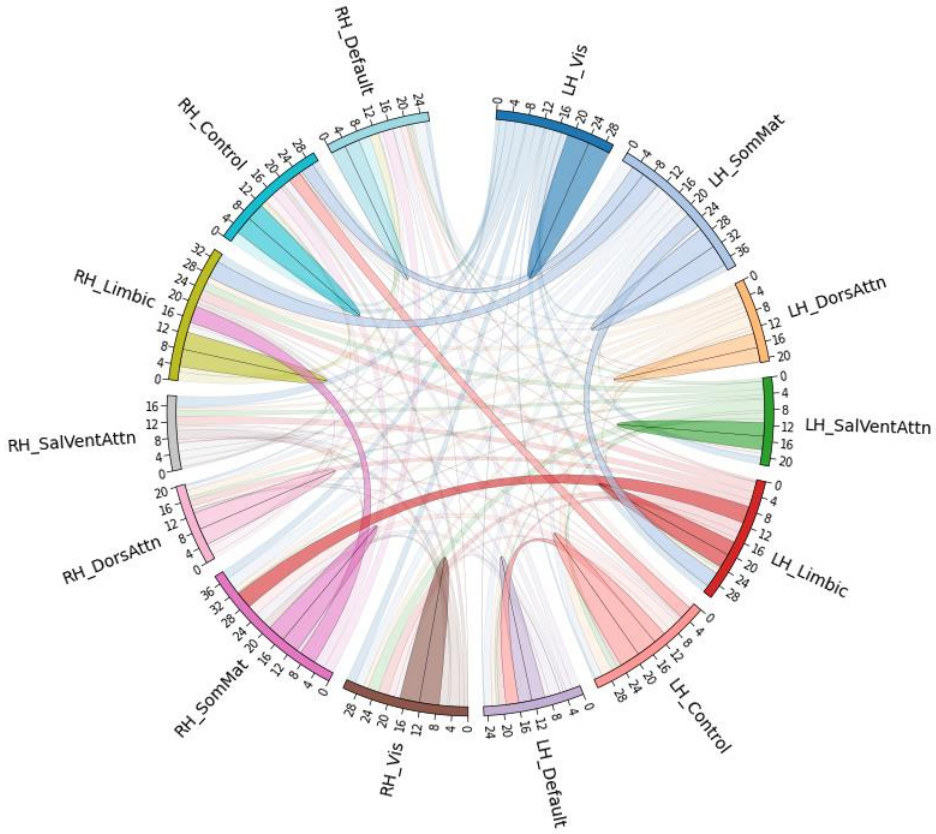

Figure 4-25 Preterm Infants: Asleep within-subject similarity – Network Edge Dissimilarity (t-values)

For the preterm asleep infants shared asleep connectivity (inter-subject FC) matrices (Schaefer 400 parcel level) showed practically no significant shared connectivity (Figure 4-26). This is a similar finding to term born infants (Figure 4-11).

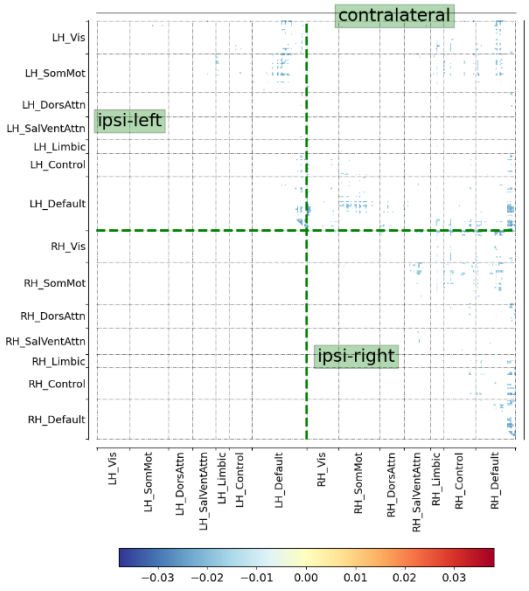

Figure 4-26 Preterm infants: Asleep inter-subject similarity of functional connectivity.

Schaefer et al. 400 parcel level. Values shown surviving bootstrapping significance p<0.05 (with multiple comparisons correction).

4.4.8.2 Preterm Infants: Movies state

For each preterm infant who watched movies an average of 1.7 (min-max: 1-3) runs survived the motion threshold criterion (an average of 1.2 runs per infant were excluded). Only 3 preterm infants had runs surviving the stricter motion threshold, and so analysis was precluded at the stricter motion threshold. Of all preterm infants with included runs, the one run with the least motion was chosen to represent that infant.

Table 4-8 Movies – Preterm group average characteristics

	Motion threshold 3mm 18 infants (mean/std; min-max)	**Motion threshold 0.5mm (mean/std; min-max)**
Gestational age (weeks)	31.7/2.9; 23.9-36.0	N/A
Scan age (mo.)	2.63/0.63; 2.0-4.1	N/A
FWD (mm)	0.75/0.38; 0.13-1.33	N/A

The group average within-subject functional connectivity matrix showed a very similar pattern of movies state connectivity between the preterm group (Figure 4-27) and term groups (Figure 4-12) with lowest FC occurring at edges containing limbic network (left/right/inter-hemispheres).

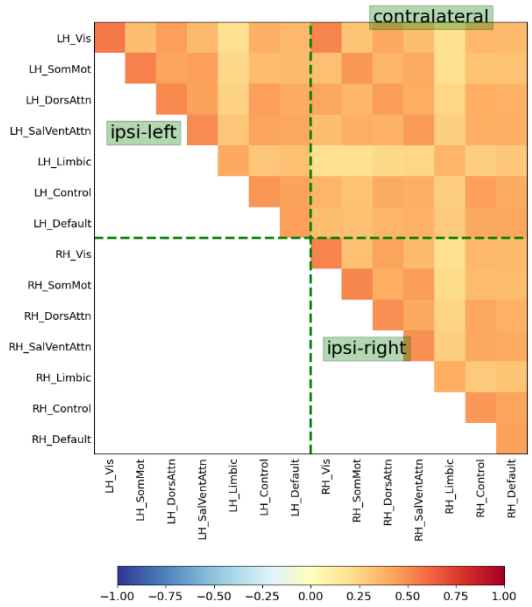

Figure 4-27 Preterm infants: Movies within-subject similarity of functional connectivity.

Yeo et al. 7 network level. Values shown surviving bootstrapping significance p<0.05 (with multiple comparisons correction).

Examining network edge dissimilarity (Figure 4-28) for movies state within-subject similarity, top 20 t-values (values range: 3.0 to 6.7) included within network edges (visual, somatomotor, dorsal-attention, and salience), bilateral homologous edges (visual only), and inter-hemispheric network edges containing the limbic network (limbic to: visual, somatomotor and dorsal-attention networks).

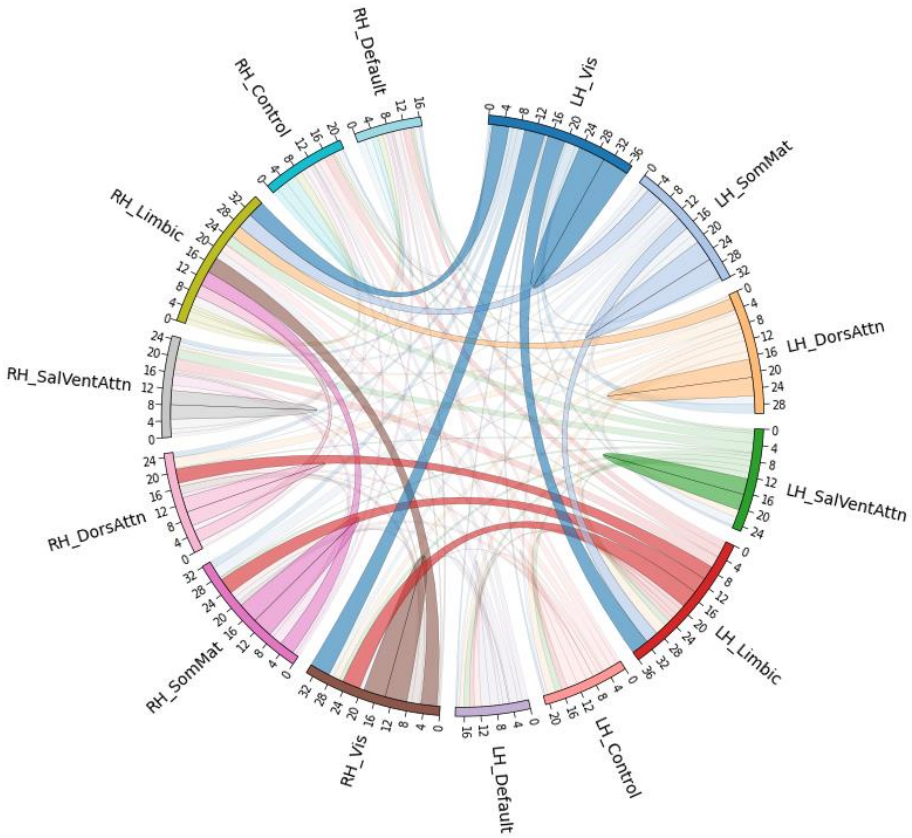

Figure 4-28 Preterm Infants: Movies within-subject similarity – Network Edge Dissimilarity (t-values)

Examining shared (evoked) functional connectivity amongst the preterm infant group, only the left somatomotor network stood out as a notable within network connectivity edge (Figure 4-29). Between network edges containing the somatomotor network (plus another) appeared strongest (left unilateral and inter-hemispheric edges) (right hemispheric shared connectivity was notably weaker/absent). Similar to term infants (Figure 4-14), edges containing visual networks seem to have minimal shared (evoked) connectivity during the movies state in the preterm infant group (Figure 4-29).

Looking at network edge dissimilarity (Figure 4-30) for inter-subject connectivity, top 20 t-values (values range: 1.6 to 2.8) included only one within network edge (left somatomotor), and both intra- and inter-hemispheric network edges containing the visual and somatomotor networks.

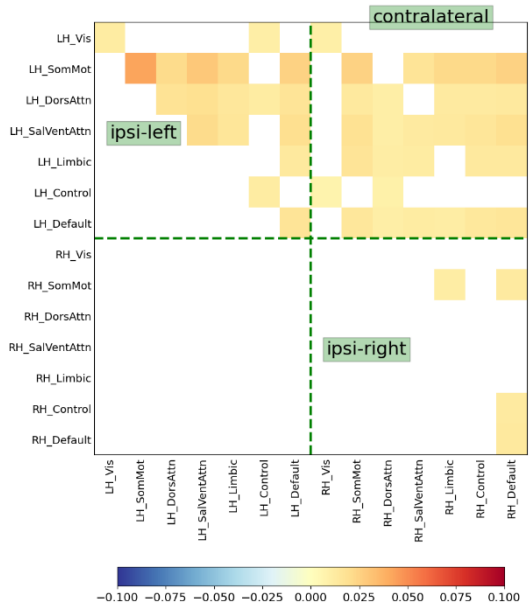

Figure 4-29 Preterm infants: Movies inter-subject similarity of functional connectivity.

Yeo et al. 7 network level. Values shown surviving bootstrapping significance p<0.05 (with multiple comparisons correction).

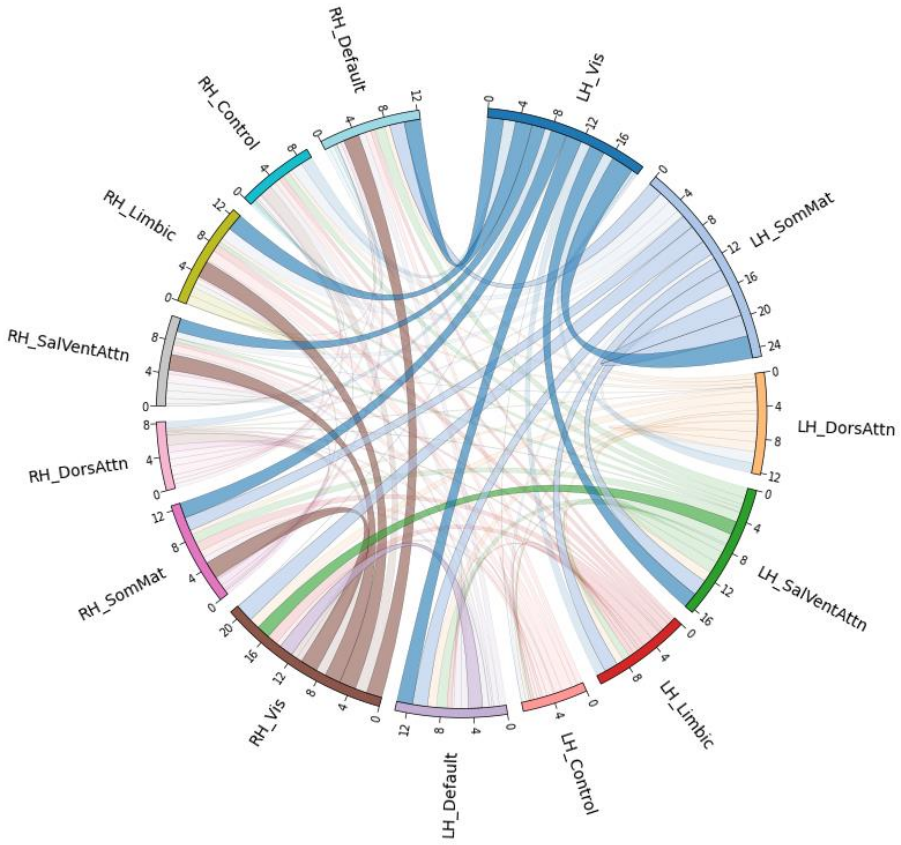

Figure 4-30 Preterm Infants: Movies inter-subject similarity – Network Edge Dissimilarity (t-values)

Analysis of state-independent similarity (18 preterm infants with movies runs, and 20 preterm infants with asleep runs) showed, like for term infants, no significant connectivity independent of infant state (i.e., no shared connectivity across infants and across movies/asleep states).

4.4.8.3 Preterm infants; State differences

As previously for term born infants, we examined state connectivity values (average for whole brain) and connectivity differences between states for the preterm born group.

For preterm born infants mean within-subject FC for movies was 0.37 (std 0.09) versus 0.33 (std 0.12) for asleep state (like previous), with no significant difference ($p<0.2$). Mean shared (inter-subject) FC for movies was 0.010 (std 0.02) versus -0.005 (std 0.014) for asleep state, with a significant difference ($p<0.006$). State-independent connectivity had mean -0.004 (std 0.014). These differences are shown in Figure 4-31 and zoom in Figure 4-32.

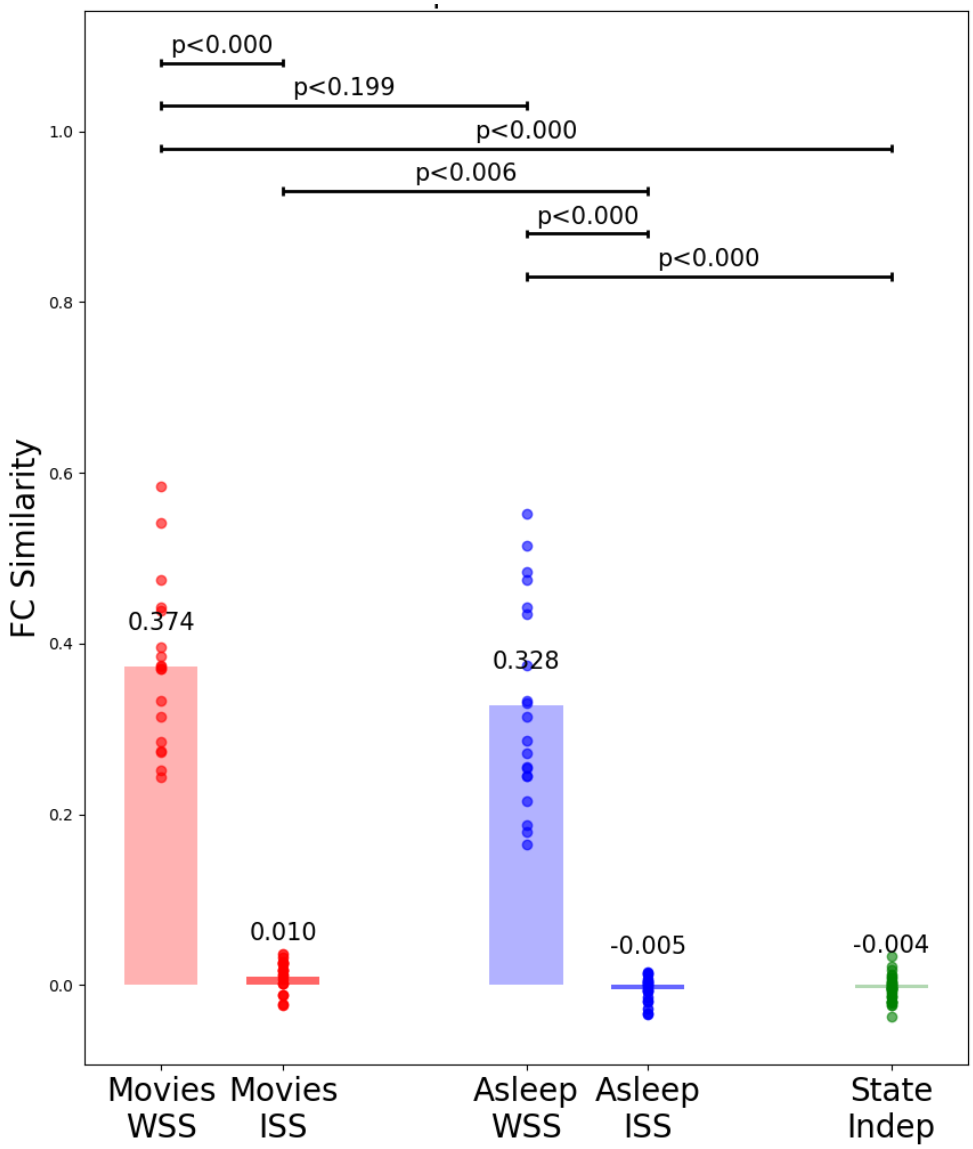

Figure 4-31 Preterm Infants: Functional connectivity (standard motion threshold).

Average connectivity (across 400 parcels/ROIs) for each preterm infant (dots shown) and group average (bar) for within subject similarity (WSS) and inter-subject similarity (ISS) in both movies and asleep states respectively. State independent similarity (SIS) (green) is the inter-subject similarity across states.

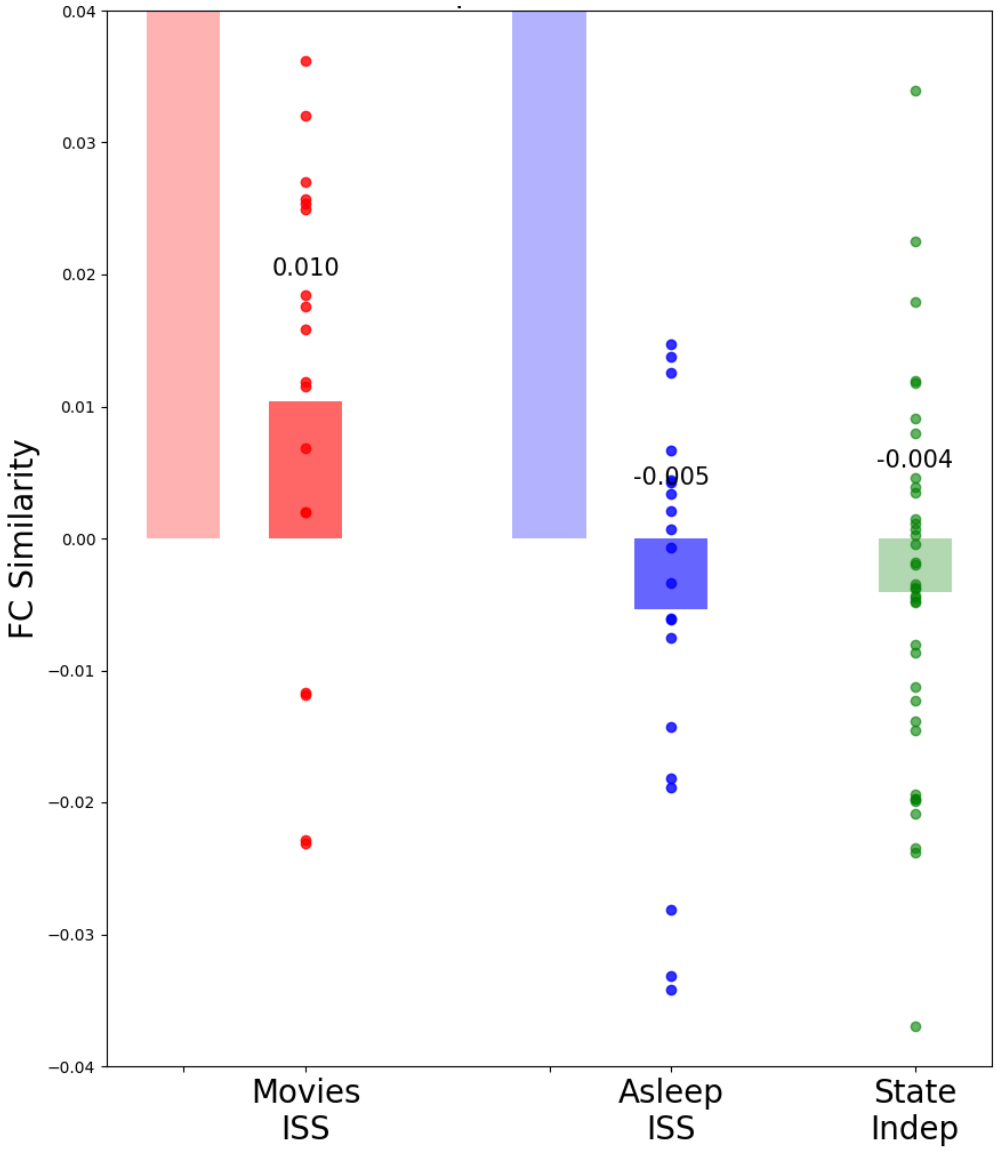

Figure 4-32 Preterm Infants: Functional connectivity (standard motion threshold), y-axis zoom

Zoom of Figure 4-31 y-axis. Average connectivity (across 400 parcels/ROIs) for each infant (dots shown) and group average (bar) for inter-subject similarity (ISS) in both movies and asleep states respectively. State independent similarity (SIS) (green) is the inter-subject similarity across states.

Functional connectivity differences were assessed using data from preterm born infants (Figure 4-33). The same colorbar scales (i.e. Pearson-r correlation ranges) were used as per the term born analysis (Figure 4-21 and Figure 4-22). Overall, there were few FC differences between movies versus asleep states in this preterm population (Figure 4-33 and Figure 4-34). Compared to term born infants, the preterm group state differences in connectivity did not show negative differences in edges containing the limbic network (i.e. limbic network edges connectivity was similar between movies and asleep states) (Figure 4-33 and Figure 4-34).

Task-evoked connectivity in the preterm born group appeared to follow patterns similar to the term born (stricter motion threshold), with positive connectivity values in edges containing the somatomotor or default networks (Figure 4-33 and Figure 4-34), albeit that connectivity was weaker in magnitude. This difference in magnitude may possibly be due motion effects (i.e. comparing preterm data meeting the standard motion criterion (at least 90% TRs with FWD<3mm) to term born data meeting the stricter motion criterion (at least 90% TRs with FWD<0.5mm)).

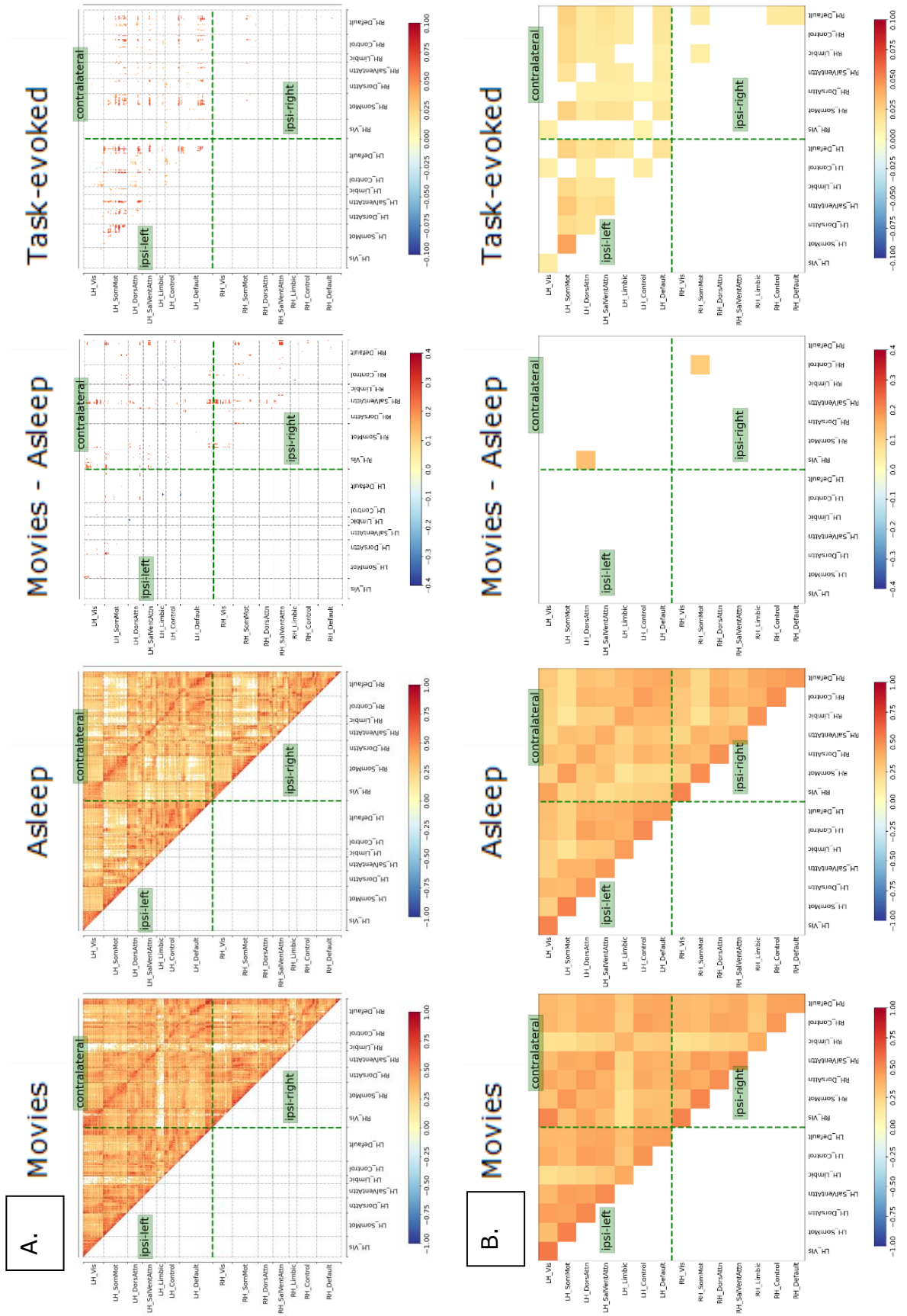

Figure 4-33 State Difference versus Task-evoked Connectivity. <u>Preterm</u> infants: <u>standard</u> motion threshold (>90% of frames with <3mm FWD).

Functional connectivity with two levels of resolution; A. (top) Schaefer et al. 400-region functional parcellation, B. (bottom) Yeo et al. 7 -network parcellation. Functional connectivity matrices corresponding to FC during movie watching (far left), asleep state (middle left), FC difference during movie relative to asleep (middle right), and the task-evoked FC using the inter-subject approach (far right). The colorbar indicates the average Pearson correlation values (only significant correlations are displayed, $p<0.05$, corrected for multiple comparisons). Abbreviations for Yeo parcellation: LH, left hemisphere; RH, right hemisphere; Vis, visual; SomMot, somatomotor; DorsAttn, dorsal attention; SalVentAttn, salience ventral attention; Limbic; Control; Default.

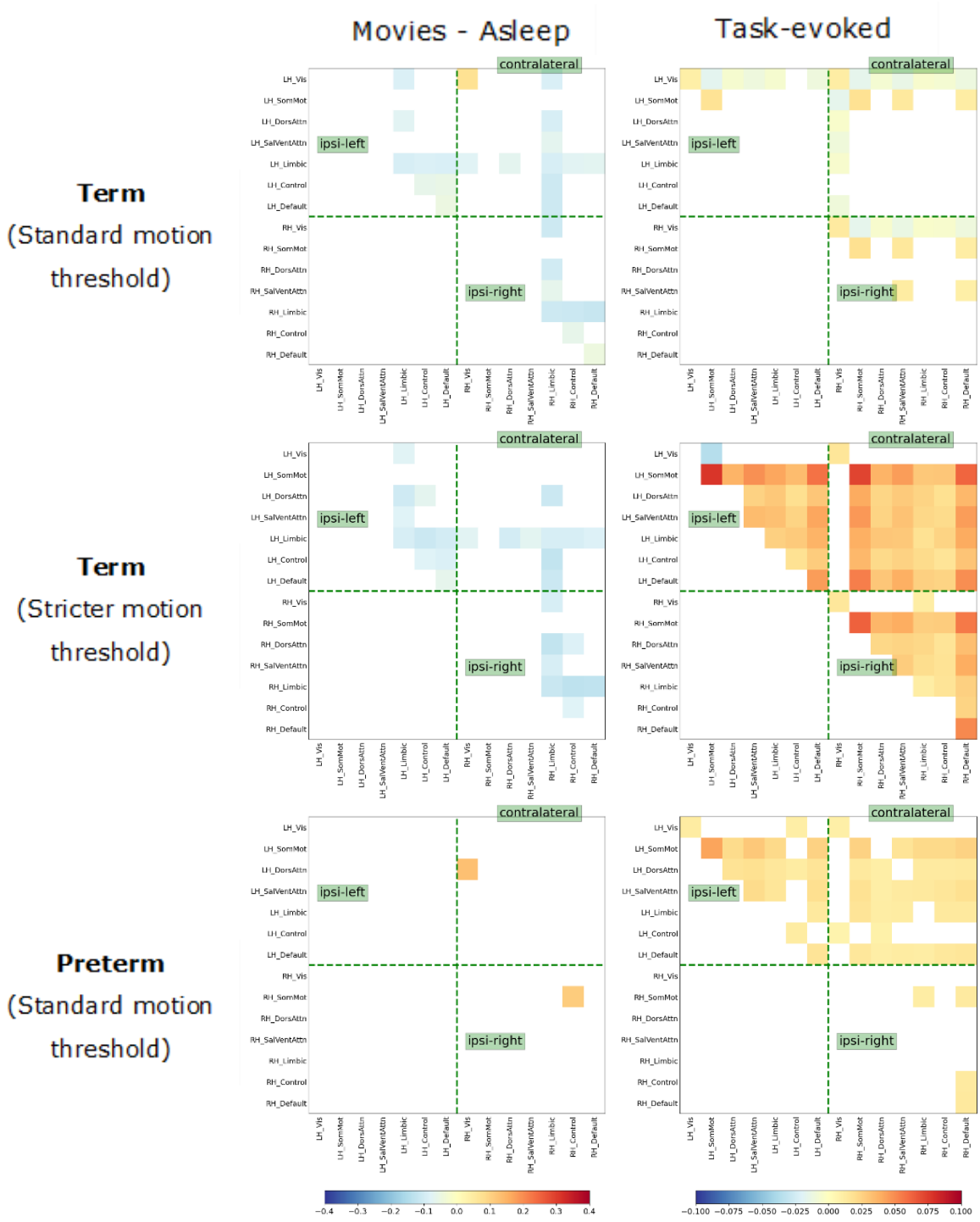

Figure 4-34 State Difference versus Task-evoked Connectivity. Term versus Preterm born infants.

Functional connectivity matrices corresponding to FC difference during movie relative to asleep (left), and the task-evoked FC using the inter-subject approach (right). The colorbar indicates the average Pearson correlation values (only significant correlations are displayed, p<0.05, corrected for multiple comparisons). Abbreviations for Yeo parcellation: LH, left hemisphere; RH, right hemisphere; Vis, visual; SomMot, somatomotor; DorsAttn, dorsal attention; SalVentAttn, salience ventral attention; Limbic; Control; Default.

4.5 DISCUSSION

4.5.1 Differences in within-subject FC between states

For the first time, we have measured FC in a cohort of infants within the same scanning session in both the awake (movie) and asleep (resting) states. These 2-month-olds had strong and consistent patterns of FC in both states. Reassuringly, as in adult studies, there was considerable similarity in FC across states. However, there were also notable differences, both in the overall global FC and in the specific patterns of FC. These highlight the importance of considering state when examining FC, and the risk of state confounding infant-adult comparisons, when infants are scanned asleep and adults awake.

In adults a state of greater arousal – specifically, wakefulness rather than sedation with the anaesthetic propofol – was associated with greater modularity in the brain (Naci et al., 2018). Corresponding to this, we found that infants awake watching movies appear to have more modular brain activity, with stronger connectivity within networks than across them, relative to the sleeping state.

In previous studies including healthy adults and comparing resting-state and movies paradigms it has been seen that movie-watching modulates mean FC in visual and higher order networks, especially the frontoparietal network, and also the default and dorsal attention networks (Betti et al., 2013; Gao and Lin, 2012; Vanderwal et al., 2015). Similarly in a study including children (age 5 – 15yo) movies watching significantly altered the mean FC with differences involving frontoparietal network FC with many other networks, including sensorimotor processing networks (somatomotor, auditory, visual), top-down control networks (cinguloopercular, dorsal attention), and the default-mode network (Greene et al., 2018). In a study of 6 year old children undergoing both resting state and movies runs the children showed an adult-like pattern of network connectivity among the dorsal attention, default, and frontal control networks, however in contrast to adults the 6 year old children showed marginally

significant changes (immature pattern) in the magnitude of the network connections between movies and rest (Emerson et al., 2015). These changes included increased edge connection between frontal control and default networks during movies relative to rest, and decreased edge connections between frontal control and dorsal attention networks (Emerson et al., 2015).

This study showed, at the group level, that whole-brain functional connectivity in young infants (2 months PMA) differs between state (asleep versus movie watching). However, as our participants were younger (infants) compared to those in previous studies (above), it is understandable that the differences in group-level connectivity between states (asleep and movies) were few.

Within network connectivity (shorter anatomical distance) in this age group was stronger than between network connectivity (longer distance connections), as has been noted in the literature. Lower within network functional connectivity was seen in the limbic, control and default mode networks, compared to visual and somatomotor networks, and this is evident in both asleep and movies states (within subject connectivity). This is in keeping with the development of these networks during the first year of life (Gao et al., 2015a, 2015b, 2009).

Interestingly, in the movies state, the lower magnitude of connectivity between edges containing the limbic network (left/right/inter-hemispheres) (e.g. limbic-visual, limbic-somatomotor, limbic-dorsal attention) seen in term born infants specifically stands out as a unique finding. The limbic network consists of amygdala (emotional processing) and hippocampus (memory formation and sensory impact). It has been seen in an adult fMRI study that evoked cortical activity can interact negatively with ongoing neural activity, such that higher pre-stimulus baseline results in either less activation or more deactivation (He, 2013). Perhaps our term healthy controls had heightened limbic activity at baseline (prior to movie onset) with later relatively more limbic deactivation (during movies).

In contrast, connectivity in edges containing limbic networks was similar across states for preterm born infants (i.e. no state difference), compared to dissimilar connectivity values in term infants (i.e. negative state difference). Multiple studies to date have shown alterations in functional connectivity network

development associated with prematurity (Ball et al., 2016; Cao et al., 2017; Doria et al., 2010; Fransson et al., 2007, p. 20; Smyser et al., 2010). Perhaps our preterm infants have lower baseline limbic activity, followed by no apparent limbic deactivation (during movies).

4.5.2 Shared (task-evoked) connectivity during movies

Qualitative comparison of group functional matrices suggests that shared connectivity (task-evoked) in the movies state does not account for the differences in connectivity (movies minus asleep) between states, both at the standard and stricter motion thresholds (summary figure: Figure 4-34). This fact that task-evoked FC does not explain the task minus rest FC difference suggests that ongoing activity that occurs during the movie but not in synchronization with movie has altered its correlational patterns and/or strengths compared with those in the resting state. In a previous study in adults, researchers sought to examine whether task-evoked functional connectivity was additive to spontaneous functional connectivity (resting-state adults; eyes closed awake), and if it was able to explain the changes in FC during movie watching relative to the resting state (Lynch et al., 2018). Their results found that the movies minus rest FC difference was largely different from the task-evoked FC during movies (Lynch et al., 2018).

Our results indicate that visual networks and their connectivity with other networks do not appear to contribute towards shared connectivity (inter-subject) in the awake movies state in these young infants (despite the visual movie stimuli). This is understandable as, in our case, infants did not see the exact same order of 6 movie clips (each clip 23 seconds duration) but instead a random order sequence of these 6 movie clips. Analysis was collapsed across all movies (despite various random clip orders).

When confining data analysis to term born infants who met the stricter motion threshold criterion, significant shared connectivity (inter-subject) was seen in the movies state (compared to minimal/none in the asleep state). While this finding was also seen in preterm born infants, the shared connectivity was lower in magnitude and somewhat limited in its extent in the right hemisphere (more

left and inter-hemispheric). This analysis showed how cortical edges containing the somatomotor and default networks (left/right/inter-hemispheres) dominated the pattern of shared (inter-subject) connectivity in infants watching movies. In the preterm born group, this finding was limited to edges containing the somatomotor network (i.e., not including edges containing the default network), with the caveat that there was more motion (FWD) in these preterm infant movies runs (likely weakening the results compared to term infants).

In adults the use of an intermediate movie ('Inscapes': a movie featuring abstract shapes without narrative or scene-cuts) was shown to decrease mean functional connectivity in somatomotor regions (compared to adult resting state) using traditional within-subject functional correlation analysis (Vanderwal et al., 2015). Using inter-subject (shared) connectivity analysis during movie watching in a group of adults, it was seen that the somatomotor network was one of the least variable networks (Vanderwal et al., 2017). Results from these studies are in contrast to our results which showed that shared (inter-subject) somatomotor activity was seen during movies (compared to asleep). We postulate that this may be due to infants shared interpretation of action (during movies) or indeed due to motion in the scanner (despite our use of strict motion thresholds).

The default mode network (DMN) consists of functional brain areas that historically were felt to decrease activity when the brain shifted from baseline to goal directed tasks, i.e. that the brain has a default mode of brain function that is suspended during goal directed behaviours (Raichle et al., 2001). Previous fMRI resting state adult studies show that DMN connectivity is reduced/altered under altered states of consciousness, such as sleep (non-REM sleep more so) (Houldin et al., 2021).

In the seminal ISFC study Simony et al. examined a group of adults listening to a real-life auditory narrative and to temporally scrambled versions of the narrative and, using ISFC to isolate correlation patterns within the default network, they showed that ISFC uncovered positive and negative stimulus-induced correlation patterns extending beyond the auditory cortex and involving regions in the DMN and between edges containing the DMN (Simony et al., 2016). Recent task-related adult studies it has been seen that the DMN

increased connectivity with other task-related networks during the performance of a wide variety of external tasks (Elton and Gao, 2015; Gao et al., 2013a). Other adult studies have shown that when watching a movie the default network shares a high connectivity (Hasson et al., 2008), and that the default network is activated during cognitively demanding tasks (Murphy et al., 2018).

In asleep infant FC studies it has been seen that the DMN is one of the first higher order networks to show a well-distributed network structure starting at 6 months of age (Gao et al., 2015a). This thought to be in response to the infant's social and emotional environment promoting DMN development during early infancy. While studies directly comparing infant resting-state to movies are few/limited, a previous study examining resting-state from movie-watching FC patterns in a cross-sectional developmental sample (from 6 to 20 years of age) demonstrated that whole-brain FC can reliably distinguish between movie-watching and rest irrespective of age, and that movie-watching modulates FC, particularly in the default mode and dorsal-attention networks (Sanchez-Alonso et al., 2021). Our findings suggest that younger infants (2 months age) do have increased DMN activity when watching movies, and that this can be captured/measured using inter-subject (shared) connectivity analysis.

We showed that there does not appear to be a baseline state-independent (shared) connectivity (inter-subject) in young infants across movies/asleep states (only within states). This fact, coupled with the fact that the asleep state showed minimal/no significant shared connectivity, emphasises how the findings of a positive shared connectivity in the movies state in early infancy is a significant finding.

4.5.3 Practical considerations of awake infant scanning

It is important to point out that the significant cortical connectivity shared (task-evoked) in the movies state was seen from data passing the stricter motion threshold criterion (0.5 mm FWD in fewer than 10% of scans), and ultimately came from 14 of 73 term born infants. Similarly, only 3 infants (not analysed) of 23 preterm born infants could have contributed data passing the stricter

motion threshold (in the movies state). All told, these small proportions of the term/preterm infant cohorts indicate how achieving awake/movies state data, useful for functional connectivity analysis, is quite challenging. This fact is important for researchers planning similar analyses. Future analyses could examine whether more liberal thresholds in combination with additional denoising (i.e., spike regression; global signal regression; ICA) might allow for the inclusion of a greater number of subjects.

Within network connectivity was stronger than between network connectivity (i.e. modularity) in both asleep and movies states. This modularity was stronger in the movies state (compared to asleep). This difference was most marked in the smaller sub-group of 14 infants (stricter motion threshold) compared to the 62 infants (standard motion threshold) watching movies. It is known that motion increases local connectivity and decreases distant connectivity (Power et al., 2012; Satterthwaite et al., 2012; Van Dijk et al., 2012), and while motion artefact was present in both groups (standard and stricter motion thresholds), it is thought that perhaps motion was more global in the standard threshold group and more local in the stricter threshold group, thus resulting in the more marked modular pattern in the sub-group of 14 infants (stricter motion threshold).

While the use of inter-subject correlation (shared responses) acted as a natural denoiser (mitigating artifacts from within brains), and the observed signal variance is likely from a shared neuronal origin (Simony et al., 2016), motion effects in this infant population likely still contribute somewhat towards the signal. Efforts to mitigate this included using the stricter motion threshold sub-cohort of infants/runs (FWD < 0.5mm, similar to asleep/resting-state thresholds used in infant/adult studies).

We presumed that very few infants would achieve an anatomical MRI sequence during the session (awake/movies runs were prioritised). As such, our analysis pipeline registered each infant's fMRI run (movies/asleep) to a fMRI reference image (not anatomical image, but an EPI functional image), and then next normalised the infant's fMRI runs to the chosen T2-weighted infant template. This induces less accuracy in terms of precise anatomical location of the regional/network fMRI signal. In retrospect, a large proportion of infants with

asleep fMRI runs also achieved anatomical T2-weighted images (this appears unique to this 2-month age group). These could be used for future registration to an anatomical reference image. At the time of study design the literature only included adult functional parcellation schemes. We chose the Schaefer 400 parcellation scheme (Schaefer et al., 2018) for this study. However, future work could use recent infant parcellations published in the literature (Myers et al., 2024; Oishi et al., 2019; Wang et al., 2023).

In our study awake/movies scan duration was relatively short (5 minutes) and literature shows that longer scan durations produce more reliable connectivity estimates, likely due to the fact that biologically relevant haemodynamic (BOLD) changes occur predominantly at lower frequencies (Birn et al., 2013; Noble et al., 2019; Shah et al., 2016). While recognising this fact, we suggest that the practical limit of scanning young infants watching movies (while remaining settled) may be limited to 5 minutes, as seen by the increasing FWD prior to movies run end (Figure 4-5).

Finally, while infants were confirmed asleep (by eyes closed and no active movements as witnessed by the researcher, and also by assessment of facial camera footage/tags), the level of sleep was not assessed (i.e. no contemporaneous EEG-fMRI was conducted) and so association of the functional connectivity patterns (asleep n = 56 term infants, n = 20 preterm infants) may not be uniform across subjects. Infants born at term gestation average 16 to 18 hours per day sleeping, 50% of it in REM sleep, and premature infants spend even more time asleep; 80% of it in REM sleep (André et al., 2010). Adult EEG-fMRI studies of adult asleep/wake states have shown positive wake correlations trending towards negative correlations in NREM and back towards positive correlations in REM (Houldin et al., 2021). As participants in our study were young infants, it is postulated that a considerable proportion of time asleep in the MRI scanner was spent in REM sleep. If so, this supports the findings of positive network connectivity patterns seen in the asleep analysis (and not dissimilar to awake/movies connectivity).

CHAPTER 5 USING A MACHINE LEARNING MODEL TO CLASSIFY CONNECTIVITY IN AWAKE INFANTS

5.1 ABSTRACT

Estimating 'brain age' has become a popular tool in fMRI in recent years. Models are trained on datasets spanning an age range, then tested on unseen data. Subjects with a 'brain age' higher/lower than their chronological age are then compared to behaviours/morbidities. Already some recent studies have used asleep fMRI data from older infants/toddlers to classify age groups and to predict brain age with reasonable successes.

The hypothesis of this current study was that FC from movies would be more revealing of key phenotypes (birth gestation and scan age) than FC from sleeping infants (aged 2-months PMA), and this would be seen as a difference in classification ability (preterm versus term birth) and prediction ability (birth gestation, brain age) using a machine learning model.

Infants (75 term born, 29 preterm born) attending as part of the FOUNDCOG project undertook MRI scanning at 2-months age (corrected age for preterm). Infants watched naturalistic movies (485 frames, 5 mins) during awake movies runs, and underwent asleep fMRI (1000 frames, 10 mins) if they fell asleep. Functional connectivity was calculated as the Pearson correlation of the timeseries for a parcel with every other parcel across the number of TRs (volumes) within the subject's own run. The indices of the upper triangle (including the leading diagonal values) of the Yeo et al. (14, 14) network level connectivity matrices were taken to achieve a series of 105 unique network to network connections/edges. These 105 functional edges were used as features for the machine learning models. Support vector classification was used to classify state (awake/asleep) and birth gestation (preterm/term), while support vector regression was used to predict birth gestation and brain age.

The median birth gestation of the 23 preterm infants included (6 infants excluded due to known structural brain injury) was 32 (IQR 29-33) weeks PMA. Incidence of serious co-morbidities were few in this group (1 infant had history of sepsis, 5 infants had history of chronic lung disease). A support vector machine classifier (using functional edge data) was able to classify state (asleep/movies) with high ability in both preterm ($F1=0.82$, $p<0.00$) and term ($F1=0.93$, $p<0.00$) born infant groups. However, when the models were trained using only motion data (FWD) as the training feature (not functional edge data),

F1 scores were very similar, indicating that motion is an important driver of this classification. A support vector classifier (using functional edge data) was moderately able to classify birth gestation (F1 = 0.66, $p<0.00$) (training on asleep data and testing on movies), but not while training/testing on data from the same state (movies F1=0.57, asleep F1=0.50). Support vector regression (using functional edge data) was only able to weakly predict brain age ($R2 = 0.09$, $p<0.01$) (using asleep FC edges but not movies edges), but was not able to predict birth gestation (either state).

Ultimately, while this study indicates that FC data from 2-month aged infants can classify brain state (asleep/movies) during a scan (both ex-preterm and term born infants) and can weakly predict brain age (asleep state only), it is likely that methodological challenges in our analysis, and perhaps the relatively low incidence of co-morbidities in the preterm group, limited our ability to classify and predict birth gestation. Future work adopting SVM analysis, but also using more rigorous motion censoring; registration to anatomical images; and bespoke infant atlases/parcellation (to include subcortical regions); may perhaps lend towards improved classification of birth gestation (and subsequent analysis of networks/features driving same).

5.2 INTRODUCTION

5.2.1 Machine Learning - background

Machine learning is rapidly expanding in application in medicine, and has recently entered the infant clinical domain and examples include decision models for febrile infants at risk of serious bacterial infection (Ramgopal et al., 2020), identification of sub-cohorts of children with septic shock who may be more likely to benefit from corticosteroids (Wong et al., 2016), and the development of algorithms to identify children recently admitted who need to transfer to paediatric intensive care (Zhai et al., 2014). Machine learning with EEG has been used to aid health-care professionals to identify neonates with electrographic seizures (Pavel et al., 2020) and to predict infants who would later develop seizures following neonatal hypoxic ischaemic encephalopathy (Pavel et al., 2023).

Machine learning can be used to create a model that estimates an individual's phenotypic characteristics (e.g., executive function, diagnostic category) from neuroimaging data. Model features are used to estimate continuous outcome measures (known as regression) or categorical outcome measures (known as classification). In recent years machine learning has been investigated as a tool in infant neuroimaging due to its ability to perform classical statistical inference while also allowing the capture of more complex associations (Dosenbach et al., 2010). In addition, outputs from machine learning are often more generalisable than simple correlations since they are/should be defined and validated with independent data (held back/out data) (Pollatou et al., 2022).

Machine learning as a domain can be divided in different ways (Scheinost et al., 2022; Shah et al., 2023; Zhu et al., 2019). One critical division is between supervised and unsupervised training strategies. Supervised machine learning uses labelled datasets where each data sample is associated with an outcome measure. Example algorithms include linear discriminant analysis or deep neural network classifiers. In contrast, unsupervised machine learning uses unlabelled datasets to discover patterns in the data. Some examples of unsupervised machine learning algorithms include K-means clustering (clusters data

comprising continuous variables), latent class analysis (clusters data using both categorical and continuous variables), or contrastive learning in deep neural networks. Compared to conventional machine learning algorithms, deep neural networks methods can identify more complex patterns but require larger datasets (Scheinost et al., 2022; Shah et al., 2023; Zhu et al., 2019).

Articles applying machine learning to infant imaging were sparse but have increased in recent years. It has been applied to EEG, structural MRI and multimodal approaches, but neuroimaging techniques such as fMRI, magneto-encephalography (MEG), and arterial spin labelling (ASL) MRI remain underused currently in this field (Scheinost et al., 2022). In a systematic review of literature that includes machine learning prediction models in the under 3 year old community (toddler or younger), Scheinost et al (2022) showed that most studies have made predictions in the cognitive/development domain (e.g Bayleys scores) (31%), the physical characteristics domain (e.g. brain maturation/age) (29%), the neurological phenotype domain (e.g. seizures/encephalopathy) (27%), with the final neurodiversity domain (e.g. autism) (12%).

Importantly, in addition to classifying the present phenotype from neuroimaging data, it is possible to use machine learning to predict future state – such as motor (Saha et al., 2020) and later social-emotional and cognitive outcomes at both 18 months age (Fenchel et al., 2022) and two years of age (He et al., 2018).

5.2.2 Machine learning - simple versus complex models

While machine learning has exciting potential for infant neuroimaging, it is important to understand the balance of aims, whether it is being used to aid interpretation (and inference between predictors and outcomes) versus black box prediction (complex models) (Figure 5-1). Simpler models include multiple regression using linear relationships between predictors and outcomes. Simpler models require less computational power and less training data. On the other

hand, are complex models such as non-linear support vector machine (SVM) models and deep neural networks. These exploit non-linear relationships between predictors and outcomes, which can be more powerful, but requires more training data, more computational power, and can be difficult to interpret (i.e., they are black boxes).

Infant/toddler asleep fMRI machine learning studies to date have leaned towards using more simpler/explainable algorithms (Kardan et al., 2022; Pruett et al., 2015), however even these models have been seen to maintain high accuracy even while excluding the principal "consensus" features (e.g. functional connectivity edges that appear most discriminatory), indicating that inference is not necessarily easy, even with simpler models.

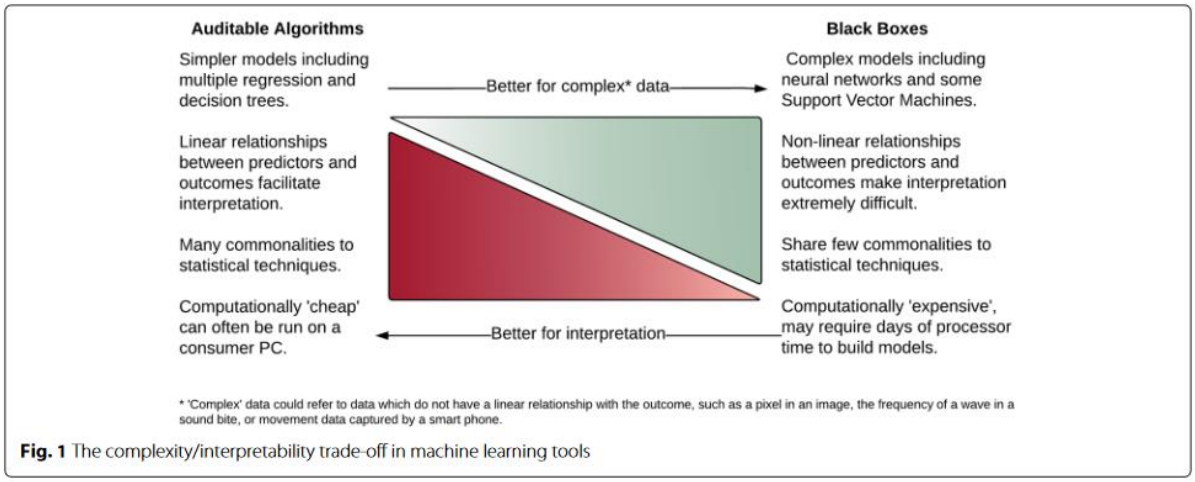

Figure 5-1 Balance between statistical (inference) and black box (prediction) methods in machine learning.

Sidey-Gibbons, J.A.M., Sidey-Gibbons, C.J., 2019. Machine learning in medicine: a practical introduction. BMC Med Res Methodol 19, 64. https://doi.org/10.1186/s12874-019-0681-4

5.2.3 Machine learning - important steps

In machine learning, a process called cross-validation is used to avoid circularity. The dataset is split, and the model is trained on the 'training set' and tested on the 'test set'. Prior to testing on an external/independent test set, the

model can be trained using a k-fold cross-validation technique as described below.

The k-fold cross-validation technique involves splitting the dataset into k equally sized, non-overlapping subsets. Machine learning then learns the model for the k-1 folds. Individuals in these k-1 folds comprise the training data. The model is tested in the left-out fold (testing data). This process is repeated for each set of k-1 folds for training and the corresponding left-out fold for testing (Figure 5-2). Commonly recommended approaches include 10-fold (i.e., a 90/10 split for training and testing), 5-fold (i.e., an 80/20 split), leave-one-out (k = sample size), and split-half (k = 2) cross-validation. Repeating the random splits (iterations) is generally recommended to obtain more stable estimates than a single split (Dangeti, 2017).

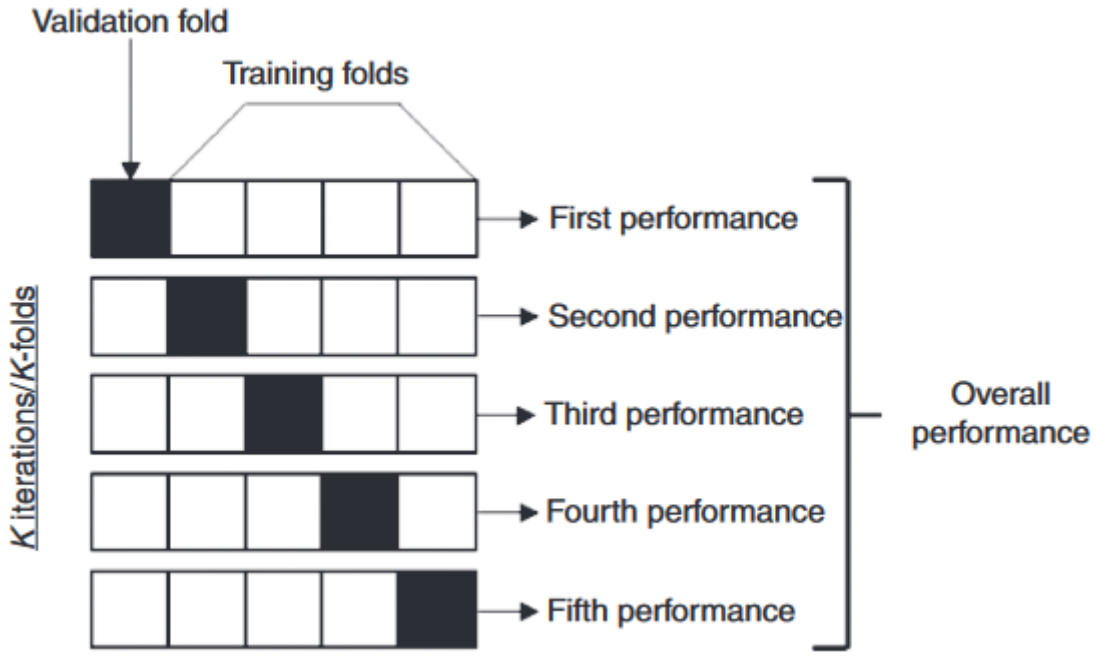

Figure 5-2 K-fold cross-validation

Shah, N., Arshad, A., Mazer, M.B., Carroll, C.L., Shein, S.L., Remy, K.E., 2023. The use of machine learning and artificial intelligence within pediatric critical care. Pediatr Res 93, 405–412. https://doi.org/10.1038/s41390-022-02380-6

As infant fcMRI imaging data is of high dimensionality (many features), support vector machine (SVM) multi-variate pattern analysis/classification can be used to determine patterns/differences within sub-groups of data (Ben-Hur et al., 2008). Support vector machine (SVM) analysis is effective in instances where

number of dimensions (features) are greater than number of samples. Through transforming data into higher-dimensional space, an SVM can convert complex classification/regression problems (with complex decision surfaces) into simpler problems that can use linear discriminant functions (Mechelli and Vieira, 2019). For support vector classification (SVC), the SVM finds the hyperplane (i.e., plane in high-dimensional space, line in 2-dimensional space) that separates classes by maximizing the distance between observations closest to the separating hyperplane.

Machine learning classification has been further extended to support vector regression (SVR) models, allowing quantitative predictions in individual subjects, and this has been used previously in infant studies (Nielsen et al., 2023, 2019; C. D. Smyser et al., 2016a). For support vector regression (SVR), the SVM finds the hyperplane that allows predictions to be within a specified error band, where observations just outside the error band define the hyperplane. In the context of age prediction, SVR uses a training set of observations with known ages and calculates the multi-variate relationship between features (i.e. functional connections/edges) and age (Pereira et al., 2009).

5.2.4 Studies of brain age

Using multivariate machine learning to estimate from brain features the age of the participant, has proven a powerful tool in recent years. It can be trained on large datasets spanning the age range. Then, when tested on unseen data, people with a "brain age" higher than their chronological age have been found to be at higher risk of various mental morbidities (Franke and Gaser, 2019). Diverse measures can be used to predict brain age. It has been used with structural and diffusion MRI to predict brain age in children and young adults (Erus et al., 2015). Further, in a study using structural and diffusion MRI features (creating 'morphometric similarity networks' derived from: regional volumes/diffusion tensor metrics/neurite orientation dispersion/image density) in a cohort of neonates (preterm and term scanned between 38 and 45 weeks PMA), the researchers regression model predicted PMA at scan with a mean

absolute error of 0.70 ± 0.56 weeks, and the classification model achieved 92% accuracy (Galdi et al., 2020).

As a next step from structural/diffusion models, it is natural to expect that differences in functional MRI connectivity (instead of brain structure/tractography measures) may be particularly useful indicators of function/dysfunction in infant brain development. Since the initial measurements of rsfMRI in term infants asleep (Fransson et al., 2009) investigators have studied the changing functional network configurations in infants during infancy (Damaraju et al., 2014; Fransson et al., 2011; Gao et al., 2013a, 2011). While higher-order resting state functional networks have been seen to develop slower (compared to primary motor/sensory networks) during the third trimester (Doria et al., 2010; Eyre et al., 2021) and infancy (Gao et al., 2015a; C. D. Smyser et al., 2016b), by 18 months age functional networks are relatively similar in architecture (Damaraju et al., 2010). It is during this period of rapid changing/developing resting state functional networks that there may be an opportunity to discern aberrant neurodevelopment. Indeed, the infant connectivity literature has shown differences in functional connectivity between preterm and term born infants/toddlers scanned asleep (Damaraju et al., 2010; Eyre et al., 2021; C. D. Smyser et al., 2016a, 2016b; Smyser et al., 2010).

Functional MRI connectivity has been used in multivariate models relating age and FC in a training set and predicting the age of test individuals in an adolescent/young adult group (Dosenbach et al., 2010), and also in an older adults group (Meier et al., 2012). Compared to the adolescent/adult literature in this area, Kardan et al have used FC fMRI data from the Baby Connectome Project study (Howell et al., 2019) to measure the reliability, uniqueness, and to predict age in a sample of older infants and toddlers (mean age 16 months: range 8-to-26 months) (Kardan et al., 2022). Using functional network features, a SVR (linear kernel) model (with 10-fold cross-validation) was used to predict infants' and toddlers' ages in months from their resting-state (asleep) FC pattern. The model successfully predicted novel infants' age within ± 3.6 months error and a prediction coefficient of determination of $R^2 = 0.51$ (Kardan et al., 2022). This ability to predict brain age in toddlers was also extended to a fully infant cohort in another study where infants aged 6 months and 12 months

underwent asleep rsfMRI (these infants were at low/high risk for autism based on family history) (Pruett et al., 2015). These researchers used feature selection to choose the top 200 features from the pairwise correlations (26,335 edges) to use in their classifier model. While their study did not show the ability to classify risk of autism, the study did successfully classify 6 month versus 12 month age with 88% accuracy (Pruett et al., 2015).

5.2.5 Aims and Objectives

Previously in this thesis (Chapter 4), it has been shown that infants watching movies have a different FC matrix (group wise) and that the shared/evoked component of the awake FC is stronger in the term born group compared to the preterm born group. The evoked FC did not simply equate to a difference between 'awake minus asleep' FC but appeared distinct and more complex in origin. However, it was felt that certain attributes of this awake FC, specifically the strong connectivity of the somatomotor and default mode networks, may lend towards a discriminatory power (classification/prediction) in awake infants. Indeed, previously other studies in asleep infants/toddlers have shown how the DMN connectivity matures during the first 2 years of life (Gao et al., 2013b) and that the DMN contains important edges involved in age classification in asleep 6 – 12 month old infants (Pruett et al., 2015).

The hypothesis of this current study was that FC from movies will be more revealing of key phenotypes (birth gestation and scan age) than FC from sleeping infants (aged 2 months PMA) and this would be seen as a difference in classification/prediction ability.

To achieve this aim, the following objectives were tasked:

- To use simple machine learning techniques to enable classification/prediction of dependent clinical variables.
- To examine the impact of various machine learning parameters on model function.
- To assess whether asleep brain state data allows classification/age prediction ability in this age group.

- To assess whether awake (movie watching) brain state data allows classification/age prediction ability in this age group.
- To identify any differences in classification/prediction ability between the asleep and awake brain states.
- If successful classification/prediction was seen, to then analyse model features/weights to allow some inference of what brain networks were important regarding birth gestation/brain age differences.

5.3 METHODS

5.3.1 Participants

The first 100 infants recruited as part of the FOUNDCOG study were included. This consisted of 75 term controls and 25 graduates of the NICU (see previous, Figure 3-4). To allow more data representing the preterm group, four additional NICU participants (scanned Oct – Dec 2022) were included in the preterm group (in addition to the first 25 NICU participants). Details of the detailed practical setup for awake (movies) and asleep infant fMRI scanning are given previously in this thesis (Chapter 3).

Infants attended for scanning at 2 months post-menstrual age (all infants born either term or preterm were each corrected to their PMA). All infants were scanned in the same Siemens Prisma 3T MRI scanner in the one visit/session. If the infant fell asleep, we acquired resting-state fMRI (1000 volumes) and then a T2-weighted anatomical sequence, as detailed in previously in this thesis (Chapter 3). These infants fell asleep naturally (no sedation) having commenced the session awake.

5.3.2 State/Stimulus

All infant movie and asleep data came from distinct functional runs (i.e. no concatenation of volumes/frames). Movie runs were collected while infants watched 6 short movie clips. Infant asleep runs were collected during natural sleep with the display turned off, without visual stimulation. The asleep fMRI run was stopped as soon as it was felt that the infant was no longer asleep. Asleep runs were 10 min long (1000 volumes). Asleep runs (surviving motion thresholds) were successfully obtained in 76 infants (56 term controls and 20 preterms).

5.3.3 Code

The code used for pre-processing, data handling, analysis, statistics, and output graphics is available at (please contact to request access permissions): https://github.com/Grahamgithubking/foundcog_pipeline/tree/master/graham_code

5.3.4 Pre-processing

For fMRI runs the CMRR (https://www.cmrr.umn.edu/multiband/) gradient-echo multiband EPI sequence was used (acceleration factor 4), 3 x 3 mm in-plane, 36 slices of 3 mm plus 10% gap, phase encoding anterior-to-posterior, repetition time (TR) 610 ms, echo time (TE) 32 ms, flip angle 40 degrees, echo spacing 0.54 ms.

MRI data were converted from DICOM to NIfTI format using dcm2niix (https://github.com/rordenlab/dcm2niix) (Li et al., 2016). The FMRIB Software Library FSL was used in the pre-processing steps (Smith et al., 2004).

Motion was determined using FSL MCFLIRT (Jenkinson et al., 2002), using the middle volume as the standard reference, and the 6 motion parameters (3 translation, 3 rotation) were used to calculate framewise displacement (FWD, in mm) (Power et al., 2012) using Nippype software algorithm (Gorgolewski et al., 2011).

Two spin-echo reference protocols were acquired for distortion correction each time the infant was positioned in the head coil (i.e. once per session), one with phase encoding anterior-to-posterior and the other posterior-to-anterior, with the same geometry as the fMRI run but without multiband for better tissue contrast (TR=2,260 ms, TE=32 ms, FA=40 degrees, 10 volumes).
Following motion correction with FSL MCFLIRT, the field distortion estimation from FSL TOPUP (Andersson et al., 2003) was then applied to the EPI data to correct for susceptibility distortion. One subject (of these 100 participants) was excluded due to failing to obtain field maps.

As a T2-weighted anatomical scan was not presumed/expected during the session (not needed as an inclusion criterion) a bespoke method of co-registration/normalisation of the functional images was devised. To allow co-registration of a subject's multiple fMRI runs, a co-registration reference run was chosen (with asleep/resting state being the preferred co-registration run in any subject who had both resting state and movie runs). The mean of this chosen run was used as the co-registration reference. The mean images of a subject's other runs were then co-registered (FSL FLIRT) using 12 DOF. Using the transformation matrices (from these co-registrations) the mean image of each run was re-oriented (applyXFM) to the space of the reference run. Averaging (ants.AverageImages) these mean images produced a single average volume in the reference space.

For spatial normalisation to a common group space, a 2 – 5 month age infant T2-weighted template was used (Fonov et al., 2009). Using FSL FLIRT (cost function=mutual info, DOF=12) the single average volume was linearly registered (normalised) to the infant template. Combining both transformations (using fsl.utils.ConvertXFM) a subject's distortion corrected (FSL TOPUP) functional runs were then both co-registered to the reference run and normalised to the template (applyXFM). The runs were then smoothed using a gaussian kernel (FWHM=5.0) using fsl.SMOOTH to allow for inaccuracies of spatial normalisation. Of note, functional runs were not slice time corrected as the TR was short at 0.61sec, and a multiband EPI sequence was used. Global signal reduction (GSR) was not applied as this analysis aimed at determining differences between groups of infants with different noise characteristics and so the effect of GSR was not certain (Murphy and Fox, 2017).

5.3.5 Quality Control

Quality control checks were as previously documented in Section 4.3.5.

5.3.6 Motion threshold

In keeping with other recent studies (Ellis et al., 2021b; Yates et al., 2022) in awake infant fMRI a FWD threshold of 3mm was chosen. We required that less than 10% of volumes could meet this threshold (in keeping with the approximated number of similar volumes in the asleep runs). A mean of 1.4 movies runs from each infant crossed the motion threshold (min 1 – max 3 runs). Of all movies runs for all infants included the mean FWD was 0.72mm (std 0.37mm). Of all asleep runs for all infants included the mean FWD was 0.19mm (std 0.11mm).

5.3.7 Timeseries Signal Cleaning

As less than 10% of volumes were allowed to meet the FWD threshold (i.e. 90% of volumes had to be below the chosen FWD threshold) in any run (movie or asleep), it was decided to keep the 480 consecutive volumes/frames intact, and no volume scrubbing/censoring was applied. As the segment length was relatively short (480 volumes) and the high pass filter was 0.01Hz, it was considered that there was no real need to detrend the segment.

Steps of signal cleaning for included the following (in order): band pass filtering; confound regression; and z-scoring. For band pass filtering the signal was filtered between 0.01 and 0.1 Hz (as is common in infant/child connectivity literature). For confound regression the corresponding motion parameter file (FSL MCFLIRT motion correction) containing estimated 3 rotations and 3 translations for each TR was uploaded. Confound regression includes fitting a linear model using motion estimates as regressors then subtracting it out from the signal. The output was z-scored meaning the timeseries were shifted to zero mean and scaled to unit variance.

5.3.8 Functional connectivity

The Schaefer 400 parcellation (7 networks) atlas (Schaefer et al., 2018) was used for parcellation [See Appendix]. This is an adult parcellation based on the 7 functional connectivity networks as determined by Yeo et al. (Thomas Yeo et al., 2011a). The 7 functional networks consist of: visual, somatomotor, dorsal attention, ventral attention, limbic, frontoparietal control, and default networks.

As the movie runs were 480 TRs (volumes) in duration (5 initial volumes were discarded due to T1 equilibrium effects), the asleep runs were therefore similarly shortened to 480 consecutive TRs in length. This was so that both movies and asleep runs would contain the exact same number of volumes.

Functional connectivity was calculated as the Pearson correlation of the timeseries for a parcel with every other parcel across the number of TRs (volumes) within the subject's own run. This method was similar for both movies and asleep state runs. Any infants with repeat sessions of movie watching had sessions averaged within each subject.

Network level connectivity was determined by calculating the arithmetic mean of the corresponding parcels of the 2-dimensional parcel level connectivity array. Parcels located on the leading diagonal (within network) of the parcel level array (400, 400) (i.e. value of '1') were not included in the arithmetic means for their respective networks.

The indices of the upper triangle (including the leading diagonal values) of the Yeo et al. (14, 14) network level connectivity matrices were taken to achieve a series of 105 unique network to network connections/edges. These 105 connectivity edges were the column headers of the resulting dataframe. Each run (row of the dataframe) was labelled with the corresponding subject ID.

	subject	LH_visual_LH_visual	...	RH_control_RH_default	RH_default_RH_default
0	IRN76	0.598713	...	0.504570	0.511541
1	IRN74	0.353262	...	0.414129	0.404192
2	IRN72	0.770655	...	0.602056	0.515320
3	ICC193	0.464222	...	0.541683	0.594635
4	ICC185	0.722278	...	0.660923	0.632449
..	...	...	...	...	...
304	IRC21	0.498769	...	0.259935	0.223431
305	IRC19	0.389827	...	0.343346	0.310251
306	IRC13	0.469892	...	0.272443	0.262846
307	ICN2	0.301108	...	0.214974	0.224694
308	IRN1	0.309116	...	0.186139	0.178104

[309 rows x 106 columns]

Figure 5-3 Example of a dataframe used for classification/regression analysis

There were 105 network to network connections (columns). The correlation for a run (row) in the dataframe was labelled with the corresponding subject ID.

5.3.9 Classification and regression variables

Gestational age at birth was acquired through medical records upon study enrolment and was determined by best obstetric estimate (American College of Obstetricians and Gynecologists, 2017) including last menstrual period or earliest ultrasound dating available. For classification analyses an infant was classed as preterm if they were born less than 37 weeks 0 days post-menstrual age (PMA), and term if they were born on or after 37 and 0 days gestation (PMA).

An infant's state was classed as asleep as judged from: their eyes were closed, they had minimal movements, and based on both researchers (one with direct vision inside the scanner room and the other visually monitoring via the MR compatible camera) agreeing that the infant was asleep.

An infant's state was classed as movies (awake) as judged from: their eyes were open, and they were attending the visual stimuli as much as possible, to such an extent that they completed the movie run duration and that both researchers (one in the scanner room and one in the control room) agreed that the infant was comfortable and cooperative during the run.

Scan age (corrected age on day of scanning) was determined based on the infant's birth gestation and chronological age since birth. This decision was to achieve similarity in PMA between infants (in as much as possible) on the day of MRI scanning.

Head circumference (cm) was measured by the specialist registrar doctor (with expertise in the technique) on the day of attending for MRI scanning.

Motion was determined by calculating the average FWD (Power et al., 2012) for the run (or across runs for infants with more than run).

To determine an approximate level of neurodevelopment the Ages & Stages Questionnaire (ASQ) (Squires and Bricker, 2009) (parent reported questionnaire) was conducted at 9-months corrected age. Most infants received the 10-month ASQ (age range: 9mo 0d to 10mo 30d). However, based on an infant's corrected age a small number of infants were slightly younger than 9 months. Parents of those infants younger than 9 months corrected gestational age (CGA) were given the 8-month ASQ (age range: 7mo 0d to 8mo 30d). The total ASQ score for each infant was used as a variable in the regressor analyses.

5.3.10 Support Vector Machine (SVM) Analyses

Both support vector classification (SVC) and regression (SVR) was conducted using the package scikit-learn 1.0.2 (Pedregosa et al., 2011) in Python 3.8.10.

5.3.10.1 SVM Classification (SVC)

The first classification analysis was conducted to determine asleep versus movie state (sub-divided by preterm and term born infants). The second classification analysis was conducted to determine preterm versus term birth (sub-divided by asleep and movie state).

In the context of SVC, sampling was stratified (stratified k-fold) so that train/test sets represented the ratio of the vector for the entire dataset (for example: the ratio of term/preterm runs in the dataset).

We used stratified 10-fold cross-validation to train/test the models. The cost parameter C of the SVC (kernel = linear) was tuned using another 10-fold inner loop. The cost parameter achieving the model with the highest balanced-accuracy score was then used in the SVC for the 10-fold test sets. This whole process was iterated 10 times to ensure stability of the result and to ensure performance was not due to random seeding.

By applying the classifier model for state (asleep versus movie) trained using term infant data only, to the features/data from the preterm group, we were able to assess whether the same features (network edges) that were important in classifying state (asleep/movies) in term infants were also important in preterm infants (and visa-versa). Similarly, by applying the classifier model for birth gestation (preterm versus term birth) trained using movie state data only, to the features/data from the asleep state, we were able to assess whether the same features that were important in classifying birth gestation (preterm/term) in the movies state were also important in asleep state (and vice-versa).

5.3.10.2 SVM Regression (SVR)

Multivariate regression analysis was conducted to predict variables (predicted gestational age, predicted scan age) using FC data from either the movie or asleep states respectively. Further SVR analysis was conducted using the combined (concatenated) movie and asleep run data for a subject ('both states').

We used k-fold cross-validation to train/test the models. The cost parameter C of the SVR (kernel = linear) was tuned using a 10-fold inner loop. The cost parameter achieving the model with the highest R^2 score (coefficient of determination) was then used in the SVR model for the 10-fold test sets. This whole process was iterated 10 times to ensure stability of the result and to ensure performance was not due to random seeding.

5.3.10.3 *Parameter C*

Regularization/penalty parameter C is a hyperparameter with values between 0 and infinity. The strength of the regularization is inversely proportional to C. If noisy data, C should be lower (larger margin, more violations). Parameter C was determined by a gridsearch [https://scikit-learn.org/stable/modules /generated/sklearn.model_selection.GridSearchCV.html] in a 10-fold validation inner loop, and the C value producing the best score (balanced-accuracy for SVC, R^2 for SVR) in the inner loop was used for k-fold train/test sets of the model.

5.3.11 Support Vector Machine Performance Metrics

5.3.11.1 *SVC Classification:*

Classification accuracy is the proportion of correctly classified instances over the total number of instances in the test set. Accuracy can be misleading in imbalanced datasets where the majority class dominates the accuracy score leading to falsely positive accuracy.

Precision measures the proportion of true positives over the total number of predicted positives. Recall (sensitivity) measures the proportion of true positives over the total number of actual positives. A useful measurement in imbalanced data sets is the F1-score which relies on both precision and recall. The F1-score is calculated as 2 x (precision x recall) / (precision + recall). The F1-score gives an indication of how precise and robust a classifier is. Importantly, the F1-score only improves when both the amount and accuracy of predictions gets better (i.e. it considers how the data is distributed/balanced). F1-scores are useful in scenarios where it is important to identify both positive and negative cases for a chosen class.

An initial assessment of unbalanced datasets (movies versus asleep, preterm versus term) used in this study showed that in some instances the accuracy score was impacted by unbalanced groups. An initial method to tackle this issue was to use a weighted SVM based on class frequency. The class weight is used

to give more importance to a certain class (i.e. the magnitude of the positive support vector will be higher than the negative vector). The SVM can penalize the errors made on the minority class more than the errors made on the majority class and balance the influence of both classes. The "balanced" mode uses the values of y to automatically adjust weights inversely proportional to class frequencies in the input data as n_samples / (n_classes * np.bincount(y)). While weighted classes are helpful when using unbalanced datasets, it was felt that the accuracy score was still not a transparent measure of performance, and so ultimately it was decided to use the F1-scores as a more transparent indication of the true predictive power for a class.

Additional analysis (using F1-scores as performance metric) included random under-sampling of the largest class (term infants) for the 'gestation' classifier only (the 'state' classifier was already balanced in the original subject groups). This random under-sampling produced 'balanced classes' with equal numbers of preterm and term infants (compared to the original 'unbalanced classes').

5.3.11.2 SVR Regression:

Performance of SVR was determined using R^2 values. R-squared (R^2), also known as the coefficient of determination (and similar to the correlation coefficient squared), is a statistical measure that represents the proportion of the variance for a dependent variable that's explained by one or more independent variables in a regression model.

$R^2 = 1 - (RSS/TSS)$

where
RSS represents the residual sum of squares.
TSS represents the total sum of squares.

5.3.12 Significance of prediction

5.3.12.1 Classification significance

To evaluate the significance of the classification scores (F1 scores for each class), for each of the 10 iterations we generated a null distribution by calculating 1000 permutations of randomly shuffled labels (thereby removing dependency between the features and the labels). The p-value was the fraction of the 1000 permutations for which the average cross-validation score obtained by the model of shuffled labels was better than the cross-validation score obtained by the model using the original data. The p-values (10 iterations used to calculate the final classification score) were summed and divided by 10 to get the p-value for the final score. A small p-value suggests that there is a real dependency between features and targets which has been used by the estimator to give good predictions.

5.3.12.2 Regression significance

To assess the significance of the regression scores (R^2), we used SVR to model the relationship between the FC features and randomly permuted samples of the dependent variable to create a null model. This process was repeated for 1000 resamples. The p-value was the fraction of the 1000 permutations for which the average cross-validation score obtained by the null model was better than the score obtained by the model using the original data. The p-values (10 iterations used to calculate the final classification score) were summed and divided by 10 to get the p-value for the final score.

5.3.12.3 Differences in group means

When comparing group means (e.g. preterm versus term) for differences in predicted versus actual data an independent t-test was used for statistical significance.

5.4 RESULTS

5.4.1 Participants contributing to functional models

The first 75 term control participants were included (as seen previously Figure 3-4). To allow more data representing the preterm group, four additional NICU participants (scanned Oct – Dec 2022) were included in the preterm group (in addition to the first 25 NICU participants, seen previously Figure 3-4). Of the 75 control participants, two did not have any functional MRI data. Of the 29 NICU (preterm) participants: one was excluded due to not having field maps; four were excluded due to having known structural brain pathology; and one was excluded due to poor registration to template. Characteristics of the remaining 23 NICU graduates are shown (Table 5-1).

Table 5-1 Population characteristics of included NICU graduates:

	NICU (n=23)
Birth gestation (wks, median)	32 (IQR 29-33)
Sex (M:F)	10:13
NICU days (mean)	39 (std 24)
Chorioamnionitis (no.)	1
Early onset sepsis (no.)	1
Late onset sepsis (no.)	0
Necrotising enterocolitis (no.)	0
Chronic Lung Disease (no.)	5

The remaining 96 infants (73 controls, 23 NICU) had functional runs (movies and asleep) assessed to see if they met the defined standard motion threshold for inclusion. The number of participants contributing runs meeting the standard motion threshold are shown in Figure 5-4.

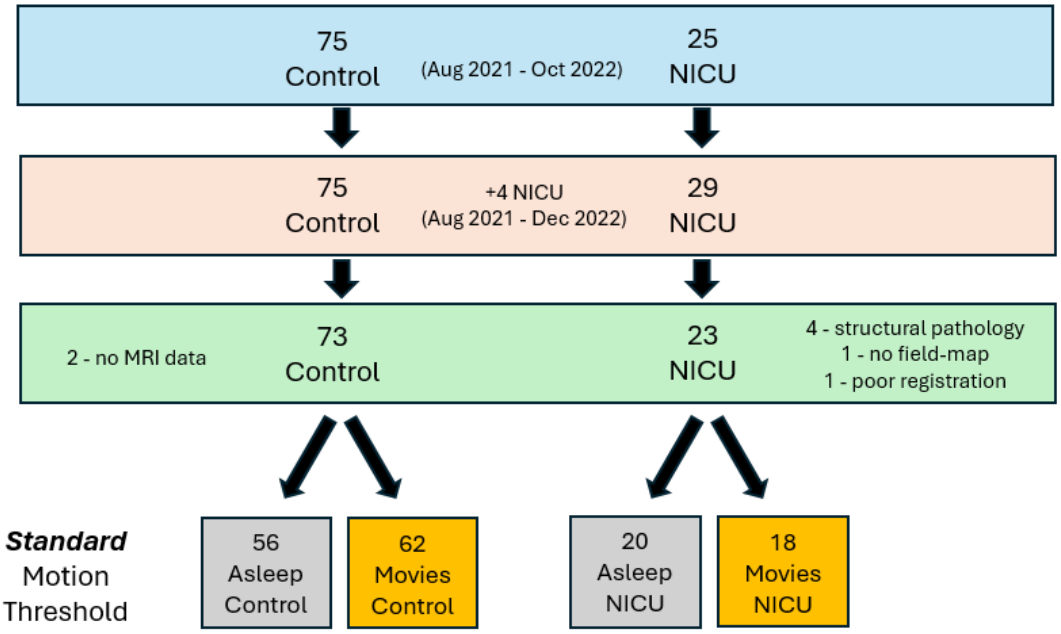

Figure 5-4 Number of participants (Control/NICU) contributing to functional models (using standard motion threshold)

5.4.2 Classification of birth gestation using connectivity features from different states

5.4.2.1 Classifier models

Classifier models of birth gestation (preterm/term) were created using features/data from asleep and movies states respectively. As can be seen in Table 5-2 there was an expected significant difference in birth gestation (the classifier vectors). In addition, motion/FWD approached significance, with slightly higher motion in the preterm infants scanned watching movies.

Table 5-2 Population characteristics: Movies model

	Preterm (n=18)^	**Term (n=62)^**	**P-value¥**
Birth gestation (wks)	31.7 (2.9)	39.3 (1.1)	0.0001
OFC (cm)**	40.6 (1.6)	40.6 (1.4)	0.94
Scan age (mo.)	2.6 (0.6)	2.4 (0.5)	0.133
Motion/FWD (mm)	0.8 (0.3)	0.7 (0.3)	0.09

^ Mean (SD), unless otherwise stated

¥ Student t-test, unless otherwise stated
** preterm n =16, term n = 59

Using FC data from infants watching movies, the classifier was unable to classify term gestation from FC with an F1-score similar to the null/permuted classifier (Figure 5-5). The movie classifier showed true positives of 40, true negatives of 6, false positives of 12, and false negatives of 22.

In the asleep model it can be seen that there were minimal differences in characteristics of infants born preterm versus term (only birth gestation different as expected) (Table 5-3).

Table 5-3 Population characteristics: Asleep model

	Preterm (n=20)^	**Term (n=56)^**	**P-value¥**
Birth gestation (wks)	32.5 (2.9)	39.2 (1.1)	0.0001
OFC (cm)**	39.8 (1.8)	40.4 (1.3)	0.13
Scan age (mo.)	2.5 (0.5)	2.3 (0.4)	0.29
Motion/FWD (mm)	0.21 (0.16)	0.18 (0.09)	0.28

^ Mean (SD), unless otherwise stated
¥ Student t-test, unless otherwise stated
** preterm n =18, term n = 53

In asleep infants the classifier model was also unable to classify gestation in unbalanced model (Figure 5-5), with true positives of 41, true negatives of 9, false positives of 11, and false negatives of 15.

Similarly, gestation could not be classified in a balanced model (Figure 5-6), either for the movies, with true positives of 9, true negatives of 11, false positives of 7, and false negatives of 9, or for asleep with true positives of 10, true negatives of 10, false positives of 10, and false negatives of 10.

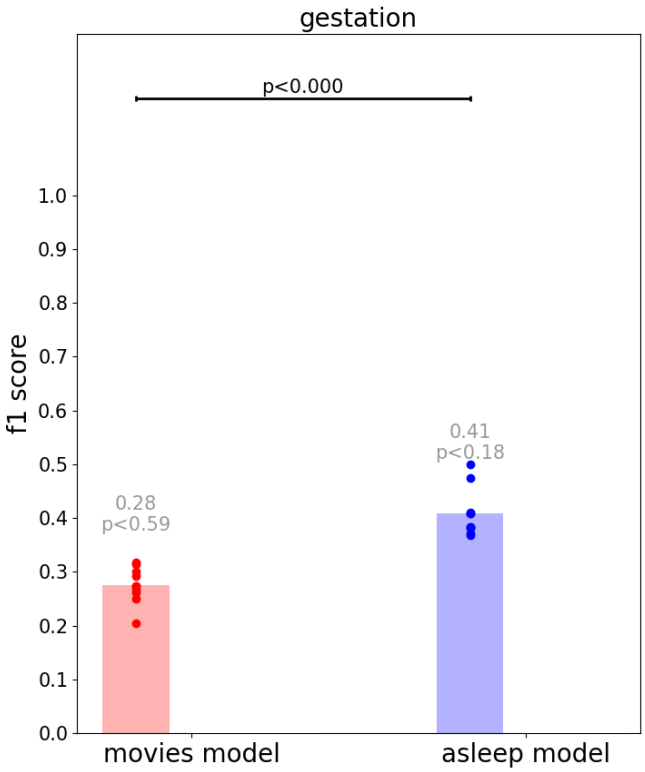

Figure 5-5 F1-scores for classification (unbalanced classes) of birth gestation in asleep and movie states.

(dots = F1-score for each of 10 model iterations, bar = mean F1-score)

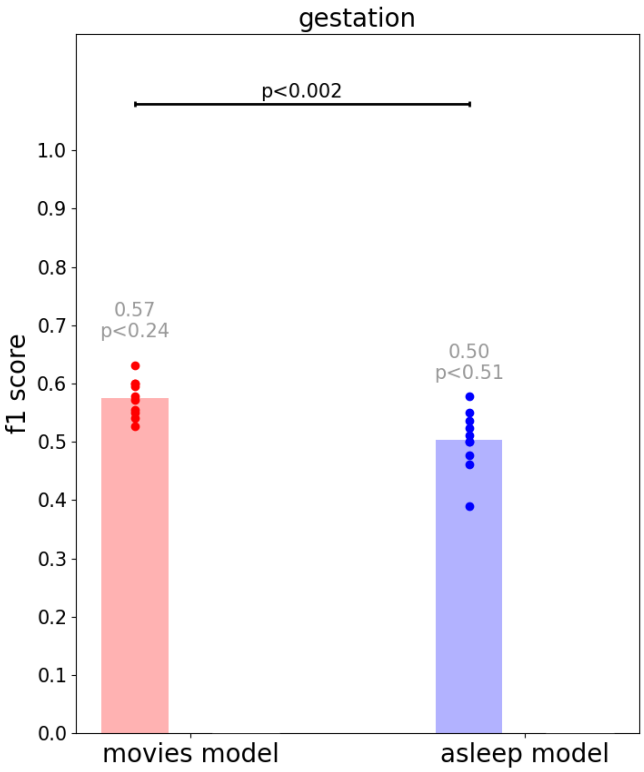

Figure 5-6 F1-scores for classification (balanced classes) of birth gestation in asleep and movie states.

(dots = F1-score for each of 10 model iterations, bar = mean F1-score)

Examining differences in classification between models based on movies versus asleep data, unbalanced classes models appeared to indicate greater classification ability of gestation with infants in the asleep state compared to watching movies (F1-scores; 0.41 asleep versus 0.28 awake) (Figure 5-5). However, using balanced classes, this greater ability of gestation classification in the asleep state disappeared, in this case the movies model (F1-score 0.57) performed slightly better than asleep model (F1-score 0.50), $p<0.002$ (Figure 5-6).

Overall, it appears that the FC network features in both movies and asleep states, using a support vector classifier with a linear kernel, were poorly able to classify birth gestation in infants at 2 months corrected age (i.e. scan age approximately 2 months corrected age).

5.4.2.2 *Generalisation of birth gestation classifier across states*

As there was considerable overlap in the infants who both fell asleep (asleep data set) and watched movies (movies data set), it was decided to determine whether indeed the difference in FC networks (difference in FC network features between movies and asleep states) might lend towards determination/classification of gestation. This analysis involved creation of the same SVC models (movies model trained on movies data, and asleep model trained on asleep data) but instead the models were tested on FC network features from infants in the other state (i.e. movies model tested on asleep data, and asleep model tested on movies data). In general, models performed worse (Figure 5-7 and Figure 5-8) (i.e. worse classification of gestation), however in the case of balanced models, the model trained on asleep data and tested on movies data, showed that the classification of gestation improved (F1-score 0.66, $p<0.001$) (Figure 5-8) compared to when the same asleep model was tested on asleep data (F1-score 0.50, $p<0.51$) (Figure 5-6). This suggests that when a classifier is training on FC data with less motion noise from sleeping infants, it can effectively discriminate gestation when tested on movies.

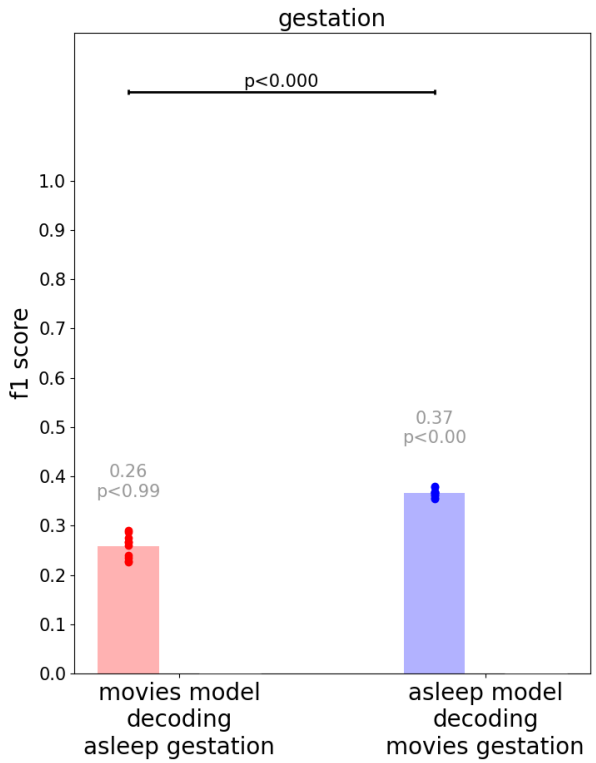

Figure 5-7 F1-scores for classification models (unbalanced classes) tested on FC features from the other state (to classify gestation)

(dots = F1-score for each of 10 model iterations, bar = mean F1-score)

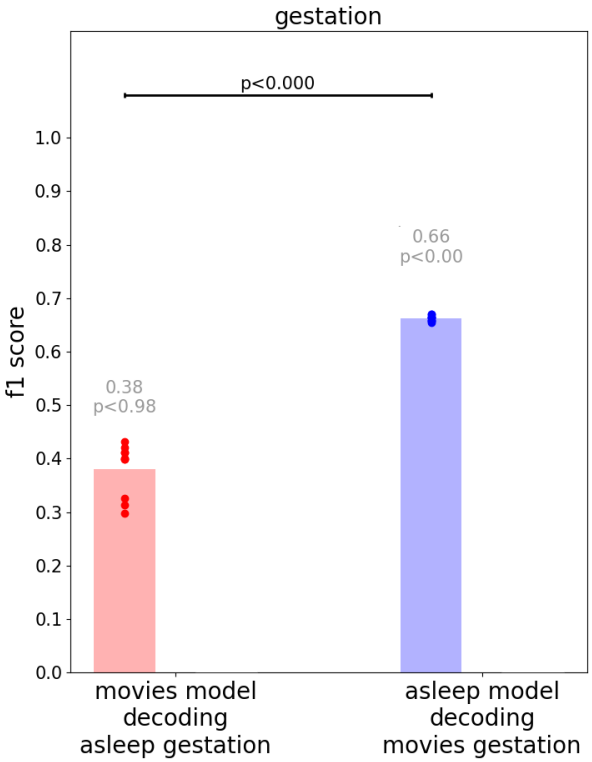

Figure 5-8 F1-scores for classification models (balanced classes) tested on FC features from the other state (to classify gestation).

(dots = F1-score for each of 10 model iterations, bar = mean F1-score)

5.4.2.3 Impact of confounders on birth gestation classifier

To assess the impact of motion on classification of birth gestation the balanced classifiers (under-sampling the largest class to equal the smallest class) were re-run but trained with only FWD as the feature. This achieved F1-scores of 0.58 and 0.16 from infants watching movies and asleep respectively. These scores are no greater than the F1-scores achieved when trained on FC network features (and indeed specifically asleep preterm infants had a considerably higher F1-score when the model was trained on FC network features).

Similarly, to assess the impact of head circumference (OFC) on classification power, the balanced classifiers models were trained using only OFC as the model feature. This achieved F1-scores of 0.38 and 0.59 from infants watching movies or asleep respectively (i.e. no greater ability to classify birth gestation versus models using FC network features).

Lastly, to assess the impact of scan age on classification of birth gestation, the balanced classifiers were trained with only scan age as the model feature. This achieved F1-scores of 0.51 and 0.15 from infants watching movies or asleep respectively. Again, these scores are no greater than the F1-scores achieved using FC networks features (and again, specifically, asleep preterm infants had a considerably higher F1-score when the model was trained on FC network features).

5.4.4 Classification of state using connectivity features from infants born at different gestation

5.4.4.1 Classifier models

Classifier models of state (asleep/movies) were created using features/data from preterm infants only and term infants only respectively. Classes were approximately equally balanced (Table 5-4 and Table 5-5). Importantly, the single and significant difference between infants scanned asleep versus watching movies was motion/FWD (as seen by significant p-values).

Table 5-4 Population characteristics: Preterm model

	Movies (n=18)^	**Asleep (n=20)^**	**P-value¥**
Birth gestation (wks)	31.7 (2.9)	32.5 (2.8)	0.38
OFC (cm)**	40.6 (1.6)	39.8 (1.8)	0.20
Scan age (mo.)	2.6 (0.6)	2.5 (0.5)	0.39
Motion/FWD (mm)	0.85 (0.3)	0.21 (0.16)	0.001

^ Mean (SD), unless otherwise stated
¥ Student t-test, unless otherwise stated
** movies n = 16, asleep n = 18

In the preterm model classification of state was high (f1 0.82, $p<0.001$) (Figure 5-9). The classification model using FC network data from term infants only was able to classify state even better (f1 0.93, $p<0.001$) (Figure 5-9).

Table 5-5 Population characteristics: Term model

	Movies (n=62)^	**Asleep (n=56)^**	**P-value¥**
Birth gestation (wks)	39.3 (1.1)	39.2 (1.1)	0.70
OFC (cm)**	40.6 (1.4)	40.4 (1.3)	0.48
Scan age (mo.)	2.4 (0.5)	2.3 (0.4)	0.28
Motion/FWD (mm)	0.70 (0.3)	0.18 (0.1)	0.001

^ Mean (SD), unless otherwise stated
¥ Student t-test, unless otherwise stated
** movies n = 59, asleep n = 53

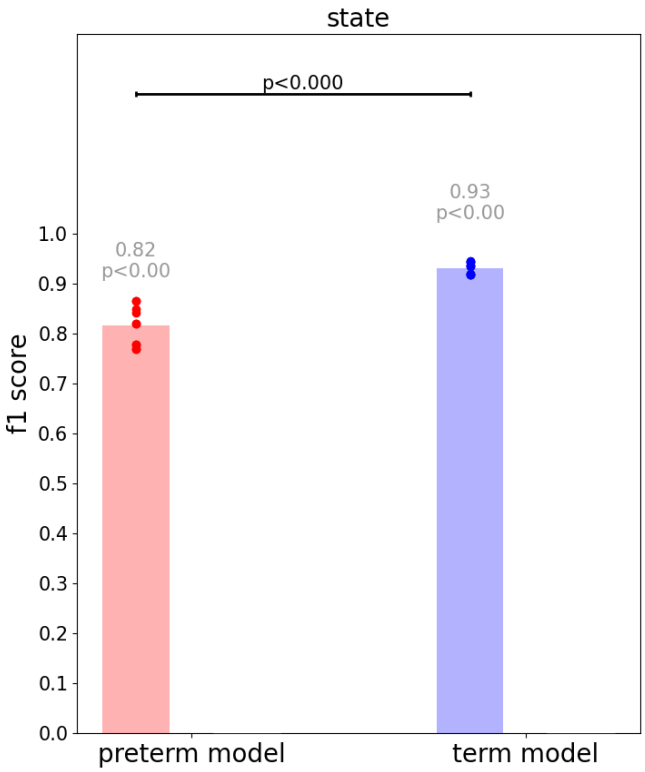

Figure 5-9 F1-scores for classification of state (asleep/movies) in preterm and term born infants.

(dots = F1-score for each of 10 model iterations, bar = mean F1-score)

Initial reflection on these results appeared to show that infants born at term gestation had FC network features that allowed stronger/better classification of brain state (asleep versus movies) when undergoing fMRI at 2 months corrected age i.e. perhaps arousal/concentration or some other brain network connectivity features were more discriminatory in term infants.

5.4.4.2 Generalisation of state classifier across birth gestation

When assessing how the models (preterm/term data) performed when tested on FC network features from infants born a different gestation, it could be seen that F1-scores (classification) changed somewhat, likely due the fact that features used to decode state in the respective models were different between preterm and term born infants. In the case of the preterm model classification slightly increased, while in the case of the term model classification slightly decreased (Figure 5-10).

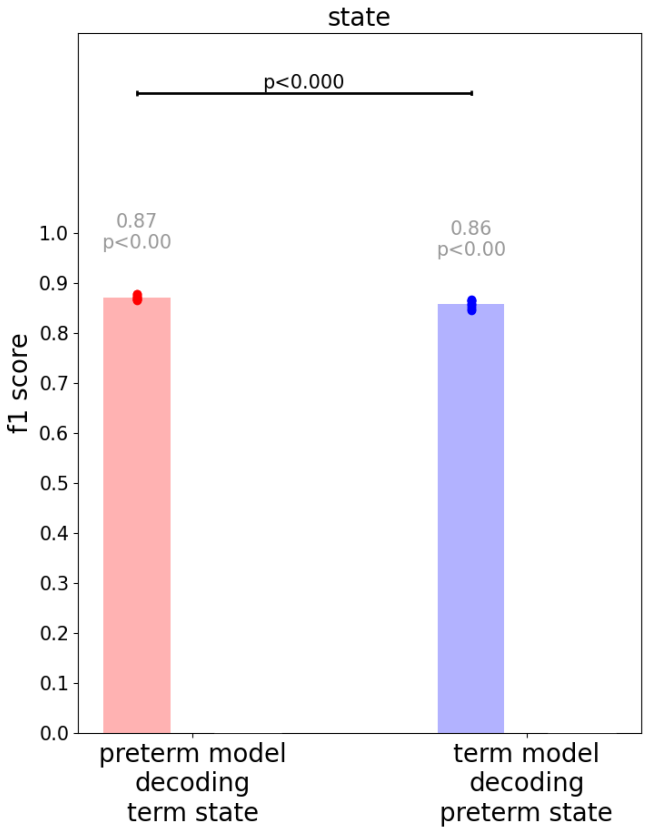

Figure 5-10 F1-scores for classifier models tested on FC features from infants born a different gestation (preterm/term) (to classify movies/asleep state).

(dots = F1-score for each of 10 model iterations, bar = mean F1-score)

5.4.4.3 Impact of confounders on state classification

To assess the impact of motion on the classification of state, the models were trained using only motion/FWD as the training feature. These achieved F1-scores of 0.82 and 0.92 from preterm and term infants respectively. These F1-scores are practically the exact same as those calculated from models using the 105 FC network edges features indicating that it is possible that the classification of state was driven by motion impacting the FC network feature values. This is an important finding, that merits deeper investigation in future studies.

Similarly, to assess the impact of OFC on classification power, the classifier models were trained with only OFC as the feature. This achieved F1-scores of 0.53 and 0.46 from preterm and term infants respectively. These indicate that

OFC had less impact than either functional connectivity or motion on state classification for both preterm and term born infants.

Lastly, to assess the impact of scan age on state classification, the classifier models were trained with only scan age as the feature. This achieved F1-scores of 0.39 and 0.36 from preterm and term infants respectively. This shows that scan age likely holds some factor which explains a considerable amount of the variance associated with asleep infant state.

5.4.5 Prediction of birth gestation using connectivity data from different states

Using SVR machine learning models, estimates of predicted gestational age at birth were calculated using the FC data from infants who fell asleep and watched movies awake respectively.

Initial characteristics of the asleep infant group were examined using Pearson-r correlation values with birth gestation (Table 5-6). This showed that more premature born infants (younger gestation) were scanned at a slightly older corrected age (r = -0.15), had slightly smaller head circumferences (r = 0.13) likely reflecting slower ex-utero growth in the NICU, and had slightly more motion/FWD (r = -0.19).

Table 5-6 Variables potentially related to birth gestation – Asleep fMRI data

	No. Infants	**Mean (std); min-max**	**Correlation w/ birth gestation^**
Birth gestation (wks)	76	37.4 (3.4); 28.6-41.7	n/a
Scan age (mo.)	76	2.37 (0.43); 1.60-4.10	-0.15
OFC (cm)	71	40.3 (1.5); 35.7-44.0	0.13
FWD (mm)	76	0.19 (0.11); 0.07-0.65	-0.19

^Pearson r correlation

Using the FC network features from the asleep data (76 infants), a SVR model was fitted to the actual gestational age data. The model performed poorly with the given data and predicted all ages between 37 and 40 weeks gestation (Figure 5-11). The coefficient of determination (R^2 = -0.14) was slightly negative implying that the fit of the model was worse than that of fitting a horizontal straight line through the mean of the data (null hypothesis).

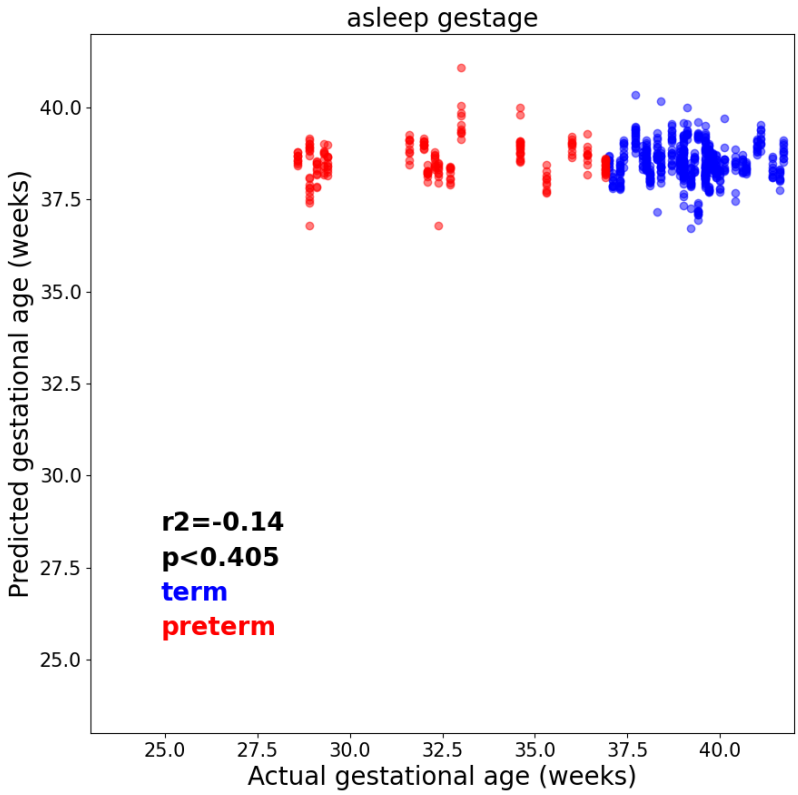

Figure 5-11 Support vector regression results depicting actual (x-axis) versus predicted (y-axis) gestational age at birth for term and preterm infants determined using asleep connectivity data at 2 months corrected age.

Characteristics of the infant group watching movies were examined using Pearson-r correlation values with birth gestation (Table 5-7). Again, this showed that more premature born infants (younger gestation) were scanned at a slightly older corrected age (r = -0.10), had slightly smaller head circumferences (r = 0.06) and had slightly more motion/FWD (r = -0.12).

Table 5-7 Variables potentially related to birth gestation – Movies fMRI data

	No. Infants	Mean (std); min-max	Correlation w/ birth gestation^
Birth gestation (wks)	80	37.6 (3.5); 23.9-41.7	n/a
Scan age (mo.)	80	2.5 (0.5); 1.6-4.1	-0.1
OFC (cm)	75	40.60 (1.4); 37.0-44.0	0.06
FWD (mm)	80	0.74 (0.33); 0.20-1.5	-0.12

^Pearson r correlation

Again, using the FC network features from the awake movies data (80 infants), a SVR model was fitted to the actual gestational age data. Again, this model performed poorly with the given data and predicted all ages between 37 and 40 weeks gestation (Figure 5-12). The coefficient of determination (R^2 = -0.14) was similar to that of the asleep state and was slightly negative implying that the fit of the model was worse than that of fitting a horizontal straight line through the mean of the data (null hypothesis).

The difference (error) between predicted versus actual gestational age (absolute value) was calculated for each infant using their asleep followed by movie data. The average for the groups was calculated and showed a difference of 6 weeks and 1.1 weeks for preterm and term groups respectively (p value <0.001) for asleep state. Similarly, the average difference was 7.1 weeks and 1.0 weeks for preterm and term groups respectively (p value <0.001) for the movie state.

Overall, these results imply that the FC network features (at the Yeo et al. 7 network edge level) in these infants at scan age (2 months corrected age) did not contain information explaining the variance of gestational age at birth in these infants (both asleep and movies states).

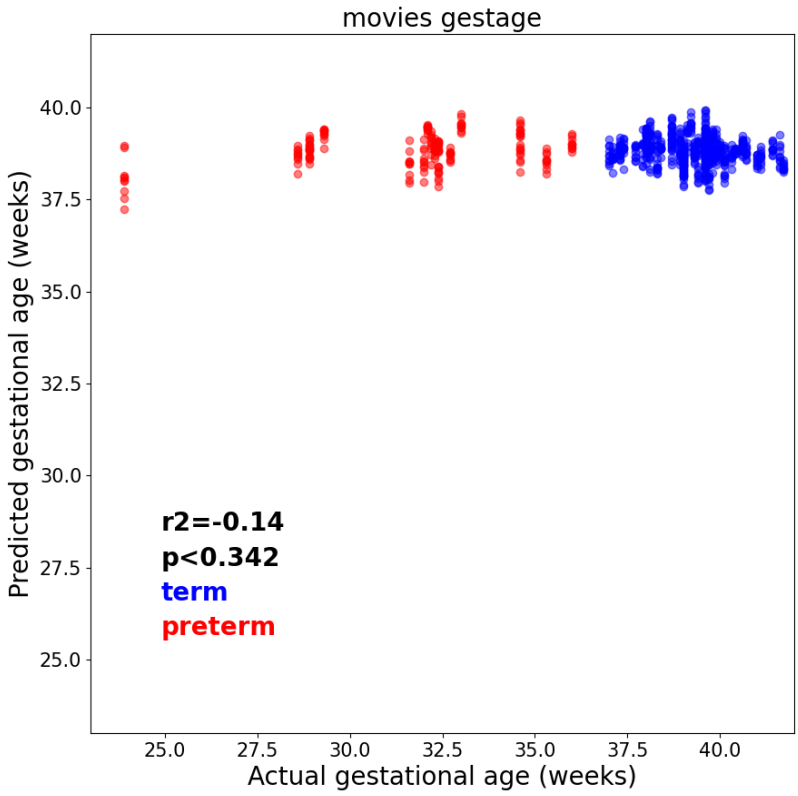

Figure 5-12 Support vector regression results depicting actual (x-axis) versus predicted (y-axis) gestational age at birth for term and preterm infants determined using movie (awake) data at 2 months corrected age.

5.4.6 Prediction of scan age using connectivity data from different states

Estimates of predicted scan age (corrected age a scan visit) were calculated using the fMRI data from infants who fell asleep and watched movies respectively. Characteristics of the asleep infant group were examined using Pearson-r correlation values with birth gestation (Table 5-8). These showed that those scanned at an older corrected scan age (min 1.6 – max 4.1 months age) were born at a younger gestation (Pearson-r = -0.15), had larger head size (Pearson-r = 0.34) and has more motion/FWD (Pearson-r= 0.05).

Table 5-8 Variables potentially related to scan age – Asleep fMRI data

	No. Infants	**Mean (std); min-max**	**Correlation w/ scan age^**
Scan age (mo.)	76	2.37 (0.43); 1.60-4.10	n/a
Birth gestation (wks)	76	37.4 (3.4); 28.6-41.7	-0.15
OFC (cm)	71	40.3 (1.5); 35.7-44.0	0.34
FWD (mm)	76	0.19 (0.11); 0.07-0.65	0.05

^Pearson r correlation

Using the asleep FC network features the fitted model (SVR linear kernel) was able to explain a small amount of the variance associated with scan age (Figure 5-13) ($R^2 = 0.09$, $p<0.01$).

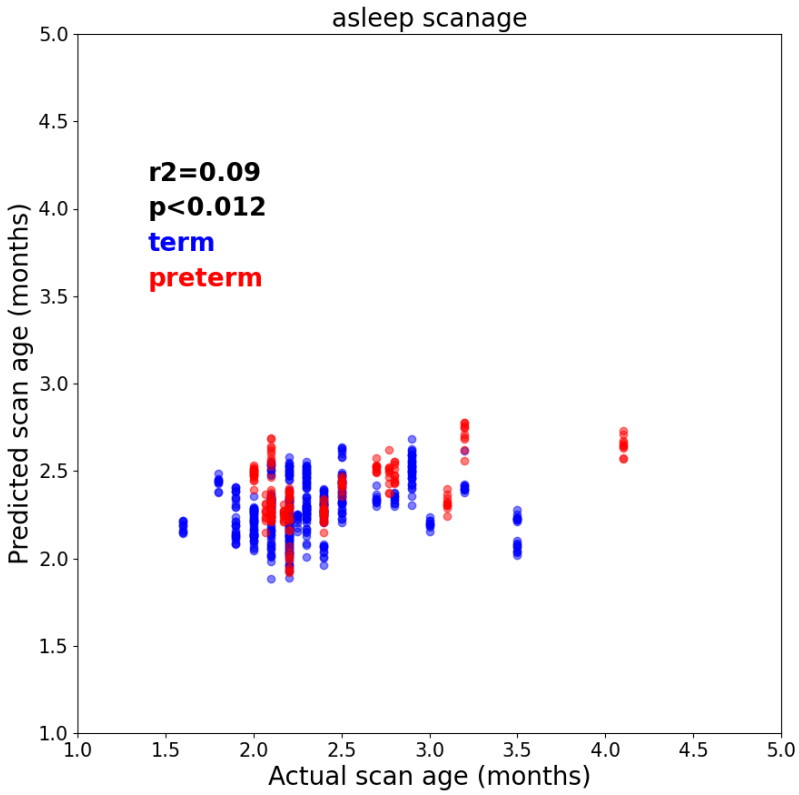

Figure 5-13 Support vector regression results depicting actual (x-axis) versus predicted (y-axis) scan age for term and preterm infants determined using asleep connectivity data at 2 months corrected age.

Next, infants with movies connectivity data were analysed to assess the relationship between FC networks and scan age as assessed by a fitted SVM regression (linear kernel) model. The characteristics of the 80 infants watching movies and the Pearson-r correlation with the variable of interest (scan age) was examined (Table 5-9). This showed stronger correlation between head size (Pearson-r = 0.45) and motion/FWD (Pearson-r = 0.23) than the data set analysed in the asleep model.

Table 5-9 Variables potentially related to scan age – Movies fMRI data

	No. Infants	Mean (std); min-max	Correlation w/ scan age^
Scan age (mo.)	80	2.5 (0.5); 1.6-4.1	n/a
Birth gestation (wks)	80	37.6 (3.5); 23.9-41.7	-0.10
OFC (cm)	75	40.60 (1.4); 37.0-44.0	0.45

	No. Infants	Mean (std); min-max	Correlation w/ scan age^
FWD (mm)	80	0.74 (0.33); 0.20-1.5	0.23

^Pearson r correlation

The previous small relationship between FC network features and scan age seen in the asleep model (previous) appears to disappear when using the infants with movies data (Figure 5-14) (R^2 = 0.00, p<0.03).

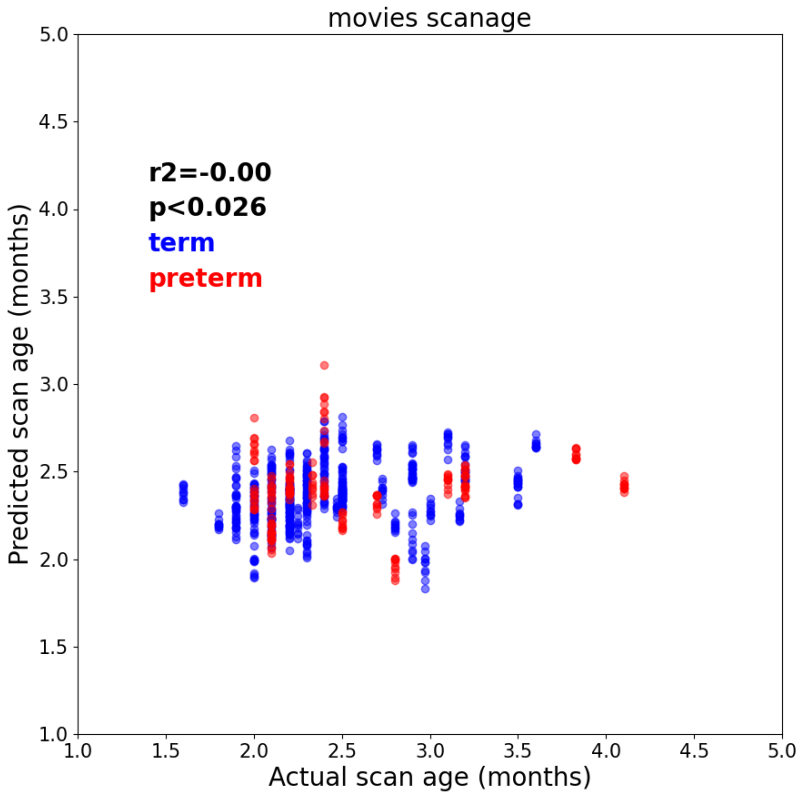

Figure 5-14 Support vector regression results depicting actual (x-axis) versus predicted (y-axis) scan age for term and preterm infants determined using movies connectivity data at 2 months corrected age.

In those infants with FC runs in both states (asleep and movies) FC network features were combined (concatenated) to create a total of 210 features (105 asleep + 105 movies). This was to assess whether perhaps the combined (larger) feature set would be able to predict (explain variance) scan age better than the individual states alone. Results showed that this was not the case (Figure 5-15) (R^2 = -0.01, p<0.03).

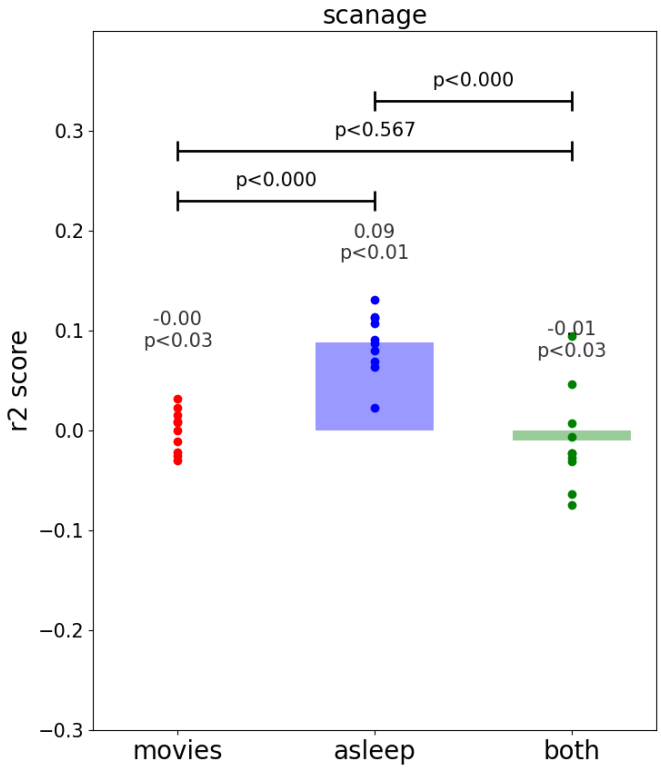

Figure 5-15 Differences in prediction (R^2 values) of scan age using data from a) movies, b) asleep, and c) both states (concatenated input features).

The difference between predicted versus actual scan age (absolute value) was calculated for each infant using their asleep followed by movie data. The average difference was calculated and showed a difference of 0.33 weeks (preterm) and 0.27 weeks (term) for asleep state (p value <0.007). On the other hand, the average difference was 0.5 weeks (preterm) and 0.32 weeks (term) for the awake movie state (p value <0.001). These differences are small, and it is unlikely that these differences represent any real difference in FC network activity.

5.4.6.1 Robustness of regressor to confounding variables

Using the SVR machine learning model, the relationship between FC network features and confounding elements was assessed. Two confounders included head size (OFC) and motion (FWD). These are commonly included as confounders in functional connectivity analyses. We further included the relationship between FC network features (at scan age, i.e. approx. 2 months)

and later neurodevelopment using scores from Ages & Stages Questionnaires (parental devised scores) which were carried out later (when infants were 9 months corrected age). Although the Ages & Stages Questionnaire was used as an early indicator of development, behavioural follow-up testing of both the preterm and term cohorts is currently ongoing, so we are unable to confirm at this time whether infants in either group are developing normally/abnormal on these more formal assessments. The Ages & Stages Questionnaire has 5 domains (maximum score 60 in each domain). While, in standard procedures, a child is assessed as normal/borderline/below in each domain, we used a cumulative score (maximum 300) as a continuous variable for the SVR regression model.

Table 5-10 Coefficient of determination (R^2) model scores for the relationship between functional connectivity (asleep/movies) and various confounder factors

	Asleep model	Movies model
ASQ score	-0.11	-0.11
OFC	-0.19	-0.17
Motion/FWD	0.16 ($p<0.01$)	0.25 ($p<0.01$)

While the regression models (SVR) showed a lack of relationship between the FC network features and both head circumference and Ages & Stages scores, the models did show some relationship between FC network features and motion (FWD), with the variance explained by motion (asleep R^2 = 0.16, movies R^2 = 0.25) greater than the previously weakly positive variance explained by scan age (R^2= 0.09).

5.5 DISCUSSION

5.5.1 Classification of brain state in young infants

We have previously shown in this thesis (Chapter 4) that significant differences in group-level FC matrices between awake (movies) versus asleep states exist. While our SVC classifier was able to classify state (asleep/movies) with high ability (F1-scores range = 0.82 – 0.93) in both preterm and term born infants, it is difficult to dissect whether this classification is driven by true FC features (neural processing) or the confounding motion (in movies state) (motion values inputted into the SVC model had equal classification ability as FC features). However, supporting this finding of an ability to classify state is a recent study by (Tristan S Yates et al., 2023) which examined asleep versus movies states in a cohort of young children (asleep age range 4-21 months, movies age range 4-32 months) with a mean age of 12 months. Only a few children overlapped having runs in both states in their study (unlike the cohort in this study). In their study the authors found that they could classify a child's asleep versus movie state with 91% accuracy score (similar classification of state to this study) (Tristan S Yates et al., 2023).

5.5.2 Classification of birth gestation in young infants

We showed that a SVM classifier (with a linear kernel) using 105 whole-brain network functional connectivity features (Thomas Yeo et al., 2011a) from young infants both asleep and watching movies was poorly able to classify birth gestation. The one exception to this finding was the use of an SVC model trained on asleep FC and tested using movies FC and which was able to classify preterm birth with low-moderate ability (F1-score 0.66). It is of note that motion and scan age did not appear to drive this finding, which potentially shows that discriminating FC features can be identified when trained on a low-motion asleep dataset. Further, the richer data in the test set (movies FC) may underly this improved classification of preterm birth. Future work might investigate training regimes that will allow the network to focus on age-related features while ignoring motion features, perhaps by stratifying on both dimensions. Possible

reasons for this inability to classify birth gestation are multiple and are discussed below.

5.5.2.1 Possibility that preterm infants already have similar FC at 2 months age

We have seen previously in this thesis (Chapter 4) that while group-wise FC differences existed between these term/preterm groups, the magnitude of the FC differences was small. So perhaps the FC features themselves did not contain enough difference/information allowing classification? While most literature has shown disrupted connectivity in ex-preterm infants scanned at term corrected age (Ball et al., 2016; Gozdas et al., 2018; Smyser et al., 2010), less literature reports ongoing disrupted connectivity in ex-preterm children scanned at 3 years age (but no differences in connectivity at 18 months) (Damaraju et al., 2010) and at school age (Wehrle et al., 2018). Indeed developmental plasticity can allow preserved brain function and this has been shown in preterm infants (Herzmann et al., 2017).

However, to counter this argument is an important study by Smyser et al. in which term born and preterm infants were scanned at term equivalent age and in which a machine learning classifier was able to classify birth gestation with 84% accuracy (C. D. Smyser et al., 2016a). These authors showed that both early maturing (motor/sensory) and later maturing higher-order (default/dorsal attention/salience) networks all contributed towards their classification accuracy (i.e., it is unlikely that these higher-order networks would have normalised by the age of infants in our study). Important differences exist between their study and our study and these include (not limited to): preterm birth gestation (more extreme in their study), group numbers (they had more numbers with 50 infants in equal term and preterm groups), motion handling (they scrubbed/censored frames with FWD>0.5mm), number of features (they used feature selection to choose consensus features from 22,791 functional edges) and age of scanning (they scanned at a younger age i.e. term equivalent age).

5.5.2.2 Possibility that un-suitable brain networks/parcellation were adopted

In another study of a large group of ex-preterm infants scanned at term equivalent age, researchers were able to classify preterm (n=105) versus term (n=26) born infants with 80% accuracy (Ball et al., 2016). Interestingly their

classification power came from both cortical and subcortical nodes, with over 50% of edges connecting one or more nodes with the basal ganglia (Ball et al., 2016). Consideration of subcortical nodes seems an important aspect of their success, and indeed a previous group using fMRI connectivity analysis in very preterm infants have shown that connectivity between thalamo-cortical regions correlated with standardised neurocognitive assessments at 20 months PMA (Toulmin et al., 2020). While we did not consider using an atlas including subcortical brain regions, this would be an important consideration for future analysis.

Because there is not yet consensus on the spatial layout of neonatal functional networks (Doria et al., 2010; Eyre et al., 2021; Gao et al., 2015a; Lin et al., 2008) we used definitions of functional networks derived in one thousand healthy young adults (Thomas Yeo et al., 2011b). This allowed us to calculate our 105 edges/features for the support vector machine analyses. Indeed, not having anatomical images for each infant (co-registration of our infants' fMRI images was to a chosen fMRI reference run: see "Pre-processing Section") led to the decision to adopt the 105 edges/features instead of 79,800 edges using the Schaefer parcellation scheme (Schaefer et al., 2018), as it was felt that a considerable proportion of these thousands of edges may not be registered accurately (given the limitation of not having anatomical images). Another reason for choosing only 105 network edges (105 features) was due to the fact that it is known that SVM models over-fit when they have many more features than samples (i.e. risk of over-fitting was considered).

However perhaps these functional networks, derived from an adult cohort, are not ideal for this infant age and impacted results? Indeed Ball et al. used group independent component analysis (ICA) to determine functional parcellation in their asleep machine learning classifier of preterm versus term birth (Ball et al., 2016). Similarly, using their defined Baby Connectome Project infant/toddler functional networks (Howell et al., 2019), researchers in another study trained separate SVR models using features from each of the 11 infant/toddler networks separately. Networks involving temporal regions, regions overlapping with the canonical dorsal attention network (DAN), motor areas, anterior fronto-parietal network (aFPN), and frontal parts of the default mode network (infant-DMN) all reliably changed over 8–26 months in manner that facilitated age prediction in

their toddler group (Kardan et al., 2022). Further conflict with the results of this current study using adult functional networks it the fact that Nielsen et al. were able to predict PMA at scan in a group of infants at term age using various adult network parcellation schemes (Nielsen et al., 2023).

5.5.2.3 Possibility of minimal phenotypic difference between preterm and term infants

Another reason for poor classification of birth gestation may be due to the fact that our NICU (preterm) group had a relatively complication-free NICU course, with relatively few morbidities of prematurity (see Table 5-1) (this is in addition to the fact that NICU graduates with structural brain injury were already excluded). There is a possibility that our preterm group did indeed have similar FC to the term born group when scanned at 2 months age. Indeed, many functional networks present in adults are evident in preterm infants by the time they reach term equivalent age (Doria et al., 2010; Fransson et al., 2009). However, in refute of this suggestion is the findings of a study of healthy term born infants scanned shortly after birth, in which researchers found that SVR was able to predict differences in PMA at scan (R^2 = 0.51) of healthy term neonates even within the narrow window of development (38–45 weeks PMA) (Nielsen et al., 2023). Pending developmental follow-up in the cohort will allows us to investigate this hypothesis.

5.5.3 Prediction of birth gestation and scan age

In this current study the SVR regression model (linear kernel) was not able to predict gestation at birth using FC data from either asleep infants or infants watching movies. It is known that data from complementary imaging modalities lend towards improved model accuracies in machine learning (Brown et al., 2012; Erus et al., 2015; Temko et al., 2011). Our results show that combining data from infants who had FC data in both states (asleep/movie) did not improve prediction compared to models using data only in one state. In contrast to our regression findings, Smyser et al. showed a significant difference in predicted birth gestation (using SVR analysis) between their preterm (30+4 PMA) and term (36+4 PMA) groups scanned asleep at term equivalent age (C. D. Smyser et al., 2016a) (study differences given already, above).

Our SVR model was weakly able to predict scan age (R2 = 0.09) in the asleep FC dataset only (scan age range 1.6 to 4.1 months age). This was not achieved using movies FC data. Whether this prediction is related to FC (neural) maturation (asleep state) that is only evident in the asleep state (and not shared in movies state) is uncertain. Importantly, it is notable that the asleep state had less motion compared to movies state (however asleep FC data also predicted FWD with greater prediction power than that of scan age).

It is likely that motion plays a significant impact on both the inability to predict birth gestation in our study and the weak ability to predict scan age. Indeed a previous study has shown that, in a group of children and adults in resting state (awake viewing a cross-hair), that prior to rigorous motion denoising, 50% of the variance was explained by motion (reducing to 4% after motion denoising) (Nielsen et al., 2019). Using stringent motion denoising (frames >0.2mm were censored) they showed that FC was able to predict brain age/maturity (Nielsen et al., 2019). While global signal regression (GSR) has been shown to mitigate the impact of motion on SVM models (age prediction), we did not perform GSR. The use of GSR is considered controversial and to date there is no clear consensus in the literature (Murphy and Fox, 2017).

5.5.4 Conclusion

In summary, while our study indicates that FC data from 2-month aged infants can classify brain state (asleep/movies) during the scan (both ex-preterm and term born infants) and can predict scan age (asleep state only), it is likely that methodological challenges in our analysis limited our ability to classify and predict birth gestation. This lack of classification/prediction ability for birth gestation, precluded planned 'next step' analysis of functional network/edge contributions (Dosenbach et al., 2010; C. D. Smyser et al., 2016a).

Future work adopting SVM analysis, but also using more rigorous motion censoring; registration to anatomical images; and bespoke infant atlases/parcellation (to include subcortical regions); may perhaps lend towards improved classification of birth gestation (and subsequent analysis of networks/features driving same).

CHAPTER 6 GENERAL DISCUSSION

6.1 INTRODUCTION

This study is one of the few functional MRI studies of awake infants worldwide and the first awake infant fMRI study in Ireland. This study used naturalistic stimuli (movies) to command infants' attention and complemented this with a carefully planned scanning protocol, team (including parents), and environment. It is known that watching movies in the MRI scanner can both achieve better fMRI data quality (less movement) in child populations (Vanderwal et al., 2015) while also constraining variability (noise) in the functional data (but still preserving meaningful differences in a subject's connectome) (Finn, 2021). This study presents results from functional connectivity analysis of these infants (term born and preterm born) in both awake and asleep states. It examines the group connectivity patterns seen in both states while also investigating whether there is an individual component of the connectome that is stronger/unique in either state. It is this individual component which ultimately may link with behaviours in the future (i.e. a potential neuroimaging biomarker for preterm infants).

6.2 OVERVIEW OF RESULTS AND LIMITATIONS

6.2.1 Practicalities and challenges of awake infant fMRI

In the hospital setting infant MRI requires careful sedation protocols (Sury et al., 2005). In neonates, it is possible to avoid sedation with a stepwise approach with feed-and-wrap technique and infant immobilization (vacuum pillows), which can also ensure good image capture success rates in asleep MRI (R. King et al., 2023). However, by 2-3 months-old, success rates using this method are less than 50% (Wild et al., 2017), too low for clinical practice, and sedation is necessary for asleep MRI.

In this study, the use of naturalistic stimuli (movies) was successful in this young infant population undergoing MRI scanning. The movies held the infants' attention, as determined from the facial video footage rating of 'interested and

scanning' (i.e. the infant was eye scanning the visual stimulus) for at least 85% of the run time. While infants in this study viewed both movie runs and picture runs (pictures runs not analysed in this thesis), movie runs were more successful (i.e. most infants completed approximately 2 full video runs compared to 1 full picture run). The unique added benefit of a 2-month age infant scan appears to be the fact that many infants fall asleep later in the session (allowing gathering of asleep state FC in 80% of infants and T2-weighted sequences in 70% of infants).

Motion does impact awake infant MRI scanning. In this study 87% (62/71) of term infants and 69% (20/29) of preterm infants had a movie run meeting the inclusion criterion (>90% of frames with FWD less than 3 mm). However, only 20% and 10% of term and preterm infants respectively met the stricter motion inclusion criterion (>90% of frames with FWD less than 0.5 mm). These inclusion rates are similar to those seen in a recent infant awake FC MRI study using similar motion thresholds (Tristan S Yates et al., 2023) confirming the generalisability of this finding.

Further this study showed how there is a 'settling in' phase for an infant who transitions from an awake run into an asleep run in the same fMRI session. It is thought that this 'settling in' phase is due to motion associated with early active (REM) sleep in these young infants. The effect of this 'settling in' phase is a drop in BOLD signal (which then slowly recovers over the period). This is an important realisation for any future awake infant scanning protocol design.

In addition to ensuring appropriate acoustic noise (from gradient magnetic fields) level reduction (noise inside the ear cup was monitored continuously during scanning), this study found that active noise cancelling (ANC) headphones were of more benefit during asleep runs (especially the transition period from awake through to asleep), however the need for a 'learning phase' for the ANC headphones undermined their benefit during awake movies runs (movies with audio input).

Neonatal/infant research is considered complex, hands-on and time intensive and due consideration is needed for deciding the balance or risk exposure versus benefit from research. This is compounded by the fact that parents have to

make the decision/consent on behalf of their infant (Krishna and Fuloria, 2022). In this study a carefully planned non-intrusive/delicate approach to participant recruitment was prioritised. This resulted in satisfactory recruitment rates (13% for parents of controls and 27% for parents of NICU infants). During the scanning session parents were encouraged to be active helpers (hands-on) to ensure infant comfort. Feedback form parents surveyed showed that they felt that infants had been comfortable during awake scanning and that their visit/session has contributed towards usable data.

In this study only a few awake infants achieved runs meeting the stricter motion threshold criterion. As such, the generalisability of study findings/analysis is limited. However, future pooling of these data with other awake infant/toddler fMRI studies would be an important future step. Our findings are being shared with the foetal/infant/toddler neuroimaging community (FIT'NG community) which is an increasingly active and growing community of researchers (Pollatou et al., 2022; Vaughn et al., 2022).

6.2.2 Important confounds in infant fMRI fingerprinting

This study compared functional fingerprinting within a session and across sessions. Confounding variables were identified and included motion, head size, inter-session interval and head position in the head coil. Head position was impacted the most with 98 - 100% success in within-session fingerprinting using only the regional SNR located in the head coil. This finding likely explains the discrepancy in success rates for within-session and across-session fingerprinting in infants. Future infant across-session studies (i.e. studies where infants are placed down in the head coil more than once, and/or where there is head growth in the intervening period) will need to allow for this finding in their study design, to mitigate head position/SNR induced artifact. This study discussed developments in infant head coil design which are timely given these findings.

6.2.3 Functional connectivity in awake and asleep infants

This study scanned young infants in the awake (movies) conscious state using a neuroimaging modality (fMRI) that allows assessment of functional networks deep to the cortical surface (unlike EEG for example). This study has shown that there is a different pattern of fMRI connectivity between sleep and awake (movies) states, and that infants born preterm (assessed at 2 months PMA) have similar connectivity in limbic network edges in both states (while term born infants have lower limbic connectivity in the awake/movies state). This study also found that infants watching movies appear to have more modular brain activity, with stronger connectivity within networks than across them, relative to the sleeping state.

This study adopted the inter-subject functional connectivity method (Hasson et al., 2004; Simony et al., 2016) to determine if there is a shared connectivity in these young awake infants and to determine what RSN pattern it might take. Analysis showed how cortical edges containing the somatomotor and default networks (left/right/inter-hemispheres) dominated the pattern of shared (inter-subject) connectivity in infants watching movies. This finding that movie-watching modulates FC in the DMN has been shown previously in older children/adolescents (Sanchez-Alonso et al., 2021). In contrast, in preterm born infants this finding was limited to edges containing the somatomotor network only (i.e., not including edges containing the default network).

In a recent study of toddlers (mean participant age 12 months) (Tristan S Yates et al., 2023) researchers found that the average FC was not significantly different between asleep and movies states. This is a similar result to the findings of this thesis. These investigators also found that these functional networks in toddlers were equally similar to adult functional networks regardless of sleep/movie state, suggesting that infant consciousness might not impact overall measures of functional network maturity (Tristan S Yates et al., 2023).

6.2.4 Using machine learning to examine functional connectivity

One hypothesis of this current study was that FC from movies will be more revealing of key phenotypes (birth gestation and scan age) than FC from

sleeping infants (aged 2-months PMA) and this would be seen as a difference in classification/prediction ability using a machine learning model. Ultimately, while this study indicates that FC data from 2-month aged infants can classify brain state (asleep/movies) during a scan (both ex-preterm and term born infants) and can weakly predict scan age (asleep state only), it is likely that methodological challenges in our analysis limited our ability to classify and predict birth gestation. Future work adopting SVM analysis, but also using more rigorous motion censoring; registration to anatomical images; and bespoke infant atlases/parcellation (to include subcortical regions); may perhaps lend towards improved classification of birth gestation (and subsequent analysis of networks/features driving same).

6.3 FUTURE WORK

Infant participants in this project (FOUNDCOG: https://www.foundcog.org/) are already undergoing longitudinal follow up investigations. Firstly, all infants who attended for the 2-month MRI scan visit have been asked to attend again for a further MRI scan at 9-months (PMA). These 9-month scan have just recently been completed (data yet to be analysed). This 9-month fMRI data will allow future functional connectome analysis (fingerprinting) across-sessions (2-month versus 9-month visit) using data from awake (movies) and asleep states. This future analysis will include analysis of within-subject connectivity and between-subject connectivity (ISFC, shared connectivity) (Hasson et al., 2004). Further, functional connectivity patterns that are more stereotyped in certain subjects than others may be captured by dynamically tracking the temporal profiles of the shared (ISFC) changes (Bolton et al., 2018) and this new approach may prove useful in the awake (movies) state in this infant cohort.

The awake infant MRI data acquired in this project (FOUNDCOG project) can further lend towards the understanding of early brain patterns of categorical representation in early infancy. Awake functional data has been analysed by the project team to investigate infant brain processing of categories (semantic development) and has been used in conjunction with computational modelling (deep neural networks) to provide insights into the developmental origins of the

visual system. Using design matrices (regressors for categories) and generalised linear models, the awake infant data in this study has been fit (convolved with the haemodynamic response function), and correlations between voxel-wise response patterns (for each category) have been calculated. Using representational similarity analysis, patterns of brain activity across different conditions have been determined. Patterns of brain activity have also been compared to deep neural network patterns.

All infant participants (term controls and preterm/NICU) are being asked to complete the Vineland-3 Adaptive Behavioural Scales (Sparrow and Cicchetti, 1985) at 18-months age (PMA). This is a parent questionnaire, and it is used to measure communication, activities of daily living, social development, and risk of autism in this study population. Parental questionnaires are well established, but have confounding effects of the parent's opinions, and an alternative is to directly test the infants. Therefore, at 24 months age (PMA) we are also acquiring a new touch-screen based measure of infant executive function, the Cognitot (www.liltoda.com). These data from all participants will allow correlation with the 2-month and 9-month MRI data in both the control group and NICU group participants. Those participants recruited from the NICU (n = 29) are being offered a Bayley Scales of Infant Development (BSID) (Version 3) at 2-years age (PMA). The BSID is a face-to-face assessment of toddler cognitive, receptive language and expressive language (Mental Development Index) and fine/gross motor (Psychomotor Developmental Index) (Michalec, 2011). This assessment will allow more in-depth analysis/correlations of MRI data and developmental outcomes in the NICU participant group.

6.3.1 Future work – dealing with physiological noise

In infants the cardiac and respiratory cycles are faster than older children/adults. It is known that infants have relatively prominent occiputs and forward/backward (z-axis of the MRI scanner) head movements can occur with respiration. While the facial camera (in-bore) provided real-time footage of gross infant head movements, it was challenging to know whether the infant head was having small/micro movements (e.g. due to respiratory or cardiac pulsations). Attaching heart rate and/or respiratory rate monitoring devices to

an apprehensive awake infant can be detrimental to ensuring a comfortable/happy infant is relaxed at the start of watching movies in the scanner. Historically fMRI sampling rate was too slow to filter this physiological noise out of the signal and often this noise was aliased in the true BOLD signal. In recent years multiband accelerated MRI has allowed multiple slices of the brain to be acquired at the same time (through multiple radio-frequency coils which separate the overlapping images into their separate slices) (Griffanti et al., 2014). This technique allows shorter TR times (i.e. fractions of seconds). Shorter TR times allows more time points (improving statistical power) but also prevents the aliasing of high frequency noise, such as infant heart rate and infant respiratory rate, into the lower frequency functional BOLD signal (Cordes et al., 2001). Independent component analysis (ICA) is a technique used in functional neuroimaging to separate statistically independent components from linearly mixed signals (Beckmann, 2012; Kiviniemi et al., 2003). Future work on this infant dataset could include inspection of the spatial maps, timeseries and frequency spectrum in order to label these physiological noise parameters and to then filter this physiological noise out of the signal. An example of a useful platform for this future work would be FMRIB's ICA-based Xnoisefier (FIX) (Salimi-Khorshidi et al., 2014). An alternative solution could also be probe free (marker-less) measurement of these small movements. Novel motion capturing methods, such as TracInnovations (Slipsager et al., 2019) can both provide real-time motion estimates, and motion data for image correction. This technology uses invisible infrared light to construct high resolution 3D surfaces, enabling marker-less tracking of a participant's head. Using advanced algorithms, the motion data can be used to reconstruct a new image eliminating the effect of the motion artifacts up to ±10-15 mm (Slipsager et al., 2019). This technology could improve delineation of signal versus motion in future imaging data.

6.3.2 Future work – monitoring researcher position

One important data that was not measured in this study, but that is realised as a potential confound/noise, was the position of the researcher relative to the main static magnetic field (B_0). In the optimal case (an awake, minimally moving infant) the researcher stood away from the infant at approximately the 5 Gauss line. However, in some cases, if the infant needed reassurance, the researcher

placed their hand on the infant's leg or pelvis to sooth the infant. As the infant watched the movies, often the researcher then remained in this position close to the infant and within the stronger magnetic field of the bore of the scanner. As the infant settled, sometimes the researcher would then move away from this closer position, and retreat to the 5 Gauss line. In summary, this variable position of the researcher (during a run), relative to the static magnetic field, may have introduced variation in the magnetic field during a run. Future work should track the position of the researcher (e.g. camera identifying the proximity of researcher to the infant during a run) to mitigate this technical confounder.

6.3.3 Future work - registration of infant functional MRI images

A limitation of this study is that infant fMRI frames/volumes were registered to a functional (fMRI) reference volume (i.e. not an anatomical MRI image). This was because awake runs were prioritised. However, in retrospect 70% of infants in this study fell asleep allowing collection of T2-weighted anatomical MRI images. Future work will include use of these T2-weighted images to register the fMRI data to the anatomical landmarks, ideally using surface-based registration techniques (surface-based registration achieves better cross-subject alignment of functional areas compared to volume-based registration) and has been used in large infant studies such as the dHCP (Makropoulos et al., 2018). Also, for those infants still without anatomical images (i.e. never fell asleep), future work will include investigation of the potential for alignment of fMRI data using 'functional' signal instead. This 'hyper-alignment' can be accomplished using evoked BOLD-signal time courses during movie-watching (Conroy et al., 2013; Sabuncu et al., 2010) and may offer a future solution to infant awake scanning where anatomical MRI sequences are not obtained.

6.3.4 Future work – measurement of level of arousal or sleep

In this study infants were labelled/tagged as asleep state or awake state (various facial footage tags e.g. 'eyes_scanning'), however the level of arousal

(awake) or level of sleep were not directly measure. It is known that infants born at term (controls) average 16 – 18 hours sleep per day (with 50% of sleep in REM sleep), while premature born infants spend even longer periods asleep (80% of sleep in REM sleep) (André et al., 2010). Ultimately these differences suggest that infants in this study may have had different levels of asleep which were not measure. A future consideration would be to included fMRI-EEG simultaneously in future infant studies. Simultaneous fMRI-EEG has been previously been demonstrated to be safe and feasible in newborn infants (Arichi et al., 2017).

6.3.5 Future work - comparing infant to older children/adult populations

Longitudinal analysis comparing infant resting-state (i.e. asleep) fMRI data to older resting-state (i.e. awake) child/adult populations is challenged by the difference in state in which the data is acquired. Methods for transforming awake/movie FC patterns into sleep FC patterns (and vice-versa) are needed for longitudinal studies using fMRI. Future work using data form this study could include regression of the shared (ISFC) awake/movie evoked timecourse from each parcel (ROI) in the infant data and using the residuals as a comparable representation of FC (infant versus child/adult resting-state). Another future method may include using models (deep neural network models) for transformation of sleep into movies FC patterns (and vice-versa) in infants. Already one research group (UNC/UMN Baby Connectome Project) have used this type of model in a small cohort of infants and has shown how it out-performed other models in prediction of state and maintenance of modular connectivity structure (Hu et al., 2021b).

While a future focus may be on this transformation of sleep into movies FC patterns, it is important to recognised that likely it is no single state (asleep/resting/awake/movies) that can a full picture of brain functional organisation, but rather functional organisation is better estimated from multiple task states (rather than rest alone), and that behaviour prediction models trained on data from a combination of tasks states outperforms models trained on resting-state data alone (Elliott et al., 2019).

6.4 CONCLUSION

This thesis explored the important practical aspects and challenges of awake functional MRI in the young infant population. While methods used resulted in successful completion of awake fMRI runs and good infant comfort/attendance (as reported by researcher and parents), still motion had an impact on data analysed. Future pooling of low motion awake infant fMRI data will be important for the infant neuroimaging research community. This thesis highlighted important confounders impacting the stability of the infant functional connectome (fingerprint) when comparing within-session versus between-session functional analysis. While there were more similarities than differences in functional connectivity patterns between asleep and awake states, this thesis showed the existence of a shared connectivity (awake state) in infants watching movies. While functional connectivity patterns were able to differentiate state (asleep/awake), this study was unable to differentiate measures of brain maturity (birth gestation/brain age) using the minimally pre-processed data acquired and simple machine learning models. Future work and methodological improvements are shared, ultimately in the hope that infant functional MRI analysis will prove an important biomarker during this pre-verbal early life period.

REFERENCES

Aarnoudse-Moens, C.S.H., Weisglas-Kuperus, N., Goudoever, J.B. van, Oosterlaan, J., 2009. Meta-Analysis of Neurobehavioral Outcomes in Very Preterm and/or Very Low Birth Weight Children. Pediatrics 124, 717–728. https://doi.org/10.1542/peds.2008-2816

Abujarir, R., Salama, H., Greer, W., Al Thani, M., Visda, F., 2012. The impact of earmuffs on vital signs in the neonatal intensive care unit. J. Neonatal-Perinat. Med. 5, 249–259. https://doi.org/10.3233/NPM-2012-57511

Aertsen, A.M., Gerstein, G.L., Habib, M.K., Palm, G., 1989. Dynamics of neuronal firing correlation: modulation of "effective connectivity." J. Neurophysiol. 61, 900–917. https://doi.org/10.1152/jn.1989.61.5.900

Ahmadi, H., Fatemizadeh, E., Motie-Nasrabadi, A., 2023. A Comparative Study of Correlation Methods in Functional Connectivity Analysis Using fMRI Data of Alzheimer's Patients. J. Biomed. Phys. Eng. 13, 125–134. https://doi.org/10.31661/jbpe.v0i0.2007-1134

Allotey, J., Zamora, J., Cheong-See, F., Kalidindi, M., Arroyo-Manzano, D., Asztalos, E., van der Post, J., Mol, B.W., Moore, D., Birtles, D., Khan, K.S., Thangaratinam, S., 2018. Cognitive, motor, behavioural and academic performances of children born preterm: a meta-analysis and systematic review involving 64 061 children. BJOG Int. J. Obstet. Gynaecol. 125, 16–25. https://doi.org/10.1111/1471-0528.14832

Almli, C.R., Rivkin, M.J., McKinstry, R.C., 2007. The NIH MRI study of normal brain development (Objective-2): Newborns, infants, toddlers, and preschoolers. NeuroImage 35, 308–325. https://doi.org/10.1016/j.neuroimage.2006.08.058

American College of Obstetricians and Gynecologists, 2017. Committee Opinion No 700: Methods for Estimating the Due Date. Obstet. Gynecol. 129, e150. https://doi.org/10.1097/AOG.0000000000002046

Anderson, P.J., Treyvaud, K., Neil, J.J., Cheong, J.L.Y., Hunt, R.W., Thompson, D.K., Lee, K.J., Doyle, L.W., Inder, T.E., 2017. Associations of Newborn Brain Magnetic Resonance Imaging with Long-Term Neurodevelopmental Impairments in Very Preterm Children. J. Pediatr. 187, 58-65.e1. https://doi.org/10.1016/j.jpeds.2017.04.059

Andersson, J.L., Hutton, C., Ashburner, J., Turner, R., Friston, K., 2001. Modeling geometric deformations in EPI time series. NeuroImage 13, 903–919. https://doi.org/10.1006/nimg.2001.0746

Andersson, J.L.R., Graham, M.S., Drobnjak, I., Zhang, H., Campbell, J., 2018. Susceptibility-induced distortion that varies due to motion: Correction in diffusion MR without acquiring additional data. NeuroImage 171, 277–295. https://doi.org/10.1016/j.neuroimage.2017.12.040

Andersson, J.L.R., Graham, M.S., Drobnjak, I., Zhang, H., Filippini, N., Bastiani, M., 2017. Towards a comprehensive framework for movement and distortion correction of diffusion MR images: Within volume movement. NeuroImage 152, 450–466. https://doi.org/10.1016/j.neuroimage.2017.02.085

Andersson, J.L.R., Skare, S., Ashburner, J., 2003. How to correct susceptibility distortions in spin-echo echo-planar images: application to diffusion tensor imaging. NeuroImage 20, 870–888. https://doi.org/10.1016/S1053-8119(03)00336-7

André, M., Lamblin, M.-D., d'Allest, A.M., Curzi-Dascalova, L., Moussalli-Salefranque, F., Nguyen The Tich, S., Vecchierini-Blineau, M.-F., Wallois, F., Walls-Esquivel, E., Plouin, P., 2010. Electroencephalography in premature and full-term infants. Developmental features and glossary. Neurophysiol. Clin. Neurophysiol. 40, 59–124. https://doi.org/10.1016/j.neucli.2010.02.002

Arichi, T., Counsell, S.J., Allievi, A.G., Chew, A.T., Martinez-Biarge, M., Mondi, V., Tusor, N., Merchant, N., Burdet, E., Cowan, F.M., Edwards, A.D., 2014. The effects of hemorrhagic parenchymal infarction on the establishment of sensori-motor structural and functional connectivity in early infancy. Neuroradiology 56, 985–994. https://doi.org/10.1007/s00234-014-1412-5

Arichi, T., Whitehead, K., Barone, G., Pressler, R., Padormo, F., Edwards, A.D., Fabrizi, L., 2017. Localization of spontaneous bursting neuronal activity in the preterm human brain with simultaneous EEG-fMRI. eLife 6, e27814. https://doi.org/10.7554/eLife.27814

Arulkumaran, S., Tusor, N., Chew, A., Falconer, S., Kennea, N., Nongena, P., Hajnal, J.V., Counsell, S.J., Rutherford, M.A., Edwards, A.D., 2020. MRI Findings at Term-Corrected Age and Neurodevelopmental Outcomes in a Large Cohort of Very Preterm Infants. Am. J. Neuroradiol. 41, 1509–1516. https://doi.org/10.3174/ajnr.A6666

Back, S.A., Luo, N.L., Borenstein, N.S., Volpe, J.J., Kinney, H.C., 2002. Arrested Oligodendrocyte Lineage Progression During Human Cerebral White Matter Development: Dissociation Between the Timing of Progenitor Differentiation and Myelinogenesis. J. Neuropathol. Exp. Neurol. 61, 197–211. https://doi.org/10.1093/jnen/61.2.197

Badke D'Andrea, C., Kenley, J.K., Montez, D.F., Mirro, A.E., Miller, R.L., Earl, E.A., Koller, J.M., Sung, S., Yacoub, E., Elison, J.T., Fair, D.A., Dosenbach, N.U.F., Rogers, C.E., Smyser, C.D., Greene, D.J., 2022. Real-time motion monitoring improves functional MRI data quality in infants. Dev. Cogn. Neurosci. 55, 101116. https://doi.org/10.1016/j.dcn.2022.101116

Baldoli, C., Scola, E., Della Rosa, P.A., Pontesilli, S., Longaretti, R., Poloniato, A., Scotti, R., Blasi, V., Cirillo, S., Iadanza, A., Rovelli, R., Barera, G., Scifo, P., 2015. Maturation of preterm newborn brains: a fMRI–DTI study of auditory processing of linguistic stimuli and white matter development. Brain Struct. Funct. 220, 3733–3751. https://doi.org/10.1007/s00429-014-0887-5

Ball, G., Aljabar, P., Arichi, T., Tusor, N., Cox, D., Merchant, N., Nongena, P., Hajnal, J.V., Edwards, A.D., Counsell, S.J., 2016. Machine-learning to characterise neonatal functional connectivity in the preterm brain. NeuroImage 124, 267–275. https://doi.org/10.1016/j.neuroimage.2015.08.055

Ball, G., Counsell, S.J., Anjari, M., Merchant, N., Arichi, T., Doria, V., Rutherford, M.A., Edwards, A.D., Rueckert, D., Boardman, J.P., 2010. An optimised tract-based spatial statistics protocol for neonates: Applications to prematurity and chronic lung disease. NeuroImage 53, 94–102. https://doi.org/10.1016/j.neuroimage.2010.05.055

Ball, G., Pazderova, L., Chew, A., Tusor, N., Merchant, N., Arichi, T., Allsop, J.M., Cowan, F.M., Edwards, A.D., Counsell, S.J., 2015. Thalamocortical Connectivity Predicts Cognition in Children Born Preterm. Cereb. Cortex 25, 4310–4318. https://doi.org/10.1093/cercor/bhu331

Ball, G., Srinivasan, L., Aljabar, P., Counsell, S.J., Durighel, G., Hajnal, J.V., Rutherford, M.A., Edwards, A.D., 2013. Development of cortical

microstructure in the preterm human brain. Proc. Natl. Acad. Sci. 110, 9541–9546. https://doi.org/10.1073/pnas.1301652110
Banks, M.S., Salapatek, P., 1978. Acuity and contrast sensitivity in 1-, 2-, and 3-month-old human infants. Invest. Ophthalmol. Vis. Sci. 17, 361–365.
Barkovich, A.J., 2005. Magnetic resonance techniques in the assessment of myelin and myelination. J. Inherit. Metab. Dis. 28, 311–343. https://doi.org/10.1007/s10545-005-5952-z
Barkovich, M.J., Barkovich, A.J., 2019. MR Imaging of Normal Brain Development. Neuroimaging Clin. N. Am. 29, 325–337. https://doi.org/10.1016/j.nic.2019.03.007
Barnett, M.L., Tusor, N., Ball, G., Chew, A., Falconer, S., Aljabar, P., Kimpton, J.A., Kennea, N., Rutherford, M., David Edwards, A., Counsell, S.J., 2018. Exploring the multiple-hit hypothesis of preterm white matter damage using diffusion MRI. NeuroImage Clin. 17, 596–606. https://doi.org/10.1016/j.nicl.2017.11.017
Bartels, A., Zeki, S., 2005. Brain dynamics during natural viewing conditions—A new guide for mapping connectivity in vivo. NeuroImage 24, 339–349. https://doi.org/10.1016/j.neuroimage.2004.08.044
Bartels, A., Zeki, S., 2004. Functional Brain Mapping during Free Viewing of Natural Scenes. Hum. Brain Mapp. 21, 75–85. https://doi.org/10.1002/hbm.10153
Bassett, D.S., Nelson, B.G., Mueller, B.A., Camchong, J., Lim, K.O., 2012. Altered resting state complexity in schizophrenia. NeuroImage 59, 2196–2207. https://doi.org/10.1016/j.neuroimage.2011.10.002
Batalle, D., Hughes, E.J., Zhang, H., Tournier, J.-D., Tusor, N., Aljabar, P., Wali, L., Alexander, D.C., Hajnal, J.V., Nosarti, C., Edwards, A.D., Counsell, S.J., 2017. Early development of structural networks and the impact of prematurity on brain connectivity. NeuroImage 149, 379–392. https://doi.org/10.1016/j.neuroimage.2017.01.065
Bäuml, J.G., Meng, C., Daamen, M., Baumann, N., Busch, B., Bartmann, P., Wolke, D., Boecker, H., Wohlschläger, A., Sorg, C., Jaekel, J., 2017. The association of children's mathematic abilities with both adults' cognitive abilities and intrinsic fronto-parietal networks is altered in preterm-born individuals. Brain Struct. Funct. 222, 799–812. https://doi.org/10.1007/s00429-016-1247-4
Baxter, L., Moultrie, F., Fitzgibbon, S., Aspbury, M., Mansfield, R., Bastiani, M., Rogers, R., Jbabdi, S., Duff, E., Slater, R., 2021. Functional and diffusion MRI reveal the neurophysiological basis of neonates' noxious-stimulus evoked brain activity. Nat. Commun. 12, 2744. https://doi.org/10.1038/s41467-021-22960-0
Becker, R., Reinacher, M., Freyer, F., Villringer, A., Ritter, P., 2011. How ongoing neuronal oscillations account for evoked fMRI variability. J. Neurosci. Off. J. Soc. Neurosci. 31, 11016–11027. https://doi.org/10.1523/JNEUROSCI.0210-11.2011
Beckmann, C.F., 2012. Modelling with independent components. NeuroImage 62, 891–901. https://doi.org/10.1016/j.neuroimage.2012.02.020
Ben-Hur, A., Ong, C.S., Sonnenburg, S., Schölkopf, B., Rätsch, G., 2008. Support vector machines and kernels for computational biology. PLoS Comput. Biol. 4, e1000173. https://doi.org/10.1371/journal.pcbi.1000173
Benjamini, Y., Hochberg, Y., 1995. Controlling the False Discovery Rate: A Practical and Powerful Approach to Multiple Testing. J. R. Stat. Soc. Ser. B Methodol. 57, 289–300. https://doi.org/10.1111/j.2517-6161.1995.tb02031.x

Betti, V., Della Penna, S., de Pasquale, F., Mantini, D., Marzetti, L., Romani, G.L., Corbetta, M., 2013. Natural scenes viewing alters the dynamics of functional connectivity in the human brain. Neuron 79, 782–797. https://doi.org/10.1016/j.neuron.2013.06.022

Biagi, L., Crespi, S.A., Tosetti, M., Morrone, M.C., 2015. BOLD Response Selective to Flow-Motion in Very Young Infants. PLOS Biol. 13, e1002260. https://doi.org/10.1371/journal.pbio.1002260

Bijsterbosch, J., Smith, S.M., Beckmann, C.F., 2017. Introduction to Resting State fMRI Functional Connectivity, Oxford Neuroimaging Primers. Oxford University Press, Oxford, New York.

Birn, R.M., Molloy, E.K., Patriat, R., Parker, T., Meier, T.B., Kirk, G.R., Nair, V.A., Meyerand, M.E., Prabhakaran, V., 2013. The effect of scan length on the reliability of resting-state fMRI connectivity estimates. NeuroImage 83, 550–558. https://doi.org/10.1016/j.neuroimage.2013.05.099

Biswal, B., Yetkin, F.Z., Haughton, V.M., Hyde, J.S., 1995. Functional connectivity in the motor cortex of resting human brain using echo-planar mri. Magn. Reson. Med. 34, 537–541. https://doi.org/10.1002/mrm.1910340409

Biswal, B.B., Van Kylen, J., Hyde, J.S., 1997. Simultaneous assessment of flow and BOLD signals in resting-state functional connectivity maps. NMR Biomed. 10, 165–170. https://doi.org/10.1002/(sici)1099-1492(199706/08)10:4/5<165::aid-nbm454>3.0.co;2-7

Blasi, A., Lloyd-Fox, S., Sethna, V., Brammer, M.J., Mercure, E., Murray, L., Williams, S.C.R., Simmons, A., Murphy, D.G.M., Johnson, M.H., 2015. Atypical processing of voice sounds in infants at risk for autism spectrum disorder. Cortex J. Devoted Study Nerv. Syst. Behav. 71, 122–133. https://doi.org/10.1016/j.cortex.2015.06.015

Blasi, A., Mercure, E., Lloyd-Fox, S., Thomson, A., Brammer, M., Sauter, D., Deeley, Q., Barker, G.J., Renvall, V., Deoni, S., Gasston, D., Williams, S.C.R., Johnson, M.H., Simmons, A., Murphy, D.G.M., 2011. Early Specialization for Voice and Emotion Processing in the Infant Brain. Curr. Biol. 21, 1220–1224. https://doi.org/10.1016/j.cub.2011.06.009

Blencowe, H., Lee, A.C., Cousens, S., Bahalim, A., Narwal, R., Zhong, N., Chou, D., Say, L., Modi, N., Katz, J., Vos, T., Marlow, N., Lawn, J.E., 2013. Preterm birth–associated neurodevelopmental impairment estimates at regional and global levels for 2010. Pediatr. Res. 74, 17–34. https://doi.org/10.1038/pr.2013.204

Bolton, T.A.W., Jochaut, D., Giraud, A.-L., Van De Ville, D., 2018. Brain dynamics in ASD during movie-watching show idiosyncratic functional integration and segregation. Hum. Brain Mapp. 39, 2391–2404. https://doi.org/10.1002/hbm.24009

Breeman, L.D., Jaekel, J., Baumann, N., Bartmann, P., Wolke, D., 2016. Attention problems in very preterm children from childhood to adulthood: the Bavarian Longitudinal Study. J. Child Psychol. Psychiatry 57, 132–140. https://doi.org/10.1111/jcpp.12456

Brown, T.T., Kuperman, J.M., Chung, Y., Erhart, M., McCabe, C., Hagler, D.J., Venkatraman, V.K., Akshoomoff, N., Amaral, D.G., Bloss, C.S., Casey, B.J., Chang, L., Ernst, T.M., Frazier, J.A., Gruen, J.R., Kaufmann, W.E., Kenet, T., Kennedy, D.N., Murray, S.S., Sowell, E.R., Jernigan, T.L., Dale, A.M., 2012. Neuroanatomical Assessment of Biological Maturity. Curr. Biol. 22, 1693–1698. https://doi.org/10.1016/j.cub.2012.07.002

Brummelte, S., Grunau, R.E., Chau, V., Poskitt, K.J., Brant, R., Vinall, J., Gover, A., Synnes, A.R., Miller, S.P., 2012. Procedural pain and brain

development in premature newborns. Ann. Neurol. 71, 385–396. https://doi.org/10.1002/ana.22267
Brydges, C.R., Landes, J.K., Reid, C.L., Campbell, C., French, N., Anderson, M., 2018. Cognitive outcomes in children and adolescents born very preterm: a meta-analysis. Dev. Med. Child Neurol. 60, 452–468. https://doi.org/10.1111/dmcn.13685
Buckner, R.L., Andrews-Hanna, J.R., Schacter, D.L., 2008. The brain's default network: anatomy, function, and relevance to disease. Ann. N. Y. Acad. Sci. 1124, 1–38. https://doi.org/10.1196/annals.1440.011
Burger, C., Hammerl, M., Neubauer, V., Pupp Peglow, U., Kiechl-Kohlendorfer, U., Griesmaier, E., 2020. Early preterm infants with abnormal psychomotor neurodevelopmental outcome at age two show alterations in amplitude-integrated electroencephalography signals. Early Hum. Dev. 141, 104935. https://doi.org/10.1016/j.earlhumdev.2019.104935
Cabral, L., Zubiaurre, L., Wild, C., Linke, A., Cusack, R., 2020. Category-Selective Visual Regions Have Distinctive Signatures of Connectivity in Neonates. bioRxiv 675421. https://doi.org/10.1101/675421
Cao, M., Huang, H., He, Y., 2017. Developmental Connectomics from Infancy through Early Childhood. Trends Neurosci. 40, 494–506. https://doi.org/10.1016/j.tins.2017.06.003
Carney, O., Hughes, E., Tusor, N., Dimitrova, R., Arulkumaran, S., Baruteau, K.P., Collado, A.E., Cordero-Grande, L., Chew, A., Falconer, S., Allsop, J.M., Rueckert, D., Hajnal, J., Edwards, A.D., Rutherford, M., 2021. Incidental findings on brain MR imaging of asymptomatic term neonates in the Developing Human Connectome Project. EClinicalMedicine 38, 100984. https://doi.org/10.1016/j.eclinm.2021.100984
Castellanos, F.X., Di Martino, A., Craddock, R.C., Mehta, A.D., Milham, M.P., 2013. Clinical applications of the functional connectome. NeuroImage 80. https://doi.org/10.1016/j.neuroimage.2013.04.083
Cayam-Rand, D., Guo, T., Grunau, R.E., Benavente-Fernández, I., Synnes, A., Chau, V., Branson, H., Latal, B., McQuillen, P., Miller, S.P., 2019. Predicting developmental outcomes in preterm infants: A simple white matter injury imaging rule. Neurology 93, e1231–e1240. https://doi.org/10.1212/WNL.0000000000008172
Chau, V., Brant, R., Poskitt, K.J., Tam, E.W.Y., Synnes, A., Miller, S.P., 2012. Postnatal infection is associated with widespread abnormalities of brain development in premature newborns. Pediatr. Res. 71, 274–279. https://doi.org/10.1038/pr.2011.40
Ciarrusta, J., Christiaens, D., Fitzgibbon, S.P., Dimitrova, R., Hutter, J., Hughes, E., Duff, E., Price, A.N., Cordero-Grande, L., Tournier, J.D., Rueckert, D., Hajnal, J.V., Arichi, T., McAlonan, G., Edwards, A.D., Batalle, D., 2021. The developing brain structural and functional connectome fingerprint. bioRxiv 2021.03.08.434357. https://doi.org/10.1101/2021.03.08.434357
Ciarrusta, J., Dimitrova, R., Batalle, D., O'Muircheartaigh, J., Cordero-Grande, L., Price, A., Hughes, E., Kangas, J., Perry, E., Javed, A., Demilew, J., Hajnal, J., Edwards, A.D., Murphy, D., Arichi, T., McAlonan, G., 2020. Emerging functional connectivity differences in newborn infants vulnerable to autism spectrum disorders. Transl. Psychiatry 10, 1–10. https://doi.org/10.1038/s41398-020-0805-y
Collins, S.E., Thompson, D.K., Kelly, C.E., Yang, J.Y.M., Pascoe, L., Inder, T.E., Doyle, L.W., Cheong, J.L.Y., Burnett, A.C., Anderson, P.J., 2021. Development of brain white matter and math computation ability in

children born very preterm and full-term. Dev. Cogn. Neurosci. 51, 100987. https://doi.org/10.1016/j.dcn.2021.100987
Conroy, B.R., Singer, B.D., Guntupalli, J.S., Ramadge, P.J., Haxby, J.V., 2013. Inter-subject alignment of human cortical anatomy using functional connectivity. NeuroImage 81, 400–411. https://doi.org/10.1016/j.neuroimage.2013.05.009
Constable, R.T., Vohr, B.R., Scheinost, D., Benjamin, J.R., Fulbright, R.K., Lacadie, C., Schneider, K.C., Katz, K.H., Zhang, H., Papademetris, X., Ment, L.R., 2013. A left cerebellar pathway mediates language in prematurely-born young adults. NeuroImage 64, 371–378. https://doi.org/10.1016/j.neuroimage.2012.09.008
Cordes, D., Haughton, V.M., Arfanakis, K., Carew, J.D., Turski, P.A., Moritz, C.H., Quigley, M.A., Meyerand, M.E., 2001. Frequencies Contributing to Functional Connectivity in the Cerebral Cortex in "Resting-state" Data. Am. J. Neuroradiol. 22, 1326–1333.
Cordes, D., Haughton, V.M., Arfanakis, K., Wendt, G.J., Turski, P.A., Moritz, C.H., Quigley, M.A., Meyerand, M.E., 2000. Mapping functionally related regions of brain with functional connectivity MR imaging. AJNR Am. J. Neuroradiol. 21, 1636–1644.
Counsell, S.J., Shen, Y., Boardman, J.P., Larkman, D.J., Kapellou, O., Ward, P., Allsop, J.M., Cowan, F.M., Hajnal, J.V., Edwards, A.D., Rutherford, M.A., 2006. Axial and radial diffusivity in preterm infants who have diffuse white matter changes on magnetic resonance imaging at term-equivalent age. Pediatrics 117, 376–386. https://doi.org/10.1542/peds.2005-0820
Courage, M.L., Adams, R.J., 1996. Infant peripheral vision: the development of monocular visual acuity in the first 3 months of postnatal life. Vision Res. 36, 1207–1215. https://doi.org/10.1016/0042-6989(95)00204-9
Craddock, R.C., Holtzheimer, P.E., Hu, X.P., Mayberg, H.S., 2009. Disease state prediction from resting state functional connectivity. Magn. Reson. Med. 62, 1619–1628. https://doi.org/10.1002/mrm.22159
Currie, D.C., Manny, R.E., 1997. The Development of Accommodation. Vision Res. 37, 1525–1533. https://doi.org/10.1016/S0042-6989(97)85022-5
Cusack, R., Ball, G., Smyser, C.D., Dehaene-Lambertz, G., 2016. A neural window on the emergence of cognition. Ann. N. Y. Acad. Sci. 1369, 7–23. https://doi.org/10.1111/nyas.13036
Cusack, R., McCuaig, O., Linke, A.C., 2018. Methodological challenges in the comparison of infant fMRI across age groups. Dev. Cogn. Neurosci. 33, 194–205. https://doi.org/10.1016/j.dcn.2017.11.003
Dall'Orso, S., Fifer, W.P., Balsam, P.D., Brandon, J., O'Keefe, C., Poppe, T., Vecchiato, K., Edwards, A.D., Burdet, E., Arichi, T., 2021. Cortical Processing of Multimodal Sensory Learning in Human Neonates. Cereb. Cortex N. Y. N 1991 31, 1827–1836. https://doi.org/10.1093/cercor/bhaa340
Dall'Orso, S., Steinweg, J., Allievi, A.G., Edwards, A.D., Burdet, E., Arichi, T., 2018. Somatotopic Mapping of the Developing Sensorimotor Cortex in the Preterm Human Brain. Cereb. Cortex N. Y. N 1991 28, 2507–2515. https://doi.org/10.1093/cercor/bhy050
Damaraju, E., Caprihan, A., Lowe, J.R., Allen, E.A., Calhoun, V.D., Phillips, J.P., 2014. Functional connectivity in the developing brain: a longitudinal study from 4 to 9months of age. NeuroImage 84, 169–180. https://doi.org/10.1016/j.neuroimage.2013.08.038
Damaraju, E., Phillips, J.R., Lowe, J.R., Ohls, R., Calhoun, V.D., Caprihan, A., 2010. Resting-state functional connectivity differences in premature

children. Front. Syst. Neurosci. 4. https://doi.org/10.3389/fnsys.2010.00023
Dangeti, P., 2017. Statistics for Machine Learning. Packt Publishing Ltd.
Daw, N.W., 2013. Visual Development. Springer Science & Business Media.
De Asis-Cruz, J., Bouyssi-Kobar, M., Evangelou, I., Vezina, G., Limperopoulos, C., 2015. Functional properties of resting state networks in healthy full-term newborns. Sci. Rep. 5, 17755. https://doi.org/10.1038/srep17755
De Luca, M., Beckmann, C.F., De Stefano, N., Matthews, P.M., Smith, S.M., 2006. fMRI resting state networks define distinct modes of long-distance interactions in the human brain. NeuroImage 29, 1359–1367. https://doi.org/10.1016/j.neuroimage.2005.08.035
Dean, J.M., Bennet, L., Back, S.A., McClendon, E., Riddle, A., Gunn, A.J., 2014. What brakes the preterm brain? An arresting story. Pediatr. Res. 75, 227–233. https://doi.org/10.1038/pr.2013.189
Deen, B., Richardson, H., Dilks, D.D., Takahashi, A., Keil, B., Wald, L.L., Kanwisher, N., Saxe, R., 2017. Organization of high-level visual cortex in human infants. Nat. Commun. https://doi.org/10.1038/ncomms13995
Dehaene-Lambertz, G., 2002. Functional Neuroimaging of Speech Perception in Infants. Science 298, 2013–2015. https://doi.org/10.1126/science.1077066
Dehaene-Lambertz, G., Montavont, A., Jobert, A., Allirol, L., Dubois, J., Hertz-Pannier, L., Dehaene, S., 2010. Language or music, mother or Mozart? Structural and environmental influences on infants' language networks. Brain Lang., Special Issue on Language Development 114, 53–65. https://doi.org/10.1016/j.bandl.2009.09.003
Department of Health UK, Royal College of Paediatrics and Child Health, World Health Organization, 2009. UK-WHO growth charts - neonatal and infant close monitoring (NICM).
Dimitrova, R., Arulkumaran, S., Carney, O., Chew, A., Falconer, S., Ciarrusta, J., Wolfers, T., Batalle, D., Cordero-Grande, L., Price, A.N., Teixeira, R.P., Hughes, E., Egloff, A., Hutter, J., Makropoulos, A., Robinson, E.C., Schuh, A., Vecchiato, K., Steinweg, J.K., Macleod, R., Marquand, A.F., McAlonan, G., Rutherford, M.A., Counsell, S.J., Smith, S.M., Rueckert, D., Hajnal, J.V., O'Muircheartaigh, J., Edwards, A.D., 2021a. Phenotyping the preterm brain: characterising individual deviations from normative volumetric development in two large infant cohorts. bioRxiv 2020.08.05.228700. https://doi.org/10.1101/2020.08.05.228700
Dimitrova, R., Pietsch, M., Christiaens, D., Ciarrusta, J., Wolfers, T., Batalle, D., Hughes, E., Hutter, J., Cordero-Grande, L., Price, A.N., Chew, A., Falconer, S., Vecchiato, K., Steinweg, J.K., Carney, O., Rutherford, M.A., Tournier, J.-D., Counsell, S.J., Marquand, A.F., Rueckert, D., Hajnal, J.V., Mcalonan, G., Edwards, A.D., O'Muircheartaigh, J., 2020. Heterogeneity in Brain Microstructural Development Following Preterm Birth. Cereb. Cortex. https://doi.org/10.1093/cercor/bhaa069
Dimitrova, R., Pietsch, M., Ciarrusta, J., Fitzgibbon, S.P., Williams, L.Z.J., Christiaens, D., Cordero-Grande, L., Batalle, D., Makropoulos, A., Schuh, A., Price, A.N., Hutter, J., Teixeira, R.P., Hughes, E., Chew, A., Falconer, S., Carney, O., Egloff, A., Tournier, J.-D., McAlonan, G., Rutherford, M.A., Counsell, S.J., Robinson, E.C., Hajnal, J.V., Rueckert, D., Edwards, A.D., O'Muircheartaigh, J., 2021b. Preterm birth alters the development of cortical microstructure and morphology at term-equivalent age. NeuroImage 243, 118488. https://doi.org/10.1016/j.neuroimage.2021.118488

Doria, V., Beckmann, C.F., Arichi, T., Merchant, N., Groppo, M., Turkheimer, F.E., Counsell, S.J., Murgasova, M., Aljabar, P., Nunes, R.G., Larkman, D.J., Rees, G., Edwards, A.D., 2010. Emergence of resting state networks in the preterm human brain. Proc. Natl. Acad. Sci. 107, 20015–20020. https://doi.org/10.1073/pnas.1007921107

Dosenbach, N.U.F., Nardos, B., Cohen, A.L., Fair, D.A., Power, J.D., Church, J.A., Nelson, S.M., Wig, G.S., Vogel, A.C., Lessov-Schlaggar, C.N., Barnes, K.A., Dubis, J.W., Feczko, E., Coalson, R.S., Pruett, J.R., Barch, D.M., Petersen, S.E., Schlaggar, B.L., 2010. Prediction of Individual Brain Maturity Using fMRI. Science 329, 1358–1361. https://doi.org/10.1126/science.1194144

Downing, G., 2001. Biomarkers and surrogate endpoints: Preferred definitions and conceptual framework. Clin. Pharmacol. Ther. 69, 89–95. https://doi.org/10.1067/mcp.2001.113989

Dubois, J., Alison, M., Counsell, S.J., Hertz-Pannier, L., Hüppi, P.S., Benders, M.J.N.L., 2020. MRI of the Neonatal Brain: A Review of Methodological Challenges and Neuroscientific Advances. J. Magn. Reson. Imaging n/a. https://doi.org/10.1002/jmri.27192

Duerden, E.G., Halani, S., Ng, K., Guo, T., Foong, J., Glass, T.J.A., Chau, V., Branson, H.M., Sled, J.G., Whyte, H.E., Kelly, E.N., Miller, S.P., 2019. White matter injury predicts disrupted functional connectivity and microstructure in very preterm born neonates. NeuroImage Clin. 21, 101596. https://doi.org/10.1016/j.nicl.2018.11.006

Duff, E.P., Moultrie, F., van der Vaart, M., Goksan, S., Abos, A., Fitzgibbon, S.P., Baxter, L., Wager, T.D., Slater, R., 2020. Inferring pain experience in infants using quantitative whole-brain functional MRI signatures: a cross-sectional, observational study. Lancet Digit. Health 2, e458–e467. https://doi.org/10.1016/S2589-7500(20)30168-0

Dufford, A.J., Noble, S., Gao, S., Scheinost, D., 2021a. The Instability of Functional Connectomes Across the First Year of Life. bioRxiv 2021.04.14.439877. https://doi.org/10.1101/2021.04.14.439877

Dufford, A.J., Noble, S., Gao, S., Scheinost, D., 2021b. The instability of functional connectomes across the first year of life. Dev. Cogn. Neurosci. 51, 101007. https://doi.org/10.1016/j.dcn.2021.101007

Eiselt, M., Schendel, M., Witte, H., Dörschel, J., Curzi-Dascalova, L., D'Allest, A.M., Zwiener, U., 1997. Quantitative analysis of discontinuous EEG in premature and full-term newborns during quiet sleep. Electroencephalogr. Clin. Neurophysiol. 103, 528–534. https://doi.org/10.1016/s0013-4694(97)00033-3

El-Dib, M., 2020. Survey on Neuroimaging of Premature Infants. Presented at the Newborn Brain Society, Newborn Brain Society.

Elliott, M.L., Knodt, A.R., Cooke, M., Kim, M.J., Melzer, T.R., Keenan, R., Ireland, D., Ramrakha, S., Poulton, R., Caspi, A., Moffitt, T.E., Hariri, A.R., 2019. General functional connectivity: Shared features of resting-state and task fMRI drive reliable and heritable individual differences in functional brain networks. NeuroImage 189, 516–532. https://doi.org/10.1016/j.neuroimage.2019.01.068

Ellis, C.T., Skalaban, L.J., Yates, T.S., Bejjanki, V.R., Córdova, N.I., Turk-Browne, N.B., 2021a. Evidence of hippocampal learning in human infants. Curr. Biol. CB. https://doi.org/10.1016/j.cub.2021.04.072

Ellis, C.T., Skalaban, L.J., Yates, T.S., Bejjanki, V.R., Córdova, N.I., Turk-Browne, N.B., 2020. Re-imagining fMRI for awake behaving infants. Nat. Commun. 11, 4523. https://doi.org/10.1038/s41467-020-18286-y

Ellis, C.T., Skalaban, L.J., Yates, T.S., Turk-Browne, N.B., 2021b. Attention recruits frontal cortex in human infants. Proc. Natl. Acad. Sci. 118. https://doi.org/10.1073/pnas.2021474118

Ellis, C.T., Yates, T.S., Skalaban, L.J., Bejjanki, V.R., Arcaro, M.J., Turk-Browne, N.B., 2021c. Retinotopic organization of visual cortex in human infants. Neuron 109, 2616-2626.e6. https://doi.org/10.1016/j.neuron.2021.06.004

Elton, A., Gao, W., 2015. Task-positive Functional Connectivity of the Default Mode Network Transcends Task Domain. J. Cogn. Neurosci. 27, 2369–2381. https://doi.org/10.1162/jocn_a_00859

Emerson, R.W., Adams, C., Nishino, T., Hazlett, H.C., Wolff, J.J., Zwaigenbaum, L., Constantino, J.N., Shen, M.D., Swanson, M.R., Elison, J.T., Kandala, S., Estes, A.M., Botteron, K.N., Collins, L., Dager, S.R., Evans, A.C., Gerig, G., Gu, H., McKinstry, R.C., Paterson, S., Schultz, R.T., Styner, M., Network, I., Schlaggar, B.L., Pruett, J.R., Piven, J., 2017. Functional neuroimaging of high-risk 6-month-old infants predicts a diagnosis of autism at 24 months of age. Sci. Transl. Med. 9, eaag2882. https://doi.org/10.1126/scitranslmed.aag2882

Emerson, R.W., Short, S.J., Lin, W., Gilmore, J.H., Gao, W., 2015. Network-Level Connectivity Dynamics of Movie Watching in 6-Year-Old Children. Front. Hum. Neurosci. 9, 631. https://doi.org/10.3389/fnhum.2015.00631

Engelhardt, E., Inder, T.E., Alexopoulos, D., Dierker, D.L., Hill, J., Essen, D.V., Neil, J.J., 2015. Regional impairments of cortical folding in premature infants. Ann. Neurol. 77, 154–162. https://doi.org/10.1002/ana.24313

Erus, G., Battapady, H., Satterthwaite, T.D., Hakonarson, H., Gur, R.E., Davatzikos, C., Gur, R.C., 2015. Imaging patterns of brain development and their relationship to cognition. Cereb. Cortex N. Y. N 1991 25, 1676–1684. https://doi.org/10.1093/cercor/bht425

Eves, R., Mendonça, M., Baumann, N., Ni, Y., Darlow, B.A., Horwood, J., Woodward, L.J., Doyle, L.W., Cheong, J., Anderson, P.J., Bartmann, P., Marlow, N., Johnson, S., Kajantie, E., Hovi, P., Nosarti, C., Indredavik, M.S., Evensen, K.-A.I., Räikkönen, K., Heinonen, K., Zeitlin, J., Wolke, D., 2021. Association of Very Preterm Birth or Very Low Birth Weight With Intelligence in Adulthood: An Individual Participant Data Meta-analysis. JAMA Pediatr. 175, e211058. https://doi.org/10.1001/jamapediatrics.2021.1058

Eyre, M., Fitzgibbon, S.P., Ciarrusta, J., Cordero-Grande, L., Price, A.N., Poppe, T., Schuh, A., Hughes, E., O'Keeffe, C., Brandon, J., Cromb, D., Vecchiato, K., Andersson, J., Duff, E.P., Counsell, S.J., Smith, S.M., Rueckert, D., Hajnal, J.V., Arichi, T., O'Muircheartaigh, J., Batalle, D., Edwards, A.D., 2021. The Developing Human Connectome Project: typical and disrupted perinatal functional connectivity. Brain 144, 2199–2213. https://doi.org/10.1093/brain/awab118

Feldmann, M., Rousson, V., Nguyen, T.D., Bernet, V., Hagmann, C., Latal, B., Natalucci, G., 2020. Cognitive outcome of early school-aged children born very preterm is not predicted by early short-term amplitude-integrated electroencephalography. Acta Paediatr. 109, 78–84. https://doi.org/10.1111/apa.14919

Fenchel, D., Dimitrova, R., Robinson, E.C., Batalle, D., Chew, A., Falconer, S., Kyriakopoulou, V., Nosarti, C., Hutter, J., Christiaens, D., Pietsch, M., Brandon, J., Hughes, E.J., Allsop, J., O'Keeffe, C., Price, A.N., Cordero-Grande, L., Schuh, A., Makropoulos, A., Passerat-Palmbach, J., Bozek, J., Rueckert, D., Hajnal, J.V., McAlonan, G., Edwards, A.D.,

O'Muircheartaigh, J., 2022. Neonatal multi-modal cortical profiles predict 18-month developmental outcomes. Dev. Cogn. Neurosci. 54, 101103. https://doi.org/10.1016/j.dcn.2022.101103
Ferguson, S.A., Ward, W.L., Paule, M.G., Hall, R.W., Anand, K.J.S., 2012. A pilot study of preemptive morphine analgesia in preterm neonates: effects on head circumference, social behavior, and response latencies in early childhood. Neurotoxicol. Teratol. 34, 47–55. https://doi.org/10.1016/j.ntt.2011.10.008
Fevang, S.K.E., Hysing, M., Markestad, T., Sommerfelt, K., 2016. Mental Health in Children Born Extremely Preterm Without Severe Neurodevelopmental Disabilities. Pediatrics 137. https://doi.org/10.1542/peds.2015-3002
Finn, E.S., 2021. Is it time to put rest to rest? Trends Cogn. Sci. https://doi.org/10.1016/j.tics.2021.09.005
Finn, E.S., Bandettini, P.A., 2021. Movie-watching outperforms rest for functional connectivity-based prediction of behavior. NeuroImage 235, 117963. https://doi.org/10.1016/j.neuroimage.2021.117963
Finn, E.S., Glerean, E., Khojandi, A.Y., Nielson, D., Molfese, P.J., Handwerker, D.A., Bandettini, P.A., 2020. Idiosynchrony: From shared responses to individual differences during naturalistic neuroimaging. NeuroImage 215, 116828. https://doi.org/10.1016/j.neuroimage.2020.116828
Finn, E.S., Scheinost, D., Finn, D.M., Shen, X., Papademetris, X., Constable, R.T., 2017. Can brain state be manipulated to emphasize individual differences in functional connectivity? NeuroImage 160, 140–151. https://doi.org/10.1016/j.neuroimage.2017.03.064
Finn, E.S., Shen, X., Scheinost, D., Rosenberg, M.D., Huang, J., Chun, M.M., Papademetris, X., Constable, R.T., 2015. Functional connectome fingerprinting: identifying individuals using patterns of brain connectivity. Nat. Neurosci. 18, 1664–1671. https://doi.org/10.1038/nn.4135
Fischi-Gomez, E., Muñoz-Moreno, E., Vasung, L., Griffa, A., Borradori-Tolsa, C., Monnier, M., Lazeyras, F., Thiran, J.-P., Hüppi, P.S., 2016. Brain network characterization of high-risk preterm-born school-age children. NeuroImage Clin. 11, 195–209. https://doi.org/10.1016/j.nicl.2016.02.001
Fitzgibbon, S.P., Harrison, S.J., Jenkinson, M., Baxter, L., Robinson, E.C., Bastiani, M., Bozek, J., Karolis, V., Grande, L.C., Price, A.N., Hughes, E., Makropoulos, A., Passerat-Palmbach, J., Schuh, A., Gao, J., Farahibozorg, S.-R., O'Muircheartaigh, J., Ciarrusta, J., O'Keeffe, C., Brandon, J., Arichi, T., Rueckert, D., Hajnal, J.V., Edwards, A.D., Smith, S.M., Duff, E., Andersson, J., 2020. The developing Human Connectome Project (dHCP) automated resting-state functional processing framework for newborn infants. bioRxiv 766030. https://doi.org/10.1101/766030
Fogtmann, E.P., Plomgaard, A.M., Greisen, G., Gluud, C., 2017. Prognostic Accuracy of Electroencephalograms in Preterm Infants: A Systematic Review. Pediatrics 139. https://doi.org/10.1542/peds.2016-1951
Fonov, V., Evans, A., McKinstry, R., Almli, C., Collins, D., 2009. Unbiased nonlinear average age-appropriate brain templates from birth to adulthood. NeuroImage, Organization for Human Brain Mapping 2009 Annual Meeting 47, S102. https://doi.org/10.1016/S1053-8119(09)70884-5
Franke, K., Gaser, C., 2019. Ten Years of BrainAGE as a Neuroimaging Biomarker of Brain Aging: What Insights Have We Gained? Front. Neurol. 10. https://doi.org/10.3389/fneur.2019.00789
Fransson, P., Aden, U., Blennow, M., Lagercrantz, H., 2011. The functional architecture of the infant brain as revealed by resting-state fMRI. Cereb.

Cortex N. Y. N 1991 21, 145–154. https://doi.org/10.1093/cercor/bhq071
Fransson, P., Skiöld, B., Engström, M., Hallberg, B., Mosskin, M., Åden, U., Lagercrantz, H., Blennow, M., 2009. Spontaneous Brain Activity in the Newborn Brain During Natural Sleep—An fMRI Study in Infants Born at Full Term. Pediatr. Res. 66, 301–305. https://doi.org/10.1203/PDR.0b013e3181b1bd84
Fransson, P., Skiöld, B., Horsch, S., Nordell, A., Blennow, M., Lagercrantz, H., Aden, U., 2007. Resting-state networks in the infant brain. Proc. Natl. Acad. Sci. U. S. A. 104, 15531–15536. https://doi.org/10.1073/pnas.0704380104
Friedman, L., Glover, G.H., 2006. Report on a multicenter fMRI quality assurance protocol. J. Magn. Reson. Imaging 23, 827–839. https://doi.org/10.1002/jmri.20583
Friston, K.J., 2011. Functional and effective connectivity: a review. Brain Connect. 1, 13–36. https://doi.org/10.1089/brain.2011.0008
Friston, K.J., Frith, C.D., Liddle, P.F., Frackowiak, R.S., 1993. Functional connectivity: the principal-component analysis of large (PET) data sets. J. Cereb. Blood Flow Metab. Off. J. Int. Soc. Cereb. Blood Flow Metab. 13, 5–14. https://doi.org/10.1038/jcbfm.1993.4
Gal, S., Coldham, Y., Tik, N., Bernstein-Eliav, M., Tavor, I., 2022. Act natural: Functional connectivity from naturalistic stimuli fMRI outperforms resting-state in predicting brain activity. NeuroImage 258, 119359. https://doi.org/10.1016/j.neuroimage.2022.119359
Galdi, P., Blesa, M., Stoye, D.Q., Sullivan, G., Lamb, G.J., Quigley, A.J., Thrippleton, M.J., Bastin, M.E., Boardman, J.P., 2020. Neonatal morphometric similarity mapping for predicting brain age and characterizing neuroanatomic variation associated with preterm birth. NeuroImage Clin. 25, 102195. https://doi.org/10.1016/j.nicl.2020.102195
Gao, W., Alcauter, S., Elton, A., Hernandez-Castillo, C.R., Smith, J.K., Ramirez, J., Lin, W., 2015a. Functional Network Development During the First Year: Relative Sequence and Socioeconomic Correlations. Cereb. Cortex 25, 2919–2928. https://doi.org/10.1093/cercor/bhu088
Gao, W., Alcauter, S., Smith, J.K., Gilmore, J.H., Lin, W., 2015b. Development of human brain cortical network architecture during infancy. Brain Struct. Funct. 220, 1173–1186. https://doi.org/10.1007/s00429-014-0710-3
Gao, W., Gilmore, J.H., Alcauter, S., Lin, W., 2013a. The dynamic reorganization of the default-mode network during a visual classification task. Front. Syst. Neurosci. 7, 34. https://doi.org/10.3389/fnsys.2013.00034
Gao, W., Gilmore, J.H., Giovanello, K.S., Smith, J.K., Shen, D., Zhu, H., Lin, W., 2011. Temporal and Spatial Evolution of Brain Network Topology during the First Two Years of Life. PLOS ONE 6, e25278. https://doi.org/10.1371/journal.pone.0025278
Gao, W., Gilmore, J.H., Shen, D., Smith, J.K., Zhu, H., Lin, W., 2013b. The synchronization within and interaction between the default and dorsal attention networks in early infancy. Cereb. Cortex N. Y. N 1991 23, 594–603. https://doi.org/10.1093/cercor/bhs043
Gao, W., Lin, W., 2012. Frontal parietal control network regulates the anti-correlated default and dorsal attention networks. Hum. Brain Mapp. 33, 192–202. https://doi.org/10.1002/hbm.21204
Gao, W., Zhu, H., Giovanello, K.S., Smith, J.K., Shen, D., Gilmore, J.H., Lin, W., 2009. Evidence on the emergence of the brain's default network from 2-

week-old to 2-year-old healthy pediatric subjects. Proc. Natl. Acad. Sci. U. S. A. 106, 6790–6795. https://doi.org/10.1073/pnas.0811221106
Ghotra, A., Kosakowski, H.L., Takahashi, A., Etzel, R., May, M.W., Scholz, A., Jansen, A., Wald, L.L., Kanwisher, N., Saxe, R., Keil, B., 2021. A size-adaptive 32-channel array coil for awake infant neuroimaging at 3 Tesla MRI. Magn. Reson. Med. 86, 1773–1785. https://doi.org/10.1002/mrm.28791
Gilmore, J.H., Zhai, G., Wilber, K., Smith, J.K., Lin, W., Gerig, G., 2004. 3 Tesla magnetic resonance imaging of the brain in newborns. Psychiatry Res. 132, 81–85. https://doi.org/10.1016/j.pscychresns.2004.04.004
Glass, H.C., Bonifacio, S.L., Chau, V., Glidden, D., Poskitt, K., Barkovich, A.J., Ferriero, D.M., Miller, S.P., 2008. Recurrent Postnatal Infections Are Associated With Progressive White Matter Injury in Premature Infants. PEDIATRICS 122, 299–305. https://doi.org/10.1542/peds.2007-2184
Goksan, S., Hartley, C., Emery, F., Cockrill, N., Poorun, R., Moultrie, F., Rogers, R., Campbell, J., Sanders, M., Adams, E., Clare, S., Jenkinson, M., Tracey, I., Slater, R., 2015. fMRI reveals neural activity overlap between adult and infant pain. eLife 4, e06356. https://doi.org/10.7554/eLife.06356
Golan, A., Marco, R., Raz, H., Shany, E., 2011. Imaging in the newborn: infant immobilizer obviates the need for anesthesia. Isr. Med. Assoc. J. IMAJ 13, 663–665.
Gonzalez-Castillo, J., Hoy, C.W., Handwerker, D.A., Robinson, M.E., Buchanan, L.C., Saad, Z.S., Bandettini, P.A., 2015. Tracking ongoing cognition in individuals using brief, whole-brain functional connectivity patterns. Proc. Natl. Acad. Sci. U. S. A. 112, 8762–8767. https://doi.org/10.1073/pnas.1501242112
Gordon, E.M., Laumann, T.O., Gilmore, A.W., Newbold, D.J., Greene, D.J., Berg, J.J., Ortega, M., Hoyt-Drazen, C., Gratton, C., Sun, H., Hampton, J.M., Coalson, R.S., Nguyen, A.L., McDermott, K.B., Shimony, J.S., Snyder, A.Z., Schlaggar, B.L., Petersen, S.E., Nelson, S.M., Dosenbach, N.U.F., 2017. Precision Functional Mapping of Individual Human Brains. Neuron 95, 791-807.e7. https://doi.org/10.1016/j.neuron.2017.07.011
Gorgolewski, K., Burns, C., Madison, C., Clark, D., Halchenko, Y., Waskom, M., Ghosh, S., 2011. Nipype: A Flexible, Lightweight and Extensible Neuroimaging Data Processing Framework in Python. Front. Neuroinformatics 5.
Gozdas, E., Parikh, N.A., Merhar, S.L., Tkach, J.A., He, L., Holland, S.K., 2018. Altered functional network connectivity in preterm infants: antecedents of cognitive and motor impairments? Brain Struct. Funct. 223, 3665–3680. https://doi.org/10.1007/s00429-018-1707-0
Graham, A.M., Fisher, P.A., Pfeifer, J.H., 2013. What Sleeping Babies Hear: A Functional MRI Study of Interparental Conflict and Infants' Emotion Processing. Psychol. Sci. 24, 782–789. https://doi.org/10.1177/0956797612458803
Gratton, C., Laumann, T.O., Nielsen, A.N., Greene, D.J., Gordon, E.M., Gilmore, A.W., Nelson, S.M., Coalson, R.S., Snyder, A.Z., Schlaggar, B.L., Dosenbach, N.U.F., Petersen, S.E., 2018. Functional Brain Networks Are Dominated by Stable Group and Individual Factors, Not Cognitive or Daily Variation. Neuron 98, 439-452.e5. https://doi.org/10.1016/j.neuron.2018.03.035
Greene, D.J., Koller, J.M., Hampton, J.M., Wesevich, V., Van, A.N., Nguyen, A.L., Hoyt, C.R., McIntyre, L., Earl, E.A., Klein, R.L., Shimony, J.S., Petersen, S.E., Schlaggar, B.L., Fair, D.A., Dosenbach, N.U.F., 2018. Behavioral interventions for reducing head motion during MRI scans in

children. NeuroImage 171, 234–245. https://doi.org/10.1016/j.neuroimage.2018.01.023
Greicius, M.D., Krasnow, B., Reiss, A.L., Menon, V., 2003. Functional connectivity in the resting brain: a network analysis of the default mode hypothesis. Proc. Natl. Acad. Sci. U. S. A. 100, 253–258. https://doi.org/10.1073/pnas.0135058100
Griffanti, L., Salimi-Khorshidi, G., Beckmann, C.F., Auerbach, E.J., Douaud, G., Sexton, C.E., Zsoldos, E., Ebmeier, K.P., Filippini, N., Mackay, C.E., Moeller, S., Xu, J., Yacoub, E., Baselli, G., Ugurbil, K., Miller, K.L., Smith, S.M., 2014. ICA-based artefact removal and accelerated fMRI acquisition for improved resting state network imaging. NeuroImage 95, 232–247. https://doi.org/10.1016/j.neuroimage.2014.03.034
Gruskin, D.C., Patel, G.H., 2022. Brain connectivity at rest predicts individual differences in normative activity during movie watching. NeuroImage 253, 119100. https://doi.org/10.1016/j.neuroimage.2022.119100
Guillot, M., Sebastianski, M., Lemyre, B., 2021. Comparative performance of head ultrasound and MRI in detecting preterm brain injury and predicting outcomes: A systematic review. Acta Paediatr. 110, 1425–1432. https://doi.org/10.1111/apa.15670
Hand, I.L., Shellhaas, R.A., Milla, S.S., Committee on Fetus and Newborn, S. on N., 2020. Routine Neuroimaging of the Preterm Brain. Pediatrics 146. https://doi.org/10.1542/peds.2020-029082
Hasson, U., Furman, O., Clark, D., Dudai, Y., Davachi, L., 2008. Enhanced Intersubject Correlations during Movie Viewing Correlate with Successful Episodic Encoding. Neuron 57, 452. https://doi.org/10.1016/j.neuron.2007.12.009
Hasson, U., Malach, R., Heeger, D.J., 2010. Reliability of cortical activity during natural stimulation. Trends Cogn. Sci. 14, 40–48. https://doi.org/10.1016/j.tics.2009.10.011
Hasson, U., Nir, Y., Levy, I., Fuhrmann, G., Malach, R., 2004. Intersubject Synchronization of Cortical Activity During Natural Vision. Science 303, 1634–1640. https://doi.org/10.1126/science.1089506
He, B.J., 2013. Spontaneous and task-evoked brain activity negatively interact. J. Neurosci. Off. J. Soc. Neurosci. 33, 4672–4682. https://doi.org/10.1523/JNEUROSCI.2922-12.2013
He, L., Li, H., Holland, S.K., Yuan, W., Altaye, M., Parikh, N.A., 2018. Early prediction of cognitive deficits in very preterm infants using functional connectome data in an artificial neural network framework. NeuroImage Clin. 18, 290–297. https://doi.org/10.1016/j.nicl.2018.01.032
He, L., Parikh, N.A., 2015. Aberrant Executive and Frontoparietal Functional Connectivity in Very Preterm Infants With Diffuse White Matter Abnormalities. Pediatr. Neurol. 53, 330–337. https://doi.org/10.1016/j.pediatrneurol.2015.05.001
Hendrix, C.L., Thomason, M.E., 2022. A survey of protocols from 54 infant and toddler neuroimaging research labs. Dev. Cogn. Neurosci. 54, 101060. https://doi.org/10.1016/j.dcn.2022.101060
Herzmann, C., Zubiaurre-Elorza, L., Wild, C.J., Linke, A.C., Han, V.K., Lee, D.S.C., Cusack, R., 2017. Using Functional Magnetic Resonance Imaging to Detect Preserved Function in a Preterm Infant with Brain Injury. J. Pediatr. 189, 213-217.e1. https://doi.org/10.1016/j.jpeds.2017.06.063
Hickey, M., Georgieff, M., Ramel, S., 2018. Neurodevelopmental outcomes following necrotizing enterocolitis. Semin. Fetal. Neonatal Med., NECROTIZING ENTEROCOLITIS 23, 426–432. https://doi.org/10.1016/j.siny.2018.08.005

Hintz, S.R., Barnes, P.D., Bulas, D., Slovis, T.L., Finer, N.N., Wrage, L.A., Das, A., Tyson, J.E., Stevenson, D.K., Carlo, W.A., Walsh, M.C., Laptook, A.R., Yoder, B.A., Van Meurs, K.P., Faix, R.G., Rich, W., Newman, N.S., Cheng, H., Heyne, R.J., Vohr, B.R., Acarregui, M.J., Vaucher, Y.E., Pappas, A., Peralta-Carcelen, M., Wilson-Costello, D.E., Evans, P.W., Goldstein, R.F., Myers, G.J., Poindexter, B.B., Mcgowan, E.C., Adams-Chapman, I., Fuller, J., Higgins, R.D., 2015. Neuroimaging and Neurodevelopmental Outcome in Extremely Preterm Infants. PEDIATRICS 135, e32–e42. https://doi.org/10.1542/peds.2014-0898

Hintz, S.R., Vohr, B.R., Bann, C.M., Taylor, H.G., Das, A., Gustafson, K.E., Yolton, K., Watson, V.E., Lowe, J., DeAnda, M.E., Ball, M.B., Finer, N.N., Meurs, K.P.V., Shankaran, S., Pappas, A., Barnes, P.D., Bulas, D., Newman, J.E., Wilson-Costello, D.E., Heyne, R.J., Harmon, H.M., Peralta-Carcelen, M., Adams-Chapman, I., Duncan, A.F., Fuller, J., Vaucher, Y.E., Colaizy, T.T., Winter, S., McGowan, E.C., Goldstein, R.F., Higgins, R.D., Network, for the S. study group of the E.K.S.N.I. of C.H. and H.D.N.R., 2018. Preterm Neuroimaging and School-Age Cognitive Outcomes. Pediatrics 142. https://doi.org/10.1542/peds.2017-4058

Ho, T.C., Connolly, C.G., Henje Blom, E., LeWinn, K.Z., Strigo, I.A., Paulus, M.P., Frank, G., Max, J.E., Wu, J., Chan, M., Tapert, S.F., Simmons, A.N., Yang, T.T., 2015. Emotion-Dependent Functional Connectivity of the Default Mode Network in Adolescent Depression. Biol. Psychiatry 78, 635–646. https://doi.org/10.1016/j.biopsych.2014.09.002

Hollebrandse, N.L., Spittle, A.J., Burnett, A.C., Anderson, P.J., Roberts, G., Doyle, L.W., Cheong, J.L.Y., 2020. School-age outcomes following intraventricular haemorrhage in infants born extremely preterm. Arch. Dis. Child. - Fetal Neonatal Ed. https://doi.org/10.1136/archdischild-2020-318989

Horien, C., Floris, D.L., Greene, A.S., Noble, S., Rolison, M., Tejavibulya, L., O'Connor, D., McPartland, J.C., Scheinost, D., Chawarska, K., Lake, E.M.R., Constable, R.T., 2022. Functional Connectome–Based Predictive Modeling in Autism. Biol. Psychiatry, Brain Development and Communication in Autism Spectrum Disorder 92, 626–642. https://doi.org/10.1016/j.biopsych.2022.04.008

Horien, C., Shen, X., Scheinost, D., Constable, R.T., 2019. The individual functional connectome is unique and stable over months to years. NeuroImage 189, 676–687. https://doi.org/10.1016/j.neuroimage.2019.02.002

Horne, R.S., Sly, D.J., Cranage, S.M., Chau, B., Adamson, T.M., 2000. Effects of prematurity on arousal from sleep in the newborn infant. Pediatr. Res. 47, 468–474. https://doi.org/10.1203/00006450-200004000-00010

Houldin, E., Fang, Z., Ray, L.B., Stojanoski, B., Owen, A.M., Fogel, S.M., 2021. Reversed and increased functional connectivity in non-REM sleep suggests an altered rather than reduced state of consciousness relative to wake. Sci. Rep. 11, 11943. https://doi.org/10.1038/s41598-021-91211-5

Howell, B.R., Styner, M.A., Gao, W., Yap, P.-T., Wang, L., Baluyot, K., Yacoub, E., Chen, G., Potts, T., Salzwedel, A., Li, G., Gilmore, J.H., Piven, J., Smith, J.K., Shen, D., Ugurbil, K., Zhu, H., Lin, W., Elison, J.T., 2019. The UNC/UMN Baby Connectome Project (BCP): An overview of the study design and protocol development. NeuroImage 185, 891–905. https://doi.org/10.1016/j.neuroimage.2018.03.049

Hu, D., Wang, F., Zhang, H., Wu, Z., Zhou, Z., Li, Guoshi, Wang, L., Lin, W., Li, Gang, Consortium, U.B.C.P., 2021a. Existence of Functional Connectome

Fingerprint During Infancy and Its Stability Over Months. J. Neurosci. https://doi.org/10.1523/JNEUROSCI.0480-21.2021
Hu, D., Yin, W., Wu, Z., Chen, L., Wang, L., Lin, W., Li, G., 2021b. Reference-Relation Guided Autoencoder with Deep CCA Restriction for Awake-to-Sleep Brain Functional Connectome Prediction, in: de Bruijne, M., Cattin, P.C., Cotin, S., Padoy, N., Speidel, S., Zheng, Y., Essert, C. (Eds.), Medical Image Computing and Computer Assisted Intervention – MICCAI 2021, Lecture Notes in Computer Science. Springer International Publishing, Cham, pp. 231–240. https://doi.org/10.1007/978-3-030-87199-4_22
Huettel, S.A., Song, A.W., McCarthy, G., Huettel, S.A., Song, A.W., McCarthy, G., 2014. Functional Magnetic Resonance Imaging, Third Edition, Third Edition. ed. Oxford University Press, Oxford, New York.
Hughes, E.J., Winchman, T., Padormo, F., Teixeira, R., Wurie, J., Sharma, M., Fox, M., Hutter, J., Cordero-Grande, L., Price, A.N., Allsop, J., Bueno-Conde, J., Tusor, N., Arichi, T., Edwards, A.D., Rutherford, M.A., Counsell, S.J., Hajnal, J.V., 2017. A dedicated neonatal brain imaging system. Magn. Reson. Med. 78, 794–804. https://doi.org/10.1002/mrm.26462
Huppi, P.S., Warfield, S., Kikinis, R., Barnes, P.D., Zientara, G.P., Jolesz, F.A., Tsuji, M.K., Volpe, J.J., 1998. Quantitative magnetic resonance imaging of brain development in premature and mature newborns. Ann. Neurol. 43, 224–235. https://doi.org/10.1002/ana.410430213
Huttenlocher, P.R., de Courten, C., 1987. The development of synapses in striate cortex of man. Hum. Neurobiol. 6, 1–9.
Huttenlocher, P.R., De Courten, C., Garey, L.J., Van der Loos, H., 1982. Synaptic development in human cerebral cortex. Int. J. Neurol. 16–17, 144–154.
Inder, T.E., de Vries, L.S., Ferriero, D.M., Grant, P.E., Ment, L.R., Miller, S.P., Volpe, J.J., 2021. Neuroimaging of the Preterm Brain: Review and Recommendations. J. Pediatr. 237, 276-287.e4. https://doi.org/10.1016/j.jpeds.2021.06.014
Jalbrzikowski, M., Liu, F., Foran, W., Klei, L., Calabro, F.J., Roeder, K., Devlin, B., Luna, B., 2020. Functional connectome fingerprinting accuracy in youths and adults is similar when examined on the same day and 1.5-years apart. Hum. Brain Mapp. 41, 4187–4199. https://doi.org/10.1002/hbm.25118
Jenkinson, M., Bannister, P., Brady, M., Smith, S., 2002. Improved Optimization for the Robust and Accurate Linear Registration and Motion Correction of Brain Images. NeuroImage 17, 825–841. https://doi.org/10.1006/nimg.2002.1132
Johns, C.B., Lacadie, C., Vohr, B., Ment, L.R., Scheinost, D., 2019. Amygdala functional connectivity is associated with social impairments in preterm born young adults. NeuroImage Clin. 21, 101626. https://doi.org/10.1016/j.nicl.2018.101626
Johns, C.B., Lacadie, C., Vohr, B., Ment, L.R., Scheinost, D., 2018. Amygdala functional connectivity is associated with social impairments in preterm born young adults. NeuroImage Clin. 21. https://doi.org/10.1016/j.nicl.2018.101626
Johnson, S., Marlow, N., 2017. Early and long-term outcome of infants born extremely preterm. Arch. Dis. Child. 102, 97–102. https://doi.org/10.1136/archdischild-2015-309581
Jones, I.H., Hall, N.J., 2020. Contemporary Outcomes for Infants with Necrotizing Enterocolitis-A Systematic Review. J. Pediatr. 220, 86-92.e3. https://doi.org/10.1016/j.jpeds.2019.11.011

Kardan, O., Kaplan, S., Wheelock, M.D., Feczko, E., Day, T.K.M., Miranda-Domínguez, Ó., Meyer, D., Eggebrecht, A.T., Moore, L.A., Sung, S., Chamberlain, T.A., Earl, E., Snider, K., Graham, A., Berman, M.G., Uğurbil, K., Yacoub, E., Elison, J.T., Smyser, C.D., Fair, D.A., Rosenberg, M.D., 2022. Resting-state functional connectivity identifies individuals and predicts age in 8-to-26-month-olds. Dev. Cogn. Neurosci. 56, 101123. https://doi.org/10.1016/j.dcn.2022.101123

Kaufmann, T., Alnæs, D., Brandt, C.L., Bettella, F., Djurovic, S., Andreassen, O.A., Westlye, L.T., 2018. Stability of the Brain Functional Connectome Fingerprint in Individuals With Schizophrenia. JAMA Psychiatry 75, 749. https://doi.org/10.1001/jamapsychiatry.2018.0844

Kaufmann, T., Alnæs, D., Doan, N.T., Brandt, C.L., Andreassen, O.A., Westlye, L.T., 2017. Delayed stabilization and individualization in connectome development are related to psychiatric disorders. Nat. Neurosci. 20, 513–515. https://doi.org/10.1038/nn.4511

Keil, B., Alagappan, V., Mareyam, A., McNab, J.A., Fujimoto, K., Tountcheva, V., Triantafyllou, C., Dilks, D.D., Kanwisher, N., Lin, W., Grant, P.E., Wald, L.L., 2011. Size-optimized 32-channel brain arrays for 3 T pediatric imaging. Magn. Reson. Med. 66, 1777–1787. https://doi.org/10.1002/mrm.22961

King, G., Truzzi, A., Cusack, R., 2023. The confound of head position in within-session connectome fingerprinting in infants. NeuroImage 265, 119808. https://doi.org/10.1016/j.neuroimage.2022.119808

King, R., Low, S., Gee, N., Wood, R., Hadweh, B., Houghton, J., Leijser, L.M., 2023. Practical Stepwise Approach to Performing Neonatal Brain MR Imaging in the Research Setting. Child. Basel Switz. 10, 1759. https://doi.org/10.3390/children10111759

Kinney, H.C., Volpe, J.J., 2018. Chapter 14 - Encephalopathy of Prematurity: Neuropathology, in: Volpe, J.J., Inder, T.E., Darras, B.T., de Vries, L.S., du Plessis, A.J., Neil, J.J., Perlman, J.M. (Eds.), Volpe's Neurology of the Newborn (Sixth Edition). Elsevier, pp. 389–404. https://doi.org/10.1016/B978-0-323-42876-7.00014-4

Kiviniemi, V., Kantola, J.-H., Jauhiainen, J., Hyvärinen, A., Tervonen, O., 2003. Independent component analysis of nondeterministic fMRI signal sources. NeuroImage 19, 253–260. https://doi.org/10.1016/s1053-8119(03)00097-1

Kline, J.E., Illapani, V.S.P., He, L., Altaye, M., Logan, J.W., Parikh, N.A., 2019. Early cortical maturation predicts neurodevelopment in very preterm infants. Arch. Dis. Child. - Fetal Neonatal Ed. fetalneonatal-2. https://doi.org/10.1136/archdischild-2019-317466

Koch, W., Teipel, S., Mueller, S., Benninghoff, J., Wagner, M., Bokde, A.L.W., Hampel, H., Coates, U., Reiser, M., Meindl, T., 2012. Diagnostic power of default mode network resting state fMRI in the detection of Alzheimer's disease. Neurobiol. Aging 33, 466–478. https://doi.org/10.1016/j.neurobiolaging.2010.04.013

Konkle, T., Caramazza, A., 2013. Tripartite Organization of the Ventral Stream by Animacy and Object Size. J. Neurosci. 33, 10235–10242. https://doi.org/10.1523/JNEUROSCI.0983-13.2013

Koolen, N., Dereymaeker, A., Räsänen, O., Jansen, K., Vervisch, J., Matic, V., Naulaers, G., De Vos, M., Van Huffel, S., Vanhatalo, S., 2016. Early development of synchrony in cortical activations in the human. Neuroscience 322, 298–307. https://doi.org/10.1016/j.neuroscience.2016.02.017

Korom, M., Camacho, M.C., Filippi, C.A., Licandro, R., Moore, L.A., Dufford, A., Zöllei, L., Graham, A.M., Spann, M., Howell, B., Shultz, S., Scheinost, D., 2022. Dear reviewers: Responses to common reviewer critiques about infant neuroimaging studies. Dev. Cogn. Neurosci. 53, 101055. https://doi.org/10.1016/j.dcn.2021.101055

Kosakowski, H., Cohen, M., Takahashi, A., Keil, B., Kanwisher, N., Saxe, R., 2021. Selective Responses to Faces, Scenes, and Bodies in the Ventral Visual Pathway of Infants. https://doi.org/10.31234/osf.io/7hqcu

Kosakowski, H.L., Cohen, M.A., Takahashi, A., Keil, B., Kanwisher, N., Saxe, R., 2022. Selective responses to faces, scenes, and bodies in the ventral visual pathway of infants. Curr. Biol. 32, 265-274.e5. https://doi.org/10.1016/j.cub.2021.10.064

Kostović, I., Jovanov-Milosević, N., 2006. The development of cerebral connections during the first 20-45 weeks' gestation. Semin. Fetal. Neonatal Med. 11, 415–422. https://doi.org/10.1016/j.siny.2006.07.001

Kozberg, M., Hillman, E., 2016. Chapter 10 - Neurovascular coupling and energy metabolism in the developing brain, in: Masamoto, K., Hirase, H., Yamada, K. (Eds.), Progress in Brain Research, New Horizons in Neurovascular Coupling: A Bridge Between Brain Circulation and Neural Plasticity. Elsevier, pp. 213–242. https://doi.org/10.1016/bs.pbr.2016.02.002

Kravitz, D.J., Peng, C.S., Baker, C.I., 2011. Real-World Scene Representations in High-Level Visual Cortex: It's the Spaces More Than the Places. J. Neurosci. 31, 7322–7333. https://doi.org/10.1523/JNEUROSCI.4588-10.2011

Kriegeskorte, N., Mur, M., Ruff, D.A., Kiani, R., Bodurka, J., Esteky, H., Tanaka, K., Bandettini, P.A., 2008. Matching categorical object representations in inferior temporal cortex of man and monkey. Neuron 60, 1126–1141. https://doi.org/10.1016/j.neuron.2008.10.043

Krishna, S., Fuloria, M., 2022. Ethical Considerations in Neonatal Research. NeoReviews 23, e151–e158. https://doi.org/10.1542/neo.23-3-e151

Kwong, K.K., Belliveau, J.W., Chesler, D.A., Goldberg, I.E., Weisskoff, R.M., Poncelet, B.P., Kennedy, D.N., Hoppel, B.E., Cohen, M.S., Turner, R., 1992. Dynamic magnetic resonance imaging of human brain activity during primary sensory stimulation. Proc. Natl. Acad. Sci. 89, 5675–5679. https://doi.org/10.1073/pnas.89.12.5675

Lake, E.M.R., Finn, E.S., Noble, S.M., Vanderwal, T., Shen, X., Rosenberg, M.D., Spann, M.N., Chun, M.M., Scheinost, D., Constable, R.T., 2019. The Functional Brain Organization of an Individual Allows Prediction of Measures of Social Abilities Transdiagnostically in Autism and Attention-Deficit/Hyperactivity Disorder. Biol. Psychiatry 86, 315–326. https://doi.org/10.1016/j.biopsych.2019.02.019

Lee, C.W., Blanco, B., Dempsey, L., Chalia, M., Hebden, J.C., Caballero-Gaudes, C., Austin, T., Cooper, R.J., 2020. Sleep State Modulates Resting-State Functional Connectivity in Neonates. Front. Neurosci. 14, 347. https://doi.org/10.3389/fnins.2020.00347

Leitao, S., Corcoran, P., Twomey, A., Murphy, B., Greene, R., 2020. Very Low Birth Weight Infants in the Republic of Ireland Annual Report 2018. National Perinatal Epidemiology Centre, Cork.

Levitt, P., 2003. Structural and functional maturation of the developing primate brain. J. Pediatr. 143, S35-45. https://doi.org/10.1067/s0022-3476(03)00400-1

Li, X., Morgan, P.S., Ashburner, J., Smith, J., Rorden, C., 2016. The first step for neuroimaging data analysis: DICOM to NIfTI conversion. J. Neurosci. Methods 264, 47–56. https://doi.org/10.1016/j.jneumeth.2016.03.001
Lin, W., Zhu, Q., Gao, W., Chen, Y., Toh, C.-H., Styner, M., Gerig, G., Smith, J.K., Biswal, B., Gilmore, J.H., 2008. Functional Connectivity MR Imaging Reveals Cortical Functional Connectivity in the Developing Brain. AJNR Am. J. Neuroradiol. 29, 1883–1889. https://doi.org/10.3174/ajnr.A1256
Linke, A.C., Cusack, R., 2015. Flexible Information Coding in Human Auditory Cortex during Perception, Imagery, and STM of Complex Sounds. J. Cogn. Neurosci. 27, 1322–1333. https://doi.org/10.1162/jocn_a_00780
Linke, A.C., Wild, C., Zubiaurre-Elorza, L., Herzmann, C., Duffy, H., Han, V.K., Lee, D.S.C., Cusack, R., 2018. Disruption to functional networks in neonates with perinatal brain injury predicts motor skills at 8 months. NeuroImage Clin. 18, 399–406. https://doi.org/10.1016/j.nicl.2018.02.002
Liu, H., Fan, G., Xu, K., Wang, F., 2011. Changes in cerebellar functional connectivity and anatomical connectivity in schizophrenia: A combined resting-state functional MRI and diffusion tensor imaging study. J. Magn. Reson. Imaging 34, 1430–1438. https://doi.org/10.1002/jmri.22784
Logothetis, N.K., Pauls, J., Augath, M., Trinath, T., Oeltermann, A., 2001. Neurophysiological investigation of the basis of the fMRI signal. Nature 412, 150–157. https://doi.org/10.1038/35084005
Lowe, M.J., Mock, B.J., Sorenson, J.A., 1998. Functional connectivity in single and multislice echoplanar imaging using resting-state fluctuations. NeuroImage 7, 119–132. https://doi.org/10.1006/nimg.1997.0315
Lui, K., Lee, S.K., Kusuda, S., Adams, M., Vento, M., Reichman, B., Darlow, B.A., Lehtonen, L., Modi, N., Norman, M., Håkansson, S., Bassler, D., Rusconi, F., Lodha, A., Yang, J., Shah, P.S., International Network for Evaluation of Outcomes (iNeo) of neonates Investigators, 2019. Trends in Outcomes for Neonates Born Very Preterm and Very Low Birth Weight in 11 High-Income Countries. J. Pediatr. 215, 32-40.e14. https://doi.org/10.1016/j.jpeds.2019.08.020
Lynch, L.K., Lu, K.-H., Wen, H., Zhang, Y., Saykin, A.J., Liu, Z., 2018. Task-evoked functional connectivity does not explain functional connectivity differences between rest and task conditions. Hum. Brain Mapp. 39, 4939–4948. https://doi.org/10.1002/hbm.24335
Mahadevan, A.S., Tooley, U.A., Bertolero, M.A., Mackey, A.P., Bassett, D.S., 2021. Evaluating the sensitivity of functional connectivity measures to motion artifact in resting-state fMRI data. NeuroImage 241, 118408. https://doi.org/10.1016/j.neuroimage.2021.118408
Makropoulos, A., Robinson, E.C., Schuh, A., Wright, R., Fitzgibbon, S., Bozek, J., Counsell, S.J., Steinweg, J., Vecchiato, K., Passerat-Palmbach, J., Lenz, G., Mortari, F., Tenev, T., Duff, E.P., Bastiani, M., Cordero-Grande, L., Hughes, E., Tusor, N., Tournier, J.-D., Hutter, J., Price, A.N., Teixeira, R.P.A.G., Murgasova, M., Victor, S., Kelly, C., Rutherford, M.A., Smith, S.M., Edwards, A.D., Hajnal, J.V., Jenkinson, M., Rueckert, D., 2018. The developing human connectome project: A minimal processing pipeline for neonatal cortical surface reconstruction. NeuroImage 173, 88–112. https://doi.org/10.1016/j.neuroimage.2018.01.054
McJury, M.J., 2022. Acoustic Noise and Magnetic Resonance Imaging: A Narrative/Descriptive Review. J. Magn. Reson. Imaging 55, 337–346. https://doi.org/10.1002/jmri.27525
Mechelli, A., Vieira, S., 2019. Machine Learning: Methods and Applications to Brain Disorders. Academic Press.

Meier, T.B., Desphande, A.S., Vergun, S., Nair, V.A., Song, J., Biswal, B.B., Meyerand, M.E., Birn, R.M., Prabhakaran, V., 2012. Support vector machine classification and characterization of age-related reorganization of functional brain networks. NeuroImage 60, 601–613. https://doi.org/10.1016/j.neuroimage.2011.12.052

Michalec, D., 2011. Bayley Scales of Infant Development: Third Edition, in: Goldstein, S., Naglieri, J.A. (Eds.), Encyclopedia of Child Behavior and Development. Springer US, Boston, MA, pp. 215–215. https://doi.org/10.1007/978-0-387-79061-9_295

Miller, D.J., Duka, T., Stimpson, C.D., Schapiro, S.J., Baze, W.B., McArthur, M.J., Fobbs, A.J., Sousa, A.M.M., Sestan, N., Wildman, D.E., Lipovich, L., Kuzawa, C.W., Hof, P.R., Sherwood, C.C., 2012. Prolonged myelination in human neocortical evolution. Proc. Natl. Acad. Sci. U. S. A. 109, 16480–16485. https://doi.org/10.1073/pnas.1117943109

Miranda-Dominguez, O., Feczko, E., Grayson, D.S., Walum, H., Nigg, J.T., Fair, D.A., 2018. Heritability of the human connectome: A connectotyping study. Netw. Neurosci. Camb. Mass 2, 175–199. https://doi.org/10.1162/netn_a_00029

Miranda-Dominguez, O., Mills, B.D., Carpenter, S.D., Grant, K.A., Kroenke, C.D., Nigg, J.T., Fair, D.A., 2014. Connectotyping: model based fingerprinting of the functional connectome. PloS One 9, e111048. https://doi.org/10.1371/journal.pone.0111048

Mitra, A., Snyder, A.Z., Tagliazucchi, E., Laufs, H., Elison, J., Emerson, R.W., Shen, M.D., Wolff, J.J., Botteron, K.N., Dager, S., Estes, A.M., Evans, A., Gerig, G., Hazlett, H.C., Paterson, S.J., Schultz, R.T., Styner, M.A., Zwaigenbaum, L., Schlaggar, B.L., Piven, J., Pruett, J.R., Raichle, M., 2017. Resting-state fMRI in sleeping infants more closely resembles adult sleep than adult wakefulness. PLoS ONE 12, e0188122. https://doi.org/10.1371/journal.pone.0188122

Moraczewski, D., Chen, G., Redcay, E., 2018. Inter-subject synchrony as an index of functional specialization in early childhood. Sci. Rep. 8, 2252. https://doi.org/10.1038/s41598-018-20600-0

Morgan, S.E., Achard, S., Termenon, M., Bullmore, E.T., Vértes, P.E., 2018a. Low-dimensional morphospace of topological motifs in human fMRI brain networks. Netw. Neurosci. Camb. Mass 2, 285–302. https://doi.org/10.1162/netn_a_00038

Morgan, S.E., White, S.R., Bullmore, E.T., Vértes, P.E., 2018b. A Network Neuroscience Approach to Typical and Atypical Brain Development. Biol. Psychiatry Cogn. Neurosci. Neuroimaging 3, 754–766. https://doi.org/10.1016/j.bpsc.2018.03.003

Mulder, H., Pitchford, N.J., Hagger, M.S., Marlow, N., 2009. Development of Executive Function and Attention in Preterm Children: A Systematic Review. Dev. Neuropsychol. 34, 393–421. https://doi.org/10.1080/87565640902964524

Murphy, C., Jefferies, E., Rueschemeyer, S.-A., Sormaz, M., Wang, H., Margulies, D.S., Smallwood, J., 2018. Distant from input: Evidence of regions within the default mode network supporting perceptually-decoupled and conceptually-guided cognition. Neuroimage 171, 393. https://doi.org/10.1016/j.neuroimage.2018.01.017

Murphy, K., Birn, R.M., Handwerker, D.A., Jones, T.B., Bandettini, P.A., 2009. The impact of global signal regression on resting state correlations: Are anti-correlated networks introduced? NeuroImage 44, 893–905. https://doi.org/10.1016/j.neuroimage.2008.09.036

Murphy, K., Fox, M.D., 2017. Towards a consensus regarding global signal regression for resting state functional connectivity MRI. NeuroImage 154, 169–173. https://doi.org/10.1016/j.neuroimage.2016.11.052
Myers, M.J., Labonte, A.K., Gordon, E.M., Laumann, T.O., Tu, J.C., Wheelock, M.D., Nielsen, A.N., Schwarzlose, R.F., Camacho, M.C., Alexopoulos, D., Warner, B.B., Raghuraman, N., Luby, J.L., Barch, D.M., Fair, D.A., Petersen, S.E., Rogers, C.E., Smyser, C.D., Sylvester, C.M., 2024. Functional parcellation of the neonatal cortical surface. Cereb. Cortex 34, bhae047. https://doi.org/10.1093/cercor/bhae047
Naci, L., Haugg, A., MacDonald, A., Anello, M., Houldin, E., Naqshbandi, S., Gonzalez-Lara, L.E., Arango, M., Harle, C., Cusack, R., Owen, A.M., 2018. Functional diversity of brain networks supports consciousness and verbal intelligence. Sci. Rep. 8, 13259. https://doi.org/10.1038/s41598-018-31525-z
Nastase, S.A., Gazzola, V., Hasson, U., Keysers, C., 2019. Measuring shared responses across subjects using intersubject correlation. Soc. Cogn. Affect. Neurosci. 14, 667–685. https://doi.org/10.1093/scan/nsz037
Nielsen, A.N., Greene, D.J., Gratton, C., Dosenbach, N.U.F., Petersen, S.E., Schlaggar, B.L., 2019. Evaluating the Prediction of Brain Maturity From Functional Connectivity After Motion Artifact Denoising. Cereb. Cortex N. Y. N 1991 29, 2455–2469. https://doi.org/10.1093/cercor/bhy117
Nielsen, A.N., Kaplan, S., Meyer, D., Alexopoulos, D., Kenley, J.K., Smyser, T.A., Wakschlag, L.S., Norton, E.S., Raghuraman, N., Warner, B.B., Shimony, J.S., Luby, J.L., Neil, J.J., Petersen, S.E., Barch, D.M., Rogers, C.E., Sylvester, C.M., Smyser, C.D., 2023. Maturation of large-scale brain systems over the first month of life. Cereb. Cortex 33, 2788–2803. https://doi.org/10.1093/cercor/bhac242
Nielsen, J.A., Zielinski, B.A., Fletcher, P.T., Alexander, A.L., Lange, N., Bigler, E.D., Lainhart, J.E., Anderson, J.S., 2013. Multisite functional connectivity MRI classification of autism: ABIDE results. Front. Hum. Neurosci. 7, 599. https://doi.org/10.3389/fnhum.2013.00599
Nijmegen: Max Planck Institute for Psycholinguistics, 2022. ELAN (Version 6.4).
Noble, S., Scheinost, D., Constable, R.T., 2019. A decade of test-retest reliability of functional connectivity: A systematic review and meta-analysis. NeuroImage 203, 116157. https://doi.org/10.1016/j.neuroimage.2019.116157
Oishi, K., Chang, L., Huang, H., 2019. Baby brain atlases. NeuroImage 185, 865–880. https://doi.org/10.1016/j.neuroimage.2018.04.003
O'Reilly, H., Johnson, S., Ni, Y., Wolke, D., Marlow, N., 2020. Neuropsychological Outcomes at 19 Years of Age Following Extremely Preterm Birth. Pediatrics 145. https://doi.org/10.1542/peds.2019-2087
Ou, X., Glasier, C.M., Ramakrishnaiah, R.H., Mulkey, S.B., Ding, Z., Angtuaco, T.L., Andres, A., Kaiser, J.R., 2014. Impaired White Matter Development in Extremely Low-Birth-Weight Infants with Previous Brain Hemorrhage. Am. J. Neuroradiol. 35, 1983–1989. https://doi.org/10.3174/ajnr.A3988
Ousdal, O.T., Kaufmann, T., Kolskår, K., Vik, A., Wehling, E., Lundervold, A.J., Lundervold, A., Westlye, L.T., 2020. Longitudinal stability of the brain functional connectome is associated with episodic memory performance in aging. Hum. Brain Mapp. 41, 697–709. https://doi.org/10.1002/hbm.24833
Parikh, N.A., He, L., Priyanka Illapani, V.S., Altaye, M., Folger, A.T., Yeates, K.O., 2020. Objectively Diagnosed Diffuse White Matter Abnormality at Term Is an Independent Predictor of Cognitive and Language Outcomes

in Infants Born Very Preterm. J. Pediatr. 220, 56–63. https://doi.org/10.1016/j.jpeds.2020.01.034
Pascal, A., Govaert, P., Oostra, A., Naulaers, G., Ortibus, E., Van den Broeck, C., 2018. Neurodevelopmental outcome in very preterm and very-low-birthweight infants born over the past decade: a meta-analytic review. Dev. Med. Child Neurol. 60, 342–355. https://doi.org/10.1111/dmcn.13675
Pauling, L., Coryell, C.D., 1936. The Magnetic Properties and Structure of Hemoglobin, Oxyhemoglobin and Carbonmonoxyhemoglobin. Proc. Natl. Acad. Sci. U. S. A. 22, 210. https://doi.org/10.1073/pnas.22.4.210
Pavel, A.M., O'Toole, J.M., Proietti, J., Livingstone, V., Mitra, S., Marnane, W.P., Finder, M., Dempsey, E.M., Murray, D.M., Boylan, G.B., 2023. Machine learning for the early prediction of infants with electrographic seizures in neonatal hypoxic-ischemic encephalopathy. Epilepsia 64, 456–468. https://doi.org/10.1111/epi.17468
Pavel, A.M., Rennie, J.M., Vries, L.S. de, Blennow, M., Foran, A., Shah, D.K., Pressler, R.M., Kapellou, O., Dempsey, E.M., Mathieson, S.R., Pavlidis, E., Huffelen, A.C. van, Livingstone, V., Toet, M.C., Weeke, L.C., Finder, M., Mitra, S., Murray, D.M., Marnane, W.P., Boylan, G.B., 2020. A machine-learning algorithm for neonatal seizure recognition: a multicentre, randomised, controlled trial. Lancet Child Adolesc. Health 4, 740–749. https://doi.org/10.1016/S2352-4642(20)30239-X
Pedregosa, F., Varoquaux, G., Gramfort, A., Michel, V., Thirion, B., Grisel, O., Blondel, M., Prettenhofer, P., Weiss, R., Dubourg, V., Vanderplas, J., Passos, A., Cournapeau, D., Brucher, M., Perrot, M., Duchesnay, É., 2011. Scikit-learn: Machine Learning in Python. J. Mach. Learn. Res. 12, 2825–2830.
Peirce, J., Gray, J.R., Simpson, S., MacAskill, M., Höchenberger, R., Sogo, H., Kastman, E., Lindeløv, J.K., 2019. PsychoPy2: Experiments in behavior made easy. Behav. Res. Methods 51, 195–203. https://doi.org/10.3758/s13428-018-01193-y
Perani, D., Saccuman, M.C., Scifo, P., Anwander, A., Spada, D., Baldoli, C., Poloniato, A., Lohmann, G., Friederici, A.D., 2011. Neural language networks at birth. Proc. Natl. Acad. Sci. 108, 16056–16061. https://doi.org/10.1073/pnas.1102991108
Pereira, F., Mitchell, T., Botvinick, M., 2009. Machine learning classifiers and fMRI: a tutorial overview. NeuroImage 45, S199-209. https://doi.org/10.1016/j.neuroimage.2008.11.007
Peyton, C., Einspieler, C., Fjørtoft, T., Adde, L., Schreiber, M.D., Drobyshevsky, A., Marks, J.D., 2020. Correlates of Normal and Abnormal General Movements in Infancy and Long-Term Neurodevelopment of Preterm Infants: Insights from Functional Connectivity Studies at Term Equivalence. J. Clin. Med. 9, 834. https://doi.org/10.3390/jcm9030834
Pollatou, A., Filippi, C.A., Aydin, E., Vaughn, K., Thompson, D., Korom, M., Dufford, A.J., Howell, B., Zöllei, L., Martino, A.D., Graham, A., Scheinost, D., Spann, M.N., 2022. An ode to fetal, infant, and toddler neuroimaging: Chronicling early clinical to research applications with MRI, and an introduction to an academic society connecting the field. Dev. Cogn. Neurosci. 54, 101083. https://doi.org/10.1016/j.dcn.2022.101083
Power, J.D., Barnes, K.A., Snyder, A.Z., Schlaggar, B.L., Petersen, S.E., 2012. Spurious but systematic correlations in functional connectivity MRI networks arise from subject motion. Neuroimage 59, 2142–2154. https://doi.org/10.1016/j.neuroimage.2011.10.018

Pruett, J.R., Kandala, S., Hoertel, S., Snyder, A.Z., Elison, J.T., Nishino, T., Feczko, E., Dosenbach, N.U.F., Nardos, B., Power, J.D., Adeyemo, B., Botteron, K.N., McKinstry, R.C., Evans, A.C., Hazlett, H.C., Dager, S.R., Paterson, S., Schultz, R.T., Collins, D.L., Fonov, V.S., Styner, M., Gerig, G., Das, S., Kostopoulos, P., Constantino, J.N., Estes, A.M., IBIS Network, Petersen, S.E., Schlaggar, B.L., Piven, J., 2015. Accurate age classification of 6 and 12 month-old infants based on resting-state functional connectivity magnetic resonance imaging data. Dev. Cogn. Neurosci. 12, 123–133. https://doi.org/10.1016/j.dcn.2015.01.003

Raichle, M.E., MacLeod, A.M., Snyder, A.Z., Powers, W.J., Gusnard, D.A., Shulman, G.L., 2001. A default mode of brain function. Proc. Natl. Acad. Sci. U. S. A. 98, 676–682. https://doi.org/10.1073/pnas.98.2.676

Ramgopal, S., Horvat, C.M., Yanamala, N., Alpern, E.R., 2020. Machine Learning To Predict Serious Bacterial Infections in Young Febrile Infants. Pediatrics 146, e20194096. https://doi.org/10.1542/peds.2019-4096

Raschle, N., Zuk, J., Ortiz-Mantilla, S., Sliva, D.D., Franceschi, A., Grant, P.E., Benasich, A.A., Gaab, N., 2012. Pediatric neuroimaging in early childhood and infancy: challenges and practical guidelines. Ann. N. Y. Acad. Sci. 1252, 43–50. https://doi.org/10.1111/j.1749-6632.2012.06457.x

Richardson, H., Lisandrelli, G., Riobueno-Naylor, A., Saxe, R., 2018. Development of the social brain from age three to twelve years. Nat. Commun. 9, 1027. https://doi.org/10.1038/s41467-018-03399-2

Rios, N.L., Foias, A., Lodygensky, G., Dehaes, M., Cohen-Adad, J., 2018. Size-adaptable 13-channel receive array for brain MRI in human neonates at 3 T. NMR Biomed. 31, e3944. https://doi.org/10.1002/nbm.3944

Rogers, C.E., Lean, R.E., Wheelock, M.D., Smyser, C.D., 2018. Aberrant structural and functional connectivity and neurodevelopmental impairment in preterm children. J. Neurodev. Disord. 10, 38. https://doi.org/10.1186/s11689-018-9253-x

Rosenberg, M.D., Finn, E.S., Scheinost, D., Papademetris, X., Shen, X., Constable, R.T., Chun, M.M., 2016. A neuromarker of sustained attention from whole-brain functional connectivity. Nat. Neurosci. 19, 165–171. https://doi.org/10.1038/nn.4179

Sabuncu, M.R., Singer, B.D., Conroy, B., Bryan, R.E., Ramadge, P.J., Haxby, J.V., 2010. Function-based intersubject alignment of human cortical anatomy. Cereb. Cortex N. Y. N 1991 20, 130–140. https://doi.org/10.1093/cercor/bhp085

Saha, S., Pagnozzi, A., Bourgeat, P., George, J.M., Bradford, D., Colditz, P.B., Boyd, R.N., Rose, S.E., Fripp, J., Pannek, K., 2020. Predicting motor outcome in preterm infants from very early brain diffusion MRI using a deep learning convolutional neural network (CNN) model. NeuroImage 215, 116807. https://doi.org/10.1016/j.neuroimage.2020.116807

Salimi-Khorshidi, G., Douaud, G., Beckmann, C.F., Glasser, M.F., Griffanti, L., Smith, S.M., 2014. Automatic denoising of functional MRI data: Combining independent component analysis and hierarchical fusion of classifiers. NeuroImage 90, 449–468. https://doi.org/10.1016/j.neuroimage.2013.11.046

Sanchez-Alonso, S., Rosenberg, M.D., Aslin, R.N., 2021. Functional connectivity patterns predict naturalistic viewing versus rest across development. NeuroImage 229, 117630. https://doi.org/10.1016/j.neuroimage.2020.117630

Satterthwaite, T.D., Wolf, D.H., Loughead, J., Ruparel, K., Elliott, M.A., Hakonarson, H., Gur, R.C., Gur, R.E., 2012. Impact of in-scanner head motion on multiple measures of functional connectivity: Relevance for

studies of neurodevelopment in youth. NeuroImage 60, 623–632. https://doi.org/10.1016/j.neuroimage.2011.12.063
Schaefer, A., Kong, R., Gordon, E.M., Laumann, T.O., Zuo, X.-N., Holmes, A.J., Eickhoff, S.B., Yeo, B.T.T., 2018. Local-Global Parcellation of the Human Cerebral Cortex from Intrinsic Functional Connectivity MRI. Cereb. Cortex 28, 3095–3114. https://doi.org/10.1093/cercor/bhx179
Scheef, L., Nordmeyer-Massner, J.A., Smith-Collins, A.P., Müller, N., Stegmann-Woessner, G., Jankowski, J., Gieseke, J., Born, M., Seitz, H., Bartmann, P., Schild, H.H., Pruessmann, K.P., Heep, A., Boecker, H., 2017. Functional Laterality of Task-Evoked Activation in Sensorimotor Cortex of Preterm Infants: An Optimized 3 T fMRI Study Employing a Customized Neonatal Head Coil. PLoS ONE 12, e0169392. https://doi.org/10.1371/journal.pone.0169392
Scheinost, D., Pollatou, A., Dufford, A.J., Jiang, R., Farruggia, M.C., Rosenblatt, M., Peterson, H., Rodriguez, R.X., Dadashkarimi, J., Liang, Q., Dai, W., Foster, M.L., Camp, C.C., Tejavibulya, L., Adkinson, B.D., Sun, H., Ye, J., Cheng, Q., Spann, M.N., Rolison, M., Noble, S., Westwater, M.L., 2022. Machine learning and prediction in fetal, infant, and toddler neuroimaging: a review and primer. Biol. Psychiatry 0. https://doi.org/10.1016/j.biopsych.2022.10.014
Schlapbach, L.J., Aebischer, M., Adams, M., Natalucci, G., Bonhoeffer, J., Latzin, P., Nelle, M., Bucher, H.U., Latal, B., Swiss Neonatal Network and Follow-Up Group, 2011. Impact of sepsis on neurodevelopmental outcome in a Swiss National Cohort of extremely premature infants. Pediatrics 128, e348-357. https://doi.org/10.1542/peds.2010-3338
Schuh, A., Makropoulos, A., Robinson, E.C., Cordero-Grande, L., Hughes, E., Hutter, J., Price, A.N., Murgasova, M., Teixeira, R.P.A.G., Tusor, N., Steinweg, J.K., Victor, S., Rutherford, M.A., Hajnal, J.V., Edwards, A.D., Rueckert, D., 2018. Unbiased construction of a temporally consistent morphological atlas of neonatal brain development. bioRxiv 251512. https://doi.org/10.1101/251512
Schultz, J., Pilz, K.S., 2009. Natural facial motion enhances cortical responses to faces. Exp. Brain Res. 194, 465–475. https://doi.org/10.1007/s00221-009-1721-9
SciPy v1.14.0 Manual, n.d. scipy.stats.bootstrap [WWW Document]. URL https://docs.scipy.org/doc/scipy/reference/generated/scipy.stats.bootstrap.html (accessed 7.20.24).
Shah, L.M., Cramer, J.A., Ferguson, M.A., Birn, R.M., Anderson, J.S., 2016. Reliability and reproducibility of individual differences in functional connectivity acquired during task and resting state. Brain Behav. 6. https://doi.org/10.1002/brb3.456
Shah, N., Arshad, A., Mazer, M.B., Carroll, C.L., Shein, S.L., Remy, K.E., 2023. The use of machine learning and artificial intelligence within pediatric critical care. Pediatr. Res. 93, 405–412. https://doi.org/10.1038/s41390-022-02380-6
Sifre, R., Olson, L., Gillespie, S., Klin, A., Jones, W., Shultz, S., 2018. A Longitudinal Investigation of Preferential Attention to Biological Motion in 2- to 24-Month-Old Infants. Sci. Rep. 8. https://doi.org/10.1038/s41598-018-20808-0
Simony, E., Honey, C.J., Chen, J., Lositsky, O., Yeshurun, Y., Wiesel, A., Hasson, U., 2016. Dynamic reconfiguration of the default mode network during narrative comprehension. Nat. Commun. 7, 12141. https://doi.org/10.1038/ncomms12141

Slipsager, J.M., Ellegaard, A.H., Glimberg, S.L., Paulsen, R.R., Tisdall, M.D., Wighton, P., van der Kouwe, A., Marner, L., Henriksen, O.M., Law, I., Olesen, O.V., 2019. Markerless motion tracking and correction for PET, MRI, and simultaneous PET/MRI. PloS One 14, e0215524. https://doi.org/10.1371/journal.pone.0215524

Smith, G.C., Gutovich, J., Smyser, C., Pineda, R., Newnham, C., Tjoeng, T.H., Vavasseur, C., Wallendorf, M., Neil, J., Inder, T., 2011. Neonatal intensive care unit stress is associated with brain development in preterm infants. Ann. Neurol. 70, 541–549. https://doi.org/10.1002/ana.22545

Smith, S.M., Fox, P.T., Miller, K.L., Glahn, D.C., Fox, P.M., Mackay, C.E., Filippini, N., Watkins, K.E., Toro, R., Laird, A.R., Beckmann, C.F., 2009. Correspondence of the brain's functional architecture during activation and rest. Proc. Natl. Acad. Sci. U. S. A. 106, 13040–13045. https://doi.org/10.1073/pnas.0905267106

Smith, S.M., Jenkinson, M., Woolrich, M.W., Beckmann, C.F., Behrens, T.E.J., Johansen-Berg, H., Bannister, P.R., De Luca, M., Drobnjak, I., Flitney, D.E., Niazy, R.K., Saunders, J., Vickers, J., Zhang, Y., De Stefano, N., Brady, J.M., Matthews, P.M., 2004. Advances in functional and structural MR image analysis and implementation as FSL. NeuroImage, Mathematics in Brain Imaging 23, S208–S219. https://doi.org/10.1016/j.neuroimage.2004.07.051

Smyser, C.D., Dosenbach, N.U.F., Smyser, T.A., Snyder, A.Z., Rogers, C.E., Inder, T.E., Schlaggar, B.L., Neil, J.J., 2016a. Prediction of brain maturity in infants using machine-learning algorithms. NeuroImage 136, 1–9. https://doi.org/10.1016/j.neuroimage.2016.05.029

Smyser, C.D., Inder, T.E., Shimony, J.S., Hill, J.E., Degnan, A.J., Snyder, A.Z., Neil, J.J., 2010. Longitudinal Analysis of Neural Network Development in Preterm Infants. Cereb. Cortex N. Y. NY 20, 2852–2862. https://doi.org/10.1093/cercor/bhq035

Smyser, C.D., Snyder, A.Z., Neil, J.J., 2011. Functional connectivity MRI in infants: Exploration of the functional organization of the developing brain. NeuroImage 56, 1437–1452. https://doi.org/10.1016/j.neuroimage.2011.02.073

Smyser, C.D., Snyder, A.Z., Shimony, J.S., Blazey, T.M., Inder, T.E., Neil, J.J., 2013. Effects of White Matter Injury on Resting State fMRI Measures in Prematurely Born Infants. PLOS ONE 8, e68098. https://doi.org/10.1371/journal.pone.0068098

Smyser, C.D., Snyder, A.Z., Shimony, J.S., Mitra, A., Inder, T.E., Neil, J.J., 2016b. Resting-State Network Complexity and Magnitude Are Reduced in Prematurely Born Infants. Cereb. Cortex N. Y. NY 26, 322–333. https://doi.org/10.1093/cercor/bhu251

Smyser, C.D., Wheelock, M.D., Limbrick, D.D., Neil, J.J., 2019. Neonatal brain injury and aberrant connectivity. NeuroImage 185, 609–623. https://doi.org/10.1016/j.neuroimage.2018.07.057

Smyser, T.A., Smyser, C.D., Rogers, C.E., Gillespie, S.K., Inder, T.E., Neil, J.J., 2016. Cortical Gray and Adjacent White Matter Demonstrate Synchronous Maturation in Very Preterm Infants. Cereb. Cortex N. Y. N 1991 26, 3370–3378. https://doi.org/10.1093/cercor/bhv164

Sokol, S., 1978. Measurement of infant visual acuity from pattern reversal evoked potentials. Vision Res. 18, 33–39. https://doi.org/10.1016/0042-6989(78)90074-3

Spann, M.N., Wisnowski, J.L., HBCD Phase I Scanning Young Populations Working Group, Smyser, C.D., Fetal, Infant, and Toddler Neuroimaging Group (FIT'NG), Howell, B., Dean, D.C., 2023. The Art, Science, and

Secrets of Scanning Young Children. Biol. Psychiatry 93, 858–860. https://doi.org/10.1016/j.biopsych.2022.09.025
Sparrow, S.S., Cicchetti, D.V., 1985. Diagnostic uses of the Vineland Adaptive Behavior Scales. J. Pediatr. Psychol. 10, 215–225. https://doi.org/10.1093/jpepsy/10.2.215
Spittle, A., Orton, J., Anderson, P., Boyd, R., Doyle, L.W., 2012. Early developmental intervention programmes post-hospital discharge to prevent motor and cognitive impairments in preterm infants. Cochrane Database Syst. Rev. https://doi.org/10.1002/14651858.CD005495.pub3
Spoormaker, V.I., Gleiser, P.M., Czisch, M., 2012. Frontoparietal Connectivity and Hierarchical Structure of the Brain's Functional Network during Sleep. Front. Neurol. 3, 80. https://doi.org/10.3389/fneur.2012.00080
Squires, J., Bricker, D., 2009. Ages & Stages Questionnaires® Third Edition - A parent-completed child-monitoring system. Paul H. Brookes Publishing Co., Baltimore.
Squires, J., Bricker, D., Twombly, E., 2012. Ages & Stages Questionnaires®: Social-Emotional. https://doi.org/10.1037/t11524-000
Sripada, C., Rutherford, S., Angstadt, M., Thompson, W.K., Luciana, M., Weigard, A., Hyde, L.H., Heitzeg, M., 2020. Prediction of neurocognition in youth from resting state fMRI. Mol. Psychiatry 25, 3413–3421. https://doi.org/10.1038/s41380-019-0481-6
Statsmodels, n.d. statsmodels.stats.multitest.fdrcorrection [WWW Document]. URL https://www.statsmodels.org/stable/generated/statsmodels.stats.multitest.fdrcorrection.html (accessed 7.20.24).
Sun, Y., Ma, J., Huang, M., Yi, Y., Wang, Y., Gu, Y., Lin, Y., Li, L.M.W., Dai, Z., 2022. Functional connectivity dynamics as a function of the fluctuation of tension during film watching. Brain Imaging Behav. 16, 1260–1274. https://doi.org/10.1007/s11682-021-00593-7
Sury, M.R.J., Harker, H., Begent, J., Chong, W.K., 2005. The management of infants and children for painless imaging. Clin. Radiol. 60, 731–741. https://doi.org/10.1016/j.crad.2005.02.014
Sylvester, C.M., Kaplan, S., Myers, M.J., Gordon, E.M., Schwarzlose, R.F., Alexopoulos, D., Nielsen, A.N., Kenley, J.K., Meyer, D., Yu, Q., Graham, A.M., Fair, D.A., Warner, B.B., Barch, D.M., Rogers, C.E., Luby, J.L., Petersen, S.E., Smyser, C.D., 2022. Network-specific selectivity of functional connections in the neonatal brain. Cereb. Cortex N. Y. N 1991 bhac202. https://doi.org/10.1093/cercor/bhac202
Sylvester, C.M., Myers, M.J., Perino, M.T., Kaplan, S., Kenley, J.K., Smyser, T.A., Warner, B.B., Barch, D.M., Pine, D.S., Luby, J.L., Rogers, C.E., Smyser, C.D., 2021. Neonatal Brain Response to Deviant Auditory Stimuli and Relation to Maternal Trait Anxiety. Am. J. Psychiatry 178, 771–778. https://doi.org/10.1176/appi.ajp.2020.20050672
Sylvester, C.M., Smyser, C.D., Smyser, T., Kenley, J., Ackerman, J.J., Shimony, J.S., Petersen, S.E., Rogers, C.E., 2018. Cortical Functional Connectivity Evident After Birth and Behavioral Inhibition at Age 2. Am. J. Psychiatry 175, 180–187. https://doi.org/10.1176/appi.ajp.2017.17010018
Tagliazucchi, E., von Wegner, F., Morzelewski, A., Borisov, S., Jahnke, K., Laufs, H., 2012. Automatic sleep staging using fMRI functional connectivity data. NeuroImage 63, 63–72. https://doi.org/10.1016/j.neuroimage.2012.06.036
Tau, G.Z., Peterson, B.S., 2010. Normal development of brain circuits. Neuropsychopharmacol. Off. Publ. Am. Coll. Neuropsychopharmacol. 35, 147–168. https://doi.org/10.1038/npp.2009.115

Temko, A., Thomas, E., Marnane, W., Lightbody, G., Boylan, G., 2011. EEG-based neonatal seizure detection with Support Vector Machines. Clin. Neurophysiol. 122, 464–473. https://doi.org/10.1016/j.clinph.2010.06.034

Thomas Yeo, B.T., Krienen, F.M., Sepulcre, J., Sabuncu, M.R., Lashkari, D., Hollinshead, M., Roffman, J.L., Smoller, J.W., Zöllei, L., Polimeni, J.R., Fischl, B., Liu, H., Buckner, R.L., 2011a. The organization of the human cerebral cortex estimated by intrinsic functional connectivity. J. Neurophysiol. 106, 1125–1165. https://doi.org/10.1152/jn.00338.2011

Thomas Yeo, B.T., Krienen, F.M., Sepulcre, J., Sabuncu, M.R., Lashkari, D., Hollinshead, M., Roffman, J.L., Smoller, J.W., Zöllei, L., Polimeni, J.R., Fischl, B., Liu, H., Buckner, R.L., 2011b. The organization of the human cerebral cortex estimated by intrinsic functional connectivity. J. Neurophysiol. 106, 1125–1165. https://doi.org/10.1152/jn.00338.2011

Thompson, D.K., Chen, J., Beare, R., Adamson, C.L., Ellis, R., Ahmadzai, Z.M., Kelly, C.E., Lee, K.J., Zalesky, A., Yang, J.Y.M., Hunt, R.W., Cheong, J.L.Y., Inder, T.E., Doyle, L.W., Seal, M.L., Anderson, P.J., 2016. Structural connectivity relates to perinatal factors and functional impairment at 7years in children born very preterm. NeuroImage 134, 328–337. https://doi.org/10.1016/j.neuroimage.2016.03.070

Tokariev, A., Roberts, J.A., Zalesky, A., Zhao, X., Vanhatalo, S., Breakspear, M., Cocchi, L., 2019. Large-scale brain modes reorganize between infant sleep states and carry prognostic information for preterms. Nat. Commun. 10, 2619. https://doi.org/10.1038/s41467-019-10467-8

Tokariev, A., Videman, M., Palva, J.M., Vanhatalo, S., 2016. Functional Brain Connectivity Develops Rapidly Around Term Age and Changes Between Vigilance States in the Human Newborn. Cereb. Cortex N. Y. N 1991 26, 4540–4550. https://doi.org/10.1093/cercor/bhv219

Toulmin, H.L., O'Muircheataigh, J., Counsell, S.J., Falconer, S., Chew, A., Beckmann, C.F., Edwards, A.D., 2020. Functional thalamocortical connectivity at term equivalent age and outcome at 2 years in infants born preterm. Cortex. https://doi.org/10.1016/j.cortex.2020.09.022

Tran, M., Cabral, L., Patel, R., Cusack, R., 2017. Online recruitment and testing of infants with Mechanical Turk. J. Exp. Child Psychol. 156, 168–178. https://doi.org/10.1016/j.jecp.2016.12.003

Turk, E., Heuvel, M.I. van den, Benders, M.J., Heus, R. de, Franx, A., Manning, J.H., Hect, J.L., Hernandez-Andrade, E., Hassan, S.S., Romero, R., Kahn, R.S., Thomason, M.E., Heuvel, M.P. van den, 2019. Functional Connectome of the Fetal Brain. J. Neurosci. 39, 9716–9724. https://doi.org/10.1523/JNEUROSCI.2891-18.2019

Twilhaar, E.S., de Kieviet, J.F., Aarnoudse-Moens, C.S., van Elburg, R.M., Oosterlaan, J., 2018. Academic performance of children born preterm: a meta-analysis and meta-regression. Arch. Dis. Child. Fetal Neonatal Ed. 103, F322–F330. https://doi.org/10.1136/archdischild-2017-312916

Uchitel, J., Vanhatalo, S., Austin, T., 2022. Early development of sleep and brain functional connectivity in term-born and preterm infants. Pediatr. Res. 91, 771–786. https://doi.org/10.1038/s41390-021-01497-4

Van Dijk, K.R.A., Sabuncu, M.R., Buckner, R.L., 2012. The Influence of Head Motion on Intrinsic Functional Connectivity MRI. NeuroImage 59, 431–438. https://doi.org/10.1016/j.neuroimage.2011.07.044

Van Steenwinckel, J., Schang, A.-L., Sigaut, S., Chhor, V., Degos, V., Hagberg, H., Baud, O., Fleiss, B., Gressens, P., 2014. Brain damage of the preterm infant: new insights into the role of inflammation. Biochem. Soc. Trans. 42, 557–563. https://doi.org/10.1042/BST20130284

Vanderwal, T., Eilbott, J., Castellanos, F.X., 2019. Movies in the magnet: Naturalistic paradigms in developmental functional neuroimaging. Dev. Cogn. Neurosci. 36, 100600. https://doi.org/10.1016/j.dcn.2018.10.004
Vanderwal, T., Eilbott, J., Finn, E.S., Craddock, R.C., Turnbull, A., Castellanos, F.X., 2017. Individual differences in functional connectivity during naturalistic viewing conditions. NeuroImage 157, 521–530. https://doi.org/10.1016/j.neuroimage.2017.06.027
Vanderwal, T., Kelly, C., Eilbott, J., Mayes, L.C., Castellanos, F.X., 2015. Inscapes : A movie paradigm to improve compliance in functional magnetic resonance imaging. NeuroImage 122, 222–232. https://doi.org/10.1016/j.neuroimage.2015.07.069
van't Hooft, J., van der Lee, J.H., Opmeer, B.C., Aarnoudse-Moens, C.S.H., Leenders, A.G.E., Mol, B.W.J., de Haan, T.R., 2015. Predicting developmental outcomes in premature infants by term equivalent MRI: systematic review and meta-analysis. Syst. Rev. 4. https://doi.org/10.1186/s13643-015-0058-7
Vaughn, K.A., Arichi, T., Aydin, E., Camacho, M.C., Dapretto, M., Ford, A., Graham, A., Gregg, C., Hendrix, C.L., Howell, B., Korom, M., Lajous, H., Licandro, R., Madsen, K.S., Manessis, A.G., McDowell, M.G., Miranda-Dominguez, O., Mooney, L.N., Moser, J., Nolvi, S., Payette, K., Pollatou, A., Scheinost, D., Schwarzlose, R.F., Short, S.J., Spann, M., Taha, H., Tuulari, J.J., Haren, N. (Neeltje) van, Weber, C.F., Zollei, L., 2022. An Opportunity to Increase Collaborative Science in Fetal, Infant, and Toddler Neuroimaging. Biol. Psychiatry 0. https://doi.org/10.1016/j.biopsych.2022.07.005
Vertes, P.E., Alexander-Bloch, A.F., Gogtay, N., Giedd, J.N., Rapoport, J.L., Bullmore, E.T., 2012. Simple models of human brain functional networks. Proc. Natl. Acad. Sci. U. S. A. 109, 5868–5873. https://doi.org/10.1073/pnas.1111738109
Vertes, P.E., Bullmore, E.T., 2015. Annual research review: Growth connectomics--the organization and reorganization of brain networks during normal and abnormal development. J. Child Psychol. Psychiatry 56, 299–320. https://doi.org/10.1111/jcpp.12365
Vincent, J.L., Patel, G.H., Fox, M.D., Snyder, A.Z., Baker, J.T., Van Essen, D.C., Zempel, J.M., Snyder, L.H., Corbetta, M., Raichle, M.E., 2007. Intrinsic functional architecture in the anaesthetized monkey brain. Nature 447, 83–86. https://doi.org/10.1038/nature05758
Volpe, J.J., 2009. Brain injury in premature infants: a complex amalgam of destructive and developmental disturbances. Lancet Neurol. 8, 110–124. https://doi.org/10.1016/S1474-4422(08)70294-1
Wang, F., Zhang, H., Wu, Z., Hu, D., Zhou, Z., Girault, J.B., Wang, L., Lin, W., Li, G., 2023. Fine-grained functional parcellation maps of the infant cerebral cortex. eLife 12, e75401. https://doi.org/10.7554/eLife.75401
Wang, J., Ren, Y., Hu, X., Nguyen, V.T., Guo, L., Han, J., Guo, C.C., 2017. Test-retest reliability of functional connectivity networks during naturalistic fMRI paradigms. Hum. Brain Mapp. 38, 2226–2241. https://doi.org/10.1002/hbm.23517
Wang, Q., Xu, Y., Zhao, T., Xu, Z., He, Y., Liao, X., 2021. Individual Uniqueness in the Neonatal Functional Connectome. Cereb. Cortex. https://doi.org/10.1093/cercor/bhab041
Wang, Y., Hinds, W., Duarte, C.S., Lee, S., Monk, C., Wall, M., Canino, G., Milani, A.C.C., Jackowski, A., Mamin, M.G., Foerster, B.U., Gingrich, J., Weissman, M.M., Peterson, B.S., Semanek, D., Perez, E.A., Labat, E., Torres, I.B., Da Silva, I., Parente, C., Abdala, N., Posner, J., 2021. Intra-

session test-retest reliability of functional connectivity in infants. NeuroImage 239, 118284. https://doi.org/10.1016/j.neuroimage.2021.118284
Wehrle, F.M., Michels, L., Guggenberger, R., Huber, R., Latal, B., O'Gorman, R.L., Hagmann, C.F., 2018. Altered resting-state functional connectivity in children and adolescents born very preterm short title. NeuroImage Clin. 20, 1148–1156. https://doi.org/10.1016/j.nicl.2018.10.002
White, T.P., Symington, I., Castellanos, N.P., Brittain, P.J., Froudist Walsh, S., Nam, K.-W., Sato, J.R., Allin, M.P.G., Shergill, S.S., Murray, R.M., Williams, S.C.R., Nosarti, C., 2014. Dysconnectivity of neurocognitive networks at rest in very-preterm born adults. NeuroImage Clin. 4, 352–365. https://doi.org/10.1016/j.nicl.2014.01.005
Wiggins, G.C., Triantafyllou, C., Potthast, A., Reykowski, A., Nittka, M., Wald, L.L., 2006. 32-channel 3 Tesla receive-only phased-array head coil with soccer-ball element geometry. Magn. Reson. Med. 56, 216–223. https://doi.org/10.1002/mrm.20925
Wild, C.J., Linke, A.C., Zubiaurre-Elorza, L., Herzmann, C., Duffy, H., Han, V.K., Lee, D.S.C., Cusack, R., 2017. Adult-like processing of naturalistic sounds in auditory cortex by 3- and 9-month old infants. NeuroImage 157, 623–634. https://doi.org/10.1016/j.neuroimage.2017.06.038
Williams, G., Fabrizi, L., Meek, J., Jackson, D., Tracey, I., Robertson, N., Slater, R., Fitzgerald, M., 2015. Functional magnetic resonance imaging can be used to explore tactile and nociceptive processing in the infant brain. Acta Paediatr. 104, 158–166. https://doi.org/10.1111/apa.12848
Wong, H.R., Atkinson, S.J., Cvijanovich, N.Z., Anas, N., Allen, G.L., Thomas, N.J., Bigham, M.T., Weiss, S.L., Fitzgerald, J.C., Checchia, P.A., Meyer, K., Quasney, M., Hall, M., Gedeit, R., Freishtat, R.J., Nowak, J., Raj, S.S., Gertz, S., Lindsell, C.J., 2016. Combining Prognostic and Predictive Enrichment Strategies to Identify Children With Septic Shock Responsive to Corticosteroids. Crit. Care Med. 44, e1000-1003. https://doi.org/10.1097/CCM.0000000000001833
Woodward, L.J., Anderson, P.J., Austin, N.C., Howard, K., Inder, T.E., 2006. Neonatal MRI to Predict Neurodevelopmental Outcomes in Preterm Infants. N. Engl. J. Med. 355, 685–694. https://doi.org/10.1056/NEJMoa053792
Woodward, L.J., Clark, C.A.C., Bora, S., Inder, T.E., 2012. Neonatal White Matter Abnormalities an Important Predictor of Neurocognitive Outcome for Very Preterm Children. PLoS ONE 7, e51879. https://doi.org/10.1371/journal.pone.0051879
World Health Organization, n.d. WHO - Preterm birth [WWW Document]. WHO Fact Sheets. URL https://www.who.int/news-room/fact-sheets/detail/preterm-birth (accessed 6.3.20).
Yamashita, M., Yoshihara, Y., Hashimoto, R., Yahata, N., Ichikawa, N., Sakai, Y., Yamada, T., Matsukawa, N., Okada, G., Tanaka, S.C., Kasai, K., Kato, N., Okamoto, Y., Seymour, B., Takahashi, H., Kawato, M., Imamizu, H., 2018. A prediction model of working memory across health and psychiatric disease using whole-brain functional connectivity. eLife 7, e38844. https://doi.org/10.7554/eLife.38844
Yates, Tristan S., Ellis, C.T., Turk-Browne, N.B., 2023. Face processing in the infant brain after pandemic lockdown. Dev. Psychobiol. 65, e22346. https://doi.org/10.1002/dev.22346
Yates, Tristan S, Ellis, C.T., Turk-Browne, N.B., 2023. Functional networks in the infant brain during sleep and wake states. Cereb. Cortex 33, 10820–10835. https://doi.org/10.1093/cercor/bhad327

Yates, T.S., Ellis, C.T., Turk-Browne, N.B., 2021. The promise of awake behaving infant fMRI as a deep measure of cognition. Curr. Opin. Behav. Sci. 40, 5–11. https://doi.org/10.1016/j.cobeha.2020.11.007

Yates, T.S., Skalaban, L.J., Ellis, C.T., Bracher, A.J., Baldassano, C., Turk-Browne, N.B., 2022. Neural event segmentation of continuous experience in human infants. Proc. Natl. Acad. Sci. 119, e2200257119. https://doi.org/10.1073/pnas.2200257119

Yeo, K.T., Thomas, R., Chow, S.S., Bolisetty, S., Haslam, R., Tarnow-Mordi, W., Lui, K., 2020. Improving incidence trends of severe intraventricular haemorrhages in preterm infants <32 weeks gestation: a cohort study. Arch. Dis. Child. - Fetal Neonatal Ed. 105, 145–150. https://doi.org/10.1136/archdischild-2018-316664

Zhai, H., Brady, P., Li, Q., Lingren, T., Ni, Y., Wheeler, D.S., Solti, I., 2014. Developing and evaluating a machine learning based algorithm to predict the need of pediatric intensive care unit transfer for newly hospitalized children. Resuscitation 85, 1065–1071. https://doi.org/10.1016/j.resuscitation.2014.04.009

Zhi, D., King, M., Diedrichsen, J., 2021. Evaluating brain parcellations using the distance controlled boundary coefficient. bioRxiv 2021.05.11.443151. https://doi.org/10.1101/2021.05.11.443151

Zhu, G., Jiang, B., Tong, L., Xie, Y., Zaharchuk, G., Wintermark, M., 2019. Applications of Deep Learning to Neuro-Imaging Techniques. Front. Neurol. 10. https://doi.org/10.3389/fneur.2019.00869

APPENDIX

APPENDIX SECTION – ETHICS APPROVAL DOCUMENTS

Coombe Women & Infants University Hospital
Excellence in the Care of Women and Babies
Ceirfeacht i gCúram Ban agus Naíonán
Cork Street
Dublin 8
telephone +353 1 408 5200
fax +353 1 453 6033
www.coombe.ie

Prof Rhodri Cusack
The Thomas Mitchell Professor of Cognitive Neuroscience
Trinity College Dublin
cusackrh@tcd.ie

8th May 2020

Re: Study No. 8 – 2019 – Using Neuroimaging to Measure Functional Brain Development in Infants from the Neonatal Intensive Care Unit and a Control Group

Dear Prof Cusack,
I have reviewed amended Application Form and Participant Information Leaflets (supplied by you on 2nd March 2020) in relation to your study entitled **'Using Neuroimaging to Measure Functional Brain Development in Infants from the Neonatal Intensive Care Unit and a Control Group'.** Your study is now approved by the Research Ethics Committee in the Coombe Women and Infants University Hospital.

Yours sincerely

Professor Jan Miletin (IMC 241348)
Consultant Neonatologist
Chairman of the Research Ethics Committee
Coombe Women and Infants University Hospital (jmiletin@coombe.ie)

cc. *Prof Eleanor Molloy (Eleanor.Molloy@tcd.ie), Professor and Chair of Paediatrics and Child Health TCD, Consultant Neonatologist and Paediatrician, AMNCH Trinity College Dublin;*
Prof Adrienne Foran (aforan@rotunda.ie), Consultant Neonatologist, Rotunda Hospital;

Dr Gabrielle Colleran (Gabrielle.Colleran@cuh.ie), Consultant Paediatric Radiologist, National Maternity Hospital;
Dr Lorijn Zaadnoordijk (lorijnzaadnoordijk@cusacklab.org), Postdoctoral researcher, Trinity College Dublin;
Dr Anna Truzzi (annatruzzi@cusacklab.org), Trinity College Dublin

Ospidéal an Rotunda
Cearnóg Parnell, Baile Átha Cliath 1, Éire.
The Rotunda Hospital
Parnell Square, Dublin 1, Ireland.
T: +353 1 817 1700 / F: +353 1 872 6523
www.rotunda.ie

31st May, 2019.

Professor Rhodri Cusack
Lloyd Institute Room 3.21
Trinity College Institute of Neuroscience,
Trinity College Dublin,
Dublin 2.

Our ref: **REC-2019-018** *(please quote this reference on all correspondence)*
Re: **Using Neuroimaging to Measure Functional Brain Development in Infants From the Neonatal Intensive Care Unit and a Control Group**

Dear Rhodri,

Many thanks for the amended documentation received in relation to the above research. I am pleased to advise that the requirements set out by the Committee in respect of your study have now been met. This being the case, ethical approval for the research is granted and it may now commence.

You are requested to submit a progress report to the Committee in twelve months, and annually thereafter as applicable.

Please advise us by email to research@rotunda.ie when you have completed your research. We would also like to know when and where you publish or present your results. Please be aware of your responsibilities with respect to the Rotunda Hospital's good research practice policies and guidelines, copies of which are available on the Q-Pulse system.

Kind regards.

Yours sincerely,

Professor Michael Geary,
Chairman,
Research Ethics Committee.

Caring for Generations
Since 1745

Coláiste na Tríonóide, Baile Átha Cliath
Trinity College Dublin
Ollscoil Átha Cliath | The University of Dublin

F.A.O. Rhodri Cusack
Approval ID: SPREC012020-10

School of Psychology Research Ethics Committee

25th February 2020

Dear Rhodri,

The School of Psychology Research Ethics Committee has reviewed your application entitled "Using Neuroimaging to Measure Functional Brain Development in Infants from the Neonatal Intensive Care Unit and a Control Group", and I am pleased to inform you that it was approved.

Please note that you will be required to submit a completed **Project Annual Report Form** on each anniversary of this approval, until such time as an **End of Project Report Form is submitted** upon completion of the research. Copies of both forms are available for download from the Ethics section of the School website.

Please note that you must be familiar with and adhere to the attached 'Safety Protocol for Adults'.
Adverse events associated with the conduct of this research must be reported immediately to the Chair of the Ethics Committee.

Yours sincerely,

SCHOOL OF PSYCHOLOGY
Aras an Phiarsaigh
Trinity College
Dublin 2

Richard Carson
Chair,
School of Psychology Research Ethics Committee

Scoil na Síceolaíochta
Dámh na nEolaíochtaí Sóisialta agus Daonna,
Áras an Phiarsaigh, Coláiste na Tríonóide,
Baile Átha Cliath 2, Éire.

School of Psychology
Faculty of Arts, Humanities and Social Sciences,
Áras an Phiarsaigh, Trinity College,
Dublin 2, Ireland.

T +353 1 896 1886
F +353 1 671 2006
psychology@tcd.ie
www.tcd.ie/psychology

APPENDIX SECTION – CLINICAL RESEARCH FORM CONTROLS

Coláiste na Tríonóide, Baile Átha Cliath
Trinity College Dublin
Ollscoil Átha Cliath | The University of Dublin

Clinical Research Form

Title of Study: Using Neuroimaging to Measure Functional Brain Development in Infants From the Neonatal Intensive Care Unit and a Control Group.

	Response:
Participant Code:	
Gestation 37-42 week (y/n)	
Vulnerable caregiver (y/n) (As per ethics definition)	
Caregiver reported* infant congenital anomaly (y/n)	
Caregiver reported* infant perinatal brain injury (y/n)	
Caregiver reported* infant visual impairments (y/n)	
Caregiver reported* infant contra-indication to MRI	
Caregiver reported* gestation (wk, d)	
Caregiver reported* birth weight (g)	
Caregiver reported* Apgar (5min)	
Caregiver reported* infant complications in newborn period (y/n) (list)	
Caregiver reported* infant developmental concerns (y/n) (list)	
Sex (m/f)	
OFC at 2months (0.1cm)	
OFC at 9 months (0.1cm)	
Ages&Stages-3_v2 Questionnaire completed (y/n)	
Ages&Stages-Social Emotional_v2 Questionnaire completed (y/n)	
Additional relevant data (freetext)	
Key: * = Data source is *caregiver reported* primarily but also healthcare record if required	

APPENDIX SECTION – CLINICAL RESEARCH FORM NICU

Coláiste na Tríonóide, Baile Átha Cliath
Trinity College Dublin
Ollscoil Átha Cliath | The University of Dublin

Clinical Research Form

Title of Study: Using Neuroimaging to Measure Functional Brain Development in Infants From the Neonatal Intensive Care Unit and a Control Group.

	ANS:
Participant Code:	
Infant DOB	
Infant Name in Hospital (eg Emmasgirl Murphy)	
Admission to NICU (y/n)	
Cranial US in NICU (y/n)	
Congenital abnormality (y/n)	
ROP (>stage 3, or treated)	
Contraindication for MRI (y/n)	
Vulnerable caregiver (y/n)	
Sex (m/f)	
Gestation (wk+d)	
Birth weight (g)	
Apgar (5mins)	
Perinatal Stress (defined as encephalopathic but not eligible for therapeutic hypothermia) (y/n)	
Chorioamnionitis – Histological Dx (y/n)	
Chorioamnionitis – Clinical Dx (y/n)	
Early Sepsis (bacteraemic) episodes (no.)	
Early Sepsis (clinical) episodes (no.)	
Late Sepsis (bacteraemic) episodes (no.)	
Late Sepsis (clinical) episodes (no.)	
Meningitis episodes (no.)	
NEC (>mod bells Stage 2a+)	
NEC (surgical) y/n	
Days in NICU (excluding hdu/scbu) (no.)	
Day 1-4 Cranial US (IVH g1-4, PHI, cPVL)	
Day 5-10 Cranial US (IVH g1-4, PHI, cPVL)	
Day 28 Cranial US (cPVL)	
36 week CGA Cranial US, i.e. pre-discharge (cPVL, mod/severe ventricular enlargement, porencephalic cyst, shunt)	
MRI at TEA (ex-preterm) – Kidokoro/Woodward Score	
MRI HIE (35-42 weeks gestation) – Barkovich/DeVries Score	
Antenatal Steroids (any)	
Postnatal Steroids (any) (Dexa/Beta/Hydrocort)	
Days on supplemental oxygen (no.)	
Days on mechanical ventilation (no.)	
Chronic lung disease (defined by oxygen > 28days, or, failure to wean at 36/40) (y/n)	

Patent ductus arteriosus needing medical closure (y/n)	
Patent ductus arteriosus needing surgical closure (y/n)	
Hypoxic Ischaemic Encephalopathy HIE (y/n)	
Therapeutic hypothermia (y/n)	
Sarnat grade (1-3)	
HIE – clinical seizures y/n	
HIE – electrographic seizures y/n	
Seizures other (in NICU) y/n	
Haemoglobin at discharge (g/dL)	
OFC at discharge (0.1cm)	
Post-discharge anaemia y/n	
Post-discharge iron/galfer Rx	
Post-discharge Early Intervention Services (list)	
Caregiver reported hearing test result (normal/other)	
Bayley BSID III (at 2yo) – Scores	
OFC at 2months corrected (0.1cm)	
OFC at 9 months corrected (0.1cm)	
Ages&Stages-3_v2 Questionnaire completed (y/n)	
Ages&Stages-Social Emotional_v2 Questionnaire completed (y/n)	
Additional relevant data (freetext)	

APPENDIX SECTION – SCHAEFER ATLAS PARCEL/NETWORK DESCRIPTIONS

Label Name	Network Name	Full component name
7Networks_LH_Vis	visual	visual
7Networks_LH_SomMot	somatomotor	somatomotor
7Networks_LH_DorsAttn_Post	dorsal attention	posterior
7Networks_LH_DorsAttn_FEF	dorsal attention	frontal eye fields
7Networks_LH_DorsAttn_PrCv	dorsal attention	precentral ventral
7Networks_LH_SalVentAttn_ParOper	salience / ventral attention	parietal operculum
7Networks_LH_SalVentAttn_TempOcc	salience / ventral attention	temporal occipital
7Networks_LH_SalVentAttn_FrOperIns	salience / ventral attention	frontal operculum insula
7Networks_LH_SalVentAttn_PFCl	salience / ventral attention	lateral prefrontal cortex
7Networks_LH_SalVentAttn_Med	salience / ventral attention	medial
7Networks_LH_Limbic_OFC	limbic	orbital frontal cortex
7Networks_LH_Limbic_TempPole	limbic	temporal pole
7Networks_LH_Cont_Par	control	parietal
7Networks_LH_Cont_Temp	control	temporal
7Networks_LH_Cont_PFCd	control	dorsal prefrontal cortex
7Networks_LH_Cont_PFCl	control	lateral prefrontal cortex
7Networks_LH_Cont_OFC	control	orbital frontal cortex
7Networks_LH_Cont_PFCv	control	ventral prefrontal cortex
7Networks_LH_Cont_pCun	control	precuneus
7Networks_LH_Cont_Cing	control	cingulate
7Networks_LH_Cont_PFCmp	control	medial posterior prefrontal cortex
7Networks_LH_Default_Par	default	parietal
7Networks_LH_Default_Temp	default	temporal
7Networks_LH_Default_PFC	default	prefrontal cortex
7Networks_LH_Default_pCunPCC	default	precuneus posterior cingulate cortex
7Networks_LH_Default_PHC	default	parahippocampal cortex
7Networks_RH_Vis	visual	visual
7Networks_RH_SomMot	somatomotor	somatomotor
7Networks_RH_DorsAttn_Post	dorsal attention	posterior
7Networks_RH_DorsAttn_FEF	dorsal attention	frontal eye fields
7Networks_RH_DorsAttn_PrCv	dorsal attention	precentral ventral
7Networks_RH_SalVentAttn_TempOccPar	salience / ventral attention	temporal occipital parietal
7Networks_RH_SalVentAttn_PrC	salience / ventral attention	precentral
7Networks_RH_SalVentAttn_FrOperIns	salience / ventral attention	frontal operculum insula
7Networks_RH_SalVentAttn_PFCv	salience / ventral attention	ventral prefrontal cortex
7Networks_RH_SalVentAttn_PFCl	salience / ventral attention	lateral prefrontal cortex
7Networks_RH_SalVentAttn_Med	salience / ventral attention	medial
7Networks_RH_Limbic_OFC	limbic	orbital frontal cortex
7Networks_RH_Limbic_TempPole	limbic	temporal pole
7Networks_RH_Cont_Par	control	parietal
7Networks_RH_Cont_Temp	control	temporal
7Networks_RH_Cont_PFCv	control	ventral prefrontal cortex
7Networks_RH_Cont_PFCl	control	lateral prefrontal cortex
7Networks_RH_Cont_pCun	control	precuneus
7Networks_RH_Cont_Cing	control	cingulate
7Networks_RH_Cont_PFCmp	control	medial posterior prefrontal cortex
7Networks_RH_Default_Par	default	parietal
7Networks_RH_Default_Temp	default	temporal
7Networks_RH_Default_PFCv	default	ventral prefrontal cortex
7Networks_RH_Default_PFCdPFCm	default	dorsal prefrontal cortex medial prefrontal cortex
7Networks_RH_Default_pCunPCC	default	precuneus posterior cingulate cortex

APPENDIX SECTION – DEFINITIONS OF CAMERA FOOTAGE TAGS

These are in alphabetical order:

- Adult_hand
    - Anytime the adult (supervising the infant in the scanner) places their adult hand near to the baby's face/head.
    - Usually this is to place the soother into the infant's mouth, or to hold/keep it in the baby's mouth for a brief period of time. This can happen multiple times when a baby continues to spit out the soother.
- Asleep
    - Their eyes are ***fully closed*** and their lack of movement suggests they are asleep. Note: a sucking reflex can occur in infants when asleep
    - Asleep tag can last seconds or minutes (and is often alternated sequentially with tags of 'sleepy')
- Baby_out
    - The baby has disappeared from the camera location.
- Eyes_blocked (this concerns the **ability to tag by the tagger**)
    - The **camera view** of the baby's eyes is blocked (i.e. neither of the two eyes are visible enough to allow confident tagging). This can be due to an obstructed view or an unclear view (e.g poor light, e.g. blurred focus, etc)
    - Note: in many videos the distal/furthest eye is invisible or partially visible, however this tag relates to moments when neither eye is visible.
    - This tag does not preclude the use of other tags (i.e. other tags can be given in parallel)
- Eyes_closed_awake (the emphasis is on the *awake* baby)
    - When a baby has their eyes ***fully*** closed for >1sec
    - This can be e.g. while crying, or e.g. rubbing their eyes, or other reason, (crying does not necessarily mean eyes closed)
    - Avoid giving this tag in the 'sleepy/asleep baby' setting.
- Fussing
    - When the baby appears upset (detail below)
    - Baby does not have to be fully crying (e.g mouth-open/vocalising) to get this tag. Instead this tag is based on details of the baby's facial expression.

    - This tag is given if at least 2 (out of 4) of the following are present in the facial expression:
        - Brow bulging/lowering: bulging, creasing, above and between brows resulting from lowering and drawing the brows together
        - Nasolabial furrowing: pulling upwards and deepening in the nasolabial fold
        - Opening lips/mouth: any separation of the lips (even when an object present in the mouth)
        - Eye squeeze (eyelid must close): squeezing/bulging of the eyelid (fatty pad of eyelid)
- Interest_enjoyment
    - Time periods (>1sec) when the baby is any of: Smiling, or talking/babbling happily
    - Only tag this when confident that baby is enjoying
    - This is an infrequent tag
- Interest_scanning
    - These tags will generally be anything from, e.g. 3-4s >> e.g. 40-60s, and signify the 'continuous' time period when a baby is conducting 'eye scanning' of the visual stimuli
    - This is NOT JUST when the eyes/pupils are physically moving, but includes the time between eye movements when the baby appears to be in a continuous state of interest (with intermittent eye scanning movements).
    - This is NOT simply when the baby is 'looking/attending' the stimuli (c.f 'Looking_away' tags below)
- Looking_away_internal
    - Baby's eyes are deviated to an angle/extreme that it appears as though they are not looking towards the stimuli. There appears no external reason for the baby to have looked_away other than an active decision internally
- Looking_away_camera
    - Baby's eyes are deviated to an angle/extreme that it appears as though they are not looking towards the stimuli. They appear to have chosen to look directly at the mri camera itself.
- Looking_away_foreignobject

    - Baby's eyes are deviated to an angle/extreme that it appears as though they are not looking towards the stimuli. They appear to have chosen to look directly at a foreign object (e.g. a toy, e.g. a hand)
- Object_in_mouth
    - This is to record when a baby has the sensory stimulation of a soother/object in their mouth. The object is actually inside their mouth (not nearby, not outside the mouth). This causes them to suck/bite the object.
    - An object includes (not limited to): soother/doody/teether/finger/thumb/hand/ (continue)
- Sleepy
    - When a baby appears quiet, as if heading towards sleep.
    - A common sign is when eyelids begin to close
    - However, their eyelids must still be partially open (NOT fully closed). They must not be 'asleep' (a separate tag)
- Vocalising
    - When the baby appears to vocalise.
    - Note: Do include vocalising during tag fussing if you think the baby is vocalising while fussing. However, these two tags are not totally dependent on each other being present.

APPENDIX SECTION – PARENTAL FEEDBACK QUESTIONNAIRE

Title of Study: Using Neuroimaging to Measure Functional Brain Development in Infants from the Neonatal Intensive Care Unit and a Control Group

Participant Code: [- _RC_FOUNDCOG] (Date:)

[First / Second] visit (please select one)

How was your experience?

We are interested to find out what you thought of your visit for your infant's research MRI scan. Please fill out this questionnaire and return to us at the end of the session. Thank you.

*NOTE: Please ***CIRCLE*** as appropriate (to select your response).

1. I feel that the hospital post-natal ward (or in the NICU) was an appropriate time for the study team to introduce me to this study (receive the study leaflet/flyer)?

Strongly Disagree	Disagree	Neither Disagree/Agree	Agree	Strongly Agree

2. I feel the study information received BEFORE attending for the research MRI was helpful.

Strongly Disagree	Disagree	Neither Disagree/Agree	Agree	Strongly Agree

3. BEFORE attending for the research MRI I feel I understood the difference between 'Structural MRI' compared to 'Functional MRI' of the brain.

Strongly Disagree	Disagree	Neither Disagree/Agree	Agree	Strongly Agree

4. The duration (2 - 2.5 hours) of the visit was acceptable to me.

Strongly Disagree	Disagree	Neither Disagree/Agree	Agree	Strongly Agree

5. I found it helpful to be able to hear my infant during the scan

Strongly Disagree	Disagree	Neither Disagree/Agree	Agree	Strongly Agree

6. I found it helpful to be able to see my infant's face during the scan

Strongly Disagree	Disagree	Neither Disagree/Agree	Agree	Strongly Agree

7. I found it helpful to be able to see the visual stimuli (what infant is seeing) during the scan

Strongly Disagree	Disagree	Neither Disagree/Agree	Agree	Strongly Agree

8. I felt my infant was comfortable for the majority of the scan session

Strongly Disagree	Disagree	Neither Disagree/Agree	Agree	Strongly Agree

9. During the scan session, my infant's awake state (e.g. tired/crying or settled/happy) allowed the gathering of usable MRI data for analysis.

Strongly Disagree	Disagree	Neither Disagree/Agree	Agree	Strongly Agree

10. During the scan session, my infant's **asleep** state allowed the gathering of usable MRI data for analysis.

Strongly Disagree	Disagree	Neither Disagree/Agree	Agree	Strongly Agree

11. I received debriefing at the end of the research MRI session.

Strongly Disagree	Disagree	Neither Disagree/Agree	Agree	Strongly Agree

12. AFTER attending for the research MRI I feel I understood the difference between 'Structural MRI' compared to 'Functional MRI' of the brain.

Strongly Disagree	Disagree	Neither Disagree/Agree	Agree	Strongly Agree

13. Functional MRI brain imaging may prove a useful tool for measuring infant brain development in the hospital in the future.

Strongly Disagree	Disagree	Neither Disagree/Agree	Agree	Strongly Agree

14. I was overall satisfied with my child's experience of visiting for the research MRI scan.

Strongly Disagree	Disagree	Neither Disagree/Agree	Agree	Strongly Agree

15. What is/are the reason(s) that you wished your baby(s) to be part of this research study? (enter below):

16. Do you have any other comments or suggestions about your visits [2month / 9 month]? (enter below):

APPENDIX SECTION – INFANT MRI STANDARD OPERATING PROCEDURES

Trinity College Institute of Neuroscience

Infant MRI
Standard Operating Procedures and Guidelines

(Version 1.1)
(Date: 16/08/2021)

1. Infant Standard Operating Procedures

A. Procedure for infant MRI scanning

The pre-scan MRI checklist will be conducted initially by the Principal Investigator (PI) (or their nominee) with a potential participant as a screening to exclude persons with medical implants or other conditions.

It is the responsibility of the PI to ensure that prior to scanning the participant's parent/guardian completes all consent forms including permission for:

1) Principal Investigator (PI) to conduct the overall study
2) TCIN to conduct the MRI scan and store MRI scan data of participant
3) TCIN to contact the named radiologist in the participant's neonatal hospital
4) TCIN to contact the named neonatologist in participant's neonatal hospital
5) TCIN radiographer to send MRI scan data to named radiologist in participant's neonatal hospital
6) Named radiologist to store data in a hospital system with the same care as other patient data
7) Named radiologist to contact participant's named neonatologist
8) TCIN to store data on the study for a period of 10 years

Notes:
Consent(1) refers to the PI's specific consent form and must be initially approved by their ethics committee and shown to the MRI Committee.

The named radiologist will be sent image data in a format that allows participant identification so that if a clinical response is required the radiologist can act quickly. This will be stored in the hospital system and treated like other medical data, as per the rules of that institution. The raw scan data will be stored at TCIN in

pseudo-anonymous form for research purposes as agreed on the consent form of the particular research project.

A dated standard letter, signed by the appropriate PI, will be sent to a participant's named radiologist and named neonatologist. It is the responsibility of the PI to ensure that this letter is sent at least two days before scanning to allow for postal delays.

The named neonatologist must be made aware by means of this letter that a scan will take place at TCIN and that a named radiologist acting for TCIN may be in contact with them, in the event of reported radiological evidence of anomalies/irregularities, to recommend appropriate and timely clinical/radiological follow-up for the participant. This letter must be received by the named neonatologist before the scan details reach the named radiologist.

A photocopy of this signed & dated letter should be brought to the TCIN radiographer (Sojo Joseph) to be stored on file in the TCIN MRI area.

Failure to contact the named neonatologist before scanning or before the radiologist reads the scan could jeopardise the TCIN scanning agreement, which stipulates that there shall be no cold calling involved between the named radiologist and the named neonatologist.

Consequently, failure to follow this procedure is considered a serious disciplinary matter and may result in the revocation of scanning rights for an individual and or research group for a period to be determined by the director of TCIN in consultation with the MRI committee.

Information Flow:

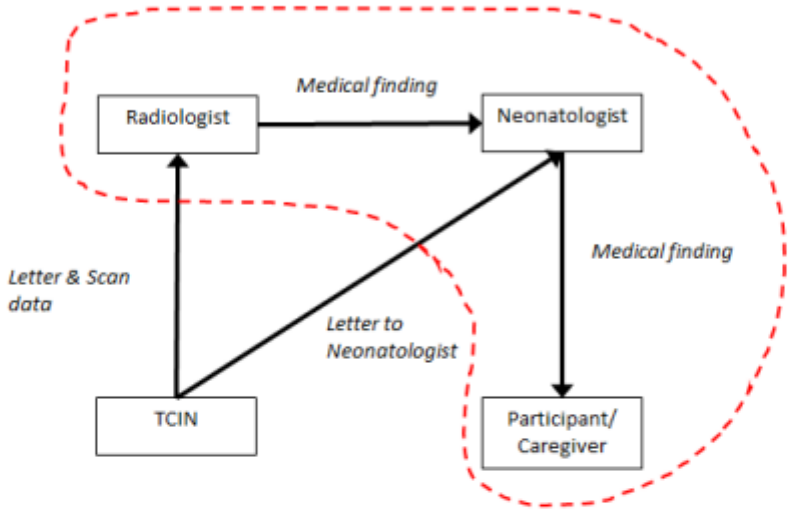

(figure 1)

Before scanning the TCIN radiographer (Sojo Joseph/other) will once again go through the MRI screening checklist. After scanning, appropriate data will be sent to the named radiologist by the TCIN radiographer. The data will be in the format agreed and specified with the named radiologist acting for TCIN.

The scan data may be sent to the named radiologist by encrypted USB in the postal system (a certificate of postage or swift post receipt will be required) OR via BEAM Image Sharing Network.

The data does not become of medical nature until it is interpreted by the radiologist, at which point it will be stored in the hospital system and only imparted to other medical professionals and the participant's parent/guardian (Figure 1, dotted line region.) The dotted line region is depicted to show that medical data should remain within the

medical domain as a rule. The raw data will be stored at TCIN in pseudo-anonymous form for research purposes as agreed on the consent form.

The PI is responsible for their project at all times. This means that the PI, or a nominated member of their research team, conducts the study with the assistance of the MRI radiographer.

The important general documentation (shown below) includes the following:

- TCIN Infant MRI Data Consent Form
- Standard letter to (named) neonatologist
- Standard letter to (named) radiologist
- Agreements between TCIN and (named) radiologist
    - Scientific Publication agreement
    - Monetary compensation agreement

Infant MRI Data Consent Form

Trinity College Institute of Neuroscience (TCIN) is performing research, utilising an MRI scanner at Trinity College, Dublin 2. These scans are primarily for research purposes however structural MRI images will be clinically reported by a named radiologist(a doctor specializing in medical imaging such as MRI imaging/other).

The TCIN named radiologist will be sent image data in a format that includes participant demographics. This is in order to allow the named radiologist to act appropriately on any radiological image evidence of suspected anomalies/irregularities. The image data will be stored in the hospital system with the same rigour and attention to confidentiality as all other medical data.

Separately, the raw scan image data will be stored at TCIN in a pseudo-anonymous format(this means that the participant's image data will only be identifiable by a unique code to which only the principal researcher will have the key to link the image data with the participant demographics in the future).

In the unlikely event of an irregularity being found, the named radiologist [Dr A - Hospital A, or Dr B - Hospital B, or Dr C - Hospital C] (*delete as appropriate*) will inform the named neonatologist(newborn and infant doctor) [Dr A - Hospital A, or Dr B - Hospital B, or Dr C - Hospital C] (*delete as appropriate*) that a follow-up (non-research) clinical scan may be required to determine whether or not a radiological finding is of clinical significance.

To enable us to perform the research scan you as the parent/guardian are asked to write your initials in the box beside the following statements if you agree. If you do not agree with a statement please leave the box blank.

	Parent/ Guardian Initials:
• I give permission for TCIN to conduct the MRI scan and store MRI scan data of my child	
• I give permission for TCIN to contact the named radiologist in my child's neonatal hospital	

• I give permission for TCIN to contact the named neonatologist in my child's neonatal hospital	
• I give permission for the TCIN radiographer to send MRI scan data to named radiologist in my child's neonatal hospital	
• I give permission for the named radiologist to store data in a hospital system with the same care as other patient data	
• I give permission for the named radiologist to contact my child's named neonatologist	
• I give permission for TCIN to store my child's raw pseudo-anonymous MRI data for a period of 10 years	

Participant/infant Name (Block Capitals):

Participant/infant date of birth: xx/xx/xxxx

Parent/Guardian Name (Block Capitals):

Relationship to participant/infant:

Parent/Guardian Signature:

Date:

Researcher Name (Block Capitals):

Researcher signature:

Date:

Standard Letter to Neonatologist from Trinity College
Institute of Neuroscience

Date:

Dear Consultant Neonatologist [Dr A - Hospital A, or Dr B - Hospital B, or Dr C - Hospital C] (*delete as appropriate*),

(Participant 's name, address, D.O.B, telephone no.) is a patient of [Hospital A, or Hospital B, or Hospital C] (*delete as appropriate*) and is taking part in the ' XXXXXXX research study' (e.g. Cusack Lab, FOUNDCOG study) utilising MRI imaging at Trinity College Institute of Neuroscience, TCD Dublin 2. These research MRI scans, although not full clinical scans, will be read by a named radiologist in your hospital [Dr A - Hospital A, or Dr B - Hospital B, or Dr C - Hospital C] (*delete as appropriate*).

In the event of an radiological irregularity being found the named radiologist in your hospital will contact you in order that you might organise a follow-up (non-research) clinical scan to determine whether or not a radiological finding is of clinical significance.

You as the neonatologist should then contact the participant's parent/guardian to advise them that a (non-research) clinical scan at your hospital is recommended to check the irregularity with appropriate clinical follow-up as necessary.

In the unlikely event that you need to contact us, the following telephone number can be used (01 - XXXXX)

Sincerely,

Name of PI:

Signature of PI:

Date:

This letter was posted to the participant's neonatologist on XX/XX/XXXX.

Standard Letter to Radiologist from Trinity College
Institute of Neuroscience

Date:

Dear Consultant Radiologist [Dr A - Hospital A, or Dr B - Hospital B, or Dr C - Hospital C] (*delete as appropriate),*

(Participant 's name, address, D.O.B, telephone no.) is a patient of [Hospital A, or Hospital B, or Hospital C] (*delete as appropriate*) and is taking part in the ' XXXXXXX research study' (e.g. Cusack Lab, FOUNDCOG study) utilising MRI imaging at Trinity College Institute of Neuroscience, TCD Dublin 2.

The participant's functional MRI (fMRI) research images will be retained in TCIN. Any structural MRI images obtained will be copied to you (including metadata/participant demographics) and will be sent to you by BEAM Imaging Sharing Network or via encrypted USB. (*Please note; if an infant does not tolerate the imaging procedure there may be no structural MRI images obtained and a follow-up letter will notify you of this occurrence)

In the event of finding a radiological irregularity please contact the named neonatologist in your hospital [Dr A - Hospital A, or Dr B - Hospital B, or Dr C - Hospital C] (*delete as appropriate*) in order that the named neonatologist may organise a follow-up (non-research) clinical scan to determine any clinical significance.

In the unlikely event that you need to contact us, the following telephone number can be used (01 - XXXXX)

Sincerely,

Name of PI:

Signature of PI:

Date:
This letter was posted to the participant's radiologist on XX/XX/XXXX.

Radiology Clinical Reading Agreement - Option 1

between

Dr. A - Hospital A/ Dr. B - Hospital B/ Dr. C - Hospital C

&

Trinity College Institute of Neuroscience (TCIN)

Dated from: XX/XX/XXXX

I agree to provide clinical readings of MRI images acquired as part of the *"XXXXXX Study"* from the 3T MRI located at TCIN, Lloyd Building, Trinity College Dublin. The scans will be sent to me via BEAM Image Sharing Network or on encrypted USB disc and will be accompanied by participant identifiers including: name; date of birth; address; and telephone number.

The MRI images and radiological report will be uploaded/stored on the NIMIS system by the PACS Manager in my hospital [Hospital A, or Hospital B, or Hospital C] (*delete as appropriate*).

Should any anomalous findings require follow-up I will contact the participant's named neonatologist [Dr A - Hospital A, or Dr B - Hospital B, or Dr C - Hospital C] (*delete as appropriate*) to communicate my observations and will request that the named neonatologist follow-up with the participant's parent/guardian.

These activities will be covered by my professional indemnity cover.

If I am unavailable (e.g. due to being on vacation/sick-leave/other) I will arrange for another radiologist in my team at [Hospital A, or Hospital B, or Hospital C] to fulfill these obligations.

In return, TCIN will ensure that I am an ongoing research collaborator in *"XXXXXX Study"* and that I am listed as an author of any of the team's research publications which include these participant's images.

Signature of consultant radiologist: .....

[Dr A - Hospital A, or Dr B - Hospital B, or Dr C - Hospital C] (*delete as appropriate*)

Date: .....

Signature of TCIN, MRI Committee Acting Chair: .....

Date: .....

Radiology Clinical Reading Agreement - Option 2

between

Dr. A - Hospital A/ Dr. B - Hospital B/ Dr. C - Hospital C

&

Trinity College Institute of Neuroscience (TCIN)

Dated from: XX/XX/XXXX

I agree to provide clinical readings of MRI images acquired as part of the *"XXXXXX Study"* from the 3T MRI located at TCIN, Lloyd Building, Trinity College Dublin. The scans will be sent to me via BEAM Imaging Sharing Network or on encrypted USB disc and will be accompanied by participant identifiers including: name; date of birth; address; and telephone number.

The MRI images and radiological report will be uploaded/stored on the NIMIS system by the PACS Manager in my hospital [Hospital A, or Hospital B, or Hospital C] (*delete as appropriate*).

Should any anomalous findings require follow-up I will contact the participant's named neonatologist [Dr A - Hospital A, or Dr B - Hospital B, or Dr C - Hospital C] (*delete as appropriate*) to communicate my observations and will request that the named neonatologist follow-up with the participant's parent/guardian.

These activities will be covered by my professional indemnity cover.

If I am unavailable (e.g. due to being on vacation/sick-leave/other) I will arrange for another radiologist in my team at [Hospital A, or Hospital B, or Hospital C] to fulfill these obligations.

In return, TCIN will pay €XX.XX euro per participant for these services and I will invoice TCIN every two months.

Signature of consultant radiologist: .....

[Dr A - Hospital A, or Dr B - Hospital B, or Dr C - Hospital C] (*delete as appropriate*)

Date: .....

Signature of TCIN, MRI Committee Acting Chair: .....

Date: .....

B. MRI Management Committee (MRI-MC)

The MRI committee deals with issues such as allocation of MRI scanning time and general policy for use of MRI. This committee shall be a diverse group with membership drawn from different disciplines including TCIN management, Physics, Psychology, and Psychiatry/Medicine. Before a study commences, evidence that it has passed the relevant ethics review should be submitted to the MRI Committee. The MRI committee has also specified an Infant General Consent Form for participants to be allowed to be scanned. The MRI Management Committee will be the final arbiter in the allocation of scanning hours on MRI.

MR Operational Group (MROG):

The MRI committee will delegate some duties to focus on day-day operational issues to members of core staff (e.g. Sojo Joseph) as well as postgrads and postdocs with the Principal Physicist (CK), as chair of this MR Operational Group (MROG) which reports to the MRI Management Committee.

The MROG can provide support with protocol planning, theoretical and practical aspects of the research. Technical aspects of MRI project from data acquisition to analysis methods can be discussed with the chair of the group. The MROG is responsible for review and approval of study protocols. Complete proposals will be reviewed by the MR Operational group on a monthly basis.

The review process will determine if the proposed research is appropriate given the technology available and whether the investigative team is prepared to carry out and analyse the experiment. In this regard, Postgrad and Postdoc training on MRI should be strongly encouraged by TCIN.

The MROG will also identify any potential problems arising from the studies (software, hardware, data processing issues, etc.) during the proposal review.

The MROG will not approve study protocols if the study plans to alter the MR scanner hardware or software without previously obtaining Trinity College Dublin research ethical approval.

Approval of the proposal does not guarantee the investigator time on the scanner. The investigator will need to schedule scanner time using the online booking system after the study has been approved.

Support may be provided for pilot studies utilizing MRI techniques that have potential to develop into full studies.

If an investigator requests scan time to gather preliminary data for a pilot study in support of a grant proposal, free pilot hours (to a maximum of 2) may be granted. However, the PI must justify why other funds to undertake the pilot study are unavailable.

After approval is obtained, a project number will be assigned and user time on the scanner can be scheduled with the TCIN online booking.

The following information is required to complete the MR scanner usage form:

- Principal and co-investigator(s), if any
- Date of proposal
- Project title
- Department and Institution of PI
- Phone number and e-mail address of PI
- Billing/account address where invoice will be sent
- Existing funding source(s) of the project
- Total number of scanner hours requested for project duration
- Total estimated duration of the project
- Data analysis methods (name of software and type of analysis)
- Additional required equipment (such as response box, physiological monitoring equipment, etc)
- Details of approval from school/faculty ethics committee and hospital ethics committee if the study involves clinical a population
- If requesting free pilot studies, the reason why other funding is not available must be provided
- Attach protocol for research project (background information, significance, preliminary data, methods, expected results, etc.) or the original grant application that includes the protocol

C. Scheduling Policy

MRI scanner time is a valuable and expensive resource and efficient use of the instrument is of utmost importance. Be aware that current and ongoing projects take precedence over newly approved and pilot studies.

1. Prior to booking slots, we recommend new studies are presented orally to the Imaging Interest Group (IIG). This should be documented in the IIG meeting minutes.

All new scans can be scheduled on TCIN online booking system https://tcin-bookingsystem.tchpc.tcd.ie. Scheduling will be handled on a first-come- first-serve basis. Scheduled scans will be confirmed via email.

2. For scheduling changes or cancellations (give at least 24-hours notice), please e-mail Sojo Joseph, josephs@tcd.ie and call the MRI research lab at 896 2963 to be certain the requested changes have been made. It should be understood that there would be occasional difficulties with participant scheduling (tardiness or absenteeism) or equipment problems beyond the investigator's control. Efforts will be made to fairly reschedule the scan at a suitable time if necessary.

3. When requesting a scan, please be clear and specific about the study details.

D. The Safe Use of the MR scanner

The following protocols must always be followed:

- The door to the scanner room must remain locked at all times when the room is not in use (also when you intend to stay away just for a few minutes).
- Upon entering the Control Room, if staff intend unlocking the Magnet room door, or indeed if it is already unlocked, they should

remove all ferromagnetic objects from their person
- **Never** work alone or without MR staff.

Responsibilities of MR personnel:

- To ensure that their name is in the current logbook of MR personnel (kept in MR Control Room)
- To sign the Sign-in/out MR personnel logbook contained within the control room (when entering Zone III/Zone IV)
- To ensure controlled access to the magnet room for participants (in questionable cases to decide as to whether an investigation should take place)
- To ensure that unauthorized persons enter the scanner room only when accompanied by an authorized person.
- To be responsible for ensuring that no ferromagnetic objects are brought into the magnet room.
- To ensure that a participant's parent/guardian has completed the necessary forms as required by the ethics committee
- To ensure that an infant participant remains no longer than1 hour in the magnet
- To never leave the control room/magnet during scanning of a human participant
- To keep his/her magnet room key only for personal use
- To ensure that the scanner and stimulus equipment is in a standard configuration.
- To ensure that RF coils are used only in the way recommended/specified by their manufacturer.

E. Post-scanning

Upon completion of scan, please follow the guidelines below:

- Clean up any untidiness resulting from the scan. This includes returning all equipment to its appropriate storage space, placing soiled linens in the laundry hamper, etc.
- After data has been collected, archive all your data on the data server. After 2 weeks data will be removed from the scanner computer.
- An invoice will be generated and sent to the appropriate billing address or charged to the appropriate account.
- In case of any adverse events promptly inform the responsible PI

F. Participant Confidentiality Notice

The MRI Research group will not share any information and/or data gained about the participant to other investigators or any other individual unless consented by the principal investigator of the project (provided that all participant confidentiality procedures are followed according to the consent form of the study).

G. Conventions governing data files and information contained there-in

Files exported from the scanner will be in NIfTI or DICOM format.

The files from the scans that are necessary to facilitate the universal radiological screening program will typically be in DICOM format.

The files exported from the scanner control workstation for research must conform to the following format:
1. The first 2-3 characters must be the initials of the PI.
2. The second 2 characters must be the day of the month. For example, 02, 10, 31.
3. The third 2 characters must be the month of the year. For example 01 for January, 02 for February and so on to 12 for December.
4. The next 2 characters must be the last two digits of the current year. For example, 06 for 2006.
5. The next 2-3 digits are the initials of the person conducting the study.
6. The next 3-4 digits is the volunteer's number within the study.
7. The next digit is an underscore.
8. (Optional) A short word identifying the study followed by an underscore. This will be useful if you are running many studies in parallel.
9. The next 2-3 (or more) is the sequence number of the scan (see below).
10. The next character is an underscore.
11. The next character is usually the number 1.
12. The next character is a full-stop i.e. a '.'.
13. Finally the final 3 characters are the extension of the file. This is usually DCM.
14. These files must NOT contain any information that may identify the volunteer.
(Note that points 9 to 13 inclusive are under the control of the export software on that scanner and may change with software upgrades.)

DICOM files will be named according to the convention used by the scanner or the PACS storage software.

The DICOM files are usually produced only from the scans that are necessary to facilitate the universal radiological screening program. These DICOM files may contain **ONLY** the participant's name, date of birth, telephone number, and responsible clinician contact details. These files are to be stored in a PACS system and only these files will be sent to the named radiologist.

The DICOM files will be pseudo-anonymised, or converted to pseudo-anonymised NIFTI (BIDS) format before release to researchers. **NO** tags that identify the volunteer will be included in the files. Researchers will be informed that they must also "de-face" any MRI structural images prior to sharing of data.

2. Infant MRI Safety Guidelines

A. Infant Clinical Safety/Supervision

***Note:** This section pertains to the clinical safety/supervision of infant research participants by a qualified paediatric doctor/nurse. For definitions of a qualified paediatric doctor/nurse please see Appendix.

****Note:** Both the Infant Emergency Procedure and Adult Emergency Procedure guidelines are documented in Section 3 (below).

Safety Equipment and the Infant Emergency Bag:

- All infant emergency equipment including the emergency bag should be labelled with MR Safety stickers as follows:
    - [MR safe (green), MR conditional (yellow), MR unsafe (red)]
- The Infant Emergency Bag should be permanently located in the MR Control Room (MR safety label RED). It should never be brought into the magnet room (Zone IV).
- In an infant emergency the infant should immediately be brought out of the magnet room and into the Control Room (and placed on a dedicated baby mat on a designated table space, the 'Baby Table')
- The following items are essential equipment for an infant emergency (all these items fit into the Infant Emergency Bag):
    - Airway equipment:
        - WelchAllyn 17462P Disposable Uniscope Stethoscope (MR safe/green), Ambu Spur II self-inflating bag (MR conditional/yellow), endotracheal tubes (MR safe/green), PediCap end-tidal CO2 detector (MR safe/green), white-tape (MR safe/green), oro/naso-gastric tubes (MR safe/green), suction catheters (MR safe/green), oropharyngeal airways (MR safe/green), laryngeal mask airways (MR safe/green), laryngoscope (MR unsafe/red),

Ambujet Jet Compact 300D portable suction machine (MR unsafe/red)

- Oxygen equipment
  - BOC Ireland - Category AZ cylinder (aluminium, 137 Bar, MR compatible), Product Code 298121-AZ, with oxygen regulator (MRI compatible)
- Other equipment
  - Medical gloves (MR safe/green)
  - Plastic syringes (MR safe/green)
  - Fluids (Saline 0.9% and Dextrose 10%) (MR safe/green)
  - Draeger infant transwarmer mattress (MR conditional/yellow)

Before the MR Scan:

- An infant participant and their parent/guardian will be greeted in the MR Reception room.
- An infant participant's parent/guardian must fill in the Infant MRI Data Consent Form as requested by the ethics committee (check if all answers are YES and initialled, if NO exclude from study!).
- The paediatric doctor/nurse will initially meet the infant and parent/guardian in the MR Reception to assess whether the infant is clinically well on the day of the MR scan.
  - The paediatric doctor/nurse will complete the Infant Clinical Status Screening Questions (see Appendix)
  - If the paediatric doctor/nurse has a concern that the infant may have an intercurrent illness or is unwell the paediatric doctor/nurse shall ask the parent/guardian for permission to clinically examine the infant. If the parent/guardian refuses this the infant shall be precluded from going for the MR scan.
  - Only an infant who is considered to be clinically well by the paediatric doctor/nurse should be allowed to continue for a MR scan.
- Prior to admission to Zones III/IV the infant's parent/guardian must have completed the Infant MR Safety Screening Questionnaire (see Appendix) both in writing and verbally with at least two MR personnel (one of whom must be a level 2 MR personnel). A positive response to an item on this questionnaire may preclude the infant from the MR scan.

- Should the parent/guardian wish to accompany/assist the infant into Zones III/IV the parent/guardian themselves must complete the Parent MR Safety Screening Questionnaire (see Appendix) both in writing and verbally with at least two MR personnel (one of whom must be a level 2 MR personnel). A positive response to an item on this questionnaire may preclude the parent/guardian from entering zones III/IV. The parent should be reassured that should the infant become upset that the researcher/doctor/nurse will manage this as specified below (See section: Upset Infant - Management)
- Infant participants will be required to wear a nappy, vest, and a baby-grow (all clothing items should contain no metal fasteners/buttons). An infant's parent/guardian should also bring a baby blanket (non metal containing) with them on the day of the scan.
    - TCIN will ensure a backup supply of nappies, vests, baby-grows (non-metallic containing) along with spare blankets for an infant in the scanner.
- The contents of the infant emergency bag (stored in Zone III) should be checked by the paediatric doctor/nurse. This includes checking the portable MR safe oxygen cylinder and MR safe regulator/flow meter (stored in Zone III)

<u>During the MR Scan:</u>

- A paediatric doctor/nurse must be present in the Control Room or Magnet Room at all times when the infant is in the MR scanner
- Infant monitoring equipment (MR camera, MR bluetooth portable pulse-oximetry, MR noise-cancelling headphones with microphone) must be checked and in working order prior to initiating the first MR sequence.
- Always record the time the participant went into and out of the magnet
- The infant should be placed supine (on their back) on the MR table and gently secured in this position using a blanket, soft positioning blocks/cushions, and gentle velcro strapping.
- For MRI brain imaging the infant's head (with headphones in-situ) will be positioned in the MR receiver coil (soft padded).
- Infant/baby headphones must be worn.
- The paediatric doctor/nurse will continuously review the infant monitoring equipment data output during the infant MR scan ensuring that the infant is well throughout the scan.
- Upset Infant - Management:

  - Should the infant become upset (some crying or moving) the parent/guardian/researcher/doctor/nurse will attempt to reassure and calm the infant using verbal and soft tactile cues.
  - Should the infant become further upset (excessive crying or movements) the parent/guardian/researcher/MR technician/doctor/nurse will make the decision to terminate the MR scan and to extract the infant from the MR scanner to comfort and calm the infant, and to return the infant to their parent/guardian immediately.
- Should the infant appear unwell/compromised at any stage (data from monitoring equipment/other) the paediatric doctor/nurse can request the MR operator to terminate the scan at any stage. The paediatric doctor/nurse should clinically assess the infant immediately and initiate the Infant Emergency Procedure (see Section 3).

<u>After the MR Scan:</u>

- The infant should be checked to ensure that they are well and at clinical baseline
- The paediatric doctor/nurse will update the parent/guardian on how the infant tolerated the MR scan.
- The contact details of the research PI and research team shall be given to the parent/guardian should they have any further questions/concerns.

B. Static Magnetic Field Issues: Site Access Restriction

1. Zoning:

The MR site is conceptually divided into 4 zones (see Appendix & Figure):

a. Zone I: This region includes all areas that are freely accessible to the general public. This area is typically outside the MR environment itself and is the area through which participants, health care personnel, and other employees of the MR site access the MR environment.
b. Zone II: This area is the interface between the publicly accessible, uncontrolled Zone I and the strictly controlled Zones III and IV. Typically, participants are greeted in Zone II and are not free to move throughout Zone II at will, but rather are under the supervision of MR personnel (see section below). It is in Zone II that the answers to MR-screening questions, participant histories, etc are typically obtained.
c. Zone III: This area is the region in which free access by unscreened non-MR personnel or ferromagnetic objects or equipment can result in serious injury or death as a result of interactions between the individuals or equipment and the MR scanner's particular environment. These interactions include, but are not limited to, those involving the MR scanner's static and time-varying magnetic fields. All access to Zone III is to be strictly restricted, with access to regions within it (including Zone IV, see below) controlled by, and entirely under the supervision of, MR personnel (see below). Specifically identified MR personnel (typically—but not necessarily only—the MR technologists) are to be charged with ensuring that this MR safe practice guideline is strictly adhered to for the safety of the participants and other non-MR personnel, the health care personnel, and the equipment itself.
d. Zone IV: This area is synonymous with the MR scanner magnet room itself, i.e., the physical confines of the room within which the MR scanner is located. Zone IV, by definition, will always be located within Zone III, as it is the MR magnet and its associated magnetic field that generates the existence of Zone III. As part of the Zone IV site restriction, all MR installations should provide for direct visual observation by level 2 MR personnel to access pathways into Zone IV.

2. MR personnel and non-MR personnel (see below):

    a. All individuals working within at least Zone III of the MR environment will be documented as having successfully completed at least one of the MR safety lectures. Attendance will be repeated annually, and appropriate documentation will be provided to confirm these ongoing educational efforts.
    b. A logbook of current MR personnel shall be kept in the MR Control Room
    c. There are 3 levels of MR personnel:
        (1) Level 1a MR personnel: Those who have passed minimal safety educational efforts to ensure their own safety as they work within Zone III will be referred to henceforth as level 1a MR personnel.
        (2) Level 1b MR personnel: Individuals who have passed both initial MRI safety educational teaching/testing (as per their institution) and who have attended a mandatory practical training/walk-through of the Infant Emergency Procedure steps. These personnel will typically be research team members or PIs involved in infant research MRI scanning. Level 1b MR personnel are only permitted to supervise an infant participant in Zone IV when a Level 2 MR person is present and has direct vision of those within Zone IV. A list of Level 1b MR Personnel (and dates of completed training) is in the Appendix.
        (3) Level 2 MR personnel: Those who have been more extensively trained and educated in the broader aspects of MR safety issues, including, for example, issues related to the potential for thermal loading or burns and direct neuromuscular excitation from rapidly changing gradients, will be referred to henceforth as level 2 MR personnel. It is the responsibility of the MR physicist not only to identify the necessary training, but also to identify those individuals who qualify as level 2 MR personnel.
    d. All those not having successfully complied with these MR safety instruction guidelines shall be referred to henceforth as non-MR personnel. Specifically, non-MR personnel will be the terminology used to refer to any individual or group who has not, within the previous 12 months, undergone the designated form safety training.

Participant and non-MR personnel screening:

a. All non-MR personnel wishing to enter Zone III must first pass an MR safety–screening process. Only MR personnel are authorized to perform an MR safety screening prior to permitting non-MR personnel into Zone III.
b. Non-MR personnel will be accompanied by, or under the immediate supervision of and in visual and verbal contact with, one specifically identified level 2 MR personnel for the entirety of their stay within Zone III or IV. Level 1a/1b MR personnel are permitted unaccompanied access throughout Zones III and IV. Level 1a/1b MR personnel are also explicitly permitted to be responsible for accompanying non-MR personnel into and throughout Zone III, excluding Zone IV. However, level 1a/1b MR personnel are not permitted to directly admit, or be designated responsible for, non-MR personnel in Zone IV. In the event of a shift change, lunch break, etc, no level 2 MR personnel shall relinquish their responsibility to supervise non-MR personnel still within Zone III or IV until such supervision has been formally transferred to another of the level 2 MR person.
c. Participants and their parent/guardian should be MR safety–screened on-site by a minimum of 2 separate individuals. At least one of these individuals should be level 2 MR personnel. At least one of these 2 screens should be performed verbally or interactively.
d. Any participant and their parent/guardian entering Zone III must remove all readily removable metallic personal belongings and devices, e.g., watches, jewelry, pagers, cell phones, body piercing (if removable), contraceptive diaphragms/coils, metallic drug-delivery patches, cosmetics containing metallic particles (such as eye makeup), and items of clothing that may contain metallic fasteners, hooks, zippers, loose metallic components, or metallic threads.
e. Infant participants will be required to wear a nappy, vest, and a baby-grow (all clothing items should contain no metal fasteners/buttons). An infant's parent/guardian should also bring a baby blanket (non metal containing) with them on the day of the scan.

   TCIN will ensure a backup supply of nappies, vests, baby-grows (non-metallic containing) along with spare blankets for an infant in the scanner.
f. All participants, their parent/guardian, and non-MR personnel with a history of potential ferromagnetic foreign object penetration must undergo further investigation prior to being permitted entrance to Zone III. Examples of acceptable methods of screening include participant history,

prior plain X-ray films, prior CT or MR studies of the questioned anatomic area, or access to written documentation of the type of implant or foreign object that might be present. Failure to comply with this further investigation will preclude the relevant person from entering Zones III/IV.

g. Final determination of whether or not to scan any given participant with any given implant, foreign body, etc is to be made by the attending MR radiologist, a MR medical director, or specifically designated level 2 MR personnel following criteria for acceptability pre-determined by the MR medical director.
h. All non-MR personnel (e.g. participants and their parents/guardians, and varied site employees and professionals) with implanted cardiac pacemakers, auto defibrillators, diaphragmatic pacemakers, nerve stimulators, or other electromechanically activated devices upon which the non-MR personnel is dependent should be precluded from entering Zone IV and physically restrained from passing the 5-G line unless specifically cleared in writing by a level 2–designated person. In such circumstances, specific risk-benefit rationale should be provided in writing and signed by an authorizing radiologist.

   Should it be determined that non-MR personnel wishing to accompany a participant into an MR scan room require their eye orbits to be cleared by plain-film radiography, a radiologist must first discuss with the non-MR personnel that plain X-ray films of their orbits are required prior to permitting them access to the MR scan room. Should they still wish to proceed with access to Zone IV or within the 5-G line, and should the attending radiologist deem it medically advisable that they do so (e.g., for the care of their child about to undergo an MR study), written informed consent should be provided by these accompanying non-MR personnel prior to undergoing X-ray examination of their orbits.

3. MR personnel screening:
   All MR personnel are to undergo an MR-screening process as part of their employment interview process to ensure their safety in the MR environment. For their own protection, and for the protection of the non-MR personnel under their supervision, all MR personnel must immediately report to the TCIN director any trauma, procedure, or surgery they experience or undergo where a ferromagnetic metallic object or device may have been introduced within or on them. This will permit appropriate screening to be performed on the employee to determine the

safety of permitting the MR personnel–designated employee into Zone III.

4. Device and object screening:
   As part of the Zone III site restriction and equipment testing and clearing responsibilities, all sites should have ready access to a strong handheld magnet (≥1000 G). This will enable the site to test external, and even some superficial internal, devices or implants for the presence of grossly detectable ferromagnetic attractive forces.
   a. All portable metallic or partially metallic devices that are on or external to the participant (e.g., oxygen cylinders) are to be positively identified in writing as non-ferromagnetic and either MR safe or MR compatible prior to permitting them into Zone III. For all device or object screening, verification and positive identification should be in writing. Examples of devices that need to be positively identified include fire extinguishers, oxygen tanks, and aneurysm clips.
   b. External devices or objects demonstrated to be ferromagnetic and MR unsafe or MR incompatible may still, under specific circumstances, be brought into Zone III if, for example, they are deemed by MR personnel to be necessary and appropriate for the care of the participant. They should only be brought into Zone III if they are under the direct supervision of specifically designated level 1 or 2 MR personnel who are thoroughly familiar with the device, its function, and the reason supporting its introduction to Zone III. The safe utilization of these devices while they are present in Zone III will be the responsibility of a specifically named level 1 or 2 MR personnel. The devices must be appropriately physically secured or restricted at all times during which they are in Zone III to ensure that they do not inadvertently come too close to the MR scanner and accidentally become exposed to static magnetic fields or gradients that might result in their becoming either hazardous projectiles or no longer accurately functional.
   c. Never assume MR compatibility or safety information about the device if it is not clearly documented in writing. All unknown external objects or devices being considered for introduction to Zone III should be tested with a strong handheld magnet (≥1000 G) for ferromagnetic properties prior to permitting them entry to Zone III. The results of such testing, as well as the date, time, and name of the tester and the methodology used for that particular device, should be documented in writing. If a device has not been tested, or if its MR compatibility or safety status is unknown, it should not be permitted unrestricted access to Zone III.

d. All portable metallic or partially metallic objects that are to be brought into Zone IV must be labeled with either a green “MR safe” label or a red “MR unsafe” label. Testing for the purpose of this labeling is to be accomplished by the site’s MR personnel exposing the metallic object to a handheld magnet (≥1000 G). If grossly detectable attractive forces are observed between the metallic object or any of its components and the handheld magnet, it is to be labeled with a red label. If no such forces are observed, a green label is to be affixed to the device or object prior to its introduction to Zone IV.
e. Decisions based on published MR compatibility or safety claims should recognize that all such claims apply to the specifically tested static field and static gradient field strengths. For example, “MR compatible up to 3.0 T at gradient strengths of 400 G/cm” or “MR safe tested up to 1.5 T up to maximum static gradient fields experienced in an unshielded 1.5T [manufacturer name] whole-body MR scanner tested 1.5 feet within the bore.”
f. It should be noted that alterations performed by the site on MR safe or compatible equipment or devices may alter the MR safety or compatibility properties of the device. For example, tying a ferromagnetic metallic twisting binder onto a sign labeling the device as MR compatible might result in artifact induction—or worse—if introduced to the MR scanner.

C. Time-Varying Gradient Magnetic Field–Related Issues: Induced Voltages

1. Although literature does not specify any known thresholds at which magnetic field strength and gradient magnetic field effects cause nerve and muscle stimulation in infants, infants will be continuously monitored for any signs of irritation or discomfort by direct visualisation (MR camera) and direct audio monitoring (MR noise-cancelling microphone). If the infant appears uncomfortable or in distress the MR scanning will be stopped immediately.
2. Infant participants with any implanted leads/wires will not be permitted to under-go MR scanning.

D. Time-Varying Gradient Magnetic Field–Related Issues: Auditory Considerations

1. During MR sequences all infant participants are to have hearing protective devices in place. These noise-cancelling earphones will have an incorporated microphone to constantly measure noise level (dB).
2. Maximum auditory exposure should be limited to 140dB (99 dB with ear protection device)
3. Infants should at all times wear Baby/Infant-headphones designed for infant MR scanning.

E. Time-Varying Radiofrequency Magnetic Field–Related Issues: Thermal

1. The infant's most recent known body weight should be requested from the parent/guardian. The level II MR personnel should continuously monitor the specific absorption ratio (SAR) during infant MR scanning.
2. The maximum permitted SAR for an infant head centred exposure is 3.4 W/kg (normal mode) and 5.0 W/kg (first level controlled mode) averaged over 6 minutes [1,2]

[1] International Electrotechnical Commission (IEC) 60601-2-33. Medical Electrical Equipment - Particular Requirements for the Safety of Magnetic Resonance Equipment for Medical Diagnosis. Geneva, 2010.
[2] Malik SJ, Beqiri A, Price AN, Teixeira JN, Hand JW, Hajnal JV. Specific absorption rate in neonates undergoing magnetic resonance procedures at 1.5 T and 3 T. NMR in Biomedicine. 2015;28(3):344–52

3. It is important to ensure the infant participant's tissues do not form large conductive loops. Therefore, care should be taken to ensure the participant's arms or legs are not positioned in such a way as to form a large caliber loop within the bore of the MR imager during the imaging process.

4. A MR compatible pulse-oximetry probe should be safely attached to the infant's foot.
5. Infant blankets should be inspected for any risk of metallic containing paints/wires within the material of the blanket.
6. Infant participants requested to undergo MR studies in whom there are skin staples or superficial metallic sutures (SMS) may be permitted to undergo the MR examination if the skin staples or SMS are not ferromagnetic and are not in the anatomic volume of RF power deposition for the study to be performed.

   Any infant with non-ferromagnetic staples/SMS but which will be within the volume to be RF irradiated for the MR study, should NOT be permitted to under-go the MR scan.

7. All unnecessary or unused electrically conductive materials should be removed from the MR system before the onset of imaging. It is not sufficient merely to "unplug" or disconnect unused, unnecessary electrically conductive material and leave it within the MR scanner with the participant during imaging. All electrical connections, such as on-surface coil leads or monitoring devices, must be visually checked by the scanning MR technologist prior to each scan to ensure the integrity of the thermal and electrical insulation.

8. Electrical voltages and currents can be induced within electrically conductive materials that are within the bore of the MR imager during the MR imaging process. This might result in the heating of this material by resistive losses. This heat might be of a caliber sufficient to cause injury to human tissue. Among the variables that determine the amount of induced voltage or current is the consideration that the larger the diameter of the conductive loop the greater the potential induced voltages or currents and, thus, the greater the potential for resultant thermal injury to adjacent or contiguous participant tissue. Therefore, when electrically conductive materials (wires, leads, implants, etc) are required to remain within the bore of the MR scanner with the participant during imaging, care should be taken to ensure no large-caliber, electrically conductive loops (including participant tissue) are formed within the MR scanner during imaging. Furthermore, it is possible, with the appropriate configuration, lead length, static magnetic field strength, and other settings, to introduce resonant

circuitry between the transmitted RF power and the lead. This could result in very rapid and clinically significant lead heating, especially at the lead tips, in a matter of seconds to a magnitude sufficient to result in tissue thermal injury or burns. This can also theoretically occur with implanted leads or wires even when they are not connected to any other device at either end. Thus, exposure of electrically conductive leads or wires to the RF-transmitted power during MR scanning should only be performed with caution and with appropriate steps taken to ensure significant lead or tissue heating does not result.

9. When electrically conductive materials are required to be within the bore of the MR scanner with the participant during imaging, care will be taken to place thermal insulation (including air, pads, etc) between the participant and the electrically conductive material while simultaneously attempting to (as much as feasible) keep the electrical conductor from directly contacting the participant during imaging. It is also appropriate to try to position the leads or wires as far as possible from the inner walls of the MR scanner if the body coil is being used for RF transmission.

10. Infants with extensive or dark tattoos will not be permitted to under-go the MR scan. This is due to the potential for radiofrequency heating of tattooed tissue in sensitive infant skin.

11. Infant participants with implants containing electrically conductive leads/wires should not be permitted to under-go the MR scan. This is due to the fact that resonant circuitry can be established during MRI between the RF energies being transmitted and specific lengths of electrically conductive wires or leads, which can thus act as efficient antennae. This can result in heating of the tips of these wires/leads to temperatures in excess of 90 degrees celcius in a few seconds.

F. Cryogen-Related Issues

For superconducting systems, in the event of a system quench, it is

imperative that all infant participants, their parent/guardian, and MR personnel be evacuated from the MR scan room as quickly and as safely feasible and that the site access be immediately restricted to all individuals until the arrival of the MR equipment service personnel. This is especially so if cryogenic gases are observed to have vented partially or completely into the scan room, as evidenced in part by the sudden appearance of white “clouds” or “fog” around or above the MR scanner. It is especially important to ensure all police and fire response personnel are restricted from entering the MR scan room with their equipment (axes, air canisters, guns, etc) until it can be confirmed that the magnetic field has been successfully dissipated, as there may still be considerable static magnetic field present despite a quench or partial quench of the magnet.

3. Fire, Flood, Quench and Infant/Adult Emergencies

Introduction

i. Research involving Magnetic Resonance Imaging (MRI) at high magnetic field strengths presents unique hazards to both research participants and individuals working within and around the MRI system. Consequently, the potential for serious personal injury is present due to the sheer size and strength of the static magnetic field along with the immense flexibility of the research system and associated peripheral hardware.

ii. The static magnetic field in the 3T MRI facility is always present. It is important that all those entering the facility be aware of the presence of the field, as it cannot be detected by our person in any way, i.e. magnetic fields cannot be felt, seen, or smelt.

iii. As a result of the potential for serious injury, access to the 3T MRI Facility is restricted, and requires permission.

iv. Working within and around the high field MRI requires in depth training on safety and Standard Operating Procedures, and documented proof of other necessary training.

v. It is imperative that all personnel who are within and around the 3T MRI facility always keep in mind the potential safety risks, and act in accordance with the guidelines set out in the Standard Operating Procedures.

vi. In case of emergency, the electrical power to the MR system can be cut abruptly without turning off or “quenching” the static magnetic field, or the static magnetic field of the MR system can be turned off. Quenching can potentially damage the MR magnet, can be dangerous, will result in several days of system down-time, and recovery to operation is expensive. It is therefore to be initiated only in the cases of 1) an uncontrollable fire, or 2) someone is pinned against the magnet by a magnetic object.

Emergency Fire Procedure

There are three basic steps to follow:

a. Ensure your own safety
b. Ensure the safety of the participant in the magnet
c. Contain the fire if possible. If it is not possible to contain the fire, follow the procedure in "Emergency Fire Procedure for Uncontrollable Fires."

1. Remove the volunteer/participant from the scanner.
    a. Manually release/withdraw the MRI table with the participant on it. This is quicker than pressing the "Home Position" button on the front face of the magnet to left of the bore.
    b. Remove the infant participant from the magnet room.
    c. If the participant is not responding or requires medical attention, follow the procedure set out in "Infant Emergency Procedure."
2. Activate the fire alarm
3. Contain the fire
    a. If possible, use the non-magnetic fire extinguisher to put the fire out.
    b. If it is not possible to contain the fire using the non-magnetic fire extinguisher, proceed to "Emergency Fire Procedure for Uncontrollable Fires."
4. Close the Magnet Room door
5. Notify the Facility Director and Security immediately following the incident.

Emergency Fire Procedure for Uncontrollable Fires

1. Always remember to:
    a. Ensure your own safety
    b. Ensure the safety of the participant in the magnet
2. Follow steps 1-5 in "Emergency Fire Procedure"

3. If the fire cannot be contained using the non-magnetic fire extinguisher, the operator must proceed to quench the magnet following "Emergency Quench Procedures". The magnet must be quenched before the fire fighting crew is allowed to enter the Magnet Room. If the magnet is not quenched, the fire fighters' equipment, which is magnetic, could cause serious injury to themselves or anyone near the magnet at the time of their entry.

   Pressing one of the two red "Stop" buttons quenches the magnet. See "Emergency Quench Procedures" for the procedure. The red "Stop" buttons are located:
   a. In the Control Room
   b. In the Magnet Room, to the left as you enter the door

4. Evacuate the building.
5. Notify the Facility Director and Security immediately following the incident.

Flood

1. If water starts to leak into the magnet room, equipment room, and control room evacuate immediately.
2. Notify the Facility Director and Security immediately.

Quench procedures

Description of a Quench

1. A "quench" is an event that occurs only in superconducting magnets and results in a loss of the magnetic field of the MRI magnet. It is caused by a loss of superconductivity; a rapid increase in the resistivity of the magnet coil windings, which generates heat that results in the rapid evaporation, or boil-off of the magnet coolant (liquid helium). This evaporated coolant is a hazard that requires emergency venting systems (quench pipe through roof) to protect participants

and operators. NOTE: once initiated a quench cannot be stopped and can potentially cause total magnet failure.

2. There are 2 situations in which a quench may occur.
    a. Spontaneously due to some force or disruption to the magnet system.
    b. The emergency "Magnet Stop" button is depressed during an emergency situation.

Depressing the "Magnet Stop" Button

1. The "Magnet Stop" button will cause the magnet to quench and must be pressed if there is a fire in the magnet room that cannot be contained using the non-magnetic fire extinguisher and requires the assistance of the fire brigade. Refer "Emergency Fire Procedure" for the emergency fire procedures.
2. The "Magnet Stop" button must be pressed if any individual is pinned to the magnet, trapped or in a potentially life threatening situation by a non-removable ferrous object.

Emergency Quench Procedure

1. Evacuate the magnet room if possible.
2. Depress one of the "Magnet Stop" buttons.
3. If the magnet was quenched because someone was pinned, and they are injured, the operator must apply first aid principles. If the victim is not responding, not breathing and has no pulse, follow the procedure outlined in "Infant Emergency Procedure" or "Adult Emergency Procedure". Once all parties are safely out of the magnet room, close the magnet room door.
4. Notify the Facility Director, and Security, immediately following the incident.

INFANT EMERGENCY:

1. An infant emergency is specifically defined as a situation in which an infant requires medical attention.
2. The paediatric doctor/nurse is responsible for initiating the Infant Emergency Procedure (set out below).
3. Unlike adults, acute cardiac arrest is extremely rare in infants/young children (usually only occurs in children with a background of congenital cardiac anomalies). Instead an unwell infant most usually presents with respiratory distress and in rare cases this may lead to respiratory arrest.
4. It is very important to monitor an infant's breathing and oxygen saturations. This can be done by direct vision (MR camera) and by oxygen saturation monitoring (MR pulse-oximetry).
5. The signs of an infant respiratory arrest include:
    a. The infant is apnoeic (no detectable breathing movements)
    b. The infant is minimally responsive
    c. The infant oxygen saturations are dropping (infant may appear cyanotic/blue)
    d. Note: if infant respiratory arrest is not managed urgently it may ultimately lead to cardiac arrest

Infant Emergency Procedure:

- Paediatric nurse/doctor – Instruct the MR operator to stop the infant MR scan if in progress.
- MR operator – Manually release/withdraw the MRI table with the participant on it. This is quicker than pressing the "Home Position" button on the front face of the magnet to left of the bore.
- Paediatric nurse/doctor – Assess the infant's condition
- Paediatric nurse/doctor – Decide if emergency response is required
- Experimental support personnel – Call Emergency (#dial 1999)
- Paediatric nurse/doctor – Extract the infant from the magnet room and place infant on the baby mat on the baby table in the control room

- MR operator - Request parent/guardian to exit the magnet room and accompany the infant and doctor/nurse into the control room (zone III).
- MR operator - Close the magnet room door
- MR operator - Open the infant emergency bag
- Paediatric nurse/doctor – Start necessary infant emergency measures as per APLS/PALS algorithms (See Appendix)
- Experimental support personnel –
    - Open the external door and wait for the paramedic emergency response team, and guide them to the Control Room when they arrive.
- MR operator - Ensure parent/guardian is being informed/updated on infant status.

ADULT EMERGENCY (adult personnel / adult caregiver):

***Note:** During infant research scanning, the contemporaneous presence of a paediatric doctor/nurse will provide additional clinical expertise to the adult emergency response. A paediatric doctor/nurse will have Basic Life Support training to allow initial adult emergency response, but will not necessarily have the clinical skill-set nor the safety/medical equipment at hand to provide more advanced adult emergency interventions/procedures.

1. An emergency is specifically defined as a situation in which a person requires medical attention.
2. The signs of an adult emergency are an adult exhibiting a change in behaviour or responsiveness.
3. The Paediatric doctor/nurse or the MR operator is responsible for initiating the Adult Emergency Procedure (set out below).
4. The signs of an adult cardiac arrest are all of the following collectively:
    a. The adult is not responding to stimulation
    b. The adult is not breathing
    c. And the adult does not have a pulse

Adult Emergency Procedure:

- MR Operator – Stop the infant MR scan if in progress
- MR Operator or Paediatric nurse/doctor – Assess the adult's condition
- MR Operator or Paediatric nurse/doctor – Decide if emergency response is required
- Experimental support personnel – Call Emergency (#dial 1999)
- MR Operator – Extract the adult from the magnet room
- Paediatric nurse/doctor – Extract the infant from the MR scanner
- MR Operator or Paediatric nurse/doctor – Start adult life-saving measures as needed
- Experimental support personnel – Open the external door, wait for paramedic emergency response team, and guide them to the Control Room when they arrive.

4. Appendix

PERSONNEL DEFINITIONS

Non-MR Personnel:
Participants, visitors, or facility staff who do not meet the criteria of level 1 or 2 MR personnel will be referred to as non-MR personnel. Specifically, non-MR personnel will be the terminology used to refer to any individual or group who has not, within the previous 12 months, undergone the designated formal training in MR safety issues defined by the MR safety director of that installation.

Level 1a MR Personnel:
Individuals who have passed initial MRI safety educational teaching/testing (as per their institution) will be referred to as level 1a MR personnel (e.g., research team members, principal investigators, MRI department office staff). Level 1a MR personnel are permitted unaccompanied access throughout Zones III and IV.

Level 1b MR Personnel:
Individuals who have passed both initial MRI safety educational teaching/testing (as per their institution) and who have attended a mandatory practical training/walk-through of the Infant Emergency Procedure steps. These personnel will typically be research team members or PIs involved in infant research MRI scanning. Level 1b MR personnel are only permitted to supervise an infant participant in Zone IV when a Level 2 MR person is present and has direct vision of those within Zone IV. A list of Level 1b MR Personnel (and dates of completed training) is in the Appendix.

Level 2 MR Personnel:
Individuals who have been more extensively trained and educated in the broader aspects of MR safety issues, including, for example, issues related to the potential for thermal loading or burns and direct neuromuscular excitation from rapidly changing gradients, will be referred to as level 2 MR personnel (physicist, radiographer/MR technologists, radiologists, certified users). Only the MR Physicist can award this designation.

Note:
All MR Personnel should be listed in the current MR Personnel logbook kept (and maintained up to date) in the MR Control Room.

ZONE DEFINITIONS

Zone I

This region includes all areas that are freely accessible to the general public. This area is typically outside the MR environment itself and is the area through which participants, health care personnel, and other employees of the MR site access the MR environment.

Zone II

This area is the interface between the publicly accessible, uncontrolled Zone I and the strictly controlled Zone III (see below). Typically, participants are greeted in Zone II and are not free to move throughout Zone II at will, but rather are under the supervision of MR personnel. It is in Zone II that the answers to MR screening questions, participant histories, medical insurance questions, etc are typically obtained. Zone II is swipe card controlled.

Zone III

This area is the region in which free access by unscreened non-MR personnel or ferromagnetic objects or equipment can result in serious injury or death as a result of interactions between the individuals or equipment and the MR scanner's particular environment. These interactions include, but are not limited to, those involving the MR scanner's static and time-varying magnetic fields. All access to Zone III is to be strictly restricted, with access to regions within it (including Zone IV, see below) controlled by, and entirely under the supervision of MR personnel. Zone III is swipe card controlled.

Zone IV (Magnet room)

This area is synonymous with the MR scanner magnet room itself. Zone IV, by definition, will always be located within Zone III, as it is the MR magnet and its associated magnetic field, which generates the existence of Zone III. Non-MR Personnel should be accompanied by, or under the immediate supervision of and in visual contact with, one specifically identified level 2 MR person for the entirety of their duration within Zone III or IV. Level 1 and 2 MR personnel may move freely about all zones. The door to the magnet room has to be locked when no Level 2 MR personnel is in Zone III. Keys are only available to Level 2 MR personnel.

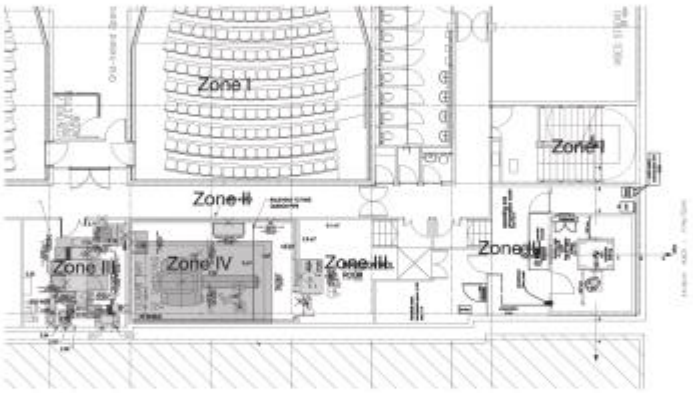
Zone I
Zone II
Zone III
Zone IV
Zone V

PAEDIATRIC DOCTOR/NURSE DEFINITIONS

A paediatric doctor, suitable for the clinical supervision of infants in the MR scanner, is someone who must:

- Be registered in the paediatric specialist trainee division or the paediatric specialist division of the Medical council of Ireland
- Have an active and up to date medical practitioners licence with the Medical council of Ireland
- Have up to date certification in Advanced Paediatric Life Support (APLS®) or Paediatric Advanced Life Support (PALS®).

A paediatric nurse, suitable for the clinical supervision of infants in the MR scanner, is someone who must:

- Be a registered children's nurse (RCN) with the Nursing and Midwifery Board of Ireland
- Have an active and up to date nursing licence with the Nursing and Midwifery Board of Ireland
- Have up to date certification in Advanced Paediatric Life Support (APLS®) or Paediatric Advanced Life Support (PALS®).

INFANT MR SAFETY SCREENING QUESTIONNAIRE

Name:	Date:		
Categories		**Yes**	**No**
Cardiac pacemaker – any type			
Heart surgery (e.g. patent ductus) or other			
Ventriculo-peritoneal shunt			
Other surgery			
Any type of surgical clip or staples			
Aneurysm clip			
Any type of biostimulator or neurostimulator pump			
Any type of internal electrode including pacing wires, cochlear implant, other			
Swan–Ganz catheter			
Any type of electronic, mechanical or magnetic implant			
Hearing aid or any type of ear implant			
Any type of foreign body, shrapnel or bullet			
Implanted drug infusion device			
Orbital/eye prosthesis			
Any type of implant held in place by a magnet			
Artificial limb or joint			
Any implanted orthopedic item			
Allergies			
Remove infant earrings/jewellery/religious artifacts			
Remove infant clothes containing metal buttons/poppers			
Change infant into MR compatible baby clothes			

If the answer to any of the above questions is 'YES' please give details.

Name: …… Date:……

Signed: …… (Parent or Guardian)

Signed:……(MR personnel)

A.

PARENT/GUARDIAN MR SAFETY SCREENING QUESTIONNAIRE

Name:	Date:		
Categories		**Yes**	**No**
Cardiac pacemaker any type			
Aneurysm clip			
Any type of biostimulator or neurostimulator pump			
Any type of internal electrode including pacing wires, cochlear implant, other			
Implanted insulin pump			
Any type of electronic, mechanical or magnetic implant			
Hearing aid			
Implanted drug infusion device (Implanon/contraceptive/other)			
Any type of foreign body, shrapnel or bullet			
Any type of ear implant			
Artificial eye			
Occupation as a metal worker, grinder, welder			
Any type of implant held in place by a magnet			
Vascular access port			
Intraventricular shunt			
Artificial limb or joint			
Any implanted orthopedic item			
Pregnancy			
Before entering the scanning room			
please remove your watch			
please take out metal hair ornaments			
please empty your pockets (some coins are ferromagnetic)			

If the answer to any of the above questions is 'YES' please give details.

Name: ..... Date:.....

Signed: .....

Signed:.....(MR personnel)

INFANT CLINICAL STATUS - SCREENING QUESTIONS

1. Infant age (months)?
2. Infant recent weight (kg)?
3. Any cough or secretions?
4. Any shortness of breath or wheeze?
5. Any recent fever?
6. Any recent medications? (include paracetamol? Ibuprofen? other?)
7. Any recent vomiting or diarrhoea?
8. When was the infant's last food and drink intake?
9. History of prematurity? (Corrected age?)
10. History of reflux?
11. History of apnoeas?
12. History of airway/lung issues?
13. History of infantile seizures?
14. History of previous MR scan (and any complications of same)?

APLS ALGORITHMS (BLS and Choking Child)

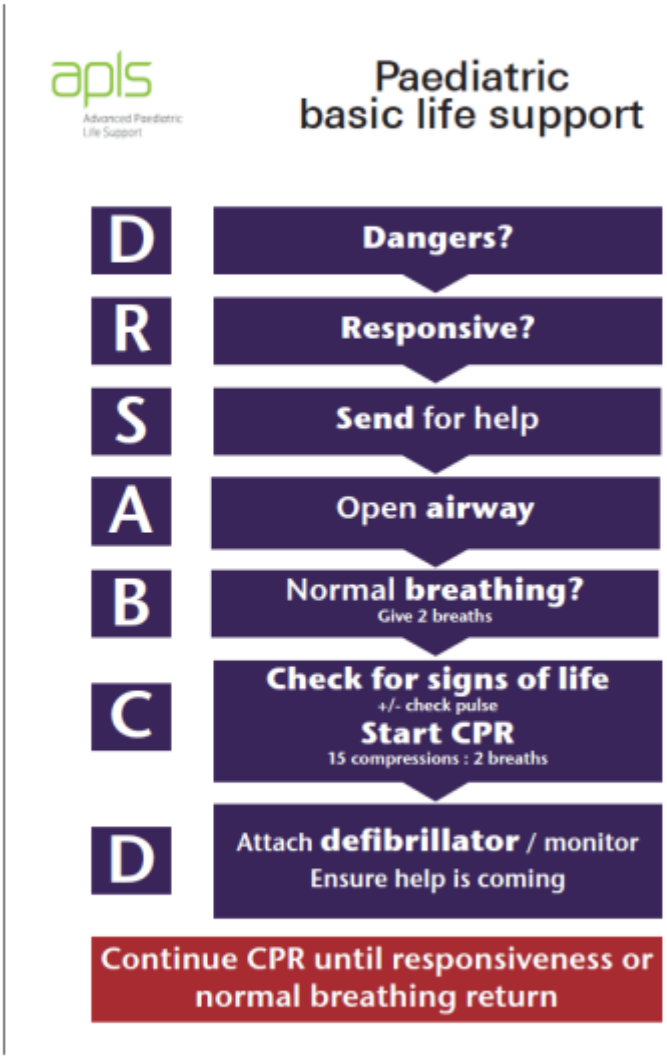

apls
Advanced Paediatric Life Support

The choking child

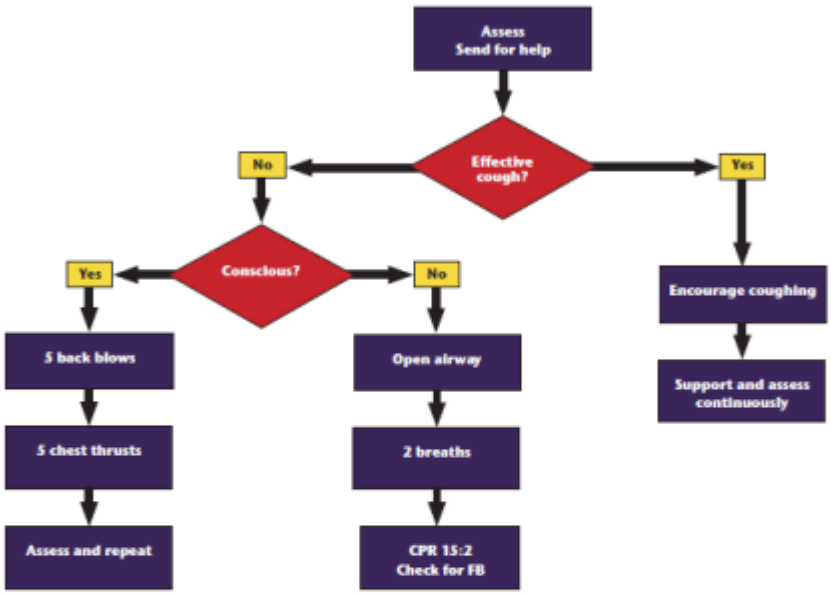

LEVEL 1b MR PERSONNEL - TRAINING RECORD

Name	Date completed MR Safety Theory	Date completed Infant Emergency Procedure practical/walk-through
E.g. Joe Bloggs	dd/mm/yyyy	dd/mm/yyyy